UNIVERSITÉ DU QUÉBEC À MONTRÉAL

INTERACTIONS ENTRE LA MICROCYSTINE INTRACELLULAIRE ET LES PROCESSUS PHYSIOLOGIQUES DE MICROCYSTIS AERUGINOSA

THÈSE

PRÉSENTÉE

COMME EXIGENCE PARTIELLE

DU DOCTORAT EN BIOLOGIE

PAR

JONATHAN NAOUM

AVRIL 2023

REMERCIEMENTS

J'aimerais principalement remercier mon directeur de thèse, Dr. Philippe Juneau, pour m'avoir encouragé à persévérer au travers de multiples embûches et qui m'a permis de mener mes recherches avec une grande liberté qui fut instrumentale à mon succès. Je lui serais toujours reconnaissant d'avoir pu identifier mon potentiel et m'avoir encouragé dans la bonne direction depuis ma première rencontre avec lui à la fin de mon baccalauréat. Sans ses conseils et son support, je n'aurais jamais pu réaliser un projet d'une telle envergure et sa confiance inébranlable en mes capacités a été très importante pour m'aider à conserver mon momentum tout au long de mes études au niveau maîtrise et doctorat. Philippe est un professeur extrêmement dévoué à ses élèves et son professionnalisme m'as été d'une grande inspiration pour la continuité de mes études.

Je tiens aussi à remercier les professeurs qui ont participé aux multiples comités d'évaluation de mon doctorat ou qui m'ont aidé de près ou de loin à répondre à d'importantes questions. Sans ordre particulier : Dr. Marcelo Pedrosa Gomes, Dr. David Dewez, Dr. Beatrix Beisner, Dr. Maikel Rosabal, Dr. Kui Xu, Dr. Catherine Jumarie, Dr. William Gerson Matias et Dr. Yves Prairie. Je tiens aussi à remercier le laboratoire du Dr. Sébastien Sauvé pour avoir procédé à l'analyse du contenu en microcystines dans mes échantillons ce qui a été d'une importance capitale à la complétion de cette thèse. De plus, je remercie également mes collègues de laboratoire pour leur aide, questions, réponses et encouragements. Ceux-ci ont su maintenir un environnement de travail positif et motivant dans le laboratoire du Dr. Philippe Juneau. Toujours sans ordre particulier : Juan Du, Disney Izquierdo, Guiqi Zhao, Fernanda Vieira, Catherine Ayotte, Ozgur Yoruk, Vitor Pereira Vaz, Alexandre Gauthier et Marie-Claude Perron. Aussi, un grand merci à ma famille et mes amis pour leur support et confiance indéfectible tout au long de mes études.

Finalement, je veux remercier les organismes subventionnaires et groupes de recherche interuniversitaire pour leur support financier et l'accès aux infrastructures qui ont été nécessaires à la conduite de mes travaux : le NSERC-CRSNG, le GRIL, le TOXEN, l'EcotoQ et la Fondation de l'UQAM.

AVANT-PROPOS

Vers la fin de mon baccalauréat, j'ai découvert un interêt particulier pour le domaine de l'écotoxicologie. En particulier, j'avais pour objectif de développer mes compétences au niveau de la bioremédiation des écosystèmes aquatiques/terrestres à l'aide de plantes et microalgues. Ainsi, le laboratoire d'écotoxicologie des microorganismes aquatiques du Dr. Philippe Juneau s'alignait parfaitement avec mon but premier. Mes premières expériences en tant que stagiaire m'ont permis de vérifier l'impact de retardateurs de flammes sur la physiologie de microalgues vertes et cyanobactéries pour ultimement déterminer leur potentiel de bioremédiation de l'eau contaminée par ces molécules. Ces expériences ont cimenté mon intérêt pour ce domaine de recherche et j'ai décidé de poursuivre mes études au niveau maîtrise dans ce même laboratoire. Toujours sous la supervision du Dr. Juneau, mon projet de maîtrise visait à déterminer les conséquences d'un inhibiteur de la biosynthèse des chlorophylles sur la physiologie de deux espèces de microalgues vertes et une cyanobactérie où j'ai pu déterminer qu'une exposition à long terme à ce toxique a mené à l'émergence d'une résistance stable chez une des microalgues vertes étudiées.

Par la suite, j'ai poursuivi un projet de doctorat dans ce même laboratoire afin d'affiner davantage mes compétences dans un sujet connexe soit l'étude de l'effet de l'impact combiné des changements climatiques et la présence de pesticides sur la physiologie et la composition des biofilms riverains. Ce projet a débuté par un séjour de trois mois en Chine à l'université Sun Yat-Sen situé à Guangzhou dans le laboratoire de recherche en microbiomique environnementale du Dr. Zhili He où j'ai pu apprendre plusieurs notions de métagénomique qui m'ont permis de complémenter l'influence de mes traitements sur la physiologie du périphyton à l'abondance et la diversité taxonomique des communautés. Malgré un intérêt particulier pour ce domaine de recherche, j'ai rapidement réalisé que je m'éloignais significativement des compétences acquises lors de ma maîtrise qui m'auraient permises de réaliser un projet de doctorat à la hauteur de ce qu'il m'était possible d'accomplir. J'ai donc cru plus sage de recentrer mon projet de doctorat vers un tout autre défi me permettant ainsi de m'appuyer sur mes compétences afin d'approfondir mon expertise sur l'étude de la physiologie des microorganismes

photosynthétiques soit l'étude du rôle physiologique d'une cyanotoxine, la microcystine intracellulaire, chez la cyanobactérie *Microcystis aeruginosa* en lien à la photosynthèse et la défense contre le stress oxydatif. Ce faisant, j'ai pu composer un projet de recherche de doctorat me permettant de repousser les limites de la connaissance sur ce sujet sous la forme de trois articles scientifiques dont je suis le principal contributeur.

TABLE DES MATIÈRES

[Cette page a été laissée intentionnellement blanche]

LISTE DES FIGURES

LISTE DES TABLEAUX

[Cette page a été laissée intentionnellement blanche]

LISTE DES ABRÉVIATIONS ET DES SYMBOLES

a^*_{φ}	Coefficient d'absorption spécifique de la lumière pour la chlorophylle *a*
ABS/RC	Surface d'absorption effective par centre réactionnel
ADN	Acide désoxyribonucléique
ADP	Adénosine diphosphate
AEPs	Voies alternatives d'électrons
ANOVA	Analyse de la variance
AOC_{OJIP}/F_M	Aire au-dessus de la courbe OJIP entre la fluorescence minimale et maximale et normalisée à la valeur de fluorescence maximale
APC	Allophycocyanine
ART	Test statistique non paramétrique avec distribution en rang aligné
ARTO	Oxydoréductase terminale alternative
ATP	Adénosine triphosphate
Atz	Atrazine
BG11	Milieu de croissance « *Blue-Green* » -11
CAR	Caroténoïdes
CAT	Catalase
Chl	Chlorophylle
Chl *a*/CAR	Ratio entre la chlorophylle *a* et les caroténoïdes
CO_2	Dioxyde de carbone
COX	Cytochrome *c* oxydase de type *aa3*
CPCC	« *Canadian Phycological Culture Center* »
CTE	Chaîne de transport d'électrons
Cyd	Cytochrome *bd* quinol oxydase
Cyt b_6f	Cytochrome b_6f
Cyt *f*	Cytochrome *f*
D-Asp^3 MC-LR	[D-Asp^3] Microcystine-LR

D-Asp^3 MC-RR	[D-Asp^3] Microcystine-RR
DBMIB	Dibromothymoquinone
DCMU	Diuron
DI_0/RC	Dissipation d'énergie par centre réactionnel
EC_{50}	Concentration d'un composé induisant 50% de l'effet maximal
ET_0/RC	Transport d'électrons par centre réactionnel
ET_0/TR_0	Probabilité qu'un exciton piégé déplace un électron dans la chaîne de transport d'électrons au-delà de la quinone A
ETC	« *Electron transport chain* »
EtOH	Éthanol
ETR	Taux de transport d'électrons
ETR_{max}	Taux maximal de transport d'électrons
F*	Spectre d'excitation de la fluorescence
F_0	Fluorescence initiale émise par la chlorophylle *a* lorsque les centres réactionnels du photosystème II sont réduits
F'_0	Fluorescence minimale de la chlorophylle *a* lorsque les centres réactionnels du photosystème II sont oxydés
FACHB	Freshwater Algae Culture Collection at the Institute of Hydrobiology
$fg \cdot \mu m^{-3}$	Femtogramme par cellules et normalisé au biovolume
FL1	Fluorescence à 533 nm avec un filtre passe-bande de 30 nm
FLV	Flavodiiron
Flv3	Protéine flavodiiron de type 3
F_M	Fluorescence maximale induite par une impulsion lumineuse de saturation lorsque les centres réactionnels du photosystème II sont réduits
F'_M	Fluorescence maximale en conditions d'équilibre du transport d'électrons lorsque les centres réactionnels du photosystème II sont réduits

$F_{M\ DCMU}$	Fluorescence maximale induite par une impulsion lumineuse de saturation lorsque les centres réactionnels du photosystème II sont réduits et en présence de DCMU
F_s	Fluorescence variable quantifiée en présence de lumière actinique soutenue et en conditions d'équilibre du transport d'électrons lors de la photosynthèse
$g \cdot L^{-1}$	Gramme par litre
H_2DCF-DA	Diacétate de 2',7'-dichlorodihydrofluorescéine
H_2O	Monoxyde de dihydrogène
H_2O_2	Peroxyde d'hydrogène
HL	Forte intensité d'illumination
HPLC	Chromatographie en phase liquide à haute performance
JTS-10	Spectrophotomètre de type Joliot
K	Taux de renouvellement des électrons
LED	Diode électroluminescente
LER	Respiration améliorée par la lumière
$mg \cdot m^{-3}$	Microgramme par mètre cube
MC-HilR	Microcystine-HilR
MC-HtyR	Microcystine-HtyR
MC-LA	Microcystine-LA
MC-LR	Microcystine-LR
MC-LW	Microcystine-LW
MC-LY	Microcystine-LY
MC-RR	Microcystine-RR
MC	Microcystine
MC+	Souche possédant la capacité de produire les MCs
MC-	Souche dépourvue de la capacité de produire les MCs
MC-WR	Microcystine-WR
mcy	Opéron responsable de la synthèse des microcystines
*mcy*B$^-$	Délétion du gène *mcy*B dans l'opéron *mcy*

*mcy*D	Gène *mcy*D dans l'opéron *mcy*
MC-YR	Microcystine-YR
MeOH	Méthanol
MT	Souche mutante
MT MC-	Souche mutante dépourvue de microcystines
MV	Méthylviologène
n	Nombre d'observations
N_2	Diazote
$NADP^+$	Forme oxydée de la nicotinamide adénine dinucléotide phosphate
NADPH	Forme réduite de la nicotinamide adénine dinucléotide phosphate
NDH	Complexe similaire à la NADH déshydrogénase
NDH-1	Complexe similaire à la NADH déshydrogénase et de type 1
O_2	Dioxygène
OCP	Protéine caroténoïde orange
OJIP	Courbe d'induction rapide de la fluorescence de la chlorophylle *a* (''O'': fluorescence minimale; ''P'': fluorescence maximale: ''J-I'': deux points d'inflexion entre O et P)
SPE-UHPLC-MS/MS	Extraction en phase solide reliée à la chromatographie liquide à ultra-haute performance couplée à la spectrométrie de masse en tandem
P680	Donneur primaire d'électrons du photosystème II
$P680^+$	Forme oxydée du donneur primaire d'électrons du photosystème II
P700	Donneur primaire d'électrons du photosystème I
$P700^+$	Forme oxydée du donneur primaire d'électrons du photosystème I
PAM	Fluorescence de la chlorophylle *a* mesuré via la méthode « *Pulse amplitude-Modulated* »
PAR	Rayonnement photosynthétiquement actif
PBS	Phycobilisomes
PC	Phycocyanine
PC/Chl *a*	Ratio entre la phycocyanine et la chlorophylle *a*

PCC	«*Pasteur Culture collection of Cyanobacteria*»
PEA	Appareil d'analyse de l'efficacité photochimique des plantes
PGR5	Protéine de régulation du gradient de proton de type 5
PGRL1	Protéine semblable à la protéine de régulation du gradient de proton de type 5
pH	Potentiel hydrogène
PlastoC	Plastocyanine
PP1	Protéine phosphatase 1
PP2A	Protéine phosphatase 2A
PQ	Plastoquinone
PQH_2	Plastoquinol
Prob > F	Valeur *p* pour le test de qualité de l'ajustement
PSI	Photosystème I
PSII	Photosystème II
Q_A	Plastoquinone A
Q_B	Plastoquinone B
qN_{REL}	Dissipation relation d'énergie par voies non-photochimiques
qP_{REL}	Dissipation relation d'énergie par voies photochimiques
R^2	Coefficient de détermination
*rbc*L	Séquence du gène codant pour une sous-unité de la ribulose-1,5-bisphosphate-carboxylase
rETR	Taux de transport d'électrons relatif
ROS	Dérivés réactifs de l'oxygène
RTO	Oxydases terminales respiratoires
RT-PCR	Réaction de polymérisation en chaîne par transcription inverse
RuBisCO	Ribulose-1,5-bisphosphate-carboxylase
SDH	Succinate déshydrogénase
SOD	Superoxyde dismutase
SP	Impulsion de saturation lumineuse

SSC	Complexité intracellulaire
TR_0/RC	Taux maximal de transfert d'énergie par centre réactionnel
Tukey HSD	Test DSH (différence significative honnête) de Tukey
µ	Taux de croissance
µM	Micromolaire
μm^3	Micromètre cube
µmol	Micromole
UQF_{REL}	Dissipation relative d'énergie sous forme de fluorescence
UV-B	Rayonnement ultraviolet de type B
UV-VIS	Spectroscopie d'absorption ultraviolet-visible
v/*v*	Concentrate en pourcentage volume/volume
WATER-PAM	Fluorescence de la chlorophylle *a* mesuré via la méthode « *Pulse amplitude-Modulated* » avec adaptateur pour culture liquide
WT	Souche de type sauvage
WT MC-	Souche de type sauvage dépourvue de production de microcystines
WT MC+	Souche de type sauvage pouvant produire les microcystines
ΔCOX	Délétion du gène codant pour la production de cytochrome *c* oxydase de type aa_3
ΔCyd	Délétion du gène codant pour la production de cytochrome *bd* quinol oxydase
ΔI/I	Changement dans l'intensité du signal mesuré par une photodiode
Δε	Écart entre l'absorptivité molaire de la forme réduite et la forme oxydée d'une molécule chimique
ϕ_M	Rendement quantique maximal du PSII
ϕ'_M	Rendement quantique opérationnel du PSII
λ	Longueur d'onde

RÉSUMÉ GÉNÉRAL

Dans les écosystèmes d'eau douce, les efflorescences cyanobactériennes sont souvent dominées par *Microcystis aeruginosa*, une espèce de cyanobactérie productrice de microcystines (MCs). Les MCs représentent une famille de cyanotoxines communément qualifiées de métabolites secondaires, or, plusieurs équipes de recherche rapportent un nombre croissant de relations entre les MCs et divers processus physiologiques. Parmi ces relations, la photosynthèse et la défense contre le stress oxydatif figurent parmi les processus intimement liés aux MCs intracellulaires ce qui pointe vers un rôle physiologique potentiel des MCs en lien au métabolisme central. Ainsi, l'objectif principal de cette thèse est d'affiner notre compréhension des relations entre les MCs et les processus physiologiques en lien à la photosynthèse et la défense contre le stress oxydatif afin de mieux définir le rôle physiologique potentiel des MCs.

Pour ce faire, le premier objectif vise à caractériser les relations intrinsèques entre le contenu en MCs et divers paramètres physiologiques reliés à la photosynthèse et la défense contre le stress oxydatif chez sept souches de *Microcystis aeruginosa* soit trois souches dépourvues de la capacité de produire les MCs (CPCC 632, CPCC 633 et CPCC 124), trois souches pouvant faire la biosynthèse de MCs (CPCC 299, CPCC 300 et PCC 7806) ainsi qu'un homologue mutant de PCC 7806 dépourvus de sa capacité à produire des MCs (PCC 7806 *mcy*B$^-$). La comparaison en tandem entre plusieurs souches sauvages et entre une souche possédant les MCs et sa souche homologue mutante dépourvue de MCs permet un examen approfondi de l'effet de la perte ou le gain de MCs sur la physiologie d'un point de vue évolutif ou par l'inactivation de la production de MCs par la mutagénèse insertionelle.

Bien que les différences physiologiques retrouvées entre les souches pouvant ou non produire les MCs et entre PCC 7806 et PCC 7806 *mcy*B$^-$ ne permettent pas d'isoler ou identifier un facteur déterminant, les relations établies entre le contenu cellulaire en MCs et la physiologie pointent vers un lien entre les MCs et la réponse contre la photoinhibition. Le deuxième objectif vise à manipuler les processus en lien à la réponse contre la photoinhibition chez PCC 7806 et PCC 7806 *mcy*B$^-$. Pour ce faire, il a été question de soumettre ces souches à des traitements visant à induire une photoinhibition soit indirectement à l'aide d'une exposition de 72h à 0.8 µM d'atrazine sous illumination à 35 µmol photons $\cdot$ m^{-2} $\cdot$ s^{-1} ou directement à l'aide d'une forte illumination sur une courte durée (1200 µmol photons $\cdot$ m^{-2} $\cdot$ s^{-1} sur 45 min) ainsi qu'en combinant ces traitements. Ces traitements ont permis de révéler des différences physiologiques entre ces deux souches et isoler des conséquences physiologiques de la perte de production de MCs. Notamment, PCC 7806 a du consacrer une plus grande quantité d'énergie que PCC 7806 *mcy*B$^-$ pour s'acclimater à une exposition simple ou combinée d'atrazine et d'un stress lumineux. Aussi, les différences physiologiques entre ces deux souches en conséquence aux traitements ont pointé vers les processus de régulation de la photoacclimatation. Une analyse des relations établies entre les congénères de la MC et la physiologie a pu relier la capacité de produire les MCs aux processus de dissipation non-photochimiques de l'énergie et la re-réduction du P700$^+$ ce qui pointe vers un changement dans la défense contre la photoinhibition et les voies alternatives de

transport d'électrons. Additionnellement, MC-LY, MC-LW et MC-LF ont pu être plus étroitement reliés aux processus en lien à la photoinhibition que les autres congénères identifiés.

Le troisième objectif est d'identifier les conséquences de la perte de production de MCs sur des processus en lien aux voies alternatives de transport d'électrons. Pour ce faire, il a été question de comparer PCC 7806 et PCC 7806 *mcy*B$^-$ au niveau de la proportion d'énergie absorbée par le PSII, la production et la consommation d'oxygène, les cinétiques d'oxydoréduction du P700, Cyt *f* et de la PlastoC et l'abondance maximale de la forme photo-oxydable de ces composantes ainsi que le pourcentage de transport cyclique d'électron autour du PSI. Ainsi, il a été possible de déterminer que la perte de production de MCs a entraîné un changement dans les processus en lien aux transports alternatifs d'électrons.

En somme, cette thèse a permis de révéler plusieurs points importants pour la détermination des rôles physiologiques des MCs. Notamment, les conclusions concernant les rôles physiologiques des MCs peuvent différer selon la composition des souches évaluées. Aussi, puisque la réponse physiologique à l'atrazine et au stress lumineux a différé entre PCC 7808 et son homologue mutant dépourvu de MCs, il existe nécessairement un lien entre les MCs et les processus reliés à la réponse contre la photoinhibition. Ensuite, la MC-LR, la [D-Asp^3]-MC-LR et la MC-HilR ont été plus étroitement reliées au ϕ'_M, qP_{REL}, ETR_{max} et Chl *a*/CAR que les autres congénères de la MC alors que la MC-LY, la MC-LW et la MC-LF ont été plus associées à la croissance, le biovolume, le qN_{REL}, le renouvellement d'électrons au niveau du PSI et le contenu en ROS. Ainsi, les différents congénères de la MC peuvent diverger par rapport à leurs relations avec la physiologie. Pour poursuivre, la perte des MCs chez PCC 7806 m*cy*B$^-$ a mené à des changements significatifs dans les voies alternatives de transport d'électrons et la production/consommation d'oxygène ce qui suggère un rôle physiologique des MCs au niveau de ces processus. Cette thèse permet ainsi d'ouvrir plusieurs avenues de recherches et supplémente la compréhension du rôle physiologique des MCs ce qui peut mener à un meilleur contrôle et capacité de prévision de la probabilité de survenance ou la sévérité des efflorescences cyanobactériennes nocives.

Mots clés : Cyanobactéries, microcystines, photosynthèse, stress oxydatif, photoinhibition, voies alternatives de transport d'électrons

INTRODUCTION GÉNÉRALE

Problématique

Les dangers pour la santé humaine et l'environnement résultants de l'apparition d'efflorescences phytoplanctoniques dominées de souches cyanobactériennes toxiques sont bien connus (Chorus *et al.*, 2021, Giannuzzi et Hernando, 2022, Hellweger *et al.*, 2022, IARC, 2010, Le Manach *et al.*, 2018, Massey *et al.*, 2022). Par exemple, l'émergence d'efflorescences phytoplanctoniques peut rapidement augmenter la turbidité de l'eau ce qui peut réduire la transmission de la lumière à travers l'eau et ainsi en diminuer l'accès aux autres organismes photosynthétiques aquatiques (Huisman *et al.*, 2004). Aussi, les efflorescences phytoplanctoniques peuvent mener à un épuisement de l'oxygène dissous dans l'eau limitant ainsi la disponibilité en oxygène pour les autres organismes (Rabalais *et al.*, 2010). De plus, les cyanotoxines produites par les cyanobactéries peuvent avoir des conséquences néfastes pour la santé des animaux d'élevage et les humains qui consomment de l'eau contaminée ou entraver l'accès aux activités récréatives et économiques liées à l'utilisation de l'eau comme la baignade et les sports nautiques (Carmichael, 2001, Merel *et al.*, 2013). Globalement, les changements climatiques et les activités anthropiques ont mené à l'intensification de la fréquence d'apparition des efflorescences cyanobactériennes toxiques (Paerl et Paul, 2012, Yang *et al.*, 2017). Parmis les cyanotoxines, les microcystines (MCs) font l'objet d'une attention particulière par la communauté scientifique notamment en raison de leur potentiel toxique mais, plus récemment, suite à l'émergence de plus en plus d'études qui démontrent des liens significatifs entre les MCs et de nombreux processus physiologiques importants chez les cyanobactéries comme la photosynthèse ou les mécanismes de défense contre le stress oxydatif. Ainsi, les MCs, autrefois considérées comme des métabolites secondaires, sont maintenant de plus en plus reconnues comme étant des molécules possédant de potentiels rôles physiologiques importants chez les cyanobactéries. Cependant, un consensus sur le rôle physiologique de la microcystine intracellulaire reste toujours en suspens (Omidi *et al.*, 2018). La biosynthèse de cette molécule nécessite un apport significatif en énergie (Briand *et al.*, 2012) et est intimement liée à la période diurne de la journée (Straub *et al.*, 2011) mettant ainsi

l'emphase sur la présence d'un rôle au niveau du métabolisme primaire (Carmichael, 1992, Straub *et al.*, 2011).

De multiples recherches ont tenté d'élucider le rôle physiologique de cette toxine par l'étude de souches toxiques de *Microcystis aeruginosa* (*M. aeruginosa*), une espèce de cyanobactérie retrouvée en eaux douces et qui prédomine fréquemment au sein d'éclosions d'efflorescences de cyanobactéries. Ces recherches ont permis d'établir des différences au niveau de la réponse physiologique en présence de stress environnementaux entre les espèces produisant ou non les microcystines (MCs) dans divers contextes expérimentaux tels que des variations dans l'apport en nutriments comme l'azote (Chaffin *et al.*, 2018, Harke et Gobler, 2013, Orr et Jones, 1998, Vézie *et al.*, 2002), le phosphore (Jähnichen *et al.*, 2011, Sinang *et al.*, 2015, Vézie *et al.*, 2002), le soufre (Jähnichen *et al.*, 2011), le fer (Sinang *et al.*, 2015, Utkilen et Gjølme, 1995, Wang *et al.*, 2018), la température (Chalifour et Juneau, 2011, Yang *et al.*, 2006) ou le régime lumineux (Chaffin *et al.*, 2018, Deblois et Juneau, 2010, Jähnichen *et al.*, 2011, Utkilen et Gjølme, 1992). Malgré la disparité des contextes expérimentaux, les processus explorés convergent majoritairement vers un lien direct entre les MCs et le métabolisme central. Parallèlement, la lumière joue un rôle décisif dans la régulation de la croissance chez les cyanobactéries (Mullineaux, 2001). Il n'existe pourtant pas de consensus quant à la relation entre la photosynthèse, la croissance et la production de MCs. Il s'agit d'aspects importants puisqu'il est possible de spéculer que les études qui définissent une relation directe entre la quantité de MCs intracellulaires et divers facteurs environnementaux peignent un portrait incomplet de la situation. En effet, il est possible que les changements dans la quantité de MCs intracellulaires soient une conséquence physiologique indirecte de la présence de ces changements environnementaux sur les mécanismes en lien avec la photosynthèse et la photoprotection. Cette hypothèse est d'autant plus confortée par les travaux de certains auteurs qui avancent que les MCs intracellulaires sont impliquées au niveau de la régulation de ces processus (transports alternatifs d'électrons, mécanismes non-photochimiques d'épuisement de l'énergie, taux d'assimilation du carbone, molécules et enzymes antioxydants) et des mécanismes de photo-acclimatation (régulation de la synthèse de constituants cellulaires, changements dans la composition pigmentaire, états de transition, changements dans le ratio PSII:PSI, modification de

la taille des complexes antennaires, réparation des photodommages) (Börner et Dittmann, 2005, Deblois et Juneau, 2010, Dittmann *et al.*, 2001, Hesse *et al.*, 2001, Jähnichen *et al.*, 2007, Jähnichen *et al.*, 2011, Kaebernick *et al.*, 2000, Makower *et al.*, 2015, Nishizawa *et al.*, 1999, Tonk *et al.*, 2005, Utkilen et Gjølme, 1995, Van de Waal *et al.*, 2011). Par exemple, en modulant l'apport en rayonnement photosynthétiquement actif (PAR) certains auteurs ont démontré qu'il existe une corrélation positive entre la production de MCs chez *M. aeruginosa* et l'intensité de la lumière jusqu'à l'atteinte du taux de croissance maximal à partir duquel la synthèse de MCs se voit inhibée (Deblois et Juneau, 2010, Wiedner *et al.*, 2003). La forte affinité des MCs pour les membranes thylacoïdales chez *M. aeruginosa* (Young *et al.*, 2008, Young *et al.*, 2005), plus spécifiquement au niveau des phycobilines (Jüttner et Lüthi, 2008), pointe d'autant plus vers un lien entre ces toxines et la photosynthèse. De plus, il a été observé que la chlorophylle *a* (Chl *a*) et les MCs peuvent être retrouvés dans un rapport de trois molécules de Chl *a* pour une MC (Deblois et Juneau, 2010). L'ensemble de ces résultats suggèrent que la production de MCs peut influencer la photosynthèse et la régulation de processus liés à la photosynthèse et vice versa, mais que les mécanismes impliqués sont toujours inconnus et nécessitent plus d'exploration.

Les cyanobactéries

Les cyanobactéries sont des procaryotes photoautotrophes ubiquistes autour du globe, polyvalents, et d'une importance biologique considérable par leur implication dans multiples cycles biogéochimiques (oxygène, carbone, azote, phosphore) (Flombaum *et al.*, 2013, Waterbury *et al.*, 1979). Les cyanobactéries sont l'une des formes de vie les plus anciennes connues avec plus de trois milliards d'années d'évolution et sont responsables de la Grande Oxygénation soit une période marquant l'ère paléoprotérozoïque où une production massive d'oxygène dans les océans a permis le développement de formes de vie plus complexes (Crowe *et al.*, 2013, Lyons *et al.*, 2014). La quasi-totalité des conditions environnementales retrouvées naturellement peuvent soutenir la croissance de ces bactéries photosynthétiques oxygéniques (Jungblut *et al.*, 2010, Nagarajan et Pakrasi, 2016). Par la conversion de l'énergie solaire en carbone organique, les cyanobactéries font partie du premier échelon de l'échelle trophique et les cyanobactéries marines sont d'ailleurs responsables de plus de 30% de la production primaire océanique soit la

synthèse chimique dans l'océan de composés organiques à partir du CO_2 atmosphérique ou dissous dans l'eau (Flombaum *et al.*, 2013). Chez les cyanophytes, la membrane plasmique est recouverte d'une paroi cellulaire typique d'une bactérie à Gram négatif, plus épaisse et formée d'une enveloppe mucilagineuse de peptidoglycane complexée de polysaccharides (Hoiczyk et Hansel, 2000). Les cyanobactéries ne comportent pas de membrane nucléaire, de réticulum endoplasmique, de mitochondries ou d'appendices motiles comme les cils ou flagelles (Wynne et Bold, 1978). L'observation et la schématisation de l'intérieur d'une cyanobactérie révèlent une différenciation entre deux zones principales: le protoplasme périphérique et le protoplasme central. La zone périphérique, lieu de la photosynthèse et la respiration, se compose d'une unique membrane thylacoïdale repliée plusieurs fois sur elle-même et intégrant les pigments photosynthétiques. Au niveau de la zone centrale se retrouve le nucléoplasme, zone riche en enzymes où repose l'ADN cyanobactérien circulaire, fibrillaire et compact. Dans le protoplasme central se retrouvent aussi les carboxysomes, microcompartiments contenant les enzymes impliqués dans les processus de fixation du carbone, des granules de polyphosphates, des ribosomes et des vésicules gazeuses (Stanier, 1988).

La photosynthèse chez les cyanobactéries

Les cyanobactéries possèdent la capacité de convertir l'énergie lumineuse et le dioxyde de carbone (CO_2) en énergie chimique et en oxygène (O_2) via la photosynthèse (Campbell *et al.*, 1998). La photosynthèse est un processus complexe intégrant l'absorption de la lumière, le transfert d'électrons au sein des centres réactionnels, la régulation des réactions d'oxydoréduction et la stabilisation de l'énergie produite grâce à des processus secondaires et concernant la fixation du carbone (Roach et Krieger-Liszkay, 2014). À la différence des algues, tous ces processus se produisent dans le cytosol, car il n'existe pas de séparation physique entre les acteurs cellulaires et moléculaires rejoignant la photosynthèse et la respiration, ceux-ci partagent donc certains transporteurs d'électrons comme la plastoquinone (PQ), le cytochrome b_6f (Cyt b_6f) et la plastocyanine (PlastoC) (Mullineaux, 2014a, Nagarajan et Pakrasi, 2016). Les antennes collectrices des cyanobactéries se retrouvent à la surface des thylacoïdes et se nomment les phycobilisomes (PBS), structures formées de phycobiliprotéines : phycoérythrine (PE), phycocyanine (PC) et

allophycocyanine (APC). Les PBS ne comportent pas toujours la PE. Aux PBS s'ajoutent des pigments accessoires, les caroténoïdes (xanthophylles et carotènes), qui forment ensemble un complexe antennaire qui capte et achemine l'énergie des photons vers les centres réactionnels de la chaîne de transport d'électrons (CTE) et ceux-ci jouent un rôle très important dans la photoprotection par l'entremise de la dissipation de l'énergie sous forme de chaleur. Les centres réactionnels des photosystèmes II (PSII) et des photosystèmes I (PSI) contiennent la chlorophylle *a* (Chl *a*) et ceux-ci sont disséminés de manière relativement homogène, en périphérie et intégré à la membrane thylacoïdale. Fait à noter, les PBS sont préférentiellement complexés aux PSII en fonction du niveau d'excitation des photopigments et la teneur en Chl *a* dans le PSI est plus élevée que dans le PSII (McConnell *et al.*, 2002).

Deux principaux types de transport d'électrons coexistent au sein de la membrane thylacoïdale, le transport photosynthétique linéaire et cyclique d'électrons (Lea-Smith *et al.*, 2016). Lors du transport linéaire d'électrons, l'énergie des photons transmise au PSII provoque l'excitation de la Chl *a* (P680 → $P680^+$) qui, en tandem avec le complexe d'oxydation de l'eau, induit l'oxydation de deux molécules d'eau (H_2O), la libération de deux électrons vers la CTE et quatre ions hydrogène (H^+) et une molécule de dioxygène (O_2) dans le lumen de la membrane thylacoïdale. Les électrons traversent ainsi le PSII : $P680^+$ → Phéophytine (Phéo) → Quinone A (Q_A) → Quinone B (Q_B) → Plastoquinone (PQ) → Plastoquinol (PQH_2). La PQH_2 quitte ensuite le PSII et migre vers le Cyt b_6f par diffusion. Les électrons traversent ensuite le Cyt b_6f et sont acheminés vers deux transporteurs solubles d'électrons, la PlastoC et le cytochrome c_6 pour ensuite rejoindre le PSI où, en aval de celui-ci, le $NADP^+$ sera réduit en NADPH. Ce processus entraîne l'établissement d'un gradient de protons transmembranaires qui permet la formation d'ATP par l'entremise d'ATP synthases (Taiz et Zeiger, 2006). Lors du transport cyclique d'électrons, les électrons acheminés au PSI divergent et retournent vers le pool de quinones, ce processus permet de recycler les électrons et ainsi d'établir un gradient de proton transthylacoïdal suffisant pour la production d'ATP sans permettre la formation de NADPH. L'ATP et le NADPH sont ensuite utilisés lors de la fixation du carbone au sein du cycle de Calvin-Benson-Bassham. Le transport cyclique d'électrons est considéré comme étant la principale voie alternative de transport électrons. Les voies alternatives de transport d'électrons servent à empêcher une surréduction de la chaîne de

transport d'électron lorsqu'il y a saturation du cycle de Calvin-Benson-Bassham qui peut entraîner la génération d'espèces réactives de l'oxygène et endommager les photosystèmes (Nikkanen *et al.*, 2021). La réparation du PSI est un processus bien plus lent que pour le PSII (Tikkanen *et al.*, 2014). Par conséquent, le PSI se situe au centre de la majorité des voies alternatives de transport d'électron afin de limiter une pression d'excitation excessive et des dommages quasi irréparables à celui-ci. Principalement, les électrons peuvent recirculer vers le pool de quinones à partir de la ferrédoxine (Fd) via le complexe nommé NADH déshydrogénase (NDH) (Miller *et al.*, 2021) ou la succinate déshydrogénase (SDH) (Liu, 2016). Autrement, le transport cyclique d'électrons vers le pool de quinones peut être médiée par les protéines de régulation du gradient de protons 5 (PGR5) et PGR5 à phénotype photosynthétique de type 1 (PGRL1) (Ma *et al.*, 2021). Puisque les chaînes de transport d'électron photosynthétique et respiratoire ne sont pas compartimentalisées chez les cyanobactéries, ceux-ci partagent plusieurs composantes et transferts d'électrons (Ogawa *et al.*, 2021). Les oxydases terminales comme la cytochome *bd* quinol oxydase (Cyd) et le complexe cytochrome *c* oxydase de type aa_3 (COX) peuvent emprunter les électrons provenant du pool de quinones et du cytochrome c_6, respectivement, afin de convertir l'oxygène moléculaire et quatre ions hydrogène (H^+) en deux molécules d'eau (Berry *et al.*, 2002, Ermakova *et al.*, 2016). Aussi, l'oxygène moléculaire peut être consommé via une réaction de type Mehler qui implique des protéines flavodiiron (FLV) (Bersanini *et al.*, 2014).

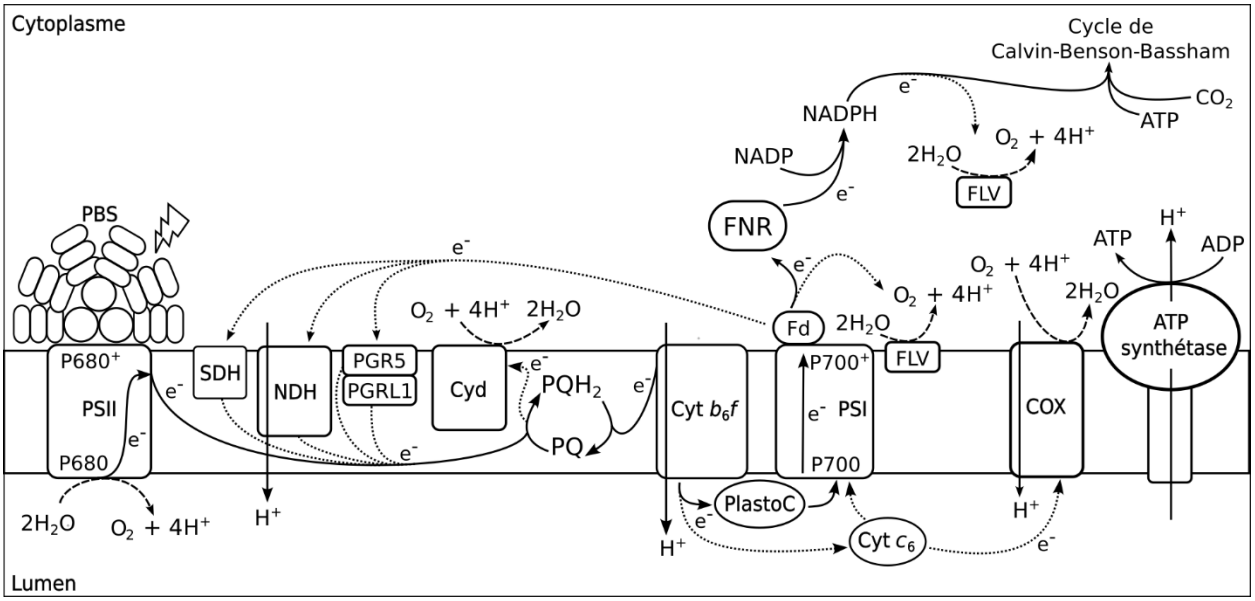

Figure 0.1 Chaîne de transport d'électron chez les cyanobactéries. Les électrons (e^-) associés aux flèches pleines représentent le transport linéaire d'électron alors les flèches pointillées représentent les transports d'électron alternatifs. Les flèches à tirets représentent les processus d'évolution de l'oxygène et de respiration. Schéma reproduit, traduit et adapté de Nikkanen *et al.* (2021).

La spectrophotométrie de type Joliot est une technique utilisée à maintes reprises lors de cette thèse et celle-ci est décrite pour la première fois dans Joliot *et al.* (1980). Lors des expériences dans le cadre de cette thèse, le JTS-10 (*Joliot-type spectrophotometer*) a été sélectionné pour cette technique puisque cet appareil comporte plusieurs avantages tel qu'un excellent rapport entre le signal capté et le bruit ainsi que la capacité d'isoler et mesurer en temps réel les changements d'absorbance au niveau de composantes spécifiques de la chaîne de transport d'électron photosynthétique. Un schéma du JTS-10 est présenté à la figure 0.2. Le JTS-10 permet une distance minimale entre l'échantillon et la diode de détection ce qui assure la possibilité d'illuminer une large surface de l'échantillon et de détecter d'une grande proportion du signal diffus. La combinaison d'un faisceau divisé et un diaphragme permet de corriger les petites variations d'une impulsion à l'autre et d'ajuster à zéro les valeurs de changements d'absorbance déterminées au début de chaque mesure. La combinaison spécifique de différentes sources de lumière actiniques et de détection ainsi que les filtres d'interférence et de coupure ont permis les applications employées lors de cette thèse. Par exemple, l'excitation sélective du PSII et du PSI ou seulement du PSI tout en surveillant les changements d'absorbance résultants au niveau du P700

a permis d'obtenir de l'information par rapport au renouvellement des électrons dans le PSI. De plus, l'ajout de diuron (DCMU) pour bloquer le flux linéaire d'électron (Pfister et Arntzen, 1979) a permis de déterminer la proportion du flux cyclique d'électron autour du PSI lors de la photosynthèse. Additionellement, il a été possible de suivre les changements d'absorbance au niveau du Cyt *f* et de la PlastoC pour la détermination des taux respectifs de renouvellement des électrons au sein de ceux-ci. En parallèle, des combinaisons entre l'ajout de DCMU pour supprimer le transport linéaire d'électron, de dibromothymoquinone (DBMIB) pour bloquer le transport linéaire et cyclique d'électron en plus des transferts d'électrons provenant de la chaîne respiratoire vers le Cyt b_6f (Liu *et al.*, 2012, Trebst, 2007) ainsi que l'ajout de méthylviologène (MV) en tant qu'accepteur d'électrons provenant du PSI (Trebst, 1972) ont permis de susciter un changement d'absorbance maximal au niveau du P700, du Cyt *f* et de la PlastoC sous illumination permettant ainsi une estimation de la concentration de ces composantes dans la cellule.

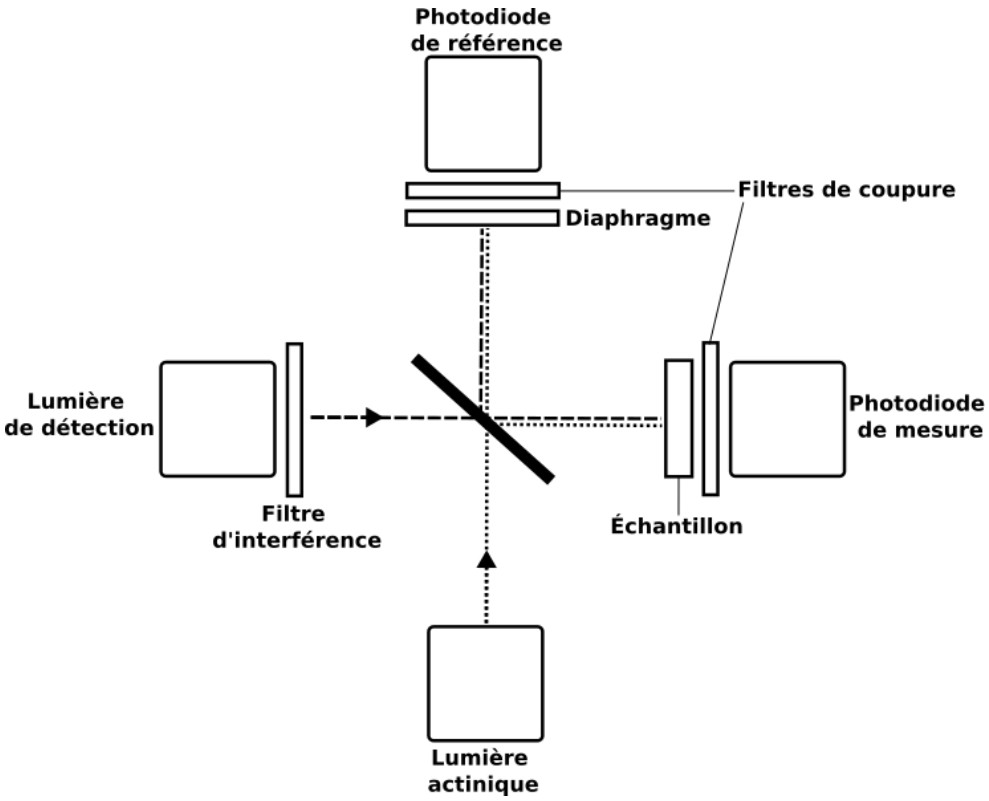

Figure 0.2 Schéma représentant les différentes composantes du *Joliot type spectrophotometer* (JTS-10). Figure reproduite, adaptée et traduite de l'anglais à partir du schéma retrouvé à la page 38 du manuel d'utilisation du logiciel du JTS-10 version 1.21.

La photoinhibition chez les cyanobactéries

Bien que les cyanobactéries nécessitent la lumière pour croître, une exposition à une illumination trop élevée ou même une illumination faible en présence de contaminants pouvant entraver le bon fonctionnement de la chaîne de transport d'électron photosynthétique peut entraîner des dommages graves pour la cellule. L'énergie lumineuse peut se retrouver transférée à l'oxygène moléculaire ce qui entraîne la génération d'espèces réactives de l'oxygène. Celles-ci émergent principalement au niveau des antennes collectrices de la lumière, le photosystème II et le photosystème I (Niyogi, 1999, 2000). La génération excessive d'espèces réactives de l'oxygène peut endommager des composantes importantes de la chaîne de transport d'électron photosynthétique qui se traduit par la photoinhibition soit une diminution de l'efficacité photosynthétique. Ces radicaux libres peuvent réagir avec les pigments photosynthétiques causant ainsi le photoblanchiment soit une altération dans la structure des pigments qui élimine

leur capacité à transférer l'énergie sous forme de fluorescence. Aussi, les radicaux libres peuvent mener à d'autres types de dommages comme la peroxydation lipidique de la membrane qui peut compromettre l'intégrité de celle-ci et empêcher l'établissement du gradient de proton transmembranaire nécessaire à la génération d'ATP lors de la photosynthèse. Pour contrer ces phénomènes, les cyanobactéries ont développé une multitude de mécanismes. Par exemple, celles-ci peuvent évacuer l'énergie en trop par l'entremise de mécanismes de dissipation non-photochimiques, éliminer les espèces réactives de l'oxygène et procéder à la réparation des dommages au niveau des photosystèmes, principalement au niveau du PSII. Un mécanisme non-photochimique important dans la réponse contre la photoinhibition chez les cyanobactéries est l'association de la protéine caroténoïde orange (OCP) à l'APC des PBS en conditions de lumière excessive (Muzzopappa et Kirilovsky, 2020). Cette association entraîne la ré-émission d'une grande proportion de l'énergie lumineuse sous forme de chaleur limitant ainsi le transfert d'énergie vers les photosystèmes (Kirilovsky, 2007, Kirilovsky et Kerfeld, 2012, Muzzopappa et Kirilovsky, 2020). Pour contrer l'émergence d'espèces réactives de l'oxygène, les cyanobactéries produisent des enzymes antioxydantes comme la superoxyde dismutase servant à dismuter l'anion superoxyde ($\cdot O_2^-$) en peroxyde de dihydrogène (H_2O_2) et en dioxygène ainsi que l'enzyme catalase servant à cataboliser le H_2O_2 en eau et en dioxygène (Pathak *et al.*, 2018). Les cyanobactéries possèdent aussi des molécules antioxydantes non-enzymatiques comme les caroténoïdes β-carotène, zéaxanthine, échinénone et myxoxanthophylle. Ces caroténoïdes servent à capter l'énergie en trop provenant de la chlorophylle excitée ou l'oxygène singulet ($^1O_2$) prévenant ainsi la formation de radicaux libres de l'oxygène. Additionellement, les conditions de photoinhibition peuvent entraîner des dommages oxydatifs irréversibles au niveau de la protéine D1 située au sein du centre réactionnel du PSII. Afin de préserver une activité photosynthétique stable, les organismes qui performent la photosynthèse possèdent un cycle continu de dégradation/réparation du PSII impliquant plusieurs kinases, phosphatases et protéases spécifiques ainsi que la synthèse *de novo* de la protéine D1 où son remplacement est régulé par l'entremise de la phosphorylation et la déphosphorylation de protéines au coeur du PSII (Nath *et al.*, 2013).

Les efflorescences de cyanobactéries et les microcystines

Les efflorescences cyanobactériennes se définissent comme étant des augmentations soudaines et rapides de la population de cyanobactéries dans les milieux aquatiques en conséquence à une variété de conditions environnementales, notamment l'excès de nutriments comme le phosphore (Jankowiak *et al.*, 2019, Kun *et al.*, 2017) et l'azote (Jankowiak *et al.*, 2019), une augmentation dans la température de l'eau (Jankowiak *et al.*, 2019, Johnk *et al.*, 2008, Paerl et Huisman, 2008), une réduction dans le débit des rivières (Mitrovic *et al.*, 2011), des faibles turbulences dans l'eau (Huisman *et al.*, 2004), de faibles vents et de basses pressions atmosphériques (Kun *et al.*, 2017). Celles-ci forment une écume dense à la surface de l'eau et peuvent se produire dans les écosystèmes d'eau douce ou marins pouvant ainsi mener à des conditions qui limitent la disponibilité en oxygène (Rabalais *et al.*, 2010) ou en lumière (Huisman *et al.*, 2004, Passarge *et al.*, 2006, Walsby *et al.*, 1997) pour les autres organismes aquatiques. *M. aeruginosa* est une espèce de cyanobactérie qui domine fréquemment au sein des efflorescences cyanobactériennes et dont certaines souches possèdent la capacité de production de cyanotoxines. Ainsi, ces efflorescences cyanobactériennes peuvent être nocives pour les autres organismes dans les écosystèmes aquatiques ou les humains qui se retrouvent exposés à celles-ci lors d'activités récréatives ou lors de la consommation d'eau contaminée. De ces cyanotoxines, les MCs sont parmi les plus étudiées par la communauté scientifique (Pearson *et al.*, 2010, Zurawell *et al.*, 2005). Jusqu'à aujourd'hui, plus de 270 variantes de la MC sont répertoriées (Massey *et al.*, 2020, Spoof et Arnaud, 2017). Les MCs sont des polypeptides cycliques hépatotoxiques qui partagent une structure commune, la cyclo(—D—Ala—X—D—MeAsp—Z—Adda—D—Glu—Mdha) où X et Z représentent des L-aminoacides variables, Adda est le diminutif de l'acide (2S, 3S, 8S, 9S)-3-amino-9-méthoxy-2,6,8-triméthyl-10-phényldéca-4,6-diénoïque, D—MeAsp est associé à l'acide D-érythro-β-iso-aspartique et Mdha correspond à la N-méthyl-déhydroalanine (Fastner et Humpage, 2021).

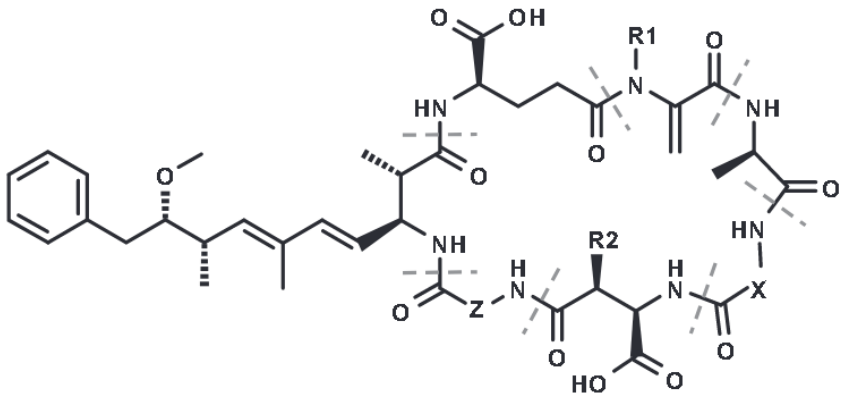

Figure 0.3 Structure commune de la microcystine. La cyclo(—D—Ala—X—D—MeAsp—Z—Adda—D—Glu—Mdha). X et Z représentent des L-aminoacides variables, Adda est le diminutif de l'acide (2S, 3S, 8S, 9S)-3-amino-9-méthoxy-2,6,8-triméthyl-10-phényldéca-4,6-diénoïque, D—MeAsp représente l'acide D-érythro-β-iso-aspartique et Mdha correspond à la N-méthyl-déhydroalanine. R1 et R2 correspondent à H (variantes de la desméthyle) ou CH_3. Adapté de Fastner et Humpage (2021).

Les MCs sont reconnues comme étant de puissants inhibiteurs de la protéine phosphatase 1 (PP1) et 2A (PP2A), enzymes responsables de la déphosphorylation des résidus sérine et thréonine dans les cellules eucaryotes (MacKintosh *et al.*, 1990). Chez l'humain, l'inhibition de la PP1 et PP2A entraîne la défaillance du foie via lésions hépatiques et l'exposition chronique aux MCs est immunotoxique, génotoxique et potentiellement carcinogène (Lone *et al.*, 2015, 2016, Zegura, 2016). Il existe très peu d'informations quant à l'influence des MCs sur les phosphatases cyanobactériennes et les informations retrouvées se limitent à une seule variante de la MC et ne peuvent donc pas reproduire la complexité des interactions entre les différents congénères de la MC et l'activité des phosphatases *in vivo* ce qui peut peindre un portrait incomplet de l'influence de ces toxines sur la physiologie des cyanobactéries (Shi *et al.*, 1999). Dittmann *et al.* (1997) ont ouvert la porte à l'étude de l'influence des MCs sur les processus physiologiques par la conception d'une souche mutante de *M. aeruginosa* PCC 7806 déficiente en production de MCs (PCC 7806 *mcy*B$^-$). La perte de la production des MCs résulte de l'inactivation du gène *mcyB* via l'insertion d'une cassette de résistance à l'antibiotique chloramphénicol dans l'opéron responsable de la synthèse des MCs. En conséquence, PCC 7806 *mcy*B$^-$ se voit dépourvue de sa

capacité de synthèse des variantes de la MC tout en permettant la production des autres peptides non ribosomaux (Dittmann *et al.*, 1997).

Relations entre la microcystine et les processus photosynthétiques et de photoprotection

Plusieurs recherches suggèrent que les MCs intracellulaires participent à la réponse physiologique de *M. aeruginosa* en présence de stress environnementaux comme une augmentation de la température (Boyer et Dyble, 2009, O'Neil *et al.*, 2012, Scherer *et al.*, 2016, Tonk *et al.*, 2005) ou des changements dans l'apport en nutriments (Paerl, 2018, Pimentel et Giani, 2014, Smith, 1983, Utkilen et Gjølme, 1995, Van de Waal *et al.*, 2011), mais que les mécanismes impliqués sont toujours largement inconnus. D'autres chercheurs ont révélé des indices de la présence de fonctions physiologiques des MCs intracellulaires en apparence intimement liés aux processus photosynthétiques, aux mécanismes de régulations dépendant de la lumière et à la protection contre le stress oxydatif (Börner et Dittmann, 2005, Dittmann *et al.*, 2001, Hesse *et al.*, 2001, Jähnichen *et al.*, 2011, Kaebernick *et al.*, 2000, Tonk *et al.*, 2005, Utkilen et Gjølme, 1992, Utkilen et Gjølme, 1995, Wiedner *et al.*, 2003, Yu *et al.*, 2019, Zilliges *et al.*, 2011). Ces recherches tentent principalement d'établir une relation cause à effet des facteurs de stress environnementaux sur la production de MCs ou la dominance des souches toxiques lors d'une efflorescence de cyanobactéries. L'utilisation d'une souche mutante de *M. aeruginosa* PCC 7806 comportant une déficience en production de MCs n'est pas une approche nouvelle, mais, à notre connaissance, il n'existe que très peu de recherche qui compare plusieurs souches non toxiques, toxiques, et une souche mutante toxique dans le but de démontrer un lien direct entre les MCs intracellulaires et la physiologie (Latour *et al.*, 2022, Mucci *et al.*, 2020, Sandrini *et al.*, 2015). Ce type d'étude est novateur par leur capacité d'observer l'impact de la perte ou le gain de production de MCs sur la physiologie d'un point de vue évolutif par rapport aux conséquences physiologiques de la perte de production de MCs via mutagénèse insertionelle. Latour *et al.*, 2022 ont suivi la densité cellulaire, le F_v/F_M et le contenu en MCs de trois souches de *M. aeruginosa* soit PCC 7005 (MC-), PCC 7806 (MC+) et PCC 7806 *mcy*B$^-$ (MC-) sous l'influence de quatre différents traitements soit une exposition prolongée à l'obscurité (24h), une exposition au H_2O_2 (0, 2 et 10 mg $\cdot$ L^{-1}) pendant 24h sous illumination continue à 10 µmol photons $\cdot$ m^{-2} $\cdot$ s^{-1}, un stress lumineux (exposition à 25

et 45 µmol photons · m^{-2} · s^{-1} pendant 2h suivi d'une incubation à 10 µmol photons · m^{-2} · s^{-1} pendant 22h) et une combinaison de H_2O_2 et les précédentes conditions d'illumination. Les auteurs ont observé que la souche MC+ est plus sensible aux conditions de stress en comparaison aux souches MC- et hypothétisent que le taux de réparation des photodommages pourrait expliquer les différences observées. Aussi, les auteurs ont observé un lien positif entre le contenu en MCs et l'activité photosynthétique. Dans l'ensemble, les auteurs concluent que les MCs ne semblent pas conférer un avantage en conditions de stress environnementaux ou contre la photoinhibition. Mucci *et al.*, 2020 ont vérifié l'influence du coagulant chitosan (0 , 0.5, 1, 2, 4 et 8 mg · L^{-1} pendant 24h) sur la physiologie de multiples souches de *M. aeruginosa* MC+ (MiRF-1, PCC 7806, PCC 7820, SAG 14.85, SAG 17.85 et CYA 140) et MC- (PCC 7805 et PCC 7806 *mcy*B^-). Les auteurs ont déterminé l'impact de ce traitement sur l'efficacité photosynthétique du PSII, la concentration en Chl *a* extracellulaire, l'intégrité membranaire ainsi que la concentration en MC-LR extracellulaire. Malgré une large disparité dans l'influence des traitements entre les différentes souches, les auteurs concluent que la présence ou non de MCs n'affecte pas la sensibilité au chitosan notamment en raison de l'influence comparable du traitement sur la physiologie de PCC 7806 et PCC 7806 *mcy*B^-. Sandrini *et al.*, 2015 ont comparé le taux de croissance de quatre souches de *M. aeruginosa* MC+ (NIES 843 et PCC 7806) et MC- (PCC 7005 et PCC 7806 *mcy*B^-) afin de déterminer si la production de MCs influence la sensibilité à l'ajout d'ions potassium (avec et sans l'addition de 11.5 mmol · L^{-1} de chlorure de potassium). En raison d'une grande variabilité par rapport à l'influence de ce traitement entre les souches ainsi qu'une sensibilité comparable entre PCC 7806 et PCC 7806 *mcy*B^-, les auteurs concluent que la production de MCs ne semble pas affecter l'influence de ce type de stress sur la physiologie de *M. aeruginosa*. Dans l'ensemble, les recherches qui comparent plusieurs souches sauvages MC+ et MC- de *M. aeruginosa* par rapport à une souche toxique mutante dépourvue de MCs contredisent la participation des MCs dans la réponse physiologique en présence de stress environnementaux tel que suggéré par les équipes de recherches citées précédemment.

Encore moins de chercheurs tentent d'explorer la question sous l'angle de la relation entre les MCs intracellulaires et la photosynthèse. Makower *et al.* (2015) ont révélé des différences dans la composition pigmentaire entre la souche PCC 7806 et PCC7806 *mcy*B^-. À l'aide de la RT-PCR

(*Reverse transcriptase polymerase chain reaction*), les travaux de Sevilla *et al.* (2012) ont permis de déterminer qu'un transport photosynthétique actif est nécessaire lors de la transcription de *mcyD*. Aussi, le mécanisme interreliant la lumière et la production de MCs ne serait pas régulé par des récepteurs de lumière ou en réponse au stress oxydatif et la présence de stress oxydatif serait liée à un déclin dans l'expression de *mcyD* et la production de MCs (Sevilla *et al.*, 2012). Certaines recherches révèlent que les MCs intracellulaires se lient au niveau des membranes thylacoïdales (Young *et al.*, 2008, Young *et al.*, 2005) ou directement sur les PBS (Jüttner et Lüthi, 2008). À la surface de l'eau, les cyanobactéries sont souvent exposées à une intensité lumineuse en excès alors que sous la surface ou au sein d'une colonie de forte densité, ceux-ci peuvent se retrouver exposés à de faibles intensités lumineuses (Tilzer, 1987). Les ajustements des processus en lien avec la photosynthèse et la photoacclimatation à différentes intensités lumineuses sont donc des mécanismes cruciaux pour optimiser la croissance des cyanobactéries et limiter les dommages en lien avec une exposition à une trop forte illumination. Deblois et Juneau (2010) suggèrent que les réactions de la phase claire de la photosynthèse interviennent dans la régulation du contenu en MCs intracellulaires. En effet, ces auteurs ont observé les mécanismes de transport d'électrons entre le PSII et le PSI, la croissance et le quota cellulaire en MCs chez la souche toxique de *M. aeruginosa* CPCC 299 en réponse à une exposition à des intensités lumineuses croissantes (24 à 820 µmol photons (PAR) m^{-2} s^{-1}) pendant cinq semaines. La photoadaptation aux différentes intensités lumineuses a permis d'établir plusieurs liens entre les processus photosynthétiques et le contenu en MCs. Une forte corrélation a été établie entre une augmentation de l'illumination et la diminution du quota cellulaire en MCs. Une corrélation très similaire a été observée pour le contenu en Chl *a*. Puisque les processus photosynthétiques interviennent dans la régulation de la synthèse de la Chl *a* et qu'il s'agit d'un mécanisme de photoacclimation, les auteurs proposent que la régulation de la synthèse des MCs pourrait fonctionner de manière similaire. Les auteurs soulignent d'ailleurs que les acteurs intervenant dans la régulation de l'expression génique et les processus impliqués dans la croissance et le développement des plantes sont influencés par les changements dans l'état d'oxydoréduction du PSII (Huner *et al.*, 1998, Wilson *et al.*, 2006). Ayant d'autant plus observé une relation inverse entre le taux de MCs intracellulaire et le transport d'électron relatif (ETR) ou l'état

d'oxydoréduction du PSII (UQF_{REL}), Deblois et Juneau (2010) avancent que ces processus pourraient fonctionner en tant que mécanismes sensibles aux pressions environnementales qui en retour modulent l'expression génique des gènes *mcy* pour éventuellement diminuer la concentration en MCs intracellulaires. Une comparaison de la quantité de transcrits géniques entre PCC7806 *mcy*B^- et sa souche homologue sauvage suggère un *cross-talk* hiérarchique et dépendant à la lumière entre les MCs et certains gènes-clés en lien avec le métabolisme central intermédiaire, la photosynthèse et le métabolisme de l'énergie (Makower *et al.*, 2015). Dans le même ordre d'idée, une augmentation de l'intensité lumineuse concorde avec une diminution de la transcription de l'opéron *mcy* (Deblois et Juneau, 2010, Kaebernick *et al.*, 2000, Utkilen et Gjølme, 1992, Wiedner *et al.*, 2003). En somme, l'étude des relations entre les MCs et la photosynthèse ainsi que les mécanismes visants à contrer la photoinhibition nécessite d'être approfondie afin de mieux définir le potentiel rôle physiologique des MCs par rapport à ces fonctions.

Structure et objectifs de la thèse

Puisqu'il a été démontré qu'il existe un lien possible entre les MCs intracellulaires et divers processus physiologiques en lien à la photosynthèse et les processus de protoprotection, il est nécessaire d'étudier ce phénomène afin d'être en mesure de déterminer l'origine et la direction de l'influence entre les MCs et la physiologie. Ainsi, le but premier de ce projet est d'isoler le rôle physiologique des MCs intracellulaires en lien aux processus liés à la photosynthèse et la réponse contre le stress oxydatif.

Dans le chapitre 1, l'objectif est d'étudier les relations intrinsèques entre les MCs et les processus physiologiques de plusieurs souches sauvages pouvant ou non produire les MCs et une souche toxique mutante dépourvue de sa capacité à produire les MCs. De plus, il est question de comparer cette caractérisation entre les souches pouvant ou non faire la biosynthèse de MCs de manière à identifier les différences physiologiques majeures entre ces groupes dans des conditions de croissance similaires, d'isoler des indices importants sur le rôle physiologique de la MC et d'établir des relations entre les MCs et les processus physiologiques quantifiés.

Pour le chapitre 2, l'objectif est de cibler le rôle physiologique des MCs intracellulaires au niveau des processus en lien à la réponse contre la photoinhibition à l'aide d'une caractérisation de la réponse physiologique de *M*. *aeruginosa* PCC 7806 et son homologue mutant dépourvu de sa capacité à produire les MCs (PCC 7806 *mcy*B$^-$) suite à l'influence seule ou combinée de l'atrazine et un stress lumineux afin de déterminer si et comment la réponse physiologique est affectée par la capacité à produire les MCs.

Pour le chapitre 3, l'objectif est de déterminer s'il existe une différence entre PCC 7806 et PCC 7806 *mcy*B$^-$ au niveau des processus en lien à l'état d'oxydoréduction des composantes au coeur de la chaîne de transport d'électrons photosynthétique. Ainsi, ce chapitre vise à mettre en lumière les liens possibles entre la capacité de produire des MCs et l'état redox de la chaîne de transport d'électrons et, conséquemment, d'obtenir de l'information sur les conséquences possibles de ces différences sur les processus régulés par l'état redox de ces composantes.

En somme, ces trois chapitres sont reliés et visent à obtenir une meilleure compréhension du rôle physiologique de la MC intracellulaire en lien aux processus impliqués dans le métabolisme central des cyanobactéries soit la photosynthèse et la réponse aux conditions oxydatives. Ainsi, la définition du rôle physiologique des MCs fourni par cette thèse peut améliorer notre connaissance en lien à la dynamique des populations au sein d'efflorescences de cyanobactéries toxiques.

[Cette page a été laissée intentionnellement blanche]

CHAPITRE 1

COMPARATIVE PHYSIOLOGICAL ANALYSIS OF SIX WILD STRAINS AND ONE MICROCYSTIN-DEFICIENT MUTANT STRAIN OF *MICROCYSTIS AERUGINOSA* REVEALS SIGNIFICANT DIFFERENCES BETWEEN MICROCYSTIN PRODUCING AND LACKING STRAINS

Jonathan Naoum[1], Juan Du[1] and Philippe Juneau[1]

[1]Département des Sciences Biologiques, GRIL-TOXEN-EcotoQ, Ecotoxicology of Aquatic Microorganisms Laboratory, University du Québec à Montréal, Succursale Centre-ville, C.P. 8888 Montréal, Québec H3C 3P8, Canada

Will be submitted to Harmful Algae

[Cette page a été laissée intentionnellement blanche]

1.1 Résumé

Dans les écosystèmes d'eau douce, les efflorescences cyanobactériennes sont souvent dominées par *Microcystis aeruginosa*, une espèce de cyanobactérie productrice de microcystines (MCs). Les MCs représentent une famille de cyanotoxines communément qualifiées de métabolites secondaires. Il existe plusieurs relations entre les MCs et divers processus physiologiques. Or, l'origine de ces relations est toujours largement incomprise. Cette étude a servi à caractériser les relations intrinsèques entre le contenu en MCs et divers paramètres physiologiques reliés à la photosynthèse et la défense contre le stress oxydatif chez sept souches de *Microcystis aeruginosa* soit trois souches sauvages dépourvus de la capacité de produire les MCs (CPCC 632, CPCC 633 et CPCC 124), trois souches sauvages pouvant faire la biosynthèse de MCs (CPCC 299, CPCC 300 et PCC 7806) ainsi qu'un homologue mutant de PCC 7806 dépourvus de sa capacité à produire des MCs (PCC 7806 *mcy*B$^-$). Une comparaison entre les différences physiologiques retrouvées entre les souches sauvages pouvant ou non produire les MCs par rapport aux différences physiologiques retrouvées entre PCC 7806 et PCC 7806 *mcy*B$^-$ a permis de déterminer que les tendances retrouvées en présence ou en absence de production de MCs diffèrent parfois selon la composition des souches sélectionnées. De plus, les relations établies entre le contenu en MCs et la physiologie ont été étroitement reliées aux processus impliqués dans la réponse contre la photoinhibition.

Mots-clés: Cyanobactéries, microcystines, souche sauvage, souche mutante, photosynthèse, systèmes de défense antioxydants, profil physiologique

[Cette page a été laissée intentionnellement blanche]

1.2 Abstract

Harmful cyanobacteria blooms are a pressing environmental issue. These blooms are often dominated by *Microcystis aeruginosa*, a species of cyanobacteria known produce microcystins (MCs). While MCs were linked to various physiological processes, little is known on it's true physiological role of MCs. In this context, this paper aimed to explore the intrinsic relationships between total MCs content and various physiological parameters related to photosynthesis and defense against oxidative stress in seven strains of *Microcystis aeruginosa* which consisted of three wild-type strains lacking the ability to produce MCs (CPCC 632, CPCC 633 and CPCC 124), three wild-type strains capable of MCs biosynthesis (CPCC 299, CPCC 300 and PCC 7806) and a mutant homologue of PCC 7806 lacking the ability to produce MCs (PCC 7806 *mcy*B$^-$). A comparison between the physiological differences found between wild type strains capable or not of producing MCs versus the physiological differences found between PCC 7806 and PCC 7806 *mcy*B$^-$ allowed us to determine that the trends found in the presence or absence of MC production may differ depending on the selection of the studied strains. Furthermore, the relationships established between total MCs content and physiology were closely related to the processes involved in the response against photoinhibition.

Keywords: Cyanobacteria, microcystins, photosynthesis, antioxidant defense, physiological profile

[Cette page a été laissée intentionnellement blanche]

1.3 Introduction

Freshwater harmful cyanobacterial blooms occur frequently in freshwater bodies and are composed of several species which are known to produce microcystins (MCs), a family of known hepatotoxins, thereby constituting a pressing environmental and public health issue (Chorus *et al.*, 2021, Giannuzzi and Hernando, 2022, Hellweger *et al.*, 2022, IARC, 2010, Le Manach *et al.*, 2018, Massey *et al.*, 2022). In these blooms, *M. aeruginosa* is often found to dominate the species distribution and is known to significantly contribute to MC production within those blooms (Duan *et al.*, 2022). Today, more than 270 variants of MCs have been identified (Massey *et al.*, 2020, Spoof and Arnaud, 2017). While MCs are conventionally classified as secondary metabolites, a growing number of research groups identified close relationships between intracellular MCs and major physiological processes related to growth (Omidi *et al.*, 2018). These relationships point toward a physiological role of intracellular MCs within central metabolism of the producing cells. Indeed, MCs were found to bind to specific proteins and enzymes in response to oxidative stress conditions (Zilliges *et al.*, 2011), may act as scavengers of free radicals (Dziallas and Grossart, 2011, Malanga *et al.*, 2019) and it was shown that inactivation of MC production led to altered expression of genes regulated by light exposure (Dittmann *et al.*, 2001) which points toward a strong link between MCs and processes related to photosynthesis and the stress response. Even if multiple relationships were established between intracellular MCs and physiology, the dynamics between these relationships are still under debate (Deblois and Juneau, 2010, Hellweger *et al.*, 2022, Omidi *et al.*, 2018). Moreover, contrasting results sometimes arise depending on the context and methodology. Zilliges *et al.* (2011) demonstrated that addition of increasing concentrations of hydrogen peroxide or growth under high light intensity was better tolerated by the MC-producing strain PCC 7806 than its non-MC-producing mutant homologous strain PCC 7806 *mcy*B$^-$ and that high light exposure led to the binding of MCs to specific proteins thereby raising the possibility of a protective role of MCs in oxidative stress conditions. In contrast, Latour *et al.* (2022) examined the physiological response of the same MC producing strain PCC 7806 and its homologous MC-deficient mutant strain PCC 7806 *mcy*B$^-$ or a wild non-MC-producing strain PCC 7005 to varying concentrations of hydrogen peroxide combined to different light regime and intensity. They concluded that the MC-producing strain was more sensitive to these

experimental conditions than the MC-devoid strains and speculated that the rate of photodamage and/or repair of PSII may be a defining parameter of these results as addition of protein synthesis inhibitors produced a stronger decrease in photosynthetic efficiency in the non-MC-producing strains compared to the MC-producing strain under high light stress conditions. One may ask if intracellular MCs are directly involved in the regulation of correlated physiological endpoints or if MC content is influenced by a change in these physiological processes ensuing from a change in environmental conditions such as light intensity or temperature. Most studies characterizing the relationships between MC content and physiology will either compare wild MC-producing (WT MC+) strains with wild non-MC-producing (WT MC-) strains or will aim to compare WT MC+ strains with a mutant counterpart from which the ability to produce MCs was inactivated through insertional mutagenesis (MT MC-) (Dittmann *et al.*, 1997). Very few studies can link the relationships between intracellular MCs and the physiology of wild strains with the consequences of the inactivation of MC production on the same physiological parameters (Latour *et al.*, 2022, Mucci *et al.*, 2020, Sandrini *et al.*, 2015). Such comparisons are necessary to allow a better understanding on the direction of the influence between MC content and physiology and should provide valuable insight on the role of MCs in relation with important growth-related physiological processes such as photosynthesis and the oxidative stress response.

To accomplish this task, we conducted a comparative analysis of the physiology (growth, photosynthesis, antioxidant enzyme activity and morphology) between seven strains of *M. aeruginosa* comprising of WT MC+, WT MC- and MT MC- strains. This holistic approach allows for a direct comparison between intracellular MCs, or lack thereof, and the physiology of all strains studied. In parallel, we compared general trends between wild strains and the consequence of induced loss of MC production in order to hypothesize on the direction of the influence between MC content and linked physiological parameters. The comparison between wild type strains and between a wild strain and its non-MC-producing mutant strain will allow for an examination of the potential role of MCs in relation to the physiology from an evolutionary perspective and through inactivation of MC production using insertional mutagenesis.

1.4 Methods

1.4.1 Cultures

Seven strains of *Microcystis aeruginosa* including three WT MC- strains (CPCC 632, CPCC 633 and CPCC 124), two WT MC+ strains (CPCC 299 and CPCC 300) and one WT MC+ strain PCC 7806 and its MT MC- counterpart PCC 7806 *mcy*B$^-$ were selected for this research. PCC 7806 was selected as it is a model toxic strain of *M. aeruginosa* commonly found in literature. PCC 7806 *mcy*B$^-$ was selected to place emphasis on the consequences of the loss of the capacity of MC production on the physiology of PCC 7806. The other strains were randomly selected based on their capacity or not to produce MCs. Cultures of CPCC 632, CPCC 633, CPCC 124, CPCC 299 and CPCC 300 were obtained from the Canadian Phycological Culture Centre (CPCC, University of Waterloo, Ontario, Canada) while the strains PCC 7806 and PCC 7806 *mcy*B$^-$ were obtained from the Pasteur Culture collection of Cyanobacteria (PCC, Pasteur Institute, Paris, France). For MT MC-, absence of MC production resulted from the knockout of the *mcy*B gene within the *mcy*ABC operon through insertional mutagenesis with a resistance gene to the antibiotic chloramphenicol (Dittmann *et al.*, 1997). Prior to the experiment, strains were maintained in exponential growth phase by transfers in fresh sterile culture media every 5 to 7 days depending on the strain. Cultures were prepared in 250 ml Erlenmeyer flasks containing 100 ml of BG11 medium at pH 7.4 (Rippka *et al.*, 1979) and inoculated at a cell density of 500 000 cells per ml. Cultures were kept in an environmental chamber at 24°C and growth light intensity of 35 µmol photons $\cdot$ m^{-2} $\cdot$ s^{-1} with a photoperiod of 12h:12h (light:dark). Illumination was provided by a combination of incandescent bulbs (Philips, 60W, USA) and white fluorescent lamps (Philips, F72T8/TL841/HO, USA). These growth conditions were selected as they offer a midpoint between the saturating light supply and maximal intracellular MC content observed by Hesse *et al.* (2001) and Deblois and Juneau (2010), respectively.

1.4.2 Growth and morphology

Cell density and biovolume were evaluated after three days of growth using a particle analyzer (Multisizer 3 Coulter Counter, Beckman Coulter Inc., USA). The growth rate was determined using the formula:

$$\mu\ (day^{-1}) = \frac{\ln[Cell]_{final} - \ln[Cell]_{initial}}{Time_{final} - Time_{initial}}$$

where μ is the maximum specific growth rate (day^{-1}) and $[Cell]_{initial}$ and $[Cell]_{final}$ relate to the initial and the final cell density, respectively. Intracellular complexity (SSC) was determined by flow cytometry (BD accuri C6 Plus, BD Biosciences, Becton-Dickinson, Franklin Lakes, NJ) according to Stachowski-Haberkorn *et al.* (2013).

1.4.3 Photosynthetic pigments

Cells were collected through gentle filtration on 0.8 µm-pore filters (Polytetrafluoroethylene, Xingya Purifying Materials Factory, Shanghai, China), flash frozen in liquid nitrogen then stored at -80°C until later extraction and quantification. Chl *a* and CAR were extracted in 95% ethanol and quantified according to Lichtenthaler (1987). Phycocyanin (PC) and allophycocyanin (APC) were extracted in phosphate saline buffer at pH 6.8 using repeated freezing/thawing cycles in liquid N_2 and a thermostated water bath at 20°C. PC and APC were then quantified according to Bennett and Bogorad (1973).

1.4.4 Photosynthetic parameters

Prior to every measurement, cultures were placed in complete obscurity for 15 min to allow for reoxidation of the electron transport chain components. Following dark acclimation, cultures were analyzed for the determination of various photosynthesis-related parameters using a WATER-Pulse-Amplitude-Modulated fluorometer (WATER-PAM) with a liquid culture attachment (WATER-PAM, Heinz Walz GmbH, Effeltrich, Germany) and a Plant-Efficiency-Analyzer (PEA) (Handy-PEA, Hansatech Instruments, Norfolk, UK). Light response curves were obtained using the WATER-PAM. For this analysis, the initial fluorescence for a dark-acclimated sample (F_0) was first recorded at the beginning of each measurement in the absence of actinic illumination. Then, a flash of saturating light (800 ms, 1685 µmol photons $\cdot m^{-2} \cdot s^{-1}$) was applied to induce the maximal fluorescence signal for a dark-acclimated sample (F_M). Subsequently, the sample was exposed to 12 incremental steps of actinic illumination (21, 31, 47, 69, 107, 158, 241, 359, 510, 706, 1153 and 1685 µmol photons $\cdot m^{-2} \cdot s^{-1}$) where each actinic light intensity was maintained for 60 sec then

followed by a pulse of saturating light (800 ms, 1685 µmol photons · m^{-2} · s^{-1}) before and during which the fluorescence signal was recorded to obtain F_s and F'_M, respectively. Afterwards, actinic illumination was turned off and the fluorescence signal was allowed to return to a stable value in order to obtain the minimum fluorescence signal of a light-acclimated sample (F'_0). Finally, DCMU was added to the sample (final concentration of 10 µM) and a flash of saturating light (800 ms, 1685 µmol photons · m^{-2} · s^{-1}) was applied to allow for the determination of the maximal fluorescence when the PSII reaction centers are fully reduced ($F_{M\ DCMU}$) (Campbell *et al.*, 1998). From the light response curves, the maximal (ϕ_M) and operational (ϕ'_M) PSII quantum yields were determined according to Kitajima and Butler (1975) and Genty *et al.* (1989), respectively. Additionally, the relative photochemical quenching (qP_{REL}) and relative non-photochemical quenching (qN_{REL}) were determined according to Buschmann (1995), while the relative unquenched fluorescence (UQF_{REL}) was determined according to Juneau *et al.* (2005). In parallel, we assessed the fast polyphasic chlorophyll fluorescence induction kinetics using the Handy-PEA and the procedure described in Strasser *et al.* (2000). We calculated the absorption (ABS/RC), trapping (TR_0/RC), electron transport (ET_0/RC) and dissipation (DI_0/RC) flux per reaction center as well as the probability that a trapped exciton moves an electron into the electron transport chain beyond Q_A (ET_0/TR_0) and the complementary area over the OJIP curve normalized to maximal fluorescence (AOC_{OJIP}/F_M) according to Force *et al.* (2003).

PSI electron turnover rate and cyclic electron transfer around PSI was evaluated through the monitoring of P700 oxidoreduction kinetics (Joliot and Joliot, 2002, 2005) using a Joliot-type spectrophotometer (JTS-10, Spectrologix, USA). PSI electron turnover rate was determined according to Joliot and Joliot (2005) where variations in the absorbance changes were recorded at 705 nm (interference filter, 10 nm bandwidth) under 5 sec of far red actinic illumination (720 nm, 1400 µmol photons · m^{-2} · s^{-1}) to preferentially excite PSI. Then, relaxation kinetics were measured in the dark for 5 sec. A 6 mm thick cut-off filter (RG695, Schott) covered the detection photodiode during measurements. The same sequence was repeated to evaluate variations in the absorbance changes recorded at 740 nm (interference filter, 10 nm bandwidth) in order to remove an unspecific contribution to the 705 nm measurement (Roberty *et al.*, 2014). Half-times of $P700^+$ re-reduction were extracted from the resulting kinetics and PSI electron turnover rate

was calculated as K = 0.693 / half-time of $P700^+$ re-reduction in seconds. The proportion of cyclic electron around PSI during active photosynthesis was quantified according to Du *et al.* (2019) where a similar procedure for the determination of the PSI electron turnover rate was repeated but with actinic illumination at 630 nm (150 µmol photons $\cdot$ $m^{-2} \cdot s^{-1}$) to excite both PSII and PSI. This measurement was then repeated in the presence of 10 µM DCMU to block linear electron flow. The proportion of cyclic electron flow around PSI in relation to the total electron flow was obtained by dividing the PSI turnover rate in the presence of DCMU (cyclic electron flow only) by the PSI turnover rate without DCMU (linear + cyclic electron flow) and expressed as a percentage.

1.4.5 Antioxidant enzyme activities

To assess intrinsic activities of antioxidant enzymes (catalase and superoxide dismutase), cells were first collected by filtration (Polytetrafluoroethylene, Xingya Purifying Materials Factory, Shanghai, China) then resuspended in 1 ml of enzyme extraction buffer. Then, the resuspended cells were broken by means of repeated cycles of flash-freezing in liquid nitrogen followed by thawing in a 20°C circulating water bath. Samples were centrifuged (25 min, 25 000 × G, 4°C) and the supernatants were separated into aliquots destined to total protein content determination and assessment of catalase and superoxide dismutase activity following the methods described in Bradford (1976), Aebi (1984) and Beyer Jr and Fridovich (1987), respectively.

1.4.6 Intracellular microcystin concentrations

To evaluate the total intracellular MC content, cells were collected by gentle filtration (Polytetrafluoroethylene, Xingya Purifying Materials Factory, Shanghai, China) and stored at -80°C until needed. The extraction process involved fully covering filters with 5 ml of MeOH/H_2O at 90/10 (*v*/*v*) followed by 20 min of sonication. This step was repeated a second time and both supernatant were combined. Subsequently, the extracts were evaporated under gentle nitrogen gas flow and the dried extracts were reconstituted in HPLC-grade water. Total intracellular MC content determination was performed using on-line solid-phase extraction connected to ultra-high-performance liquid chromatography paired with tandem mass spectrometry (on-line SPE-UHPLC-MS/MS) in positive ion mode (Munoz *et al.*, 2017, Skafi *et al.*, 2021, Zhang *et al.*, 2020).

Results were presented as total femtograms of MCs per cell normalized to the biovolume (fg MC · μm^{-3}).

1.4.7 Statistical analysis

Data distribution was tested for normality using Shapiro-wilk test and heteroscedasticity was assessed using Brown-Forsythe test. Data was transformed when distribution was found to deviate from normality or if variance was unequal between groups. When data transformation failed to produce a normal distribution or homoscedasticity between groups, data was rank-transformed and the Kruskal-Wallis test was employed to test for significant differences. Between each strain, significant differences in physiological parameters were evaluated using a one-way analysis of variance (ANOVA) and differences between groups was assessed using Tukey HSD post hoc analysis. Between wild MC+ and MC- strains, differences in the averaged means for all physiological parameters were assessed using Student's t-test or Kruskal-Wallis test. Between the wild MC+ strain and its mutant MC- counterpart, the differences in the means of each physiological parameter were compared using Student's t-test. Principal Component Analysis (PCA) and data visualization were performed using the *FactoMineR* and *factoextra* (based on *ggplot2*) R packages, respectively, using the R statistical software (R Core Team, 2020). Prior to the PCA analysis, Min – Max normalization was performed as (Value – Min/Max – Min) for all parameters.

1.5 Results

1.5.1 Growth and morphology

Growth rate, cell biovolume and intracellular complexity (SSC) of all seven studied strains of *M. aeruginosa* and the average of wild type strains are shown in Table 1.1. The growth rate differed between all strains with CPCC 300 having the highest growth rate and CPCC 299 the lowest (Table 1.1). Moreover, the average growth rate was not different between WT MC+ and WT MC- strains and between PCC 7806 and PCC 7806 *mcy*B^- (Table 1.1). The cell biovolume was variable among strains with CPCC 299 having the largest biovolume and CPCC 300 the lowest (Table 1.1). The average cell biovolume was not different between WT MC+ and WT MC- and between PCC

7806 and PCC 7806 *mcy*B$^-$ (Table 1.1). A very large diversity in intracellular complexity was observed between all strains with CPCC 299 having the highest SSC and CPCC 300 the lowest (Table 1.1). SSC was not different between the average of WT MC+ and WT MC- but was significantly higher for PCC 7806 *mcy*B$^-$ when compared to PCC 7806 (Table 1.1).

Table 1.1 Presence of intracellular microcystins, growth, cell biovolume and intracellular complexity of *M. aeruginosa* CPCC 632, 633, 124, 299, 300, PCC 7806 and 7806 *mcy*B$^-$ along with the average of WT MC+ and WT MC- strains

Strain	Presence of MCs	Growth (μ days^{-1})	Biovolume (μm^3)	Intracellular complexity (SSC)
CPCC 632	No	0.385^{b} (0.012)	$17.8^{d,e}$ (0.8)	$59\ 310^{e}$ (3573)
CPCC 633	No	0.385^{b} (0.005)	31.8^{c} (1.0)	$220\ 771^{c}$ (13 330)
CPCC 124	No	$0.376^{b,c}$ (0.017)	36.9^{b} (1.8)	$346\ 991^{b}$ (29 116)
CPCC 299	Yes	0.315^{d} (0.014)	53.8^{a} (3.8)	$559\ 738^{a}$ (32 034)
CPCC 300	Yes	0.446^{a} (0.018)	14.9^{e} (0.7)	$28\ 827^{e}$ (2 210)
PCC 7806	Yes	0.353^{c} (0.030)	18.3^{d} (1.1)	$110\ 909^{d}$ (4 879)
PCC 7806 *mcy*B$^-$	No	$0.379^{b,c}$ (0.010)	19.4^{d} (0.7)	$228\ 116^{c}$ (12 118)
Average WT MC+	Yes	0.371^{a} (0.058)	29.0^{a} (17.6)	$233\ 158^{a}$ (233 956)
Average WT MC-	No	0.382^{a} (0.011)	28.8^{a} (8.1)	$209\ 023^{a}$ (118 666)

Means (n = 3) are indicated with standard deviation in parentheses. Means not connected by the same letter are significantly different according to the Tukey HSD test between the separate strains and according to the Student's t or Kruskal-Wallis test between the average of wild type strains.

1.5.2 Photosynthesis-related parameters and pigment content

Maximal (ϕ_M) and operational (ϕ'_M) quantum yields of PSII for all seven strains of *M. aeruginosa* and the average of WT MC+ and WT MC- strains are shown in Figure 1.1. CPCC 632, CPCC 300 and CPCC 124 exhibited a comparable ϕ_M that was significantly higher than the other four strains (having similar ϕ_M values among them) (Figure 1.1A). The average ϕ_M was not different between

WT MC+ and WT MC- (Figure 1.1B). The ϕ'_M was variable among the studied strains with CPCC 632, CPCC 300 and PCC 7806 *mcy*B$^-$ having the highest ϕ'_M and CPCC 299 the lowest (Figure 1.1C). The average ϕ'_M was not different between WT MC+ and WT MC- (Figure 1.1D).

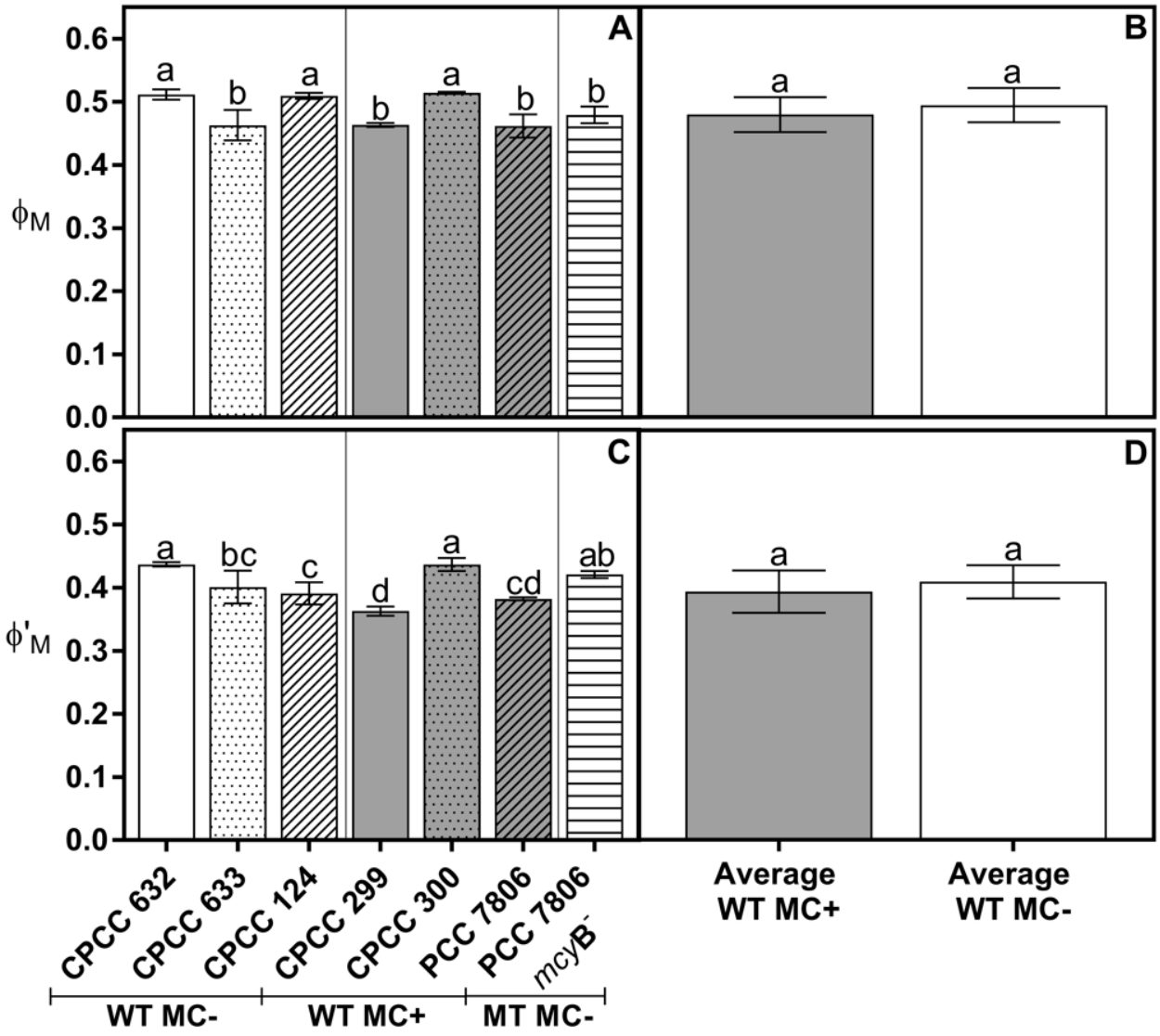

Figure 1.1 Maximal (ϕ_M) and operational (ϕ'_M) quantum yield of PSII of *M. aeruginosa* CPCC 632, 633, 124, 299, 300, PCC 7806 and 7806 *mcy*B$^-$ (**A**-**C**) and the average of WT MC+ and WT MC- (**B**-**D**). Results are presented as mean (n = 3) ± standard deviation. Means not connected by the same letter are significantly different according to the Tukey HSD test between the separate strains and according to the Student's t-test between the average of wild type strains.

Pigment content for Chl *a*, CAR, the ratio of Chl *a* and CAR, PC, APC and the ratio of PC and APC for all studied strains of *M*. *aeruginosa* and the average of WT MC+ and WT MC- strains are shown in Table 1.2. The Chl *a* content differed between all strains with CPCC 299 showing highest Chl *a* content and CPCC 124 the lowest (Table 1.2). The average Chl *a* content was not different between WT MC+ and WT MC- strains and between PCC 7806 and PCC 7806 *mcy*B$^-$ (Table 1.2). There was a wide variation in CAR content between all strains where CPCC 299 exhibited the highest CAR content and CPCC 632 the lowest. The average CAR content was significantly higher for WT MC+ strains in comparison with WT MC- strains (25%, $P < 0.01$) while PCC 7806 *mcy*B$^-$ showed a significantly higher CAR content than PCC 7806 (20%, $P < 0.05$) (Table 1.2). Chl *a*/CAR was variable among the studied strains with PCC 7806 exhibiting the highest Chl *a*/CAR and CPCC 300 the lowest (Table 1.2). The average Chl *a*/CAR was comparable between WT MC+ and WT MC- strains while PCC 7806 showed a significantly higher Chl *a*/CAR than PCC 7806 *mcy*B$^-$ (20%, $P < 0.05$) (Table 1.2). There was a wide discrepancy in PC content between strains with CPCC 633 having the highest PC content and CPCC 124 the lowest (Table 1.2). The average PC content was comparable between WT MC+ and WT MC- strains and between PCC 7806 and PCC 7806 *mcy*B$^-$ (Table 1.2). The APC content followed a similar trend as the PC content between all strains. CPCC 632 showed the highest APC content and CPCC 124 the lowest (Table 1.2). The average APC content was comparable between WT MC+ and WT MC- strains and between PCC 7806 and PCC 7806 *mcy*B$^-$ (Table 1.2). The PC/Chl *a* differed among the studied strains with CPCC 633 and CPCC 632 having the highest PC/Chl *a* and CPCC 124 the lowest (Table 1.2). The average PC/Chl *a* was comparable between WT MC+ and WT MC- strains and between PCC 7806 and PCC 7806 *mcy*B$^-$ (Table 1.2).

Table 1.2 Chlorophyll *a*, carotenoids, ratio of Chl *a* by CAR, phycocyanin, allophycocyanin and the ratio of phycocyanin and allophycocyanin content of *M. aeruginosa* CPCC 632, 633, 124, 299, 300, PCC 7806 and 7806 *mcy*B$^-$ along with the average of WT MC+ and WT MC- strains

Strain	Presence of MCs	Chl *a*	CAR	Chl *a*/CAR	PC	APC	PC/Chl *a*
CPCC 632	No	2.63^{ab} (0.36)	0.87^{e} (0.11)	3.03^{a} (0.19)	27.85^{a} (1.45)	5.79^{a} (0.39)	10.71^{a} (1.40)
CPCC 633	No	2.64^{a,b} (0.23)	0.99^{c,d} (0.02)	2.66^{b} (0.18)	28.66^{a} (1.15)	4.48^{b} (0.43)	10.90^{a} (0.71)
CPCC 124	No	2.15^{b} (0.10)	0.82^{e} (0.04)	2.62^{b} (0.06)	6.31^{e} (0.23)	0.76^{e} (0.35)	2.94^{d} (0.19)
CPCC 299	Yes	2.99^{a} (0.35)	1.28^{a} (0.04)	2.33^{c,d} (0.20)	9.31^{d} (0.55)	2.59^{d} (0.68)	3.13^{d} (0.20)
CPCC 300	Yes	2.51^{a,b} (0.30)	1.15^{b} (0.07)	2.18^{d} (0.13)	18.97^{b} (1.77)	3.11^{cd} (0.59)	7.67^{b} (1.51)
PCC 7806	Yes	2.84^{a} (0.30)	0.91^{d,e} (0.06)	3.11^{a} (0.17)	11.91^{c} (1.68)	3.40^{c,d} (0.43)	4.20^{c} (0.36)
PCC 7806 *mcy*B$^-$	No	2.87^{a} (0.35)	1.10^{b,c} (0.10)	2.60^{b,c} (0.09)	14.01^{c} (1.46)	3.66^{b,c} (0.47)	4.95^{c} (0.91)
Average WT MC+	Yes	2.78^{a} (0.33)	1.11^{a} (0.16)	2.54^{a} (0.43)	13.4^{a} (4.25)	3.03^{a} (0.58)	5.00^{a} (2.07)
Average WT MC-	No	2.47^{a} (0.31)	0.89^{b} (0.10)	2.77^{a} (0.23)	20.94^{a} (10.39)	3.68^{a} (2.15)	8.18^{a} (3.78)

Pigment concentrations are presented in femtograms of pigments per cell normalized by the cell biovolume (fg pigment · μm^{-3}). Means (n = 3) are indicated with standard deviation in parentheses. Means not connected by the same letter are significantly different according to the Tukey HSD test between separate strains and according to the Student's t-test between the average of wild type strains.

The relative energy dissipation pathways for all seven studied strains of *M. aeruginosa* and the average between WT MC+ and WT MC- are shown in Figure 1.2. The relative photochemical quenching (qP_{REL}) was variable among studied strains with PCC 7806 *mcy*B$^-$ exhibiting the highest qP_{REL} and CPCC 124 the lowest (Figure 1.2A). The average qP_{REL} was comparable between WT MC+ and WT MC- strains (Figure 1.2B) while PCC 7806 *mcy*B$^-$ was significantly higher than PCC 7806 (15%, $P < 0.05$) (Figure 1.2A). The non-photochemical quenching (qN_{REL}) also differed among the studied strains with PCC 7806 having the highest qN_{REL} and CPCC 633 the lowest (Figure 1.2C). The average qN_{REL} was comparable between WT MC+ and WT MC- strains (Figure 1.2D) while this parameter was nearly twice as high for PCC 7806 in comparison with PCC 7806 *mcy*B$^-$ (94%,

P < 0.001) (Figure 1.2C). The relative unquenched fluorescence (UQF_{REL}) was variable among the studied strains with CPCC 299 showing the highest UQF_{REL} and PCC 7806 the lowest (Figure 1.2E). The average UQF_{REL} was comparable between WT MC+ and WT MC- strains (Figure 1.2F) while this parameter was significantly higher for PCC 7806 *mcy*B$^-$ when compared to PCC 7806 (156%, P < 0.05) (Figure 1.2E).

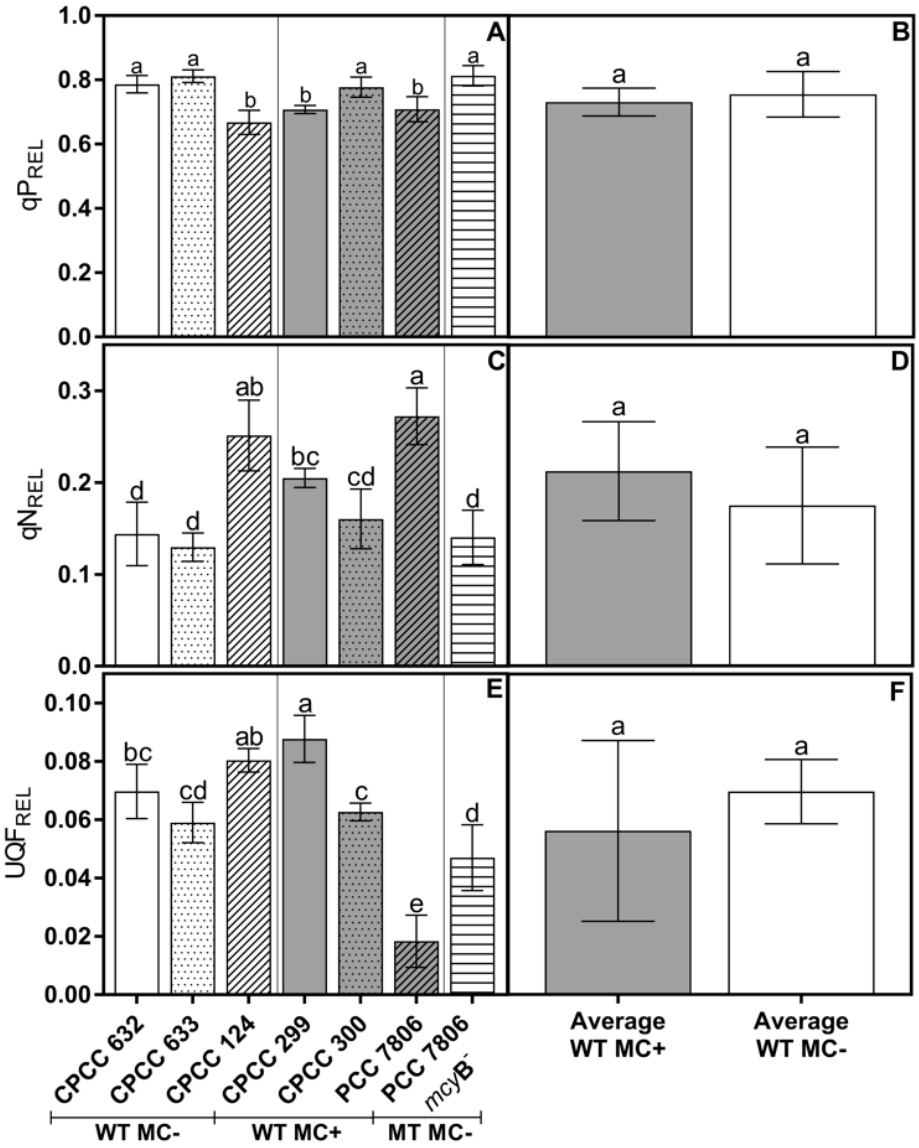

Figure 1.2 Relative photochemical quenching (qP_{REL}), non-photochemical quenching (qN_{REL}), unquenched fluorescence (UQF_{REL}). *M. aeruginosa* CPCC 632, 633, 124, 299, 300, PCC 7806 and 7806 *mcy*B$^-$ (**A**-**C**-**E**) and the average of WT MC+ and WT MC- strains (**B**-**D**-**F**). Results are presented as mean (*n* = 3) ± standard deviation. Means not connected by the same letter are significantly different according to the Tukey HSD test between the separate strains and according to the Student's t-test between the average of wild type strains.

The parameters calculated from the rapid polyphasic fluorescence induction kinetics of chlorophyll *a* (normalized O-J-I-P curve) for all studied strains of *M. aeruginosa* and the average of WT MC+ and WT MC- are shown in Table 1.3. ABS/RC differed among the studied strains with CPCC 299 having higher ABS/RC and PCC 7806 the lowest (Table 1.3). The average ABS/RC was comparable between WT MC+ and WT MC- and between PCC 7806 and PCC 7806 *mcy*B$^-$ (Table 1.3). TR_0/RC was also variable among the studied strains with CPCC 632 exhibiting the highest TR_0/RC and PCC 7806 the lowest (Table 1.3). The average TR_0/RC was comparable between WT MC+ and WT MC- and was significantly lower for PCC 7806 when compared to PCC 7806 *mcy*B$^-$ (5%, $P < 0.01$) (Table 1.3). Similarly, ET_0/RC differed between the studied strains with CPCC 633 showing the highest ET_0/RC and CPCC 124 the lowest (Table 1.3). The average ET_0/RC was comparable between WT MC+ and WT MC- and between PCC 7806 and PCC 7806 *mcy*B$^-$ (Table 1.3). DI_0/RC was dissimilar among studied strains with CPCC 299 having the highest DI_0/RC and CPCC 632 the lowest (Table 1.3). The average DI_0/RC was comparable between WT MC+ and WT MC- and between PCC 7806 and PCC 7806 *mcy*B$^-$ (Table 1.3). ET_0/TR_0 was variable among the studied strains with CPCC 633 having the highest ET_0/TR_0 and CPCC 124 the lowest (Table 1.3). The average ET_0/TR_0 was comparable between WT MC+ and WT MC- and between PCC 7806 and PCC 7806 *mcy*B$^-$ (Table 1.3). AOC_{OJIP}/F_M also differed between studied strains with PCC 7806 showing the highest AOC_{OJIP}/F_M and CPCC 124 the lowest (Table 1.3). The average AOC_{OJIP}/F_M was significantly higher for WT MC+ in comparison with WT MC- (46%, $P < 0.05$) and for PCC 7806 in comparison with PCC 7806 *mcy*B$^-$ (50%, $P < 0.05$) (Table 1.3).

Table 1.3 PSII energy fluxes, probability of electrons going past Q_A^- (ET_0/TR_0) and normalized area over O-J-I-P curve (AOC_{OJIP}/F_M) of *M. aeruginosa* CPCC 632, 633, 124, 299, 300, PCC 7806 and 7806 *mcy*B$^-$ along with the average of WT MC+ and WT MC- strains

Strain	Presence of MCs	ABS/RC	TR_0/RC	ET_0/RC	DI_0/RC	ET_0/TR_0	AOC_{OJIP}/F_M
CPCC 632	No	7.30^{d} (0.52)	3.51^{a} (0.05)	1.65^{b} (0.06)	3.78^{d} (0.47)	0.47^{b} (0.01)	7.22E-05^{b} (7.31E-06)
CPCC 633	No	10.4^{b} (0.19)	3.39^{b,c} (0.05)	1.77^{a} (0.05)	7.02^{b} (0.16)	0.52^{a} (0.01)	4.65E-05^{c} (9.18E-07)
CPCC 124	No	8.87^{c} (0.05)	3.46^{a,b} (0.05)	1.38^{d} (0.06)	5.41^{c} (0.05)	0.40^{d} (0.01)	4.22E-05^{c} (5.14E-06)
CPCC 299	Yes	11.6^{a} (0.07)	3.46^{a,b} (0.02)	1.73^{a,b} (0.04)	8.17^{a} (0.08)	0.50^{a} (0.01)	4.85E-05^{c} (1.31E-06)
CPCC 300	Yes	8.79^{c} (0.24)	3.45^{a,b} (0.09)	1.49^{c} (0.09)	5.34^{c} (0.15)	0.43^{c} (0.02)	7.11E-05^{b} (1.72E-06)
PCC 7806	Yes	7.21^{d} (0.62)	3.16^{d} (0.06)	1.45^{c,d} (0.04)	4.05^{d} (0.58)	0.46^{b} (0.01)	1.15E-04^{a} (1.78E-05)
PCC 7806 *mcy*B$^-$	No	7.65^{d} (0.24)	3.35^{c} (0.02)	1.50^{c} (0.07)	4.31^{d} (0.27)	0.45^{b,c} (0.02)	7.71E-05^{b} (9.26E-07)
Average WT MC+	Yes	9.21^{a} (1.85)	3.36^{a} (0.15)	1.56^{a} (0.13)	5.85^{a} (1.74)	0.46^{a} (0.03)	7.83E-05^{a} (2.90E-05)
Average WT MC-	No	8.86^{a} (1.30)	3.45^{a} (0.07)	1.60^{a} (0.17)	5.41^{a} (1.34)	0.46^{a} (0.05)	5.36E-05^{b} (1.39E-05)

Means (n = 3) are indicated with standard deviation in parentheses. Mean not connected by the same letter are significantly different according to the Tukey HSD test between the separate strains and according to the Student's t-test between the average of wild type strains.

The normalized $P700^+$ re-reduction kinetics and PSI electron turnover rates for the seven studied strains of *M. aeruginosa* and the average of WT MC+ and WT MC- are shown in Figure 1.3. The PSI electron turnover rate differed between the studied strains with CPCC 124 showing the highest PSI electron turnover rate and CPCC 633 the lowest (Figure 1.3A). The PSI electron turnover rate was comparable between WT MC+ and WT MC- (Figure 1.3B) while PCC 7806 *mcy*B$^-$ exhibited a significantly lower PSI turnover rate than PCC 7806 (12%, $P < 0.05$, Figure 1.3A). The proportion of cyclic electron flow around PSI for all studied strains of *M. aeruginosa* and the average of WT MC+ and WT MC- are shown in Figure 1.4. The proportion of cyclic electron flow around PSI was variable among the studied strains with CPCC 299 showing the highest value and PCC 7806 the lowest (Figure 1.4A). The cyclic electron flow around PSI was comparable between

WT MC+ and WT MC- (Figure 1.4B) and PCC 7806 *mcy*B$^-$ exhibited a significantly higher cyclic electron flow around PSI turnover rate than PCC 7806 (73%, $P < 0.01$, Figure 1.4A).

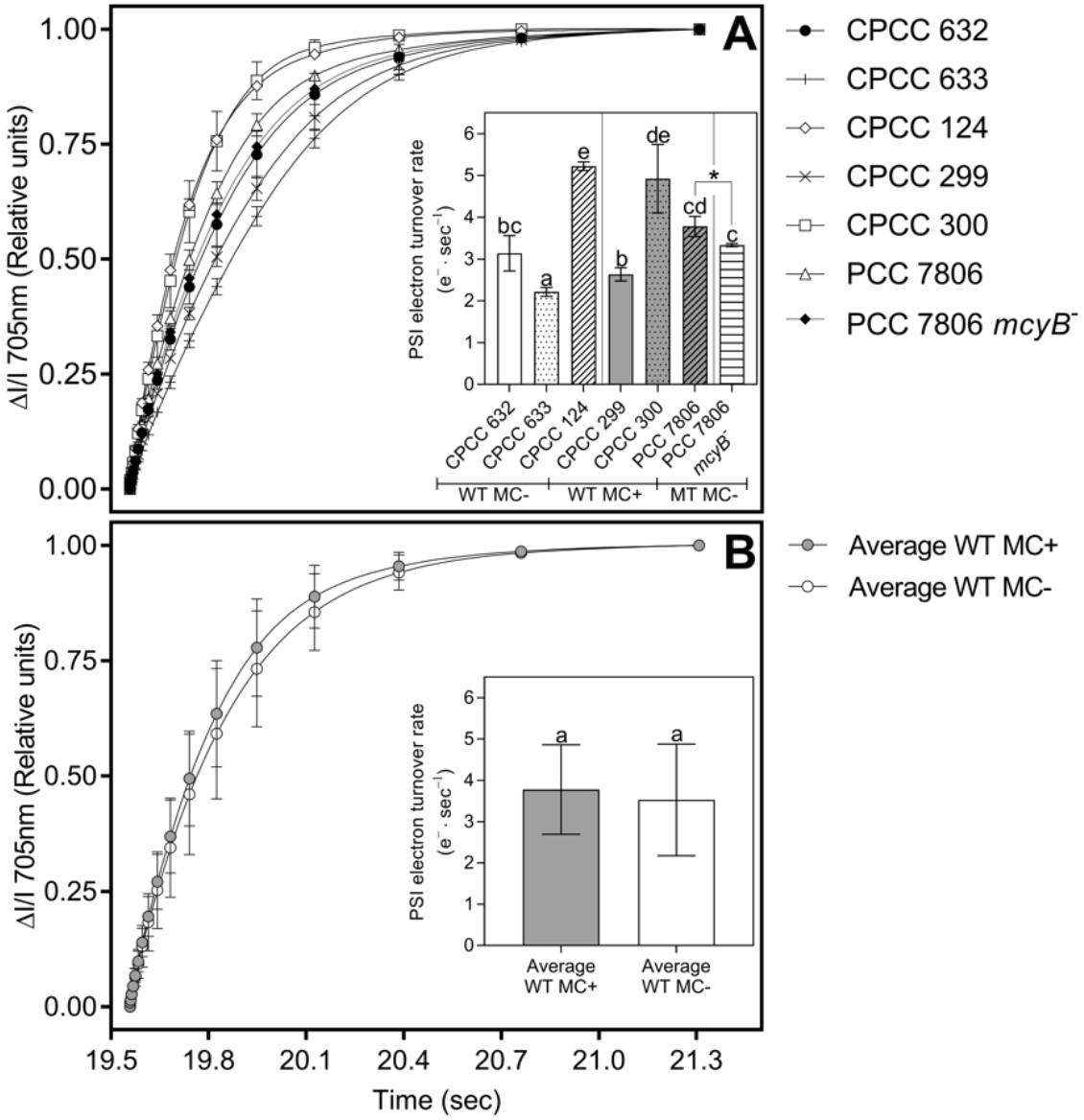

Figure 1.3 Normalized $P700^+$ re-reduction kinetics and PSI turnover rate ($e^- \cdot sec^{-1}$) of *M. aeruginosa* CPCC 632, 633, 124, 299, 300, PCC 7806 and 7806 *mcy*B$^-$ (**A**) and the average of WT MC+ and WT MC- (**B**). $P700^+$ relaxation kinetics was normalized to the minimum and maximum change in variation of signal intensity before and 1.8 sec after closing actinic illumination and PSI turnover rates are expressed as means (n = 3) ± standard deviation. Means not connected by the same letter are significantly different according to the Tukey HSD test between the separate strains and according to the Student's t-test between the average of wild type strains. An asterisk also denotes a statistically significant difference between PCC 7806 and PCC 7806 *mcy*B$^-$ according to the Student's t-test.

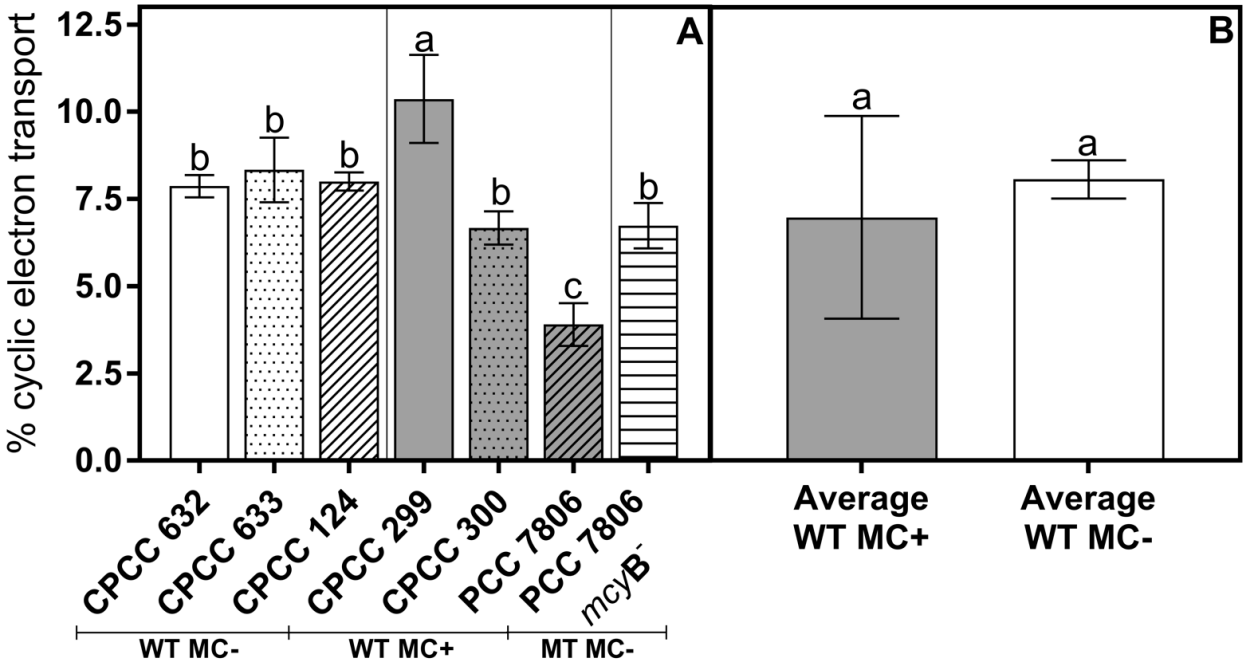

Figure 1.4 Cyclic electron flow around PSI of *M. aeruginosa* CPCC 632, 633, 124, 299, 300, PCC 7806 and 7806 *mcy*B$^-$ (**A**) and the average of WT MC+ and WT MC- (**B**). Means (n = 3) not connected by the same letter are significantly different according to the Tukey HSD test between the separate strains and according to the Student's t-test between the average of wild type strains.

1.5.3 Antioxidant enzymes activity

Catalase and superoxide dismutase activity for all seven studied strains of *M. aeruginosa* and the average of WT MC+ and WT MC- strains are shown in Figure 1.5. The catalase activity was variable among the studied strains with CPCC 632 having the highest activity and PCC 7806 the lowest (Figure 1.5A). The average CAT activity was significantly higher for WT MC- in comparison with WT MC+ (58%, $P < 0.05$, Figure 1.5B) and for PCC 7806 *mcy*B$^-$ in comparison with PCC 7806 (37%, $P < 0.01$, Figure 1.5A). Superoxide dismutase activity was variable between studied strains with CPCC 300 showing the highest SOD activity and CPCC 299 the lowest (Figure 1.5C). The average SOD activity was comparable between WT MC+ and WT MC- (Figure 1.5D) and between PCC 7806 and PCC 7806 *mcy*B$^-$ (Figure 1.5A).

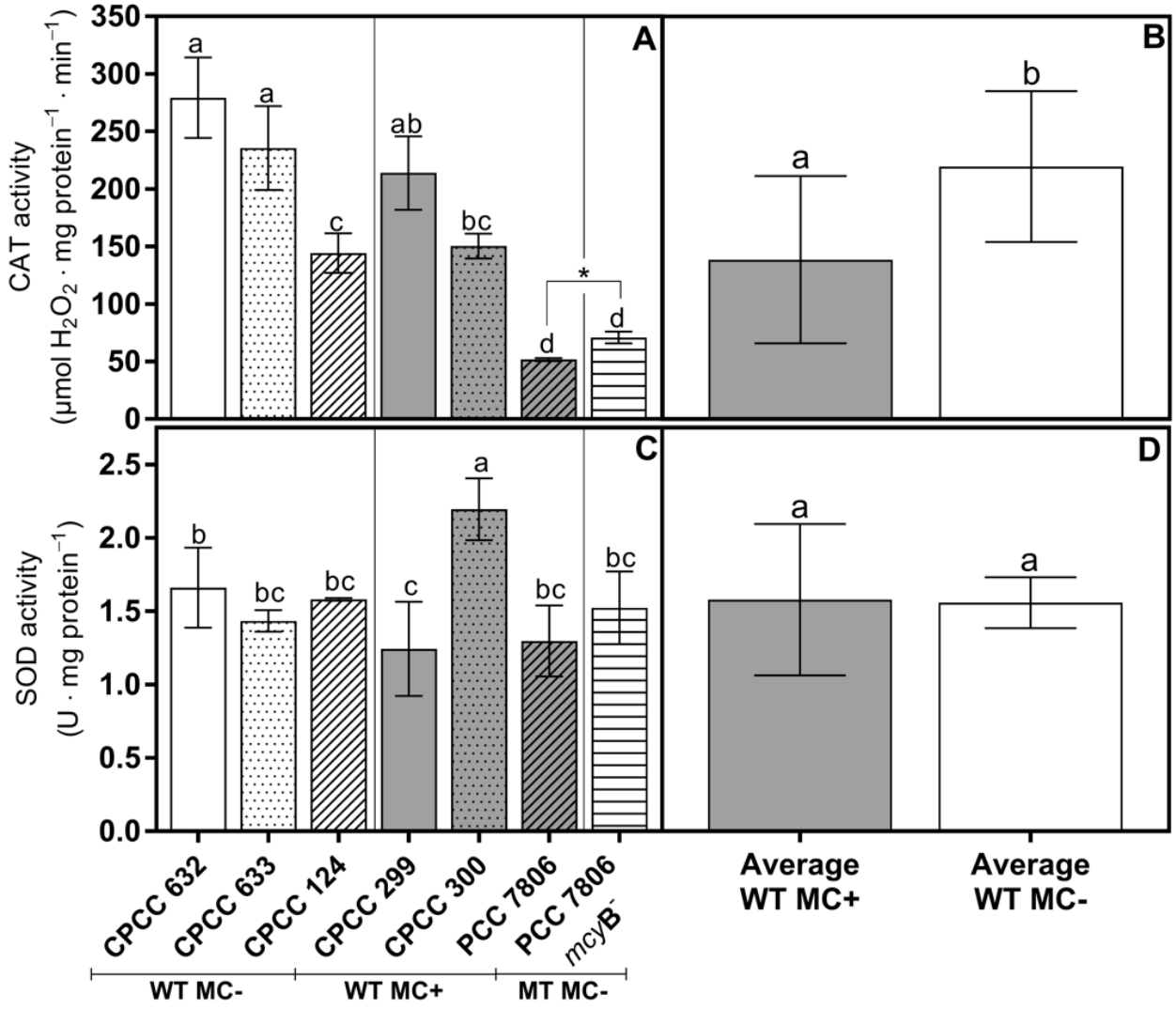

Figure 1.5 Catalase and superoxide dismutase activity of *M. aeruginosa* CPCC 632, 633, 124, 299, 300, PCC 7806 and 7806 *mcy*B$^-$ (**A**-**C**) and the average of WT MC+ and WT MC- (**B**-**D**). Results are presented as mean (n = 3) ± standard deviation. Mean not connected by the same letter are significantly different according to the Tukey HSD test between the separate strains and according to the Student's t-test between the average of wild type strains. An asterisk also denotes a statistically significant difference between PCC 7806 and PCC 7806 *mcy*B$^-$ according to the Student's t-test.

1.5.4 Total MC content normalized to biovolume and relationships with physiology

For all strains, total MC content normalized to biovolume are shown in Figure 1.6. Total MC content normalized to biovolume was significantly higher for CPCC 300 (1.76 ± 0.06 fg · µm^{-3}) than other MC+ strains, while CPCC 299 had the lowest (1.01 ± 0.02 fg · µm^{-3}) (Figure 1.6). For CPCC 632, CPCC 633, CPCC 124 and PCC 7806 *mcy*B$^-$, MC production was confirmed to be absent

(Figure 1.6). We performed a Principal Component Analysis (PCA) to identify patterns in the data, to reduce dimentionality of the dataset and to relate the total MC content normalized to biovolume with every measured physiological parameters for only MC+ strains (Figure 1.7). Two principal components together explained 87.5% of variance (scree plot, Figure S1.1). Variables were mostly explained by PC1 (51.7%) and PC2 (35.8%). Total MC content equally coincided with PC1 and PC2 and was strongly related to growth, ϕ_M, ϕ'_M, qP_{REL}, PC, PC/Chl *a*, SOD activity and PSI electron turnover on both PC1 and PC2. Total MC content was also strongly related to TR_0/ABS and AOC_{OJIP}/F_M, moderately to APC and weakly to Chl *a*/CAR and qN_{REL} on PC1. Total MC content was also strongly inversely related to biovolume, SSC, ET_0/TR_0, ET_0/RC, ABS/RC, DI_0/RC, the proportion of cyclic electron transport, CAR, CAT and UQF_{REL} and moderately inversely related to ETR_{max}, TR_0/RC and Chl *a* on PC1. On PC2, total MC content was also strongly related to ETR_{max}, TR_0/RC, UQF_{REL}, the proportion of cyclic electron transport, CAR and CAT, moderately to ABS/RC and DI_0/RC and weakly to ET_0/RC. Furthermore, total MC content was strongly inversely related to qN_{REL}, Chl *a*/CAR and AOC_{OJIP}/F_M and weakly inversely related to TR_0/ABS, ET_0/TR_0, APC, Chl *a*, SSC and biovolume on PC2.

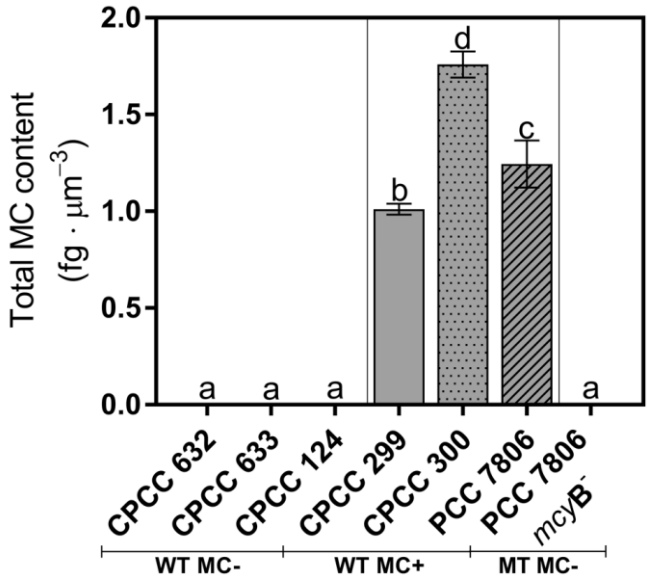

Figure 1.6 Total microcystin (MC) content per cell and normalized to biovolume (fg MC · μm^{-3}) of *M. aeruginosa* CPCC 632, 633, 124, 299, 300, PCC 7806 and 7806 *mcy*B$^-$. Results are presented as mean (*n* = 3) ± standard deviation. Mean not connected by the same letter are significantly different according to the Tukey HSD test.

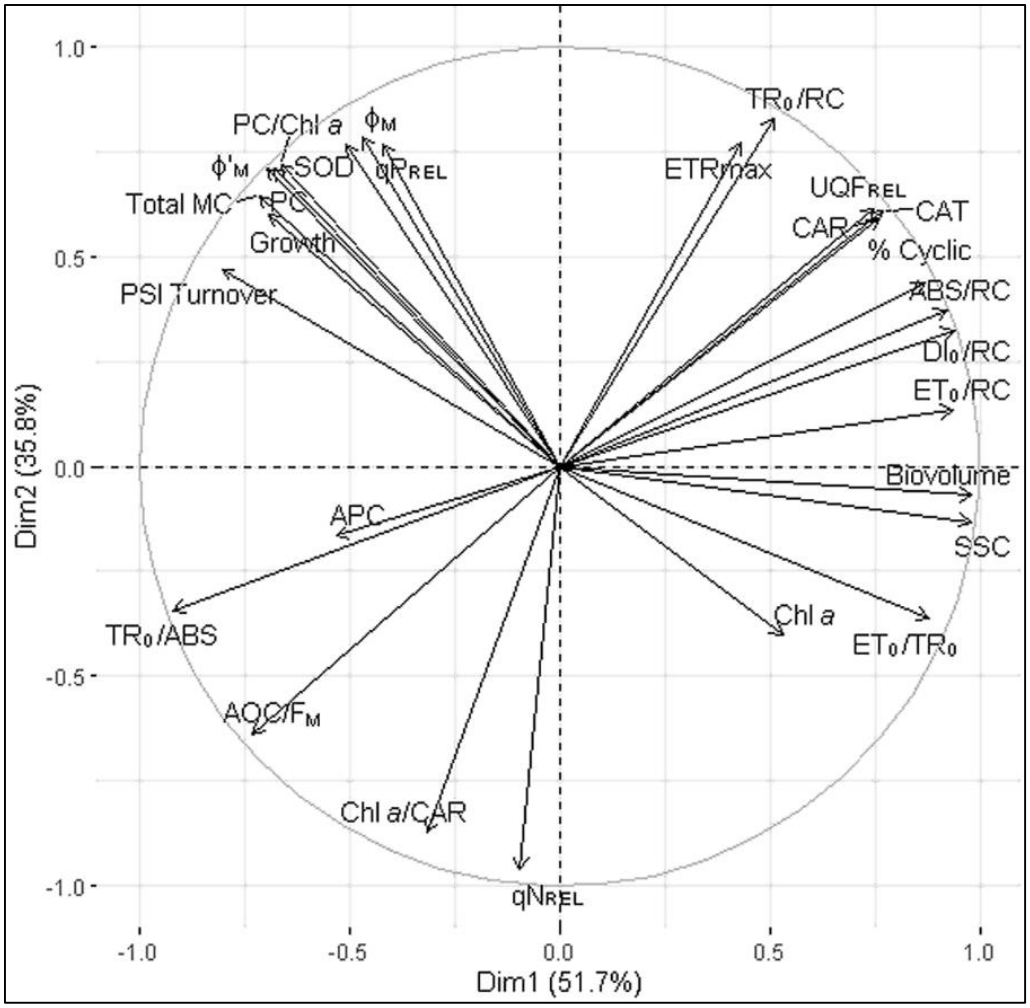

Figure 1.7 Principal Component Analysis (PCA) showing the relationships between total MC content normalized to biovolume and growth, photosynthesis, morphology and oxidative stress-related physiological parameters of three MC-producing strains of *M. aeruginosa* (CPCC 299, CPCC 300 and PCC 7806).

1.6 Discussion

In this study, we showed evidence which may allow a better understanding of the physiological role of intracellular MCs. In order to do so, we compared the interspecific physiological variation between strains which possessed or not the ability to produce MCs. Furthermore, we grouped and juxtaposed the results obtained from the average of WT MC+ and WT MC- strains with those of PCC 7806 and its MT MC- counterpart, PCC 7806 *mcy*B$^-$. This larger comparison allowed us to shed light on similarities or contrasting discrepancies in physiology which emerged from the evolutionary loss or gain of MC production as opposed to inactivation of MC production through insertional mutagenesis.

MC biosynthesis is a very energy consuming process (Briand *et al.*, 2012) and it was observed that Chl *a* and MCs can be found in a ratio of 3:1 in *M. aeruginosa* (Deblois and Juneau, 2010). Therefore, energy production should be heavily regulated to accommodate MC biosynthesis and growth-related physiological processes such as pigment production, electron transport chain component assembly and reparation, photoinhibition and the oxidative stress response according to nutrient availability, light regime and quality or other changing environmental factors. As we observed a relatively similar average growth rate between WT MC+ and WT MC- strains, this points toward a distinct restructuration of physiological processes and metabolism around growth in order to differently allocate energy in relation to the capacity to produce MCs. Among wild strains, the similar growth between MC+ and MC- strains can be explained by the general similarities seen between photosynthesis-related endpoints of both groups. Indeed, we observed comparable ϕ_M, ϕ'_M, relative energy quenching, PSII energy fluxes and PSI electron turnover rates between WT MC+ and WT MC- strains. Higher maximal fluorescence normalized area over OJIP curve for strains having the possibility to produce MC can be explained by higher CAR content which promotes better redistribution and re-emission of light energy as heat. In turn, excitation pressure would be decreased on PSII and would lead to lower fluorescence intensity at each step of the OJIP curve. Interestingly, the difference in CAR content was not significantly reflected in related photosynthetic endpoints. Generally higher fluorescence levels in the absence of DCMU but a similar shape in the OJIP for WT MC- strains in relation to WT MC+ strains could be explained by a difference in alternative electron flows such as NDH-1 mediated cyclic photophosphorylation or respiratory electron transfers (Mi *et al.*, 1992, Schuller *et al.*, 2019, Strand *et al.*, 2017) which could promote a constant slightly higher reduction in the PQ pool as these processes were found to be key to prevent over-reduction of the electron transport chain (Allahverdiyeva *et al.*, 2015, Lea-Smith *et al.*, 2013, Mullineaux, 2014a, 2014b, Schuurmans *et al.*, 2014). This corroborates with the PSI turnover rate bottlenecked to PQH_2 oxidation status as we showed that there was a trend toward a lower electron turnover around PSI for WT MC- strains in relation to WT MC+ strains. This could be, in part, due to the trend toward higher cyclic electron transport for WT MC- strains we observed during this study. As it was observed by Ma *et al.* (2010), the redox state of Q_A, which can be influenced by electron flow coming from PSII, respiratory dehydrogenases and

cyclic electron flow around PSI, is an important factor in modulating the mobility of the PBS which can affect state transition and, consequently, could affect the proportion of cyclic electron flow. Overall, comparisons between only WT MC+ and WT MC- strains revealed little to no information about the potential physiological roles of intracellular MC in relation to photosynthesis.

Between wild strains, the intrinsic activity of antioxidant enzymes CAT and SOD offered more insight on the physiological role of intracellular MCs. Indeed, CAT activity was generally higher for WT MC- strains compared to WT MC+ strains which may indicate a lesser ability for WT MC- strains to evacuate excess light energy and limit ROS production. This can be explained by the lower CAR content of WT MC- strains in relation to WT MC+ which could be counterbalanced by higher CAT activity. The similar SOD activity but higher CAT activity between wild strains could indicate higher superoxide anions production that is efficiently converted to H_2O_2 for WT MC- strains in comparison with WT MC+ strains. If H_2O_2 is more easily generated, higher CAT activity would be required to counterbalance its production (Latifi *et al.*, 2009, Tichy and Vermaas, 1999).

Absence of MC production following inactivation of the *mcy*B gene through insertional mutagenesis led to generally similar trends but significantly enhanced the slight physiological differences seen between the average of wild MC+ and MC- strains. A similar growth rate was seen between WT and MT even in the absence of the high demand in energy needed for MC production. The higher ϕ'_M for MT in relation to WT can be explained by the higher proportion of cyclic electron flow, PBS-related pigments and CAR in MT which taken together could allow for better flexibility than WT in regards to energy distribution between PSII and PSI. Moreover, inactivation of MC production decreased the capacity at which excess light energy is quenched through heat as reflected by the lower qN_{REL} parameter for MT in comparison to WT which suggests that intracellular MCs may be involved in the photoprotective response. Indeed, higher CAR content for MT following inactivation of MC production point toward a similar conclusion as carotenoids are directly involved in the photoprotective response through the association of the orange carotenoid protein (OCP) with phycobilisomes (PBS) to enhance heat dissipation (Djediat *et al.*, 2020, Kirilovsky, 2007, Kirilovsky and Kerfeld, 2012). The higher UQF_{REL} seen in MT compared to WT reflects higher fluorescence emission which is related to inefficient dissipation

of light energy via electron transport and/or through heat. In such case, energy is readily transferred to O_2 and lead to ROS production (Niyogi, 1999, 2000). Similar results were observed by Deblois and Juneau (2010) which uncovered a strong inverse relationship between UQF_{REL} and total MC content. For MT, the lack of efficient heat dissipation was unlikely to be damaging as its growth rate remained similar to WT and was most likely compensated by the reorganization of pigment content (lower Chl *a*/CAR ratio), higher ϕ'_M and through higher CAT activity. In the absence of MC production, the consequent change in pigmentation was most likely responsible for the higher trapped energy flux as CAR participate in light-harvesting and redirect light energy toward photosystems (Domonkos *et al.*, 2013, Sozer *et al.*, 2010, Zakar *et al.*, 2016). Our results corroborate those of Djediat *et al.* (2020) who employed immunogold co-localization of OCP and MCs to show that both molecules are found in close proximity from one another on the thylakoids membranes for WT MC+ strains of *Planktothrix* (PCC 7821 and PCC 10110) for control conditions indicating a possible relationship between MCs and the association of OCP and PBS. However, the authors concluded that MCs role in photoprotection was unlikely as the strains most resistant to light stress were those who did not synthesize MCs and light stress induced a decrease in MC concentration for PCC 10110 while it remained stable for PCC 7821. These observations suggest that the potential relationship between MCs, OCP and PBS is of a more complex nature.

Between wild strains, inactivation of MC production led to a lower degree of reduction of Q_A as shown by a lower normalized area over the OJIP curve (Lazár, 1999) as maximal fluorescence was higher for MT than WT. Furthermore, slower PSI electron turnover for MT compared to WT could be explained by a change in the stoichiometry in the electron transport chain within thylakoidal membranes or a change in alternative electron flow. As Chl *a* content was unchanged by the lack of MC, the change observed in the relative linear and cyclic electron flow is most likely responsible for the slower PSI electron turnover. Morphology was also clearly affected by the lack of MC production. Indeed, while biovolume remained comparable between the average of WT MC+ and WT MC- strains and between PCC 7806 and PCC 7806 *mcy*B$^-$, intracellular complexity did not follow the same trend. The intracellular complexity remained comparable between the average of WT MC+ and WT MC-, but the inactivation of MC production in MT led to a major increase in this parameter for PCC 7806 *mcy*B$^-$. Because MCs are found to be bound to photosynthetic

membranes (Djediat *et al.*, 2020, Young *et al.*, 2008, Young *et al.*, 2005), a change in intracellular complexity consequent to the inactivation of MC production could be explained by compensatory alterations in the structure of the thylakoidal membrane system. As seen by Hesse *et al.* (2001), the capacity of MC production was related to a significant difference in bio-optical properties and specific absorbance of individual pigments between PCC 7806 and PCC 7806 *mcy*B$^-$ suggesting a significant restructuration of the cell membrane system.

Total MC content showed a strong positive relationship with growth rate, ϕ_M, ϕ'_M and qP_{REL} (Figure 1.7). Similar results relating MC concentration with growth and photosynthesis were obtained by Wiedner *et al.* (2003) where growth rate and MC content showed a significant positive correlation under low light conditions. It is plausible that parameters associated with photosynthetic efficiency are positively related to the total MC content, given the positive relationship between total MC content and the growth rate and the necessary role of photosynthesis for growth. Furthermore, we observed a strong positive relationship between total MC content and PC content as well as the ratio between PC and Chl *a* which indicate that light is effectively captured, utilized and that biosynthesis of PBS-related pigments and the possible involvement of MCs becomes more and more important as the growth rate increases. This is also reflected by the inverse relationship between ET_0/TR_0 and total MC content we observed (Figure 1.7). Thus, higher MC content was shown to be related to a decrease in the probability trapped excitons will move electrons into the electron transport chain (ETC) beyond Q_A^-. Equivalent results were obtained by Wang *et al.* (2015) where comparison of the energy fluxes within PSII between three WT MC+ (FACHB 905, FACHB 912 and PCC 7806) and WT MC- (FACHB 469, FACHB 526 and PCC 7005) strains of *M. aeruginosa* showed that MC production interacted with light capture and redistribution and that WT MC- strains were more efficient at allocating light energy towards electrons transfer into the ETC than WT MC+ strains. While the close proximity of MCs and PBS were confirmed by studies such as those of Jüttner and Lüthi (2008) and Djediat *et al.* (2020), a function of intracellular MCs in relation to processes related to the PBS has yet to be directly observed. Hypothetically, MCs and PBS may be linked by a complex mechanism by which MCs interact with the binding of OCP to PBS in order to alter heat dissipation. This relationship would confer a modulatory role of MCs regarding light collection and

redistribution as well as adjustment of the evacuation of excess light energy through OCP-PBS binding thereby requiring variable CAR to PBS pigments in order to achieve efficient heat dissipation. This would explain why inactivation of MC production in MT leads to higher CAR content as no MCs consequently participate to the PBS involvement in the photoprotective response. The PCA revealed that total MC content and the CAR content were inversely related on PC1 but were positively related on PC2 (Figure 1.7). This suggests that total MC content and the CAR content are more closely related to the factors captured by PC2 and that this component may be more important for the explanation of the relationship between these two factors compared to PC1. Further research is needed to better understand the relationship between these two parameters and the driving factors but, nonetheless, these results suggest that there may be an important relationship between CAR and MCs. As such, this would-be relationship between total MC content and the photoprotective response suggests that intracellular MCs respond to a change in environmental conditions requiring the involvement of the photoprotective response rather than the opposite dynamic. Moreover, several authors observed a clear inverse relationship between total MC content and growth light intensity/high light stress (Deblois and Juneau, 2010, Liu *et al.*, 2017, Oh *et al.*, 2000, Piel *et al.*, 2020, Rapala *et al.*, 1997, Sivonen, 1990, Utkilen and Gjolme, 1992, Wiedner *et al.*, 2003) and these toxins were shown to directly respond to high light stress or addition of H_2O_2 in the growth media by binding to cysteines of various proteins (Zilliges *et al.*, 2011). It is therefore unclear whether lower MC concentration detected following growth under high light intensity or exposure to high light stress was due to either binding to intracellular components thus decreasing extraction efficiency, a decrease in MC production, cell lysis/excretion of MCs outside of the cells or a combination of these processes. Additionally, the PCA revealed that the total MC content and qN_{REL} were weakly related on PC1 but strongly inversely related on PC2 (Figure 1.7) which suggest that increasing concentrations in MCs correlates with lower requirement in non-photochemical means of energy dissipation. Overall, these results suggest that MCs may be implicated in the photoprotective response. Interestingly, there was a strong positive relationship between total MC content and the PSI electron turnover rate which could indicate that MCs play a role in the efficient function of PSI or may be promoting or enhancing electron transport throught the PSI (Figure 1.7).

However, this function is speculative and further research would be needed to confirm the relationship between MCs and PSI electron turnover rate and to identify the underlying mechanisms.

Our results highlight how physiological differences in the absence of the capacity for MC production can lead to different conclusions on the role of intracellular MC when compared to those which could be extrapolated between a WT MC+ strain and its homologous MT MC- strain in a similar comparative analysis. Inactivation of MC production through insertional mutagenesis yielded more pronounced physiological differences from the loss of the capacity to produce MCs which generally followed the same trends seen between the average of WT MC+ and WT MC- while the latter comparisons were not always significant and, in a few cases, showed a contrasting trend. This is highlighted by the significant difference we observed between WT and MT for ϕ'_M (Figure 1.1B), qP_{REL} (Figure 1.2A), qN_{REL} (Figure 1.2B), UQF_{REL} (Figure 1.2C), TR_0/RC (Table 1.3), PSI electron turnover rate (Figure 1.3A) and the proportion of cyclic electron flow around PSI (Figure 1.4) while the same comparisons were not significant between the average of WT MC+ and WT MC- strains althought they followed a similar trend. Additionally, SSC was found to be higher for PCC 7806 *mcy*B$^-$ than for PCC 7806 while this parameter trended higher for the average of WT MC+ strains in relation to the average of WT strains that did not produce MCs (Table 1.1). Similarily, the ratio of Chl *a* over CAR was higher for PCC 7806 than PCC 7806 *mcy*B$^-$ while this parameter was found to trend higher for the average of WT MC- strains in comparison with the average of WT MC+ strains (Table 1.2). Lastly, the CAR content was found to be higher for PCC7806 *mcy*B$^-$ than for PCC 7806 while this pigment was found in greater concentration in the average of wild strains containing MCs in comparison with the average of wild strains who did not contain MCs (Table 1.2).

1.7 Conclusion

Our data suggests that a comparative analysis design that includes a comparison between wild MC+ and MC- strains, as well as at least one wild MC+ strain and its corresponding non-MC-producing mutant strain, can provide a stronger range of evidence on the role of intracellular MCs in a physiological investigation. However, it is crucial to validate these results by examining strains

that have been directly isolated from the field rather than wild type strains sourced from collections of phycological culture centers as this will provide further insight into our findings. Furthermore, our results demonstrated a clear link between MC production and photoprotective mechanisms where MCs may participate in non-photochemical quenching of light energy by modulating bio-optical properties or by enhancing heat re-emission that is facilitated by the binding of OCP with PBS. As literature often shows contradictory results concerning the physiological implication of MCs in relation with photosynthesis or the oxidative stress response, we suggest that future research seeking to achieve a similar comparative analysis should increase the number of strains studied, but also include several MC-deficient mutant counterparts to broaden possible conclusions which can be extrapolated from the results.

1.8 Supplementary material

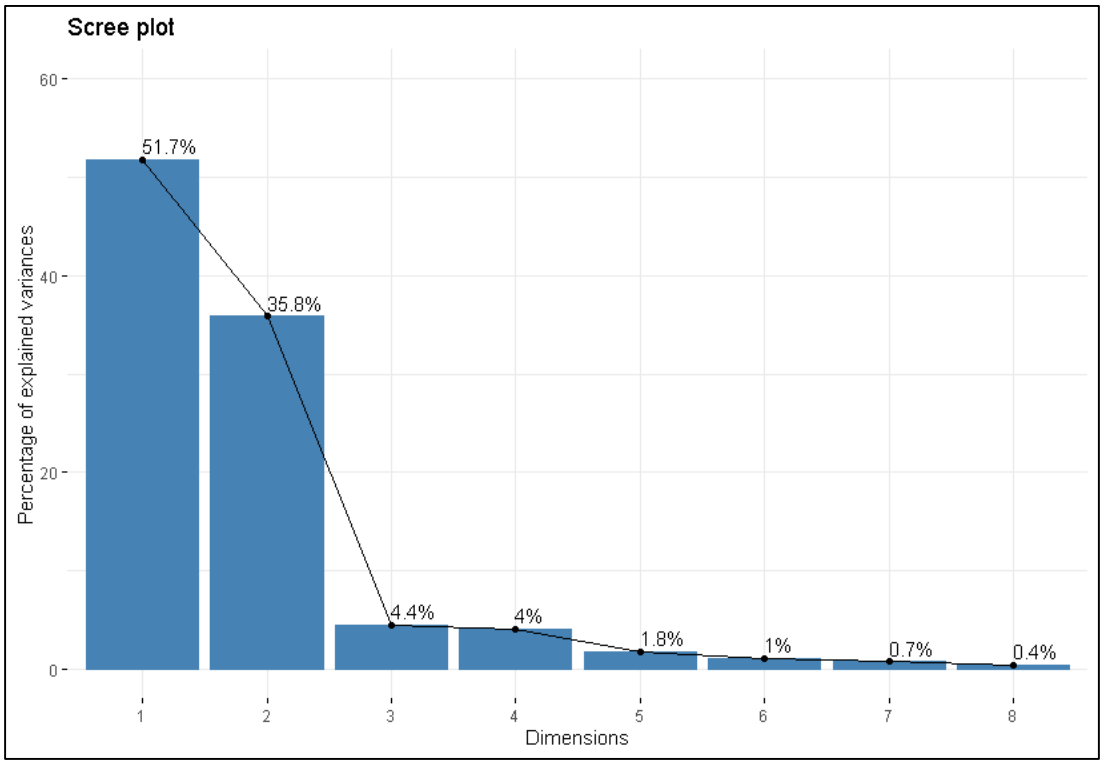

Figure S1.1 PCA scree plot, showing the eigenvalues (variances) of principal components for the physiological profile of three microcystin-producing strains of *M. aeruginosa* (CPCC 299, CPCC 300 and PCC 7806). PC1 (51.7%) and PC2 (35.8%) represented together a large proportion of the total variance.

Author Contributions: Conceptualization, J.N., and P.J.; methodology, J.N., J.D. and P.J.; validation, J.N., and P.J.; formal analysis, J.N.; investigation, J.N.; writing—original draft preparation, J.N.; writing—review and editing, J.N., J.D. and P.J.; visualization, J.N. All authors have read and agreed to the published version of the manuscript.

1.9 References

Aebi, H. (1984) Catalase in Vitro. *: Vol. 105. Methods in Enzymology* (pp. 121-126).

Allahverdiyeva, Y., Suorsa, M., Tikkanen, M. et Aro, E. M. (2015). Photoprotection of photosystems in fluctuating light intensities. *Journal of Experimental Botany*, *66*(9), 2427-2436. doi: 10.1093/jxb/eru463

Bennett, A. et Bogorad, L. (1973). Complementary chromatic adaptation in a filamentous blue-green alga. *Journal of Cell Biology*, *58*(2), 419-435. doi: 10.1083/jcb.58.2.419

Beyer Jr, W. F. et Fridovich, I. (1987). Assaying for superoxide dismutase activity: Some large consequences of minor changes in conditions. *Analytical Biochemistry*, *161*(2), 559-566. doi: 10.1016/0003-2697(87)90489-1

Bradford, M. M. (1976). A rapid and sensitive method for the quantitation of microgram quantities of protein utilizing the principle of protein-dye binding. *Analytical Biochemistry*, *72*(1-2), 248-254. doi: 10.1016/0003-2697(76)90527-3

Briand, E., Bormans, M., Quiblier, C., Salençon, M. J. et Humbert, J. F. (2012). Evidence of the cost of the production of microcystins by *Microcystis aeruginosa* under differing light and nitrate environmental conditions. *PLoS ONE*, *7*(1). doi: 10.1371/journal.pone.0029981

Buschmann, C. (1995). Variation of the quenching of chlorophyll fluorescence under different intensities of the actinic light in wildtype plants of tobacco and in an *Aurea* mutant deficient of light harvesting-complex. *Journal of Plant Physiology*, *145*(3), 245-252. doi: 10.1016/S0176-1617(11)81884-5

Campbell, D., Hurry, V., Clarke, A. K., Gustafsson, P. et Öquist, G. (1998). Chlorophyll fluorescence analysis of cyanobacterial photosynthesis and acclimation. *Microbiology and Molecular Biology Reviews*, *62*(3), 667-683. doi: 10.1128/mmbr.62.3.667-683.1998

Chorus, I., Fastner, J. et Welker, M. (2021). Cyanobacteria and cyanotoxins in a changing environment: Concepts, controversies, challenges. *Water (Switzerland)*, *13*(18). doi: 10.3390/w13182463

Deblois, C. P. et Juneau, P. (2010). Relationship between photosynthetic processes and microcystin in *Microcystis aeruginosa* grown under different photon irradiances. *Harmful Algae*, *9*(1), 18-24. doi: 10.1016/j.hal.2009.07.001

Dittmann, E., Erhard, M., Kaebernick, M., Scheler, C., Neilan, B. A., Von Döhren, H. et Börner, T. (2001). Altered expression of two light-dependent genes in a microcystin-lacking mutant of *Microcystis aeruginosa* PCC 7806. *Microbiology*, *147*(11), 3113-3119. doi: 10.1099/00221287-147-11-3113

Dittmann, E., Neilan, B. A., Erhard, M., Von Döhren, H. et Börner, T. (1997). Insertional mutagenesis of a peptide synthetase gene that is responsible for hepatotoxin production in the cyanobacterium *Microcystis aeruginosa* PCC 7806. *Molecular Microbiology*, *26*(4), 779-787.

Djediat, C., Feilke, K., Brochard, A., Caramelle, L., Kim Tiam, S., Sétif, P., Gauvrit, T., Yéprémian, C., Wilson, A., Talbot, L., Marie, B., Kirilovsky, D. et Bernard, C. (2020). Light stress in green and red Planktothrix strains: The orange carotenoid protein and its related photoprotective mechanism. *Biochimica et Biophysica Acta (BBA) - Bioenergetics*, *1861*(4), 148037. doi: 10.1016/j.bbabio.2019.06.009

Domonkos, I., Kis, M., Gombos, Z. et Ughy, B. (2013). Carotenoids, versatile components of oxygenic photosynthesis. *Progress in Lipid Research*, *52*(4), 539-561. doi: 10.1016/j.plipres.2013.07.001

Du, J., Qiu, B., Pedrosa Gomes, M., Juneau, P. et Dai, G. (2019). Influence of light intensity on cadmium uptake and toxicity in the cyanobacteria Synechocystis sp. PCC6803. *Aquatic Toxicology*, *211*, 163-172. doi: 10.1016/j.aquatox.2019.03.016

Duan, X., Zhang, C., Struewing, I., Li, X., Allen, J. et Lu, J. (2022). Cyanotoxin-encoding genes as powerful predictors of cyanotoxin production during harmful cyanobacterial blooms in an inland freshwater lake: Evaluating a novel early-warning system. *Science of The Total Environment*, *830*.

Dziallas, C. et Grossart, H. P. (2011). Increasing oxygen radicals and water temperature select for toxic *Microcystis* sp. *PLoS ONE*, *6*(9). doi: 10.1371/journal.pone.0025569

Force, L., Critchley, C. et Van Rensen, J. J. S. (2003). New fluorescence parameters for monitoring photosynthesis in plants. *Photosynthesis Research*, *78*(1), 17-33. doi: 10.1023/A:1026012116709

Genty, B., Briantais, J. M. et Baker, N. R. (1989). The relationship between the quantum yield of photosynthetic electron transport and quenching of chlorophyll fluorescence. *Biochimica et Biophysica Acta - General Subjects*, *990*(1), 87-92. doi: 10.1016/S0304-4165(89)80016-9

Giannuzzi, L. et Hernando, M. (2022). The Eco-physiological role of *Microcystis aeruginosa* in a changing world. *Microorganisms*, *10*(4). doi: 10.3390/microorganisms10040685

Hellweger, F. L., Martin, R. M., Eigemann, F., Smith, D. J., Dick, G. J. et Wilhelm, S. W. (2022). Models predict planned phosphorus load reduction will make Lake Erie more toxic. *Science*, *376*(6596), 1001-1005. doi: 10.1126/science.abm6791

Hesse, K., Dittmann, E. et Börner, T. (2001). Consequences of impaired microcystin production for light-dependent growth and pigmentation of *Microcystis aeruginosa* PCC 7806. *FEMS Microbiology Ecology*, *37*(1), 39-43. doi: 10.1016/S0168-6496(01)00142-8

IARC. (2010). Ingested nitrate and nitrite, and cyanobacterial peptide toxins. *IARC monographs on the evaluation of carcinogenic risks to humans*, *94*, v-vii, 1-412.

Joliot, P. et Joliot, A. (2002). Cyclic electron transfer in plant leaf. *Proceedings of the National Academy of Sciences of the United States of America*, *99*(15), 10209-10214. doi: 10.1073/pnas.102306999

Joliot, P. et Joliot, A. (2005). Quantification of cyclic and linear flows in plants. *Proceedings of the National Academy of Sciences of the United States of America*, *102*(13), 4913-4918. doi: 10.1073/pnas.0501268102

Juneau, P., Green, B. R. et Harrison, P. J. (2005). Simulation of Pulse-Amplitude-Modulated (PAM) fluorescence: Limitations of some PAM-parameters in studying environmental stress effects. *Photosynthetica*, *43*(1), 75-83. doi: 10.1007/s11099-005-5083-7

Jüttner, F. et Lüthi, H. (2008). Topology and enhanced toxicity of bound microcystins in *Microcystis* PCC 7806. *Toxicon*, *51*(3), 388-397. doi: 10.1016/j.toxicon.2007.10.013

Kirilovsky, D. (2007). Photoprotection in cyanobacteria: the orange carotenoid protein (OCP)-related non-photochemical-quenching mechanism. *Photosynthesis Research*, *93*(1-3), 7-16. doi: 10.1007/s11120-007-9168-y

Kirilovsky, D. et Kerfeld, C. A. (2012). The orange carotenoid protein in photoprotection of photosystem II in cyanobacteria. *BBA - Bioenergetics*, *1817*(1), 158-166. doi: 10.1016/j.bbabio.2011.04.013

Kitajima, M. et Butler, W. L. (1975). Quenching of chlorophyll fluorescence and primary photochemistry in chloroplasts by dibromothymoquinone. *BBA - Bioenergetics*, *376*(1), 105-115. doi: 10.1016/0005-2728(75)90209-1

Latifi, A., Ruiz, M. et Zhang, C. C. (2009). Oxidative stress in cyanobacteria. *FEMS Microbiology Reviews*, *33*(2), 258-278. doi: 10.1111/j.1574-6976.2008.00134.x

Latour, D., Perrière, F. et Purdie, D. (2022). Higher sensitivity to hydrogen peroxide and light stress conditions of the microcystin producer *Microcystis aeruginosa* sp PCC7806 compared to non-producer strains. *Harmful Algae*, *114*, 102219. doi: 10.1016/j.hal.2022.102219

Lazár, D. (1999). Chlorophyll a fluorescence induction. *Biochimica et Biophysica Acta - Bioenergetics*, *1412*(1), 1-28. doi: 10.1016/S0005-2728(99)00047-X

Le Manach, S. v., Sotton, B., Huet, H. l. n., Duval, C., Paris, A., Marie, A., Yépremian, C., Catherine, A., Mathéron, L. c., Vinh, J., Edery, M. et Marie, B. (2018). Physiological effects caused by microcystin-producing and non-microcystin producing *Microcystis aeruginosa* on medaka fish: A proteomic and metabolomic study on liver. *Environmental Pollution*, *234*, 523-537. doi: 10.1016/j.envpol.2017.11.011

Lea-Smith, D. J., Ross, N., Zori, M., Bendall, D. S., Dennis, J. S., Scott, S. A., Smith, A. G. et Howe, C. J. (2013). Thylakoid terminal oxidases are essential for the cyanobacterium *Synechocystis sp.* PCC 6803 to survive rapidly changing light intensities. *Plant Physiology*, *162*(1), 484-495. doi: 10.1104/pp.112.210260

Lichtenthaler, H. K. (1987) Chlorophylls and Carotenoids: Pigments of Photosynthetic Biomembranes. *: Vol. 148. Methods in Enzymology* (pp. 350-382).

Liu, H., Song, X., Guan, Y., Pan, D., Li, Y., Xu, S. et Fang, Y. (2017). Role of illumination intensity in microcystin development using *Microcystis aeruginosa* as the model algae. *Environmental Science and Pollution Research*, *24*(29), 23261-23272. doi: 10.1007/s11356-017-9888-2

Ma, W., Mi, H. et Shen, Y. (2010). Influence of the redox state of QA on phycobilisome mobility in the cyanobacterium *Synechocystis sp.* strain PCC 6803. *Journal of Luminescence*, *130*(7), 1169-1173. doi: 10.1016/j.jlumin.2010.02.015

Malanga, G., Giannuzzi, L. et Hernando, M. (2019). The possible role of microcystin (D-Leu1 MC-LR) as an antioxidant on *Microcystis aeruginosa* (Cyanophyceae). In vitro and in vivo evidence. *Comparative Biochemistry and Physiology Part - C: Toxicology and Pharmacology*, *225*, 108575. doi: 10.1016/j.cbpc.2019.108575

Massey, I. Y., Al osman, M. et Yang, F. (2022). An overview on cyanobacterial blooms and toxins production: their occurrence and influencing factors. *Toxin Reviews*, *41*(1), 326-346. doi: 10.1080/15569543.2020.1843060

Massey, I. Y., Wu, P., Wei, J., Luo, J., Ding, P., Wei, H. et Yang, F. (2020). A mini-review on detection methods of microcystins. *Toxins*, *12*(10). doi: 10.3390/toxins12100641

Mi, H., Endo, T., Schreiber, U., Ogawa, T. et Asada, K. (1992). Electron donation from cyclic and respiratory flows to the photosynthetic intersystem chain is mediated by pyridine nucleotide dehydrogenase in the cyanobacterium synechocystis PCC 6803. *Plant and Cell Physiology*, *33*(8), 1233-1237.

Mucci, M., Guedes, I. A., Faassen, E. J. et Lürling, M. (2020). Chitosan as a Coagulant to Remove Cyanobacteria Can Cause Microcystin Release. *Toxins*, *12*(11). doi: 10.3390/toxins12110711

Mullineaux, C. W. (2014a). Co-existence of photosynthetic and respiratory activities in cyanobacterial thylakoid membranes. *Biochimica et Biophysica Acta - Bioenergetics*, *1837*(4), 503-511. doi: 10.1016/j.bbabio.2013.11.017

Mullineaux, C. W. (2014b). Electron transport and light-harvesting switches in cyanobacteria. *Frontiers in Plant Science*, *5*(JAN), 7. doi: 10.3389/fpls.2014.00007

Munoz, G., Vo Duy, S., Roy-Lachapelle, A., Husk, B. et Sauvé, S. (2017). Analysis of individual and total microcystins in surface water by on-line preconcentration and desalting coupled to liquid chromatography tandem mass spectrometry. *Journal of Chromatography A*, *1516*, 9-20. doi: 10.1016/j.chroma.2017.07.096

Niyogi, K. K. (1999) Photoprotection revisited: Genetic and molecular approaches. *: Vol. 50. Annual Review of Plant Biology* (pp. 333-359).

Niyogi, K. K. (2000). Safety valves for photosynthesis. *Current Opinion in Plant Biology*, *3*(6), 455-460. doi: 10.1016/S1369-5266(00)00113-8

Oh, H. M., Lee, S. J., Jang, M. H. et Yoon, B. D. (2000). Microcystin production by *Microcystis aeruginosa* in a phosphorus-limited chemostat. *Applied and Environmental Microbiology*, *66*(1), 176-179. doi: 10.1128/AEM.66.1.176-179.2000

Omidi, A., Esterhuizen-Londt, M. et Pflugmacher, S. (2018). Still challenging: the ecological function of the cyanobacterial toxin microcystin - What we know so far. *Toxin Reviews*, *37*(2), 87-105.

Piel, T., Sandrini, G., White, E., Xu, T., Schuurmans, J. M., Huisman, J. et Visser, P. M. (2020). Suppressing Cyanobacteria with Hydrogen Peroxide Is More Effective at High Light Intensities. *Toxins*, *12*(1).

R Core Team. (2020). R: A language and environment for statistical computing. R Foundation for Statistical Computing.

Rapala, J., Sivonen, K., Lyra, C. et Niemelä, S. I. (1997). Variation of microcystins, cyanobacterial hepatotoxins, in *Anabaena spp.* as a function of growth stimuli. *Applied and Environmental Microbiology*, *63*(6), 2206-2212. doi: 10.1128/aem.63.6.2206-2212.1997

Rippka, R., Deruelles, J., Waterbury, J. B., Herdman, M. et Stanier, R. Y. (1979). Generic Assignments, Strain Histories and Properties of Pure Cultures of Cyanobacteria. *Microbiology*, *111*(1), 1-61. doi: doi:10.1099/00221287-111-1-1

Roberty, S., Bailleul, B., Berne, N., Franck, F. et Cardol, P. (2014). PSI Mehler reaction is the main alternative photosynthetic electron pathway in *Symbiodinium sp.*, symbiotic dinoflagellates of cnidarians. *New Phytologist*, *204*(1), 81-91. doi: 10.1111/nph.12903

Sandrini, G., Huisman, J. et Matthijs, H. C. P. (2015). Potassium sensitivity differs among strains of the harmful cyanobacterium *Microcystis* and correlates with the presence of salt tolerance genes. *FEMS Microbiology Letters*, *362*(16). doi: 10.1093/femsle/fnv121

Schuller, J. M., Birrell, J. A., Tanaka, H., Konuma, T., Wulfhorst, H., Cox, N., Schuller, S. K., Thiemann, J., Lubitz, W., Sétif, P., Ikegami, T., Engel, B. D., Kurisu, G. et Nowaczyk, M. M. (2019). Structural adaptations of photosynthetic complex I enable ferredoxin-dependent electron transfer. *Science*, *363*(6424), 257-260. doi: 10.1126/science.aau3613

Schuurmans, R. M., Schuurmans, J. M., Bekker, M., Kromkamp, J. C., Matthijs, H. C. P. et Hellingwerf, K. J. (2014). The redox potential of the plastoquinone pool of the cyanobacterium *Synechocystis* species strain PCC 6803 is under strict homeostatic control. *Plant Physiology*, *165*(1), 463-475. doi: 10.1104/pp.114.237313

Sivonen, K. (1990). Effects of light, temperature, nitrate, orthophosphate, and bacteria on growth of and hepatotoxin production by *Oscillatoria agardhii* strains. *Applied and Environmental Microbiology*, *56*(9), 2658-2666. doi: 10.1128/aem.56.9.2658-2666.1990

Skafi, M., Vo Duy, S., Munoz, G., Dinh, Q. T., Simon, D. F., Juneau, P. et Sauvé, S. (2021). Occurrence of microcystins, anabaenopeptins and other cyanotoxins in fish from a freshwater wildlife reserve impacted by harmful cyanobacterial blooms. *Toxicon*, *194*, 44-52. doi: 10.1016/j.toxicon.2021.02.004

Sozer, O., Komenda, J., Ughy, B., Domonkos, I., Laczk-Dobos, H., Malec, P., Gombos, Z. et Kis, M. (2010). Involvement of carotenoids in the synthesis and assembly of protein subunits of photosynthetic reaction centers of synechocystis sp. PCC 6803. *Plant and Cell Physiology*, *51*(5), 823-835. doi: 10.1093/pcp/pcq031

Spoof, L. et Arnaud, C. (ed.), (2017). Appendix 3: Tables of Microcystins and Nodularins. In J. Meriluoto, L. Spoof et G. A. Codd (dir.), *Handbook of Cyanobacterial Monitoring and Cyanotoxin Analysis* (p. 526-537). Chichester, UK : John Wiley & Sons.

Stachowski-Haberkorn, S., JérÔme, M., Rouxel, J., Khelifi, C., Rincé, M. et Burgeot, T. (2013). Multigenerational exposure of the microalga *Tetraselmis suecica* to diuron leads to spontaneous long-term strain adaptation. *Aquatic Toxicology*, *140-141*, 380-388. doi: 10.1016/j.aquatox.2013.06.016

Strand, D. D., Fisher, N. et Kramer, D. M. (2017). The higher plant plastid NAD(P)H dehydrogenase-like complex (NDH) is a high efficiency proton pump that increases ATP production by cyclic electron flow. *Journal of Biological Chemistry*, *292*(28), 11850-11860. doi: 10.1074/jbc.M116.770792

Strasser, R. J., Srivastava, A. et Tsimilli-Michael, M. (ed.), (2000). The fluorescence transient as a tool to characterize and screen photosynthetic samples. In *Probing photosynthesis: mechanisms, regulation and adaptation* (p. 445-483).

Tichy, M. et Vermaas, W. (1999). In vivo role of catalase-peroxidase in *Synechocystis sp.* strain PCC 6803. *Journal of Bacteriology*, *181*(6), 1875-1882. doi: 10.1128/jb.181.6.1875-1882.1999

Utkilen, H. et Gjolme, N. (1992). Toxin production by *Microcystis aeruginosa* as a function of light in continuous cultures and its ecological significance. *Applied and Environmental Microbiology*, *58*(4), 1321-1325. doi: 10.1128/aem.58.4.1321-1325.1992

Wang, Z., Li, D., Cao, X., Song, C. et Zhou, Y. (2015). Photosynthesis regulates succession of toxic and nontoxic strains in blooms of *Microcystis* (Cyanobacteria). *Phycologia*, *54*(6), 640-648. doi: 10.2216/15-79.1

Wiedner, C., Visser, P. M., Fastner, J., Metcalf, J. S., Codd, G. A. et Mur, L. R. (2003). Effects of light on the microcystin content of *Microcystis* strain PCC 7806. *Applied and Environmental Microbiology*, *69*(3), 1475-1481. doi: 10.1128/AEM.69.3.1475-1481.2003

Young, F. M., Morrison, L. F., James, J. et Codd, G. A. (2008). Quantification and localization of microcystins in colonies of a laboratory strain of *Microcystis* (Cyanobacteria) using immunological methods. *European Journal of Phycology*, *43*(2), 217-225. doi: 10.1080/09670260701880460

Young, F. M., Thomson, C., Metcalf, J. S., Lucocq, J. M. et Codd, G. A. (2005). Immunogold localisation of microcystins in cryosectioned cells of *Microcystis*. *Journal of Structural Biology*, *151*(2), 208-214. doi: https://doi.org/10.1016/j.jsb.2005.05.007

Zakar, T., Laczko-Dobos, H., Toth, T. N. et Gombos, Z. (2016). Carotenoids assist in cyanobacterial photosystem II assembly and function. *Frontiers in Plant Science*, *7*, 295. doi: 10.3389/fpls.2016.00295

Zhang, Y., Whalen, J. K., Vo Duy, S., Munoz, G., Husk, B. R. et Sauvé, S. (2020). Improved extraction of multiclass cyanotoxins from soil and sensitive quantification with on-line purification liquid chromatography tandem mass spectrometry. *Talanta*, *216*, 120923. doi: 10.1016/j.talanta.2020.120923

Zilliges, Y., Kehr, J. C., Meissner, S., Ishida, K., Mikkat, S., Hagemann, M., Kaplan, A., Börner, T. et Dittmann, E. (2011). The cyanobacterial hepatotoxin microcystin binds to proteins and increases the fitness of *Microcystis* under oxidative stress conditions. *PLoS ONE*, *6*(3). e17615. doi: 10.1371/journal.pone.0017615

[Cette page a été laissée intentionnellement blanche]

CHAPITRE 2

RELATIONSHIPS BETWEEN MICROCYSTINS AND THE PHYSIOLOGICAL RESPONSE TO PHOTOINHIBITION OF *MICROCYSTIS AERUGINOSA* REVEALED BY THE SINGLE AND COMBINED INFLUENCE OF HIGH LIGHT STRESS AND EXPOSURE TO ATRAZINE

Jonathan Naoum[1] and Philippe Juneau[1]

[1]Département des Sciences Biologiques, GRIL-TOXEN-EcotoQ, Ecotoxicology of Aquatic Microorganisms Laboratory, University du Québec à Montréal, Succursale Centre-ville, C.P. 8888 Montréal, Québec H3C 3P8, Canada

Will be submitted to Toxicon

[Cette page a été laissée intentionnellement blanche]

2.1 Résumé

Il existe des liens entre les processus photosynthétiques et la production de microcystines (MCs) intracellulaires. Malgré cela, il existe très peu d'information quant à l'origine de cette relation. Aussi, les souches de cyanobactéries possédant la capacité de produire les MCs répondent parfois différemment à l'influence de facteurs de stress environnementaux par rapport aux souches incapables de produire les MCs. Dans ce contexte, ce papier a pour objectif d'explorer les conséquences physiologiques d'une manipulation des processus en lien à la réponse contre la photoinhibition chez PCC 7806 et son homologue mutant incapable de produire les MCs PCC 7806 *mcy*B$^-$. Lors de cette recherche, il a été question de soumettre ces souches à diverses conditions photoinhibitrices soit à l'aide d'une exposition de 72h à 0.8 µM d'atrazine ou via une forte illumination sur une courte durée (1200 µmol photons · m^{-2} · s^{-1} sur 45 min) ainsi qu'en combinant ces traitements. Ces traitements ont permis de révéler des différences physiologiques entre ces deux souches et isoler les conséquences physiologiques de la perte de production de MCs de manière à mieux comprendre le rôle physiologique des MCs intracellulaires en liens aux processus de photoinhibition. Une plus grande diminution de la croissance en présence d'atrazine a été observée pour MT par rapport à WT, tandis que tous les paramètres liés à la photosynthèse, sauf Chl *a*, PC et qN_{REL}, ont étés plus affectés chez WT en comparaison à MT. De plus, l'atrazine a entraîné une augmentation dans la teneur en ROS et de l'activité de la SOD chez WT ainsi qu'une augmentation de la SSC et l'activité de la CAT chez MT par rapport à WT. Pour le stress lumineux, la physiologie de MT a été généralement plus sensible à ce traitement que WT, à l'exception de la Chl *a*, l'APC et la teneur en ROS. En présence d'une combinaison entre l'atrazine et le stress lumineux, la pigmentation a été différemment affectée entre les souches. Lors de ce traitement, la Chl *a*, CAR, PC et PC/Chl *a* ont étés plus affectés chez MT que chez WT, tandis que l'inverse a été observé pour Chl *a*/CAR et APC. De plus, un impact similaire des traitements combinés sur les paramètres photosynthétiques entre les souches a été observé à l'exception de qP_{REL} et du taux de transport d'électron au sein du PSI, qui ont diminué davantage chez WT que chez MT. Pour les paramètres liés au stress oxydatif, les traitements combinés ont entraîné une diminution de la teneur en ROS et de la complexité intracellulaire chez MT, tandis que l'activité de la CAT et de la SOD était plus élevée chez WT que chez MT. De manière intéressante, le taux intrinsèque de

transport d'électron au sein du PSI et la proportion de transport cyclique d'électron autour du PSI étaient presque deux fois plus élevés en l'absence de MCs intracellulaires. Une analyse en composantes principales (PCA) permettant de représenter les relations entre les différents congénères de la MC et la physiologie des cyanobactéries exposées ou non à des conditions de photoinhibition a permis de mettre en évidence une corrélation entre la présence de MCs et les processus de dissipation de l'énergie de façon non photochimique ainsi que la re-réduction du $P700^+$. En outre, certains congénères de la MC tels que MC-LY, MC-LW et MC-LF ont été plus étroitement associés aux processus de photoinhibition que les autres variantes de la MC. En somme, ces résultats suggèrent que la cyanobactérie PCC 7806 a dû dépenser plus d'énergie que la souche PCC 7806 *mcy*B^- pour faire face aux expositions individuelles ou combinées à l'atrazine et à un stress lumineux, et que plusieurs processus liés à la régulation de la photoacclimatation impliquent les MCs intracellulaires. Finalement, ces résultats indiquent un rôle potentiel des MCs dans les mécanismes de dissipation de l'énergie non photochimique et les voies alternatives de transport d'électrons, avec des différences probables entre chaque variante de la MC.

Mots-clés: Microcystines, atrazine, stress lumineux, photosynthèse, photoinhibition, dissipation non-photochimique de l'énergie, re-réduction du $P700^+$

[Cette page a été laissée intentionnellement blanche]

2.2 Abstract

There are links between photosynthetic processes and the production of intracellular microcystins (MCs). Despite this, very little is known about the origin of these relationships. Also, cyanobacterial strains with the ability to produce MCs sometimes respond differently to the influence of environmental stressors than strains unable to produce MCs. In this context, the objective of this paper was to manipulate the processes related to the response against photoinhibition in PCC 7806 and its mutant counterpart unable to produce MCs PCC 7806 *mcy*B$^-$. To this end, these strains were subjected to treatments aimed at inducing photoinhibition either using atrazine (0.8 µM for 72h) or using light stress (1200 µmol photons · m^{-2} · s^{-1} over 45 min) as well as by combining these two stress conditions. These treatments revealed differences in the photoinhibitory responses between the two strains. There was a larger decrease in growth in the presence of atrazine for MT than for WT while every photosynthesis-related parameters besides Chl *a*, PC and qN_{REL} were more affected in WT than MT. Also, atrazine led to higher ROS content and SOD activity for WT and higher CAT and SSC for MT compared to WT. For light stress, MT was generally more sensitive than WT excepted for Chl *a*, APC and the ROS content. When atrazine and light stress were combined, pigmentation was differently affected between strains with Chl *a*, CAR, PC and PC/Chl *a* being more affected for MT than WT while the opposite was seen for Chl *a*/CAR and APC. Furthermore, there was a similar impact of the combined treatments on photosynthetic parameters between strains with the exception of qP_{REL} and PSI electron turnover rate which decreased further for WT than MT. For oxidative stress-related parameters, the combined treatments led to a decrease in ROS content and intracellular complexity for MT while higher CAT and SOD activity were seen for WT compared to MT. Interestingly, the intrinsic PSI electron turnover rate and proportion of cyclic electron flow around PSI was nearly twice in the absence of intracellular MCs. PCA analysis depicting the relationships between MCs congeners and physiology with and without exposure to photoinhibitory conditions allowed us to link the presence of MCs with non-photochemical energy dissipation processes and the re-reduction of $P700^+$. In addition, MC-LY, MC-LW and MC-LF were more closely linked to photoinhibition-related processes than the other identified congeners. Overall, these results suggest that PCC 7806 had to expend a greater amount of energy than PCC 7806 mcyB$^-$ to respond to the single and

combined exposure to atrazine and high light stress and that several processes related to the regulation of photoacclimation must involve intracellular MCs. Additionally, these results points to a role of MCs in relation to NPQ mechanisms and alternative electron transport pathways which is likely to be different between each MC congeners.

Keywords: Microcystins, atrazine, high light stress, photosynthesis, photoinhibition, non-photochemical quenching, re-reduction of $P700^{+}$

[Cette page a été laissée intentionnellement blanche]

2.3 Introduction

Cyanobacteria use an extensive array of physical and biochemical defense mechanisms to cope with stress factors found in the environment (Bendall and Manasse, 1995, Ehling-Schulz and Scherer, 1999, Karapetyan, 2007, Kumar *et al.*, 2008, Müller *et al.*, 2001, Zhu *et al.*, 2010). In a species-specific manner, these mechanisms can mitigate the deleterious impact of natural or man-made sources of stress, such as light, temperature or pesticides, on the photosynthetic processes (Chalifour and Juneau, 2011, Deblois *et al.*, 2013, Deblois and Juneau, 2010, Komenda and Sobotka, 2016, Tamary *et al.*, 2012, Yu *et al.*, 2021). There is often a clear disparity between the physiological response of microcystin-producing and non-MC-producing strains of cyanobacteria. MC-producing strains frequently show greater fitness and dominance when grown in the presence of high levels of nitrogenous compounds (Chaffin *et al.*, 2018, Davis *et al.*, 2010, Suominen *et al.*, 2017) or in different stressful growth conditions such as high light intensity (Chaffin *et al.*, 2018, Deblois and Juneau, 2012, Islam and Beardall, 2017), UV-B irradiation (Yang *et al.*, 2015), increased in water temperature (Davis *et al.*, 2009) or in the presence of chemical contaminants (Perron and Juneau, 2011). The same phenomenon is seen when non-MC-producing mutant strains of toxigenic cyanobacteria are compared to its MC-producing counterpart in similar stress-inducing conditions (Feng *et al.*, 2019, Jähnichen *et al.*, 2007) (Makower *et al.*, 2015, Phelan and Downing, 2011, Zilliges *et al.*, 2011). While the list of identified MC variants keeps growing (Spoof and Arnaud, 2017), their relationship to cyanobacterial physiological processes is poorly understood and a consensus on the main physiological role of intracellular MCs has not yet been reached (Omidi *et al.*, 2018). Nonetheless, an extensive list of studies link the toxic response of bloom-forming cyanobacteria to ecological and anthropogenic pressure, connection often characterized or accompanied by a change in MCs profile (Liu *et al.*, 2016, Tonk *et al.*, 2005) and production (Ceballos-Laita *et al.*, 2015, Du *et al.*, 2017, Liu *et al.*, 2016, Qian *et al.*, 2010, Wiedner *et al.*, 2003, Zhang *et al.*, 2017), photosynthetic efficiency (Chalifour and Juneau, 2011, Deblois *et al.*, 2013), carbon concentration mechanisms (Jähnichen *et al.*, 2007) and ability to withstand oxidative stress (Schuurmans *et al.*, 2018, Zhang *et al.*, 2018, Zilliges *et al.*, 2011).

Atrazine (2-chloro-4-ethylamino-6-isopropylamino-*s*-triazine) is an herbicide commonly used worldwide for the control of broad leaf weeds in agricultural, commercial and residential activities. For photosynthetic organisms, atrazine toxicity originates from the binding of the herbicide molecule to the D1 protein at the Q_B binding site resulting in the blockage of the electron transfer towards the plastoquinone (Fedtke and Duke, 2004). This result in the organism's inability to generate the trans-thylakoid proton gradient needed to achieve ATP synthesis thus limiting growth and promoting photoinhibition (Fedtke and Duke, 2004). In addition, the inhibition of photosynthetic electron transport chain result in increased reactive oxygen species (ROS) production which can result in oxidative burst damages to cell membranes, proteins and nucleic acids (Latifi *et al.*, 2009). As of 2019, annual application of atrazine is estimated to be between 70 to 90 thousand tons (He *et al.*, 2019) despite reports of interactions between this chemical and non-target organisms in aquatic ecosystems bordering agricultural activities (DeLorenzo *et al.*, 2001). Through surface runoffs, spray drifts and leaching, atrazine can easily migrate to nearby water sources and reach non-target organisms, such as phytoplanktonic communities (Potter *et al.*, 2011). Between 2018 and 2020, 87% of tested streams and rivers in the province of Quebec revealed the presence of atrazine (Giroux and al., 2022). Moreover, some studies revealed relationships between strain capacity to produce or not MCs and the fitness of cyanobacteria grown in the presence of atrazine (Chalifour and Juneau, 2011, Deblois *et al.*, 2013). As MC-producing and non-MC-producing strains of cyanobacteria sometimes respond differently to atrazine exposure and MC content was previously linked to photosynthesis (Deblois and Juneau, 2010), there is a growing belief that intracellular MCs may be involved in the response against photoinhibition. MCs could possess important physiological functions such as modulation of proteins and enzymes and as well as playing a central role in photosynthesis and protection against oxidative stress which is further supported by the notion that the vast majority of ancient cyanobacteria produced MCs (Rantala *et al.*, 2004). However, the relationships between MCs and physiology remain unclear (Omidi *et al.*, 2018) and the process by which wild MC-producing strains sometimes perform better than non-MC-producing strains in photoinhibitory conditions (Chaffin *et al.*, 2018, Chalifour and Juneau, 2011, Deblois and Juneau, 2012, Islam and Beardall, 2017) have not yet been fully resolved. The objectives of the present study were to characterize

the physiological response of the wild MC-producing strain *Microcystis aeruginosa* PCC 7806 and its mutant non-MC-producing counterpart PCC 7806 *mcy*B$^-$ following a single or combined exposure to atrazine and high light stress to determine if and how the response is affected by the capacity to produce MCs. This research aimed to better characterize the role of intracellular MCs in *M. aeruginosa* in order to assist in clarifying population dynamics within harmful cyanobacterial blooms.

2.4 Methods

2.4.1 Cultures

A wild MC-producing strain of *Microcystis aeruginosa* PCC 7806 and its mutant non-MC-producing counterpart PCC 7806 *mcy*B$^-$ were selected for this research and were obtained from the Pasteur Culture collection of Cyanobacteria (PCC, Pasteur Institute, Paris, France). PCC 7806 (hereinafter referred to as WT) is a well-known MC-producing strain while PCC 7806 *mcy*B$^-$ (henceforth referred to as MT) was removed of its capacity to produce MCs through the deletion of the mcyB gene within the operon governing MC biosynthesis (Dittmann *et al.*, 1997). Prior to the experiment, both strains were maintained in exponential growth phase through careful periodic transfers. Cultures were prepared in 500 ml Erlenmeyer flasks containing 200 ml of BG11 medium, pH 7.4 (Rippka *et al.*, 1979) and put in environmental chambers at 24°C with a luminosity of 35 µmol photons $\cdot$ m^{-2} $\cdot$ s^{-1} and a photoperiod of 12h:12h (light:dark) provided by a combination of incandescent bulbs (Philips 60W) and white fluorescent lamps (Philips, F72T8/TL841/HO, USA).

2.4.2 Cyanobacterial toxicity test

Cultures were prepared as described in the previous section at an initial cell density of 1 000 000 cells $\cdot$ ml^{-1}. Pesticide stock solution was prepared by dissolving atrazine (Pestanal®, analytical standard CAS 1912-24-9, ≤ 100%, Sigma-Aldrich) in pure acetone. Growth rate EC_{50} for atrazine were determined by exposing cultures to increasing concentrations of atrazine (final concentrations of 0, 0.05, 0.1, 0.2, 0.4, 0.8, 1.6 µM atrazine) for 72h. Cultures were prepared in triplicate for each pesticide exposure concentration. Preliminary analysis was conducted to confirm the final acetone concentration (≤ 0.1%) did not significantly affect growth or

photosynthesis-related parameters of both strains (data not shown). The atrazine concentration closest to the growth rate-EC_{50} for both strains (0.8 µM) was selected for treatments containing atrazine. For the isolation of the role of intracellular MCs through the single or combined influence of atrazine and HL stress on the photoinhibition response of *M. aeruginosa*, cultures of WT and MT were exposed or not to atrazine at 0.8 µM for 72h followed or not by 45 min of high illumination (1200 µmol photons $\cdot m^{-2} \cdot s^{-1}$) then were sampled and separated for immediate physiological analysis (growth, cell biovolume, photosynthesis) or filtered on 0.8 µm-pore filters (Polytetrafluoroethylene, Xingya Purifying Materials Factory, Shanghai, China) and flash frozen in liquid N_2 prior to storage at -80°C until needed for pigment and MC content determination. As significant biomass was necessary for antioxidant enzyme activity determination, the treatments were repeated the following week and cultures were once again sampled and separated for immediate physiological analysis (growth, cell biovolume, ROS content determination) or filtered on 0.8 µm-pore polytetrafluoroethylene filter, resuspended in 1 ml of enzyme extraction buffer and flash frozen in liquid N_2 prior storage at -80°C for later analysis. Comparability between the cultures of both experiments was judged adequate when values of growth rate and ϕ_M deviated by less than 10% between weeks.

2.4.3 Growth and morphology

Cell density and biovolume were obtained before and after pesticide exposure using a particle analyzer (Multisizer 3 Coulter Counter, Beckman Coulter Inc., USA). The growth rate was determined using the formula:

$$\mu\ (\text{days}^{-1}) = \frac{\ln[\text{Cell}]_{\text{final}} - \ln[\text{Cell}]_{\text{initial}}}{\text{Time}_{\text{final}} - \text{Time}_{\text{initial}}}$$

where µ is the maximum specific growth rate (days^{-1}) and $[\text{Cell}]_{\text{initial}}$ and $[\text{Cell}]_{\text{final}}$ relate to the initial and the final cell density, respectively. Intracellular complexity (SSC) was determined by flow cytometry (BD accuri C6 Plus, BD Biosciences, Becton-Dickinson, Franklin Lakes, NJ) according to Stachowski-Haberkorn *et al.* (2013).

2.4.4 Intracellular microcystins determination

Cells were collected on 0.8 µm-pore filter (Polytetrafluoroethylene, Xingya Purifying Materials Factory, Shanghai, China) and stored at -80°C until the extraction process. For the determination of total intracellular MC content or 12 individual congeners, cells were collected by gentle filtration (Polytetrafluoroethylene, Xingya Purifying Materials Factory, Shanghai, China) and stored at -80°C until needed. To extract MCs, filters were fully covered with 5 ml of MeOH/H_2O at 90/10 (*v*/*v*) and sonicated for 20 min. This step was repeated a second time and both supernatants were combined. Subsequently, the extracts were evaporated under gentle nitrogen gas flow and the dried extracts were reconstituted in HPLC-grade water. Intracellular MC content determination was performed using on-line solid-phase extraction connected to ultra-high-performance liquid chromatography tandem mass spectrometry (on-line SPE-UHPLC-MS/MS) through a positive mode electro spray ionization (Munoz *et al.*, 2017, Skafi *et al.*, 2021, Zhang *et al.*, 2020). Results were presented as total femtograms of MCs per cell normalized to the biovolume. This analysis targeted 12 microcystin variants, namely MC-LR, [D-Asp^3]-MC-LR, MC-RR, [D-Asp^3]-MC-RR, MC-YR, MC-HtyR, MC-HilR, MC-WR, MC-LA, MC-LY, MC-LW and MC-LF while total intracellular MC content was obtained by addition of every congeners detected.

2.4.5 Pigments determination

Following pesticide exposure and high light treatment, aliquots of the cultures were collected on 0.8 µm-pore filters (Polytetrafluoroethylene, Xingya Purifying Materials Factory, Shanghai, China), flash frozen in liquid N_2 and stored at -80°C for later analysis. Chlorophyll *a* (Chl *a*) and total carotenoids (CAR) were determined according to Lichtenthaler (1987) and phycocyanin (PC) and allophycocyanin (APC) were determined following Bennett and Bogorad (1973).

2.4.6 Photosynthetic measurements

Prior to every measurement, cultures maintained in exponential phase were put in complete obscurity for 15 min to allow reoxidation of the electron transport chain. Dark-acclimated cultures were used for the measurements of photosynthesis–related parameters using a pulse-amplitude-modulated type fluorometer with liquid culture attachment (WATER-PAM, Heinz Walz

GmbH, Effeltrich, Germany) and to follow P700 oxidoreduction kinetics using Joliot-type spectrophotometry (JTS-10, Spectrologix, USA).

Light response curves were obtained using the WATER-PAM (Heinz Walz GmbH, Germany) as described in Chapter 1. From the light response curves, the maximal (ϕ_M, data not shown) and operational (ϕ'_M) PSII quantum yields were determined according to Kitajima and Butler (1975) and Genty *et al.* (1989), respectively. The relative dissipation pathways were measured with the determination of the relative photochemical quenching (qP_{REL}) and non-photochemical quenching (qN_{REL}) as described in Buschmann (1995) and unquenched fluorescence (UQF_{REL}) as described in Juneau *et al.* (2005).

Following the method described in Chapter 1 of this thesis, we obtained the PSI electron turnover rate and cyclic electron transfer around PSI by means of the monitoring of P700 oxidoreduction kinetics (Joliot and Joliot, 2002, 2005). These measurements were obtained using a Joliot-type spectrophotometer (JTS-10, Spectrologix, USA). The PSI electron turnover rate was calculated from re-reduction kinetics following absorbance changes under far red actinic light (720 nm, 1400 µmol photons $\cdot m^{-2} \cdot s^{-1}$) and recorded at 705 nm to isolate the P700. The PSI electron turnover rate was calculated from the half-times of $P700^+$ re-reduction as K = 0.693 / half-time of $P700^+$ re-reduction in seconds. The proportion of cyclic electron around PSI during active photosynthesis was determined using the same procedure for the determination of the PSI electron turnover rate but in the presence of 150 µmol photons $\cdot m^{-2} \cdot s^{-1}$ actinic illumination at 630 nm to oxidize both PSII and PSI. This measurement was repeated following the addition of 10 µM DCMU to shut off linear electron transfers. The percentage of cyclic electron flow was obtained by dividing the PSI turnover rate with DCMU (cyclic electron flow) by the PSI turnover rate without DCMU (linear and cyclic electron flow).

2.4.7 Determination of antioxidant enzymes activity and ROS content

To determine antioxidant enzyme activities, cells were collected by filtration, resuspended in 1 ml of enzyme extraction buffer (100 mM Phosphate buffer pH 7.8, 0.1 mM EDTA, 200 mM Polyvinylpyrrolidone), flash frozen in liquid N_2 then stored at -80°C for later analysis. Enzymes

were extracted using six cycles of freezing in liquid N_2 followed by thawing in water at 20°C. Samples were then centrifuged (25 min, 25 000 × G, 4°C) and the supernatants were separated in aliquots for determination of protein content (Bradford, 1976), catalase (CAT) activity (Aebi, 1984) and superoxide dismutase (SOD) activity (Beyer Jr and Fridovich, 1987). CAT activity was expressed as µmol H_2O_2 · mg protein^{-1} · min^{-1} while SOD activity was expressed as U · mg protein^{-1}. Determination of reactive oxygen species (ROS) was performed on aliquots of 0.488 ml of fresh culture using H_2DCF-DA and flow cytometry (BD Accuri™ C6 Plus, BD Biosciences, Becton-Dickinson, Franklin Lakes, NJ, USA) following the method described in Stachowski-Haberkorn *et al.* (2013). Results were presented as the mean FL1 fluorescence values of H_2DCF-DA-stained samples divided by the mean FL1 values of the same fresh samples without added H_2DCF-DA in order to prevent signal variations due to the influence of atrazine therefore insuring comparability between treatments.

2.4.8 Statistical analysis

The results were expressed as the average of three replicates with error bars representing standard deviation. Prior to the statistical analysis, normality and heterogeneity of variance was evaluated on residuals using the Shapiro-Wilk and Brown-Forsythe tests, respectively. Data transformation was applied when residuals were not normally distributed and showed heterogenous variance. When no data transformation yielded a normal distribution and homogeneity of variance, the data was converted to ranks. The difference between the control of both strain and the influence of atrazine on growth and biovolume was evaluated using a one-way ANOVA followed by Student's t-test. For the other parameters, the single and combined influence of atrazine and the high light treatment were determined using a two-way ANOVA (atrazine × high light treatment). When a significant influence of the treatment was identified, the ANOVA was followed by Tukey's honest significant differences (HSD) test to determine the difference between groups. For ranked data, the single influence of atrazine and the high light treatment was evaluated using a Kruskal-Wallis test followed by a post-hoc pairwise comparison while the combined influence of atrazine and the high light treatment was evaluated using an Aligned Rank Transformed (ART) ANOVA followed by a post hoc pairwise comparison with

Bonferonni correction. Principal Component Analysis (PCA) and data visualization were performed using the *FactoMineR* and *factoextra* (based on *ggplot2*) R packages, respectively, using the R statistical software (R Core Team, 2020). To preserve an equal dataset between every parameters, missing data for growth and biovolume were imputed using the *imputePCA* function from the *missMDA* package. The imputation method was performed using the default settings for the number of components used to predict the missing entries. Prior to the PCA analysis, Min – Max normalization was performed as (Value – Min/Max – Min) for every parameters.

2.5 Results

2.5.1 Growth rate and cell biovolume

Growth rate of the control was higher for MT than for WT (26%, $P < 0.01$). In the presence of 0.8 µM atrazine, the growth rate decreased in comparison with the control for WT (47%, $P < 0.001$) and MT (58%, $P < 0.001$; Table 2.1). The growth-EC_{50} for atrazine were comparable between both strains (0.73 µM for WT and 0.68 µM for MT; Table 2.1). Between strains, the biovolume of the control was slightly lower for MT than WT (6%, $P < 0.01$; Table 2.1). In response to atrazine exposure, cell biovolume decreased by 23% for WT ($P < .0001$) and by 10 % for MT ($P < 0.05$) (Table 2.1).

Table 2.1 Growth and cell biovolume of *M. aeruginosa* PCC 7806 and 7806 *mcy*B$^-$ exposed or not to 0.8 µM atrazine for 72h

Strain	Parameter	Control	Atz 0.8 µM
PCC 7806	Growth ($\mu \cdot d^{-1}$)	0.32 (0.02)^a	0.17 (0.01)^b
	Biovolume (μm^3)	22.9 (0.23)^a	17.7 (0.23)^b
	$\mu \cdot d^{-1}$ – EC_{50}	0.73 (0.08)	
PCC 7806 *mcy*B$^-$	Growth ($\mu \cdot d^{-1}$)	0.40 (0.01)^a	0.17 (0.03)^b
	Biovolume (μm^3)	21.6 (0.76)^a	19.5 (0.54)^b
	$\mu \cdot d^{-1}$ – EC_{50}	0.68 (0.05)	

n.d. : not determined. Means ($n = 3$) are indicated with standard deviation in parentheses. Letters after standard deviation represents Tukey HSD test results with the mean of a > b > c > d. Means not connected by the same letter are significantly different according to the Student's t-test or Tukey HSD.

2.5.2 Pigment content

Chl *a* and CAR contents, the ratio of Chl *a* over CAR, PC and APC contents and the ratio between PC and Chl *a* for WT and MT following the single or combined influence of atrazine and high light treatment are represented in Table 2.2. For the control, Chl *a* content was similar between WT and MT. For WT, exposure to 0.8 µM atrazine had no significant influence on Chl *a* while the same treatment led to a significant decrease in this pigment concentration for MT (22%, $P < 0.05$). The HL treatment caused a decrease in Chl *a* content for WT (19%, $P < 0.05$) but had no impact for MT. The combined influence of atrazine and HL treatment decreased Chl *a* for both WT (25%, $P < 0.05$) and MT (40%, $P < 0.01$). Between strains, the CAR content of the control was higher for MT than WT (34%, $P < 0.05$) and exposure to 0.8 µM atrazine had no influence on CAR for both strains. Exposure to the HL treatment decreased CAR for MT (23%, $P < 0.05$) but had no influence on the CAR content of WT. When combined, the HL treatment and atrazine exposure yielded contrasting result for the CAR content between both strains with a trend toward an increase for WT and a significant decrease for MT (35%, $P < 0.01$). Because of the difference in CAR content between strains, the ratio of Chl *a* over CAR for the control was lower for MT than WT (13%, $P < 0.05$). Moreover, exposure to 0.8 µM atrazine decreased the ratio of Chl *a*/CAR by 16% for WT ($P < 0.05$) and by 18% for MT ($P < 0.001$). There was a contrast in the effect of the HL treatment on the ratio of Chl *a*/CAR between both strains with a decrease for WT (15%, $P < 0.05$) and an increase for MT (16%, $P < 0.001$). Combined exposure to both treatments led to a decrease in the ratio of Chl *a*/CAR for both WT (29%, $P < 0.01$) and MT (8%, $P < .0001$). The PC content of the control was similar between strains and exposure to 0.8 µM atrazine yielded a higher PC content for both WT (89%, $P < 0.05$) and MT (110%, $P < .0001$). Exposure to the HL treatment, yielded a decrease in PC content for both WT (36%, $P < 0.01$) and MT (41%, $P < 0.01$). Combined exposure to atrazine and the HL treatment led to a decrease in PC content for both WT (27%, $P < .0001$) and MT (45%, $P < .0001$). As for the PC content, the APC content of the control was similar between strains. Exposure to 0.8 µM atrazine increased APC for WT (84%, $P < 0.05$) but had no significant influence on this pigment for MT. The HL treatment led to a decrease in APC content for both WT (61%, $P < 0.05$) and MT (44%, $P < 0.05$). The combined influence of atrazine and HL led to a decrease in APC content for WT (59%, $P < 0.001$) and MT (35%, $P < 0.001$). The ratio of PC over Chl *a* of the

control was not different between strains. Exposure to 0.8 µM increased this ratio by 77% for WT ($P < 0.001$) and by 167% for MT ($P < 0.001$). The HL treatment decreased the ratio of PC over Chl *a* for MT (34%, $P < 0.01$) but had no influence on this parameter for WT. The combined influence of atrazine and the HL treatment had no effect on the ratio of PC/Chl *a* of both strains.

Table 2.2 Chlorophyll *a* and carotenoid content per cell normalized to biovolume and their ratio, plastocyanin and allophycocyanin content per cell normalized to biovolume and the ratio between PC and Chl *a* of *M. aeruginosa* PCC 7806 and 7806 *mcy*B$^-$ exposed or not to 0.8 µM atrazine for 72h then followed or not by 45 min irradiance at 1200 µmol photons · m^{-2} · s^{-1}

Strain	Parameter	No HL treatment		HL treatment		Interaction Atz × HL
		Control	Atz 0.8 µM	Control	Atz 0.8 µM	
PCC 7806	Chl *a*	2.47 (0.13)^{ab}	2.65 (0.12)^{a}	1.99 (0.25)^{bc}	1.86 (0.25)^{c}	n.s.
	CAR	0.89 (0.02)^{ab}	1.15 (0.18)^{a}	0.84 (0.08)^{b}	0.94 (0.06)^{ab}	n.s.
	Chl *a*/CAR	2.78 (0.09)^{a}	2.33 (0.27)^{b}	2.37 (0.08)^{ab}	1.97 (0.16)^{b}	n.s.
	PC	13.2 (0.98)^{b}	25.0 (4.77)^{a}	8.47 (0.44)^{c}	9.69 (0.20)^{c}	$F(1, 8) = 16.45$ $P < 0.01$
	APC	2.58 (0.39)^{b}	4.74 (1.16)^{a}	1.01 (0.07)^{b}	1.05 (0.16)^{b}	$F(1, 8) = 8.83$ $P < 0.05$
	PC/Chl *a*	5.35 (0.30)^{b}	9.46 (0.43)^{a}	4.30 (0.63)^{b}	5.29 (0.80)^{b}	$F(1, 8) = 22.35$ $P < 0.01$
PCC 7806 mcyB$^-$	Chl *a*	2.89 (0.32)^{a}	2.27 (0.08)^{bc}	2.58 (0.28)^{ab}	1.73 (0.05)^{c}	n.s.
	CAR	1.19 (0.13)^{a}	1.14 (0.04)^{ab}	0.91 (0.11)^{bc}	0.77 (0.03)^{c}	n.s.
	Chl *a*/CAR	2.43 (0.001)^{b}	1.99 (0.05)^{c}	2.83 (0.02)^{a}	2.23 (0.04)^{d}	$F(1, 8) = 14.80$ $P < 0.01$
	PC	14.8 (0.82)^{b}	31.1 (1.49)^{a}	8.78 (1.09)^{c}	8.18 (0.54)^{c}	$F(1, 8) = 195.14$ $P < .0001$
	APC	2.77 (0.31)^{a}	2.97 (0.18)^{a}	1.54 (0.38)^{b}	1.81 (0.15)^{b}	n.s.
	PC/Chl *a*	5.15 (0.36)^{b}	13.73 (1.10)^{a}	3.39 (0.06)^{c}	4.75 (0.43)^{bc}	$F(1, 8) = 102.32$ $P < .0001$

n.s. : not significant. Pigment concentrations are presented in femtograms of pigments per cell normalized by the cell biovolume (fg pigment · μm^{-3}). Means ($n = 3$) are indicated with standard deviation in parentheses. Letters after standard deviation represents Tukey HSD test results with the mean of a > b > c > d. Means not connected by the same letter are significantly different according to the Tukey HSD test.

2.5.3 Operational PSII quantum yield

The operational quantum yields of PSII (ϕ'_M) of the control WT and MT was higher for MT in comparison with WT (14%, P < .0001; Figure 2.1). Exposure to atrazine led to a decrease in ϕ'_M for both WT (64%, P < .0001; Figure 2.1A) and MT (42%, P < .0001; Figure 2.1B). Similarly, the HL treatment led to a decrease in ϕ'_M for both WT (44%, P < .0001; Figure 2.1A) and MT (53%, P < .0001; Figure 2.1B). When combined, exposure to atrazine and a subsequent HL treatment yielded to a decrease in ϕ'_M for both WT (86%, P < .0001; Figure 2.1A) and MT (79%, P < .0001; Figure 2.1B).

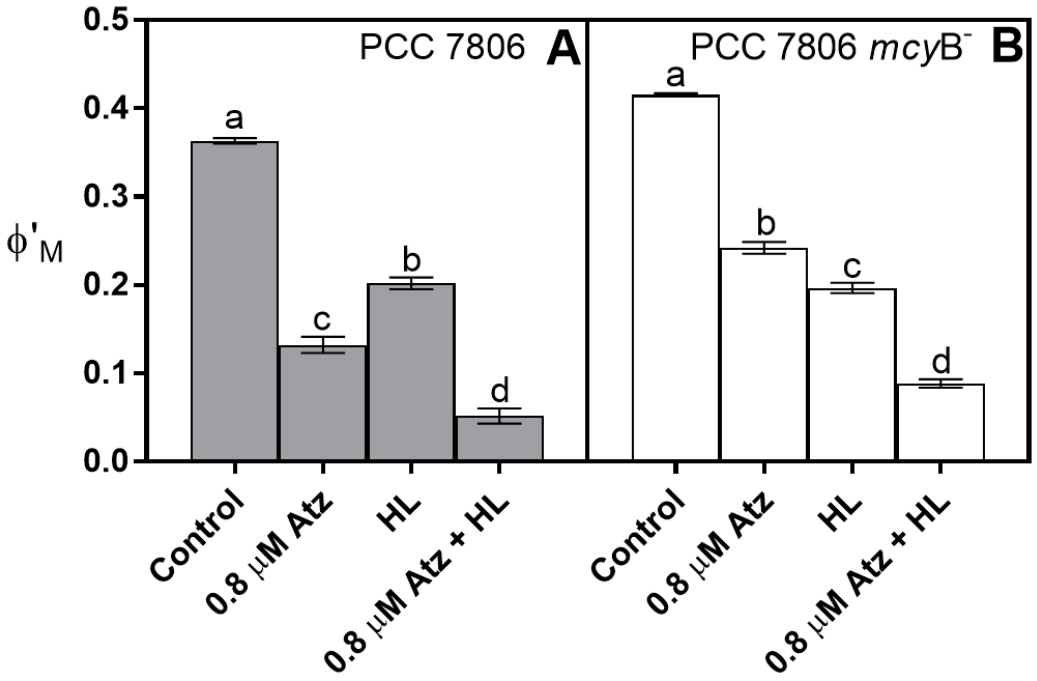

Figure 2.1 Operational quantum yield of PSII (ϕ'_M) of *M. aeruginosa* PCC 7806 (**A**) and 7806 *mcy*B$^-$ (**B**) exposed or not to 0.8 µM atrazine for 72h then followed or not by 45 min irradiance at 1200 µmol photons · m^{-2} · s^{-1}. Each bar represents the mean of three replicates. Letters above error bars represented Tukey HSD test results with the mean of a > b > c > d. Means not connected by the same letter are significantly different according to the Tukey HSD test.

2.5.4 Relative energy dissipation pathways

The relative photochemical quenching, non-photochemical quenching and unquenched fluorescence for WT and MT following the single or combined influence to atrazine and the high light treatment are represented in Figure 2.2. For the control, qP_{REL} was similar between WT and MT (Figure 2.2A-B). Exposure to atrazine yielded a decrease in qP_{REL} for WT (65%, $P < 0.001$; Figure 2.2A) and MT (38%, $P < 0.001$; Figure 2.2B). Similarly, the HL treatment led to a decrease in qP_{REL} for both WT (31%, $P < 0.01$; Figure 2.2A) and MT (40%, $P < 0.001$; Figure 2.2B). When combined, exposure to atrazine and the HL treatment led to a decrease in qP_{REL} for WT (80%, $P < .0001$; Figure 2.2A) and MT (72%, $P < .0001$; Figure 2.2B). Control cultures showed a similar qN_{REL} between WT and MT (Figure 2.2C-D). Exposure to atrazine led to a decrease in qN_{REL} for both WT (94%, $P < 0.01$; Figure 2.2C) and MT (78%, $P < 0.01$; Figure 2.2D) while the HL treatment yielded an increase in this parameter for both WT (58%, $P < 0.01$; Figure 2.2C) and MT (72%, $P < 0.05$; Figure 2.2D). Moreover, combined exposure to atrazine and the HL treatment led to a decrease in qN_{REL} for both WT (63%, $P < .0001$; Figure 2.2C) and MT (41%, $P < .0001$; Figure 2.2D). UQF_{REL} was higher for MT than WT in control cultures (229%, $P < 0.001$; Figure 2.2E-F). Exposure to atrazine increased UQF_{REL} for both WT (3925%, $P < .0001$; Figure 2.2E) and MT (740%, $P < .0001$; Figure 2.2F). The HL treatment also increased UQF_{REL} for both WT (388%, $P < 0.01$; Figure 2.2E) and MT (237%, $P < 0.01$; Figure 2.2F). When combined, the atrazine and HL treatment led to an increase in UQF_{REL} for WT (4087%, $P < .0001$; Figure 2.2E) and MT (1015%, $P < .0001$; Figure 2.2F).

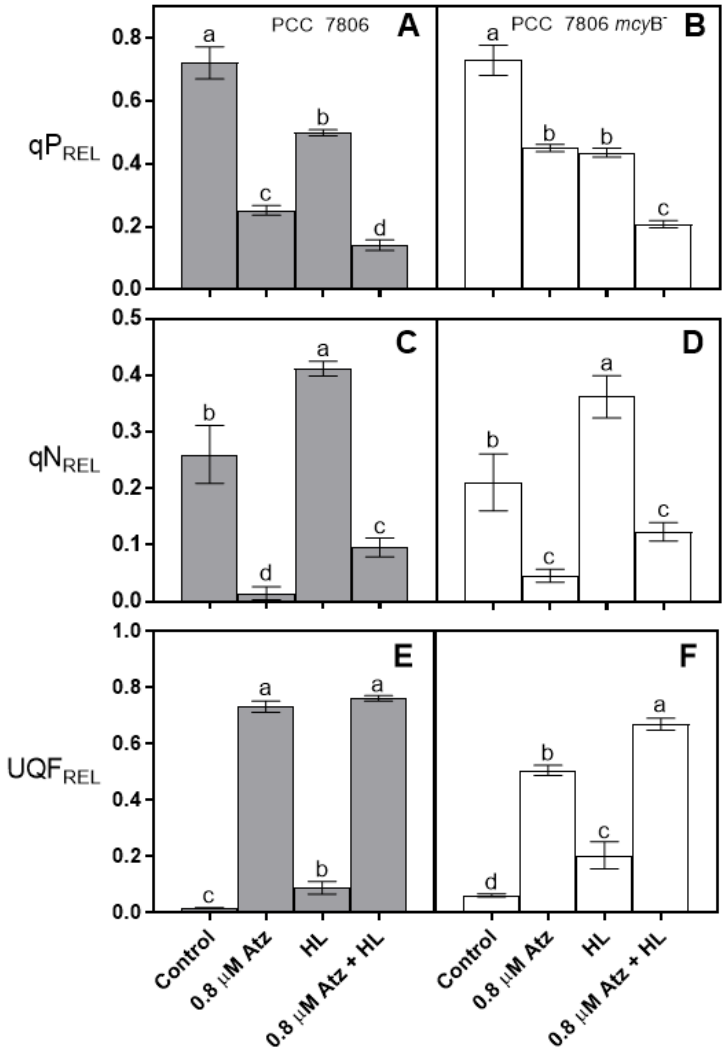

Figure 2.2 Photochemical quenching (qP_{REL}), non-photochemical quenching (qN_{REL}) and unquenched fluorescence (UQF_{REL}) of *M. aeruginosa* PCC 7806 (**A**-**C**-**E**) and 7806 *mcy*B$^-$ (**B**-**D**-**F**) exposed or not to 0.8 µM atrazine for 72h then followed or not by 45 min irradiance at 1200 µmol photons $\cdot m^{-2} \cdot s^{-1}$. Each bar represents the mean of three replicates. Letters above error bars represents Tukey HSD test results with the mean of a > b > c > d. Means not connected by the same letter are significantly different according to the Tukey HSD test.

2.5.5 Electron transport rate

For control conditions, we have shown that MT exhibited higher maximal electron transport rate (ETR_{max}) than WT (14%, $P < 0.05$; Figure 2.3). Atrazine contamination led to a decrease in ETR_{max} for both WT (81%, $P < .0001$; Figure 2.3B) and MT (65%, $P < .0001$; Figure 2.3D). Exposure to HL stress yielded a decrease in ETR_{max} for WT (26%, $P < 0.001$; Figure 2.3B) and MT (45%, $P < 0.001$; Figure 2.3D), and the combined influence of atrazine and the HL treatment led to a decrease in ETR_{max} for both WT (96%, $P < .0001$; Figure 2.3B) and MT (91%, $P < .0001$; Figure 2.3D).

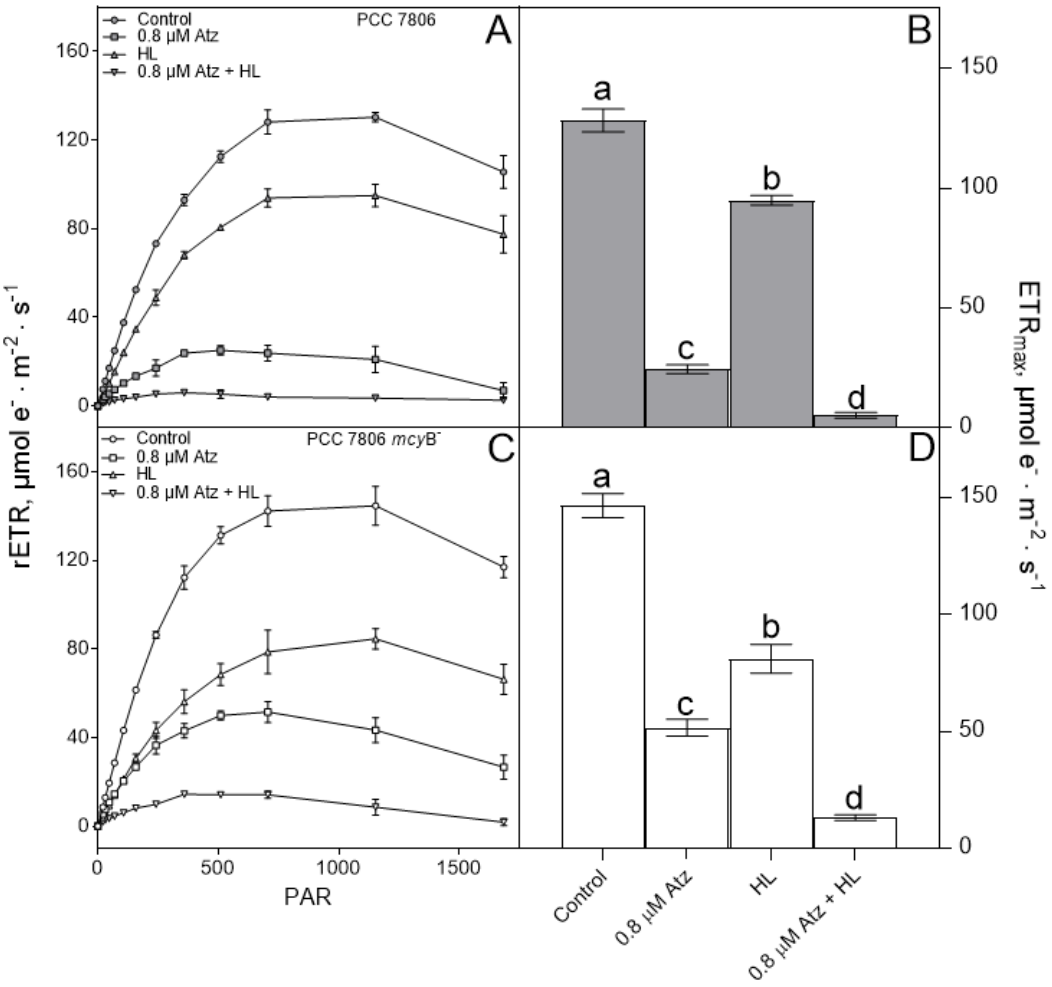

Figure 2.3 Relative electron transport rate (rETR) and maximal electron transport rate (ETR_{max}) of *M. aeruginosa* PCC 7806 (**A**-**B**) and 7806 *mcy*B^{-} (**C**-**D**) exposed or not to 0.8 µM atrazine for 72h then followed or not by 45 min irradiance at 1200 µmol photons · m^{-2} · s^{-1}. Each bar represents the mean of three replicates. Letters above error bars represents Tukey HSD test results with the mean of a > b > c > d. Means not connected by the same letter are significantly different according to the Tukey HSD test.

2.5.6 P700 kinetics and PSI turnover rate

The PSI turnover rate is represented in Figure 2.4. The intrinsic PSI electron turnover rate (e^{-} · sec^{-1}) was lower for MT in comparison with WT (45%, $P < 0.01$; Figure 2.4). When exposed to 0.8 µM atrazine, the PSI electron turnover rate decreased for both WT (82%, $P < .0001$, Figure 2.4A) and MT (48%, $P < .0001$, Figure 2.4B). Exposure to the HL treatment yielded a similar increase in PSI electron turnover rate for WT (32%, $P < 0.01$, Figure 2.4A) and MT (36%, $P < .0001$, Figure 2.4B). When combined, atrazine and HL decreased PSI electron turnover for WT only (54%, $P < .0001$, Figure 2.4A)

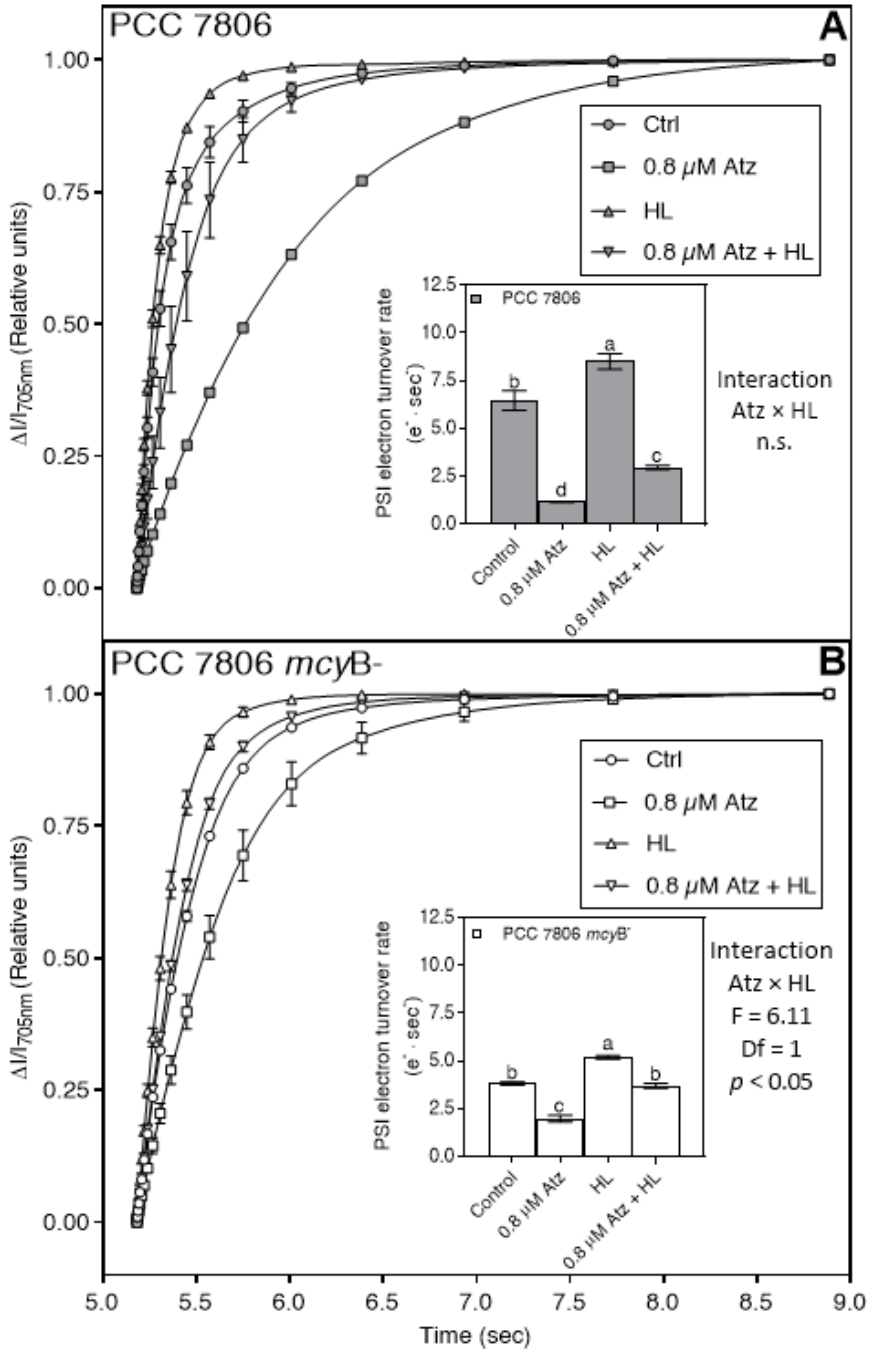

Figure 2.4 Normalized $P700^+$ re-reduction kinetics and PSI turnover rate ($e^- \cdot sec^{-1}$) of *M. aeruginosa* PCC 7806 (**A**) and 7806 *mcy*B^- (**B**) for the control (○), cultures exposed 0.8 µM atrazine for 72h (□) and the same treatments followed by 45 min irradiance at 1200 µmol photons $\cdot m^{-2} \cdot s^{-1}$ (△ and ▽, respectively). Each point represents the average of three replicates and the error bars are not shown as they are smaller than the height of the symbols. Letters above error bars represented Tukey HSD test results with the mean of a > b > c > d. Means not connected by the same letter are significantly different according to the Tukey HSD test.

2.5.7 Proportion of cyclic electron flow

The proportion of cyclic electron transport around PSI of WT and MT following the single or combined influence to atrazine and the high light treatment are represented in Figure 2.5. MT showed a much higher proportion of cyclic electron transport around PSI than WT for control conditions (149%, $P < .0001$; Figure 2.5). Exposure to atrazine had no effect on this parameter for both strains (Figure 2.5). The HL treatment induced a higher proportion of cyclic electron transport around PSI for both WT (199%, $P < 0.001$; Figure 2.5A) and MT (88%, $P < 0.001$; Figure 2.5B). Similarly, the combined influence of atrazine and the HL treatment led to an increase in the proportion of cyclic electron transport around PSI for WT (174%, $P < .0001$; Figure 2.5A) and MT (75%, $P < .0001$; Figure 2.5B).

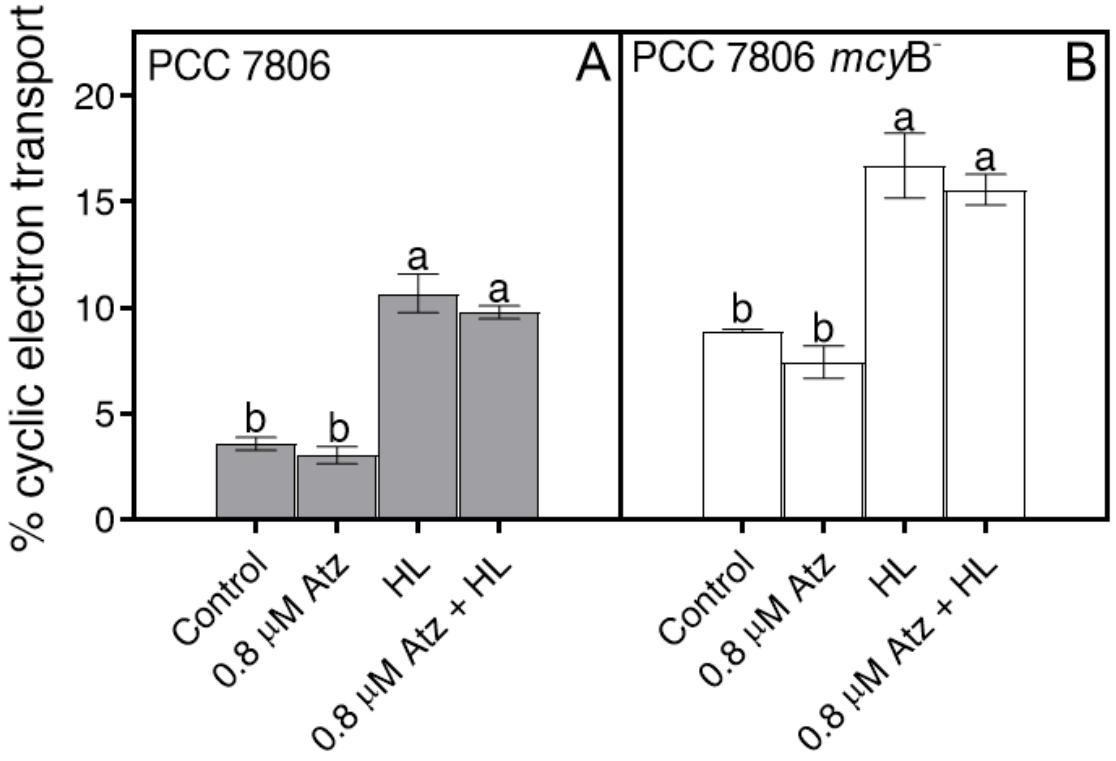

Figure 2.5 Cyclic electron flow around PSI of *M. aeruginosa* PCC 7806 (**A**) and PCC 7806 *mcy*B$^-$ (**B**) exposed or not to 0.8 µM atrazine for 72h then followed or not by 45 min irradiance at 1200 µmol photons · m^{-2} · s^{-1}. Means not connected by the same letter are significantly different according to the Tukey HSD test.

2.5.8 Reactive oxygen species content and antioxidant enzymes activity

The ROS content as well as CAT and SOD activity are represented in Table 2.3. The intrinsic ROS content of the WT strain was higher than the MT (28%, $P < 0.01$). Exposure to 0.8 µM atrazine led to a decrease in ROS content for both WT (40%, $P < 0.001$) and MT (35%, $P < 0.05$). On the other hand, HL induced a strong increase in ROS content for WT (107%, $P < .0001$) while it remained stable for MT. Combined influence of atrazine and the HL treatment led to a decrease in ROS for MT (40%, $P < 0.01$) while this treatment had no influence on ROS for WT. CAT activity of the control was similar between strains. Exposure to 0.8 µM atrazine led to an increase in CAT activity for both WT (234%, $P < 0.01$) and MT (437%, $P < 0.01$). Exposure to the HL treatment led to a strong increase in CAT activity for WT (937%, $P < 0.01$) and MT (894%, $P < 0.001$). Combined influence of atrazine and the HL treatment led to an increase in CAT activity for both WT (437%, $P < 0.001$) and MT (384%, $P < 0.01$). SOD activity of the control was higher for WT than MT (46%, $P < 0.01$). Exposure to 0.8 µM atrazine led to an increase in SOD activity for both WT (145%, $P < 0.01$) and MT (77%, $P < 0.001$). The HL treatment had no effect on SOD activity for both strains. When combined, atrazine and the HL treatment induced a rise in SOD activity for both WT (186%, $P < 0.001$) and MT (114%, $P < .0001$).

Table 2.3 Reactive oxygen species content, catalase and superoxide dismutase activity of *M. aeruginosa* PCC 7806 and 7806 *mcy*B$^-$ exposed or not to 0.8 µM atrazine for 72h then followed or not by 45 min irradiance at 1200 µmol photons · m^{-2} · s^{-1}

Strain	Parameter	No HL treatment		HL treatment		Interaction Atz × HL
		Control	Atz 0.8 µM	Control	Atz 0.8 µM	
PCC 7806	ROS	7.96 (0.36)^b	4.74 (0.26)^c	16.5 (0.54)^a	8.21 (0.59)^b	F (1,8) = 91.39 P < .0001
	CAT	55.3 (12.1)^b	184.5 (20.3)^b	573.21 (41.3)^a	536.4 (32.9)^a	n.s.
	SOD	1.65 (0.06)^b	4.04 (0.72)^a	1.47 (0.09)^b	4.71 (0.22)^a	n.s.
PCC 7806 mcyB$^-$	ROS	6.24 (0.28)^a	4.08 (1.09)^b	6.70 (0.37)^a	3.76 (0.46)^b	n.s.
	CAT	70.8 (7.23)^c	380.4 (97.6)^b	703.3 (81.1)^a	342.3 (53.9)^b	F(1,8) = 70.75 P < .0001
	SOD	1.18 (0.12)^c	1.99 (0.10)^b	0.99 (0.03)^c	2.41 (0.16)^a	F(1,8) = 17.74 P < 0.01

n.s. : not significant. ROS content is represented as mean FL1 fluorescence of H_2DCF-DA-stained cells divided by mean FL1 fluorescence of the same samples without H_2DCF-DA staining. CAT activity is represented as µmol H_2O_2 catabolized per mg protein in the extract per min. SOD activity is represented as U per mg protein in the extract where U is the amount of SOD necessary to prevent 50% formation of blue formazan. Means (*n* = 3) are indicated with standard deviation in parentheses. Letters after standard deviation represents Tukey HSD test results with the mean of a > b > c. Means not connected by the same letter are significantly different according to the Tukey HSD test.

2.5.9 Intracellular complexity

Intracellular complexity (SSC) of WT and MT following the single or combined influence to atrazine and the high light treatment are represented in Figure 2.6. Between strains, SSC of the control was higher for MT than WT (291%, P < .0001; Figure 2.6). Exposure to 0.8 µM atrazine had no influence on SSC of WT (Figure 2.6A) while this parameter decreased by 16% for MT (P < .0001; Figure 2.6B). The HL treatment caused an increase in SSC for WT (37%, P < 0.01; Figure 2.6A) and a decrease for MT (10%, P < 0.01; Figure 2.6B). Combined exposure to atrazine and the HL treatment decreased SSC for WT (5%, P < 0.001; Figure 2.6A) and MT (58%, P < .0001; Figure 2.6B).

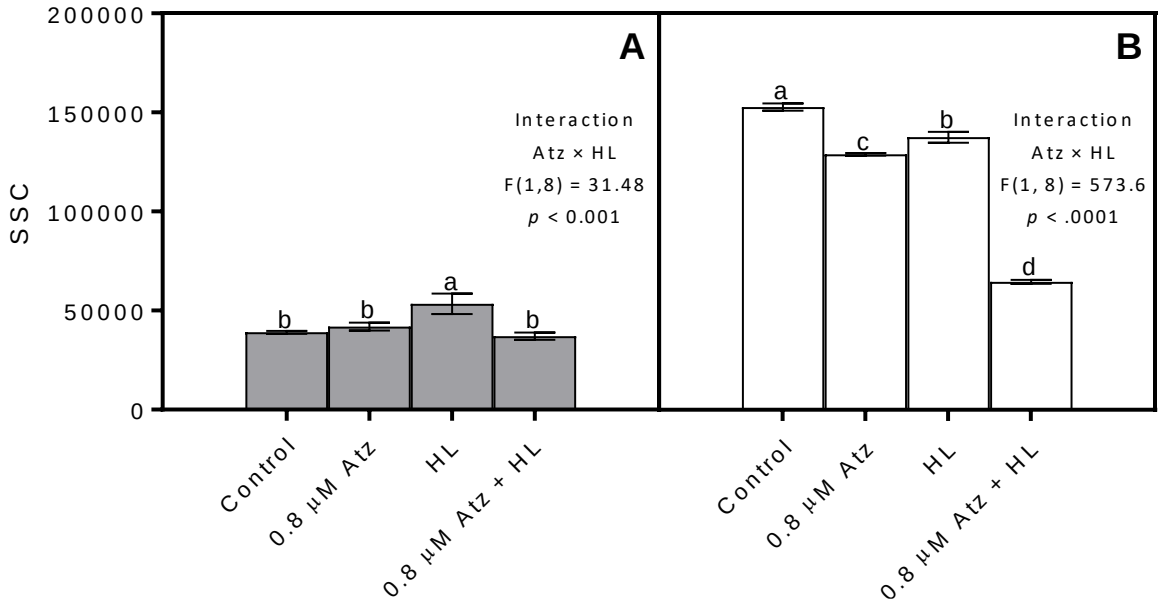

Figure 2.6 Intracellular complexity (SSC) of *M. aeruginosa* PCC 7806 (**A**) and PCC 7806 *mcy*B$^-$ (**B**) exposed or not to 0.8 µM atrazine for 72h then followed or not by 45 min irradiance at 1200 µmol photons · m^{-2} · s^{-1}. Means not connected by the same letter are significantly different according to the Tukey HSD test.

2.5.10 Total MC content and individual congeners

MC congeners and total MC content normalized to biovolume for WT following the single or combined influence to atrazine and the high light treatment are represented in Table 2.4. MC-LR was not affected by the single or combined influence of atrazine and the HL treatment. Exposure to 0.8 µM atrazine led to a 28% ($P < 0.05$) decrease in [D-Asp^3]-MC-LR content while exposure to HL or the combined influence of atrazine and HL had no effect on this congener. The single or combined influence of atrazine and the HL treatment had no effect on [D-Asp^3]-MC-RR content. Treatment with 0.8 µM atrazine led to a decrease in MC-HilR content (39%, $P < 0.05$) while exposure to HL or the combined influence of atrazine and HL had no influence on this congener. Exposure to atrazine and the combined influence of atrazine and HL yielded a 61% ($P < 0.01$) and 45% ($P < 0.01$) decrease in MC-LY content while HL had no influence on this congener. MC-LW content decreased by 63% ($P < 0.05$) and 48% ($P < 0.01$) as a response to the atrazine treatment and the combined influence of atrazine and HL stress, respectively. Exposure to atrazine completely depleted MC-LF content ($P < .0001$) while the combined influence of atrazine and HL decreased this congener by 75% ($P < .001$). The HL treatment had no effect on MC-LF. The sum of all MC congeners did not significantly change in response to our treatments but there was a clear trend toward a decrease for every treatment.

Table 2.4 MC congeners content of *M. aeruginosa* PCC 7806 exposed or not to 0.8 µM atrazine for 72h then followed or not by 45 min irradiance at 1200 µmol photons · m^{-2} · s^{-1}

Congeners	No HL treatment		HL treatment		Interaction Atz × HL
	Control	Atz 0.8 µM	Control	Atz 0.8 µM	
MC-LR	0.80 (0.06)^{a}	0.58 (0.13)^{a}	0.69 (0.04)^{a}	0.66 (0.05)^{a}	n.s.
[D-Asp^3]-MC-LR	0.44 (0.04)^{a}	0.31 (0.06)^{b}	0.35 (0.02)^{ab}	0.32 (0.02)^{ab}	n.s.
[D-Asp^3]-MC-RR	2.56 x 10^{-4} (1.14 x 10^{-5})^{a}	3.57 x 10^{-4} (3.32 x 10^{-4})^{a}	1.63 x 10^{-4} (1.25 x 10^{-4})^{a}	1.42 x 10^{-4} (1.00 x 10^{-4})^{a}	n.s.
MC-HilR	7.12 x 10^{-3} (7.59 x 10^{-4})^{a}	4.35 x 10^{-3} (1.42 x 10^{-3})^{b}	5.15 x 10^{-3} (2.67 x 10^{-4})^{ab}	5.19 x 10^{-3} (4.0 x 10^{-4})^{ab}	F(1,8) = 5.6 P < 0.05
MC-LY	3.68 x 10^{-4} (4.08 x 10^{-5})^{a}	1.43 x 10^{-4} (4.39 x 10^{-5})^{b}	3.19 x 10^{-4} (1.50 x 10^{-5})^{a}	2.03 x 10^{-4} (7.43 x 10^{-6})^{b}	F(1,8) = 6.19 P < 0.05
MC-LW	8.16 x 10^{-4} (1.26 x 10^{-4})^{a}	3.01 x 10^{-4} (9.94 x 10^{-5})^{b}	7.38 x 10^{-4} (6.10 x 10^{-5})^{a}	4.25 x 10^{-4} (3.08 x 10^{-5})^{b}	n.s.
MC-LF	8.16 x 10^{-5} (1.38 x 10^{-5})^{a}	ND	6.55 x 10^{-5} (8.06 x 10^{-6})^{a}	2.04 x 10^{-5} (3.09 x 10^{-6})^{b}	F(1,8) = 10.1 P < 0.05
Total	1.24 (0.10)^{a}	0.89 (0.20)^{a}	1.05 (0.06)^{a}	0.99 (0.07)^{a}	n.s.

n.s. : not significant. ND : Not detected. Results are presented in fg per cell normalized to the cell biovolume (fg MC · μm^{-3}). Means (n = 3) are indicated with standard deviation in parentheses. Letters after standard deviation represents Tukey HSD test results with the mean of a > b. Means not connected by the same letter are significantly different according to the Tukey HSD test.

2.5.11 Interactive effect of atrazine and high light

A two-way ANOVA produced several significant interactive effect of atrazine and the HL treatment on the physiology of both strains. When significant, the details of the interactive effect of atrazine and HL stress are found in their respective figures and tables. For WT, the combined influence of atrazine and the high light treatment yielded a significant interactive effect on PC (Table 2.2) and APC content (Table 2.2), PC/Chl *a* (Table 2.2), ϕ'_M (Figure 2.1A), qP_{REL} (Figure 2.2A), ETR_{max} (Figure 2.3B), ROS content (Table 2.3), SSC (Figure 2.6A), MC-HilR (Table 2.4), MC-LY (Table 2.4) and MC-LF (Table 2.4). For MT, the combined influence of atrazine and the high light treatment produced a significant interactive effect for Chl *a*/CAR (Table 2.2), PC content (Table 2.2), PC/Chl *a* (Table 2.2), ϕ'_M (Figure 2.1B), ETR_{max} (Figure 2.3D), PSI electron turnover rate (Figure 2.4B), SSC (Figure 2.6B), CAT (Table 2.3) and SOD activity (Table 2.3).

2.5.12 Relationships between MC content and physiological endpoints

We performed a Principal Component Analysis (PCA) in order to identify patterns in the data, to reduce dimensionality of the dataset and to relate the total MC and individual MC congeners content normalized to biovolume with every measured physiological parameters (Figure 2.7). Two principal components together explained 80.2% of variance (scree plot, Figure S2.1). Variables were mostly explained by PC1 (56%) and PC2 (24.2%). Total MC content strongly coincided with PC1 and weakly coincided with PC2. On PC1, total MC content and every MC congeners evaluated besides [D-Asp^3]-MC-RR were strongly related to ϕ'_M, qP_{REL}, ETR_{max}, Chl *a*/CAR, growth, biovolume, PSI electron turnover rate, qN_{REL} and ROS, while being moderately related to SSC and weakly related to the proportion of cyclic electron flow. Additionally on PC1, total MC content and every MC congeners evaluated besides [D-Asp^3]-MC-RR were strongly inversely related to UQF_{REL}, SOD, PC/Chl *a*, and CAR while being moderately inversely related to PC and APC and weakly inversely related to Chl *a* and CAT. On PC2, biovolume normalized cellular content in total MC, MC-LR, [D-Asp^3]-MC-LR, MC-HilR, MC-LY, MC-LW and MC-LF were weakly related to Chl *a*, Chl *a*/CAR, CAR, PC/Chl *a*, PC, APC, ϕ'_M, qP_{REL}, ETR_{max} and growth. Additionally on PC2, biovolume normalized cellular content in total MC, MC-LR, [D-Asp^3]-MC-LR, MC-HilR, MC-LY, MC-LW and MC-LF were weakly inversely related to biovolume, PSI electron turnover rate, qN_{REL}, SSC, ROS, the proportion of cyclic electron transport, CAT, SOD and UQF_{REL}. [D-Asp^3]-MC-RR weakly but equally coincided with PC1 and PC2 as well as being weakly related to every physiological parameters we measured.

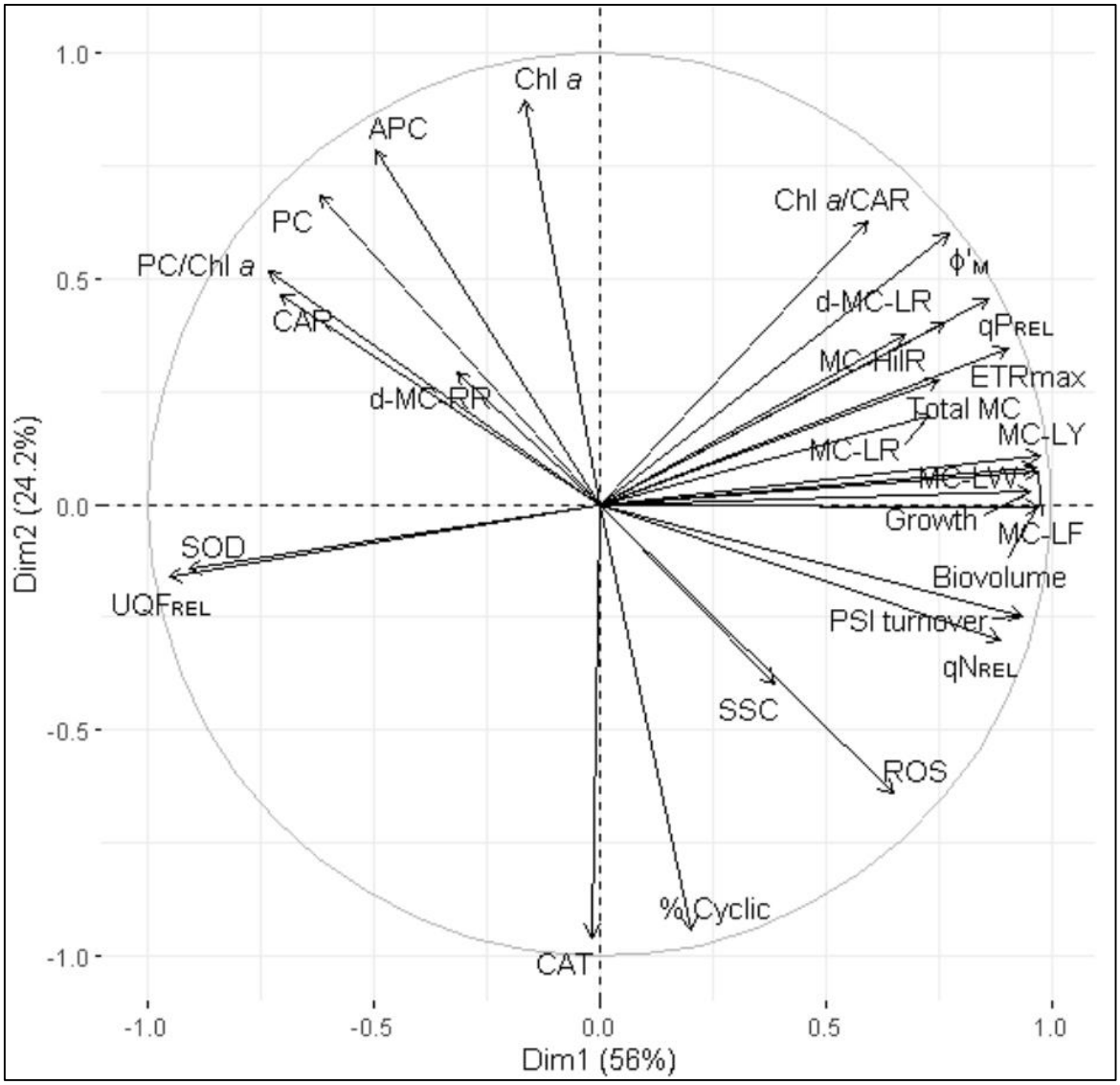

Figure 2.7 Principal Component Analysis (PCA) showing the relationship between total MC and seven individual MC congeners (MC-LR, [D-Asp^3]-MC-LR, [D-Asp^3]-MC-RR, MC-HilR, MC-LY, M-LW and MC-LF) content normalized to biovolume with growth, photosynthesis, morphology and oxidative stress-related physiological parameters for *Microcystis aeruginosa* PCC 7806 exposed or not to 0.8 µM atrazine, high light stress and the combination of both stress factors.

2.6 Discussion

In the present study, multiple endpoint analysis shed light on intrinsic physiological divergences between a *Microcystis aeruginosa* mutant (PCC 7806 *mcy*B$^-$) lacking the ability to produce MC and its wild type (PCC 7806) when exposed to atrazine and high treatment light intensity. Identification of the processes mostly affected by the loss of microcystin production and

photoinhibitory conditions provided by the single and combined influence of atrazine and HL stress allowed to focus on the potential physiological role of intracellular microcystin in relation to the physiological processes related to the response to photoinhibition and oxidative stress.

Biosynthesis of microcystins is an energy-consuming process (Briand *et al.*, 2012), and could explain the lower growth rate for WT control cultures compared to MT (Table 2.1). Moreover, the toxic effect of atrazine on cyanobacterial growth and photosynthesis can be summarized by a decrease in growth that is explained by a direct inhibition of photosynthetic linear electron transport by atrazine and this was observed by multiple research groups (Chalifour and Juneau, 2011, Chalifour *et al.*, 2016, Deblois *et al.*, 2013, González-Barreiro *et al.*, 2004, Lockert *et al.*, 2006, Qian *et al.*, 2014b, Weiner *et al.*, 2004). Therefore, as photosynthetic electron transport is necessary for energy production, the decrease in the growth we observed in both strains in response to atrazine exposure was expected (Table 2.1). Furthermore, the decrease in the growth rate following exposure to 0.8 µM atrazine was more pronounced for MT than for WT (Table 2.1) and this result highlights that the mutant strain was not able to completely adapt (in terms of physiological processes supporting growth) to the lack of MC production. Since photosynthetic electron transport is the main source of energy to support growth, monitoring PSII activity allows for the investigation of potential differences resulting from the induced treatments. The higher intrinsic photosynthetic yield of MT (Figure 2.1B, 2.2B and 2.5) can explain the higher growth rate of this strain in comparison with WT in control conditions (Table 2.1). Moreover, photosynthesis was differently affected by the treatments when MC production was present. Notably, atrazine exposure produced a stronger decrease in photosynthetic yield for WT than MT while HL stress and the combined influence of atrazine and HL produced a similar response for this parameter between both strains (Figure 2.1). Similar results can be found in literature (Chalifour *et al.*, 2016, Schuurmans *et al.*, 2018) and are mostly explained by the effect of treatments on the reparation rate of the D1 protein in PSII (Murata *et al.*, 2007, Nishiyama *et al.*, 2001). Interestingly, our results from the effect of atrazine alone on photosynthesis is in contradiction with the same treatment on growth between WT and MT. In part, this contradiction could be explained by a difference in energy allocation in consequence to inactivation of MC production where a disproportionate fraction of energy may be needed to elevate antioxidant activity and restructure pigmentation in

MT. The observed antagonistic influence of HL stress and atrazine on the photosynthetic yield (Figure 2.1) may be explained by the capacity of cyanobacteria to solicit photoregulative and photoprotective processes consequently to exposure to photoinhibitory conditions (Karapetyan, 2007, Rachedi *et al.*, 2020). As seen in our research, pre-exposure to atrazine led to higher antioxidant enzyme activity (Table 2.3) and lower ROS content (Table 2.3) which could translate to a lower inhibition of the rate of repair of the D1 protein under HL stress.

Pigment composition was key to better understand the consequences of loss of MC production on growth and photosynthetic yield for control cultures and how treatments differently affected both strains. In the presence of atrazine contamination, the pigment content of both strains was different from one another which suggests that light energy is disparately managed by both strains. While atrazine contamination led to a similar decrease in Chl *a*/CAR between strains, this treatment increased the PC/Chl *a* of both strains but significantly more for MT (Table 2.2).

Changing pigmentation in cyanobacteria following exposure to atrazine can be found in literature and shows contrasting results which appear be affected by atrazine exposure length and concentration but also differed in the presence or absence of MC production (Chalifour and Juneau, 2011, González-Barreiro *et al.*, 2004). For instance, Chalifour and Juneau (2011) exposed the microcystin-producing *M. aeruginosa* CPCC 299 and non-microcystin-producing CPCC 632 to 0.1 µM atrazine for 72h and observed an increase in CAR for CPCC 299 only and a decrease in PC for CPCC 632 only. In our case, exposure to atrazine led to an increase in CAR for the toxic strain only but showed a clear increase in PC and APC for both strains. Moreover, González-Barreiro *et al.* (2004) tested the exposure of up to 0.75 µM atrazine for 48h and 96h on the pigment content of the non-toxic cyanobacteria *Synechococcus elongatus* which resulted in a clear increase in Chl *a*, CAR, PC and APC after 48h that reverted to an overall decrease after 96h. For our study, the non-toxic strain did show a decrease in Chl *a* but maintained higher PC and APC following 72h exposure to atrazine. Inter- and intraspecific strategies of antioxidant defense with the possible involvement of MCs may explain the differences seen between our study and literature for the effect of atrazine on the cyanobacterial pigment content.

In contrast, the high light stress treatment elicited a clear overall decrease in pigment content for both strains we evaluated with the exception of CAR for WT which remained stable (Table 2.2). Photoprotection in cyanobacteria can involve redox-active CAR as well as transfers of excess light energy between CAR triplets to Chl *a* triplets which can lead to the generation of superoxide anions and degradation of Chl *a* and CAR under strong illumination (Krieger-Liszkay, 2005, Packer *et al.*, 1981, Shinopoulos *et al.*, 2014). It is also known that cyanobacteria possess high-light inducible proteins which serve to protect photosynthetic pigments (Komenda and Sobotka, 2016). Thus, intracellular MCs could serve a function in the modulation of these photoprotective processes.

The previous observations also highlight the importance of CAR in counteracting loss of MC production further suggesting a role of this cyanotoxin in photoprotection by modulating excess light energy dissipation or ROS scavenging (Kirilovsky, 2007, Kirilovsky and Kerfeld, 2012, Muzzopappa and Kirilovsky, 2020, Tóth *et al.*, 2015). This relationship seems to be of a complex nature as a direct correlation between CAR-related photoprotection and MCs has yet to be confirmed. However, it was shown that MCs and the orange carotenoid protein (OCP) are closely distributed in the thylakoid membrane and the ratio of OCP to MCs increases following HL exposure (Djediat *et al.*, 2020). It may be relevant to note that the identified MC variants and their relative proportion in Djediat *et al.* (2020) were largely dissimilar to those identified in our study and thus may differ in their potential functionality in relation to the HL stress response. When MC production was absent, phycobiliproteins also responded differently to atrazine exposure (Table 2.2) which can point to the involvement of MCs in the density or composition of phycobilisomes (PBS) or the efficiency of light capture or re-emission (Chalifour and Juneau, 2011, Chenu *et al.*, 2017, Raps *et al.*, 1985). The PBS is at the center of re-emission of light energy as heat for cyanobacteria through the binding of the OCP to APC in photoinhibitory conditions (Muzzopappa and Kirilovsky, 2020). Under HL stress, over-excitation of PBS and Chl *a* can lead to the generation of excessive heat and dismantling/degradation of the antenna complex (Rakhimberdieva *et al.*, 2007, Tamary *et al.*, 2012) which could explain the similar decrease in PC, APC and PC/Chl *a* seen in both strains. While found everywhere within the cells, MCs are often strongly concentrated in close proximity to thylakoidal membranes (Djediat *et al.*, 2020, Young *et*

al., 2008, Young *et al.*, 2005) and may bind with phycobilins (Zilliges *et al.*, 2011). The antagonistic interaction between atrazine and HL stress on PC, APC for both strains and PC/Chl *a* for WT (Table 2.2) can be explained by the increase in PBS-related pigments for both strains and in CAR for WT following atrazine exposure thereby enhancing re-emission of light energy under HL stress.

Parameters related to the relative quenching pathways were also key photosynthetic endpoints that highlighted divergences between both strains strategy and physiological response to our treatments. While qP_{REL} was similar between both strains in control conditions, this parameter decreased significantly more in atrazine-contaminated media for WT, but under HL stress we showed that qP_{REL} decreased to a similar degree between both strains (Figure 2.2A-B). As previously stated, a rapid increase in light intensity will trigger multiple processes in order to maintain a balance between energy availability and demand while preventing over-excitation and possible photodamage. As atrazine caused a much larger decrease in qP_{REL} for WT than MT, the slightly lower qP_{REL} for WT compared to MT in response to the combined influence of atrazine and HL stress (Figure 2.2A-B) may be explained by the increase in CAR and APC content following atrazine exposure for WT only (Table 2.2).

Under atrazine exposure, there was nearly no NPQ for WT, while MT was still able to solicit these processes (Figure 2.2C-D). This may be explained by the intrinsically higher CAR for MT compared to WT (Table 2.2) as cyanobacterial NPQ is regulated through activation of the OCP by strong illumination (Muzzopappa and Kirilovsky, 2020). Activation of this process was more so evident for both strains under the HL treatment (Figure 2.2C-D). Despite the response of qN_{REL} under atrazine exposure, UQF_{REL} of MT was more than twice that of WT in control cultures (Figure 2.2E-F) which could indicate that intrinsic dissipation of energy as heat may not be as efficient or may be differently regulated when MC production is inactivated. UQF_{REL} can be related to the redox state of PQ as this parameter refers to the relative amount of chlorophyll fluorescence emitted when energy dissipation pathways are inefficient and electron transport is blocked (Juneau *et al.*, 2005) which can lead to overproduction of ROS (Ledford and Niyogi, 2005, Niyogi, 1999, 2000). In response to atrazine, UQF_{REL} drastically increased for both strains but to a lesser degree for MT (Figure 2.2E-F) which may be explained by atrazine mode of action through binding to

plastoquinone B in PSII which directly inhibits electron flow to the PQ pool (Fedtke and Duke, 2004). This result could also be explained by lower Chl *a* content and Chl *a*/CAR of MT when exposed to atrazine (Table 2.2). This could also explain why treatments which involved atrazine induced a near twice fold increase in SOD activity when MC production was present (Table 2.3) as excess Chl *a* fluorescence can lead to overproduction of superoxide anions (Herbert *et al.*, 1992).

Following inactivation of MC production, the observed changes in pigment content (Table 2.2) and relative energy dissipation pathways (Figure 2.2) allowed MT to maintain an efficient and slightly higher electron flow as evidenced by the higher ETR_{max} (Figure 2.3B). Growth in atrazine-contaminated media led to a strong decrease in ETR_{max} for both strains but to a lesser degree when MC production was absent (Figure 2.3) which may be related to the higher intrinsic proportion of cyclic electron flow around PSI for MT (figure 2.5B). In contrast, HL stress decreased ETR_{max} for both strains and this decrease was not as important when MC production was present (Figure 2.3) which could also be related to the higher proportion in linear electron flow in WT compared to MT (Figure 2.5). As atrazine caused a larger decrease in ETR_{max} for WT than MT, the slightly lower ETR_{max} for WT compared to MT in response to the combined influence of atrazine and HL stress (Figure 2.3B-D) may be similarly explained as for qP_{REL}.

PSI electron turnover rate was nearly half for MT than that of WT (Figure 2.4) which point towards a difference in the processes that balance the oxidation status of the PQ pool consequent to loss of MC production. Furthermore, atrazine exposure led to decrease in PSI electron turnover rate for both strains but more so for WT (Figure 2.4) which indicates that loss of MC production may have induced a change in alternative electron flow or the distribution of light energy between PSII and PSI that could have mitigated the consequences of exposure to atrazine. The combined treatment also differently affected the PSI electron turnover rate when MC production is present as the influence of atrazine and HL stress were counterbalanced in MT (Figure 2.4B) while this parameter significantly decreased in WT (Figure 2.4A). Atrazine and HL stress had an antagonistic influence on PSI electron turnover rate for MT (Figure 2.4B) which can be explained by the higher proportion of cyclic electron flow around PSI in the absence of MC production (figure 2.5B) or a

possible change in the balance of the redox status of the PQ pool which relies on the contribution of multiple alternative electron pathways (Alric, 2015, Miller *et al.*, 2021, Nikkanen *et al.*, 2021, Qian *et al.*, 2014a, Schmetterer, 2016).

Absence of intracellular MCs was accompanied by a difference in the intrinsic oxidative stress as reflected by the slightly lower ROS content and SOD activity in control conditions for MT compared to WT (Table 2.3). In the presence of atrazine, SOD activity nearly doubled for both strains while CAT activity increased over five-fold for MT and three-fold for WT (Table 2.3) indicating higher antioxidant activity was needed to counteract the effect of atrazine on ROS production in the absence of intracellular MCs. Interestingly, exposure to HL stress increased ROS content twice-fold for WT while MT remained stable which hints toward a change in the mechanism of ROS generation or regulation under strong light in the absence of intracellular MCs. As the physiology of MT was less affected than WT under most treatments, this result was unexpected as literature often depicts MCs as protective agents in the defense against oxidative stress while referencing higher sensitivity of MC-deficient strains to oxidative stress conditions. For example, in Zilliges *et al.* (2011), the physiological response of PCC 7806 and PCC 7806 *mcy*B$^-$ to photoinhibitory conditions was evaluated after direct addition of up to 1 µM H_2O_2 or a five-day growth period under 300 µmol photons · m^{-2} · s^{-1} light intensity while our investigation followed the single and combined influence of 0.8 µM atrazine for 72h followed or not by 45 min exposure to 1200 µmol photons · m^{-2} · s^{-1} light intensity. Consequently, the dissimilarity between the findings of Zilliges *et al.* (2011) and our research (Table 2.3) could be explained by the difference in the source of oxidative stress (H_2O_2 vs atrazine) and the length of the HL exposure (five days at 300 µmol photons · m^{-2} · s^{-1} vs 45 min at 1200 µmol photons · m^{-2} · s^{-1}).

The combined influence of atrazine and HL produced different outcome on the oxidative stress response and intracellular complexity when MC production was present (Table 2.3). When combined, both stressors had no effect on the ROS content of WT while this parameter decreased in MT which can be explained by the significant rise in CAT and SOD activity in both strains but to a lesser degree in MT (Table 2.3). This result shows that loss of MC production led to the solicitation of a significantly increased activity of antioxidant systems. The antagonistic

interaction between atrazine and HL stress on the ROS content of WT can be explained by the large increase in CAT and SOD activity (Table 2.3). Exposure to atrazine can exacerbate the effect of strong illumination on photosynthetic microorganisms, as demonstrated previously by Fischer et al. (2010) where the combined influence of atrazine (up to 100 µM) and high light exposure (400 and 800 µmol photons $\cdot m^{-2} \cdot s^{-1}$) for 24h produced a synergistic decrease in growth in *Chlamydomonas reinhardtii* which was attributed to higher ROS production. This could explain the synergistic interaction we observed between atrazine and HL stress on SOD activity for MT (Table 2.3). The increase in intrinsic SSC following loss of MC production (Figure 2.6) may be related to the disparity in pigment composition between strains (Table 2.2) and could point toward a reorganization of thylakoidal membranes to compensate for processes related to light collection or transfers of light energy. However, the previous explanation may only account for part of the reason behind the increase in SSC as some authors reported that loss of MC production led to an increase in the amount of gas vesicles and intracellular inclusions (Barchewitz *et al.*, 2019, Meissner *et al.*, 2015) and a change in SSC can also be related to a number of other morphological changes or oxidative damage (Giannuzzi *et al.*, 2021). Under HL stress, the increase in SSC in WT (Figure 2.6A) may be explained by the increase in ROS content (Table 2.3) while the contrasting response of SSC for MT during this treatment (Figure 2.6B) could be related to its stable ROS content (Table 2.3). This discrepancy may be explained by the larger increase in CAT activity for MT compared to WT under HL stress (Table 2.3) and the higher intrinsic CAR content of MT compared with WT (Table 2.2). The previous phenomena could also explain why the single and combined influence of atrazine and HL stress decreased SSC in MT (Figure 2.6B). Pre-exposure of WT to atrazine prevented the increase in SSC observed following strong illumination (Figure 2.6A). This resulted in a significant antagonistic interaction between atrazine and HL on SSC which can be explained by the lack of increase in ROS for this treatment (Figure 2.6A). For MT, the previously described physiological consequences of lack of MC production may explain why the combined influence of atrazine and HL stress produced a significant synergistic interaction for SSC of MT (Figure 2.6B). It is worth noting that some of the results of this study are contradictory. For example, the growth of MT was more affected by atrazine than WT (Table 2.1) while, inversely, photosynthetic efficiency was further decreased by atrazine for WT than MT (Figure 2.1). In light

of these results, further research is needed to fully understand the complexity of the relationship between the ability to produce MCs and the effect of atrazine on photosynthesis and growth of *M*. *aeruginosa*.

From 12 MC congeners assayed, seven were identified in PCC 7806 and five responded significantly to the different photoinhibitory treatments in the presence of atrazine or HL stress (Table 2.4). While there was a clear global trend toward a decrease in total MC content in response to our treatments, this decrease was not significant (Table 2.4). However, some individual intracellular MC variants significantly decreased in response to atrazine or the combined influence of both atrazine and HL stress (Table 2.4). Indeed, atrazine decreased [D-Asp^3]-MC-LR, MC-HilR, MC-LY, MC-LW and MC-LF while the combined influence of atrazine and HL stress decreased MC-LY, MC-LW and MC-LF (Table 2.4). Similar results were observed by Qian *et al.* (2012) where exposure to atrazine led to a significant decrease in intracellular MC content for *Microcystis aeruginosa* FACHB 905. Atrazine exposure is known to decrease ATP production due to the inhibition of photosynthetic electron transport which might explain the decrease in MCs as MC biosynthesis is energy demanding (Briand *et al.*, 2012). Interestingly, there was a complete disappearance of MC-LF after atrazine exposure, but not for the combined treatment of atrazine and HL stress (Table 2.4). As exposure to ROS can lead to the binding of MCs to cysteines located on various proteins (Zilliges *et al.*, 2011), one possible explanation is that MC-LF may have been bound to specific proteins or enzymes during growth in atrazine-contaminated media and subsequent exposure to the HL treatment may have induced the release of this variant in the cytosol. Meissner *et al.* (2013) discussed the implications of LC-MS possibly underevaluating MC content in comparison with molecular methods of quantification such as Western Blot or Dot blot ELISA as the latter techniques are able to distinguish a larger proportion of MCs in the methanol insoluble protein fraction that is unseen using the LC-MS analysis. Therefore, there is a possibility that a decrease in MC content observed following HL exposure may portray an incomplete picture of the fate of MCs in response to the photoinhibitory treatment. Results from Meissner *et al.* (2013) suggests that HL stress stimulates MCs biosynthesis and that the newly synthetized MCs would directly bind to proteins rendering them unavailable for methanol extraction. While it may be important to use multiple methods to fully understand the fate of

MCs, our results still provide valuable information about the consequences of these exposure treatments on free intracellular MCs and offer a good picture of the toxicological potential of MCs in this context. Also, although we may not capture all the complex interactions that occur following specific treatments such as HL exposure, our measurements still provide important insights into the effects of these treatments on intracellular MCs levels and their relations with physiology. Furthermore, the contrasting consequences of our treatments on the different MC congeners indicates that MC variants could prioritize certain physiological functions over others depending on the environmental conditions. A similar process could explain the significant antagonistic relationship observed for the combined effect of atrazine and HL stress on MC-HilR, MC-LY and MC-LF (Table 2.4). From the PCA analysis, we were able to uncover multiple strong relationships between physiological endpoints and total MC content or individual MC congeners (Figure 2.7). The strongest positive relationships uncovered between MCs and physiology were associated to photosynthetic parameters related to photosynthetic efficiency such as ϕ', qP_{REL} or ETR_{max} while the strongest negative relationships were associated with SOD and UQF_{REL} which are parameters elicited in stress conditions (Figure 2.7). Relationships between MCs and photosynthetic efficiency can be explained by energy-intensive nature of MC biosynthesis and these results corroborate with findings that established a clear positive correlation between intracellular MC content and photosynthetic capacity (Briand *et al.*, 2012, Wang *et al.*, 2018, Wiedner *et al.*, 2003) or cell doubling time (Orr and Jones, 1998). Furthermore, modulation of photosynthetic activity through direct or indirect photoinhibitory conditions revealed a strong negative relationship between the redox state of the PSII (UQF_{REL}) and total MCs as well as every individual MC congeners detected with the exception of MC-HilR (Table 2.5). Similar results were obtained by Deblois and Juneau (2010) who speculated that the redox state of PQ (evaluated by UQF_{REL}) may act as a possible modulator of *mcy* gene expression. Moreover, as we identified a difference in the effect of the different treatments on the PSI electron turnover rate between WT and MT (Figure 2.4), the loss of MC production may have affected processes which influence redox pressure either upstream or downstream of the PSI. Such divergence may be explained by a change in alternative electron transfers, abundance and stoichiometry of various photo-oxidizable ETC components, or mechanisms linked to oxygen evolution or aerobic respiration.

Interestingly, PCA revealed that some MC congeners were more closely grouped between themselves and in relation to specific physiological parameters (Figure 2.7). For example, [D-Asp^3]-MC-LR, MC-HilR and MC-LR showed a stronger relation to Chl *a*/CAR, ϕ'_M, qP_{REL} and ETR_{max} than other congeners while MC-LY, MC-LW and MC-LF were more closely related to growth, biovolume, qN_{REL}, PSI electron turnover rate and the ROS content (Figure 2.7). Alternatively, the relationship between [D-Asp^3]-MC-RR and every physiological parameters was too weak to establish any conclusive association between physiology and this MC congener (Figure 2.7). These results suggest a divergence in the potential physiological role that individual MC congeners may possess in relation with central metabolism, photosynthesis and the response to oxidative stress. The possibility that individual MC congeners may possess distinct physiological roles in relation with physiology may explain the wide variation in intracellular concentration between MC congeners as some congeners may, for example, be required to be well distributed within the cell to quickly respond to a variation in ROS content by binding to specific proteins or enzymes. Alternatively, some MC congeners found in smaller concentrations may be involved in the regulation of physiological processes or induce enzymatic cascades in response to a change in environmental conditions or the redox state of the ETC. As such, this perspective offers a wider picture of the potential intracellular functions of MCs in relation to photosynthesis and the response to oxidative stress and highlight the need to consider potential groups of physiological roles for each MC congeners when conducting a similar investigation.

2.7 Conclusion

This investigation allowed to isolate physiological processes which were most affected by the loss of microcystin production in the context of this research thereby improving the focus on the potential physiological role of intracellular microcystin in relation to photosynthesis and the oxidative stress response to photoinhibitory conditions. By using atrazine and HL, we demonstrate that MC must be involved in the regulation of photoacclimatory processes. In sum, our results pointed toward a link between the capacity of microcystin production and NPQ-related mechanisms such as heat dissipation and re-reduction of $P700^+$.

2.8 Supplementary data

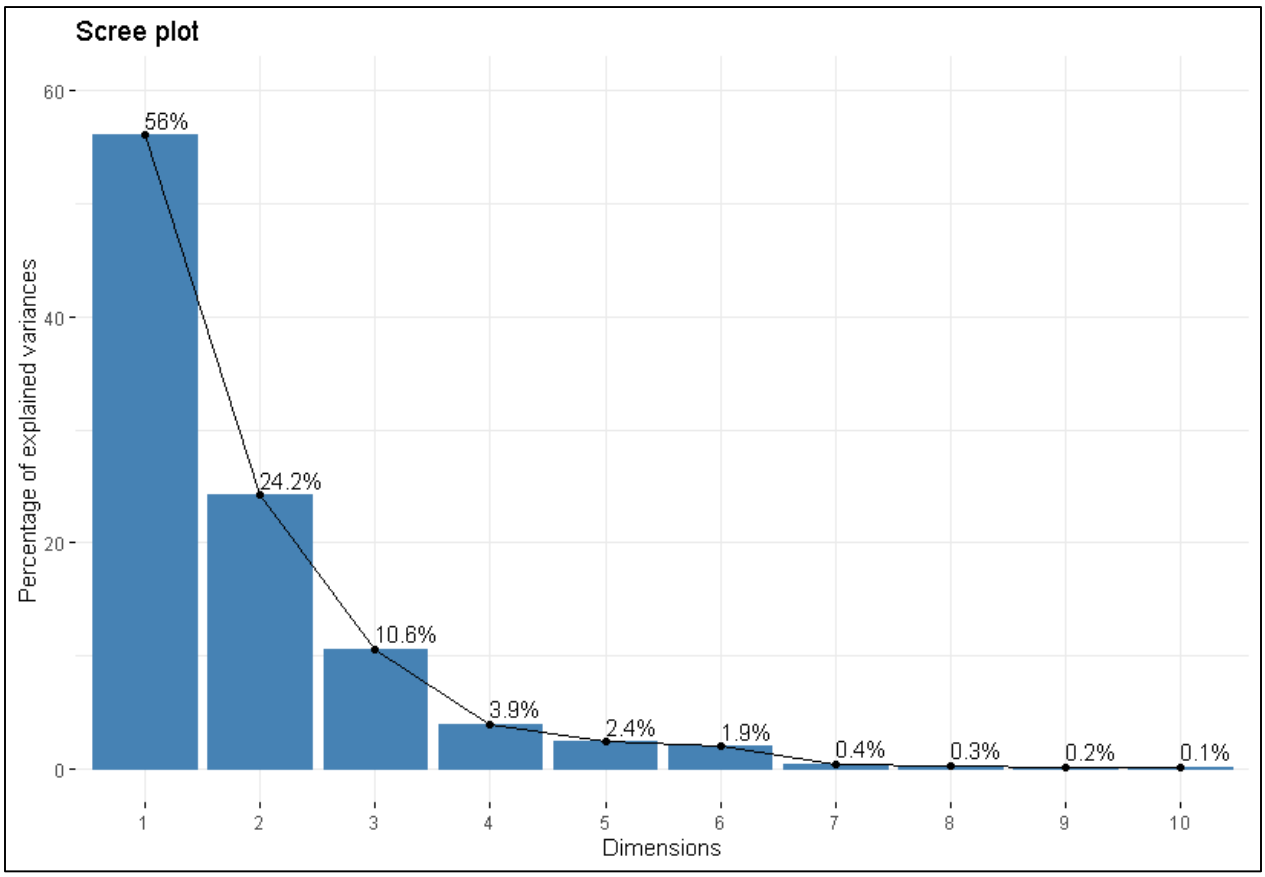

Figure S2.1 PCA scree plot, showing the eigenvalues (variances) of principal components for the physiological profile of a microcystin-producing strain of *M. aeruginosa* PCC 7806 exposed or not to 0.8 µM atrazine, high light stress or the combination of both stress factors. PC1 (56%) and PC2 (24.2%) represented together a large proportion of the total variance.

Author Contributions: Conceptualization, J.N., and P.J.; methodology, J.N. and P.J.; validation, J.N., and P.J.; formal analysis, J.N.; investigation, J.N.; writing—original draft preparation, J.N.; writing—review and editing, J.N. and P.J.; visualization, J.N. All authors have read and agreed to the published version of the manuscript.

2.9 References

Aebi, H. (1984) Catalase in Vitro. *: Vol. 105. Methods in Enzymology* (pp. 121-126).

Alric, J. (2015). The plastoquinone pool, poised for cyclic electron flow? *Frontiers in Plant Science*, *6*(JULY), 540. doi: 10.3389/fpls.2015.00540

Barchewitz, T., Guljamow, A., Meissner, S., Timm, S., Henneberg, M., Baumann, O., Hagemann, M. et Dittmann, E. (2019). Non-canonical localization of RubisCO under high-light conditions in the toxic cyanobacterium *Microcystis aeruginosa* PCC7806. *Environmental Microbiology*, *21*(12), 4836-4851. doi: 10.1111/1462-2920.14837

Bendall, D. S. et Manasse, R. S. (1995). Cyclic photophosphorylation and electron transport. *BBA - Bioenergetics*, *1229*(1), 23-38. doi: 10.1016/0005-2728(94)00195-B

Bennett, A. et Bogorad, L. (1973). Complementary chromatic adaptation in a filamentous blue-green alga. *Journal of Cell Biology*, *58*(2), 419-435. doi: 10.1083/jcb.58.2.419

Beyer Jr, W. F. et Fridovich, I. (1987). Assaying for superoxide dismutase activity: Some large consequences of minor changes in conditions. *Analytical Biochemistry*, *161*(2), 559-566. doi: 10.1016/0003-2697(87)90489-1

Bradford, M. M. (1976). A rapid and sensitive method for the quantitation of microgram quantities of protein utilizing the principle of protein-dye binding. *Analytical Biochemistry*, *72*(1-2), 248-254. doi: 10.1016/0003-2697(76)90527-3

Briand, E., Bormans, M., Quiblier, C., Salençon, M. J. et Humbert, J. F. (2012). Evidence of the cost of the production of microcystins by *Microcystis aeruginosa* under differing light and nitrate environmental conditions. *PLoS ONE*, *7*(1). doi: 10.1371/journal.pone.0029981

Buschmann, C. (1995). Variation of the quenching of chlorophyll fluorescence under different intensities of the actinic light in wildtype plants of tobacco and in an *Aurea* mutant deficient of light harvesting-complex. *Journal of Plant Physiology*, *145*(3), 245-252. doi: 10.1016/S0176-1617(11)81884-5

Ceballos-Laita, L., Calvo-Begueria, L., Lahoz, J., Bes, M.-T., Fillat, M. et Peleato, M.-L. (2015). γ-Lindane Increases Microcystin Synthesis in *Microcystis aeruginosa* PCC7806. *Marine Drugs*, *13*(9), 5666.

Chaffin, J. D., Davis, T. W., Smith, D. J., Baer, M. M. et Dick, G. J. (2018). Interactions between nitrogen form, loading rate, and light intensity on *Microcystis* and *Planktothrix* growth and microcystin production. *Harmful algae*, *73*, 84-97.

Chalifour, A. et Juneau, P. (2011). Temperature-dependent sensitivity of growth and photosynthesis of *Scenedesmus obliquus*, *Navicula pelliculosa* and two strains of *Microcystis aeruginosa* to the herbicide atrazine. *Aquatic Toxicology*, *103*(1-2), 9-17. doi: 10.1016/j.aquatox.2011.01.016

Chalifour, A., LeBlanc, A., Sleno, L. et Juneau, P. (2016). Sensitivity of *Scenedesmus obliquus* and *Microcystis aeruginosa* to atrazine: effects of acclimation and mixed cultures, and their removal ability. *Ecotoxicology*, *25*(10), 1822-1831. doi: 10.1007/s10646-016-1728-5

Chenu, A., Keren, N., Paltiel, Y., Nevo, R., Reich, Z. et Cao, J. (2017). Light Adaptation in Phycobilisome Antennas: Influence on the Rod Length and Structural Arrangement. *Journal of Physical Chemistry B*, *121*(39), 9196-9202. doi: 10.1021/acs.jpcb.7b07781

Davis, T. W., Berry, D. L., Boyer, G. L. et Gobler, C. J. (2009). The effects of temperature and nutrients on the growth and dynamics of toxic and non-toxic strains of *Microcystis* during cyanobacteria blooms. *Harmful Algae*, *8*(5), 715-725. doi: 10.1016/j.hal.2009.02.004

Davis, T. W., Harke, M. J., Marcoval, M. A., Goleski, J., Orano-Dawson, C., Berry, D. L. et Gobler, C. J. (2010). Effects of nitrogenous compounds and phosphorus on the growth of toxic and non-toxic strains of *Microcystis* during cyanobacterial blooms. *Aquatic Microbial Ecology*, *61*(2), 149-162.

Deblois, C. P., Dufresne, K. et Juneau, P. (2013). Response to variable light intensity in photoacclimated algae and cyanobacteria exposed to atrazine. *Aquatic Toxicology*, *126*, 77-84. doi: 10.1016/j.aquatox.2012.09.005

Deblois, C. P. et Juneau, P. (2010). Relationship between photosynthetic processes and microcystin in *Microcystis aeruginosa* grown under different photon irradiances. *Harmful Algae*, *9*(1), 18-24. doi: 10.1016/j.hal.2009.07.001

Deblois, C. P. et Juneau, P. (2012). Comparison of resistance to light stress in toxic and non-toxic strains of *Microcystis aeruginosa* (cyanophyta). *Journal of Phycology*, *48*(4), 1002-1011. doi: 10.1111/j.1529-8817.2012.01191.x

DeLorenzo, M. E., Scott, G. I. et Ross, P. E. (2001). Toxicity of pesticides to aquatic microorganisms: A review. *Environmental Toxicology and Chemistry*, *20*(1), 84-98. doi: doi:10.1002/etc.5620200108

Dittmann, E., Neilan, B. A., Erhard, M., Von Döhren, H. et Börner, T. (1997). Insertional mutagenesis of a peptide synthetase gene that is responsible for hepatotoxin production in the cyanobacterium *Microcystis aeruginosa* PCC 7806. *Molecular Microbiology*, *26*(4), 779-787.

Djediat, C., Feilke, K., Brochard, A., Caramelle, L., Kim Tiam, S., Sétif, P., Gauvrit, T., Yéprémian, C., Wilson, A., Talbot, L., Marie, B., Kirilovsky, D. et Bernard, C. (2020). Light stress in green and red *Planktothrix* strains: The orange carotenoid protein and its related photoprotective mechanism. *Biochimica et Biophysica Acta (BBA) - Bioenergetics*, *1861*(4), 148037. doi: 10.1016/j.bbabio.2019.06.009

Du, Y., Ye, J., Wu, L., Yang, C., Wang, L. et Hu, X. (2017). Physiological effects and toxin release in *Microcystis aeruginosa* and *Microcystis viridis* exposed to herbicide fenoxaprop-p-ethyl. *Environmental Science and Pollution Research*, *24*(8), 7752-7763. doi: 10.1007/s11356-017-8474-y

Ehling-Schulz, M. et Scherer, S. (1999). UV protection in cyanobacteria. *European Journal of Phycology*, *34*(4), 329-338. doi: 10.1080/09670269910001736392

Fedtke, C. et Duke, S. (ed.), (2004). Herbicides. In B. Hock et E. F. Elstner (dir.), *Plant toxicology* (4th éd., p. 247-330). New York, USA : CRC Press.

Feng, B., Wang, C., Wu, X., Tian, C., Tian, Y. et Xiao, B. (2019). Involvement of microcystins, colony size and photosynthetic activity in the benthic recruitment of Microcystis. *Journal of Applied Phycology*, *31*(1), 223-233. doi: 10.1007/s10811-018-1508-0

Genty, B., Briantais, J. M. et Baker, N. R. (1989). The relationship between the quantum yield of photosynthetic electron transport and quenching of chlorophyll fluorescence. *Biochimica et Biophysica Acta - General Subjects*, *990*(1), 87-92. doi: 10.1016/S0304-4165(89)80016-9

Giannuzzi, L., Lombardo, T., Juárez, I., Aguilera, A. et Blanco, G. (2021). A Stochastic Characterization of Hydrogen Peroxide-Induced Regulated Cell Death in *Microcystis aeruginosa*. *Frontiers in Microbiology*, *12*, 1-15. doi: 10.3389/fmicb.2021.636157

Giroux, I. (2022). Présence de pesticides dans l'eau au Québec : Portrait et tendances dans les zones de maïs et de soya – 2018 à 2020. 71 p. + 15 ann. Available online: https://www.environnement.gouv.qc.ca/eau/flrivlac/pesticides.htm (accessed on 24 January 2023).

González-Barreiro, Ó., Rioboo, C., Cid, A. et Herrero, C. (2004). Atrazine-Induced Chlorosis in *Synechococcus elongatus* Cells. *Archives of Environmental Contamination and Toxicology*, *46*(3), 301-307.

He, H., Liu, Y., You, S., Liu, J., Xiao, H. et Tu, Z. (2019). A review on recent treatment technology for herbicide atrazine in contaminated environment. *International Journal of Environmental Research and Public Health*, *16*(24). doi: 10.3390/ijerph16245129

Herbert, S. K., Samson, G., Fork, D. C. et Laudenbach, D. E. (1992). Characterization of damage to photosystems I and II in a cyanobacterium lacking detectable iron superoxide dismutase activity. *Proceedings of the National Academy of Sciences of the United States of America*, *89*(18), 8716-8720.

Islam, M. A. et Beardall, J. (2017). Growth and Photosynthetic Characteristics of Toxic and Non-Toxic Strains of the Cyanobacteria *Microcystis aeruginosa* and *Anabaena circinalis* in Relation to Light. *Microorganisms*, *5*(3), 45. doi: 10.3390/microorganisms5030045

Jähnichen, S., Ihle, T., Petzoldt, T. et Benndorf, J. (2007). Impact of inorganic carbon availability on microcystin production by *Microcystis aeruginosa* PCC 7806. *Applied and environmental microbiology*, *73*(21), 6994-7002.

Joliot, P. et Joliot, A. (2002). Cyclic electron transfer in plant leaf. *Proceedings of the National Academy of Sciences of the United States of America*, *99*(15), 10209-10214. doi: 10.1073/pnas.102306999

Joliot, P. et Joliot, A. (2005). Quantification of cyclic and linear flows in plants. *Proceedings of the National Academy of Sciences of the United States of America*, *102*(13), 4913-4918. doi: 10.1073/pnas.0501268102

Juneau, P., Green, B. R. et Harrison, P. J. (2005). Simulation of Pulse-Amplitude-Modulated (PAM) fluorescence: Limitations of some PAM-parameters in studying environmental stress effects. *Photosynthetica*, *43*(1), 75-83. doi: 10.1007/s11099-005-5083-7

Karapetyan, N. V. (2007). Non-photochemical quenching of fluorescence in cyanobacteria. *Biochemistry. Biokhimiia*, *72*(10), 1127-1135.

Kirilovsky, D. (2007). Photoprotection in cyanobacteria: the orange carotenoid protein (OCP)-related non-photochemical-quenching mechanism. *Photosynthesis Research*, *93*(1-3), 7-16. doi: 10.1007/s11120-007-9168-y

Kirilovsky, D. et Kerfeld, C. A. (2012). The orange carotenoid protein in photoprotection of photosystem II in cyanobacteria. *BBA - Bioenergetics*, *1817*(1), 158-166. doi: 10.1016/j.bbabio.2011.04.013

Kitajima, M. et Butler, W. L. (1975). Quenching of chlorophyll fluorescence and primary photochemistry in chloroplasts by dibromothymoquinone. *BBA - Bioenergetics*, *376*(1), 105-115. doi: 10.1016/0005-2728(75)90209-1

Komenda, J. et Sobotka, R. (2016). Cyanobacterial high-light-inducible proteins - Protectors of chlorophyll-protein synthesis and assembly. *Biochimica et Biophysica Acta - Bioenergetics*, *1857*(3), 288-295. doi: 10.1016/j.bbabio.2015.08.011

Krieger-Liszkay, A. (2005). Singlet oxygen production in photosynthesis. *Journal of Experimental Botany*, *56*(411), 337-346. doi: 10.1093/jxb/erh237

Kumar, S., Habib, K. et Fatma, T. (2008). Endosulfan induced biochemical changes in nitrogen-fixing cyanobacteria. *Science of The Total Environment*, *403*(1), 130-138. doi: https://doi.org/10.1016/j.scitotenv.2008.05.026

Latifi, A., Ruiz, M. et Zhang, C. C. (2009). Oxidative stress in cyanobacteria. *FEMS Microbiology Reviews*, *33*(2), 258-278. doi: 10.1111/j.1574-6976.2008.00134.x

Ledford, H. K. et Niyogi, K. K. (2005). Singlet oxygen and photo-oxidative stress management in plants and algae. *Plant, Cell and Environment*, *28*(8), 1037-1045. doi: 10.1111/j.1365-3040.2005.01374.x

Lichtenthaler, H. K. (1987) Chlorophylls and Carotenoids: Pigments of Photosynthetic Biomembranes. *: Vol. 148. Methods in Enzymology* (pp. 350-382).

Liu, J., van Oosterhout, E., Faassen, E., Lurling, M., Helmsing, N. et Van de Waal, D. (2016). Elevated pCO_2 causes a shift towards more toxic microcystin variants in nitrogen limited *Microcystis aeruginosa*. *92*(2), 1-8. doi: 10.1093/femsec/fiv159

Lockert, C. K., Hoagland, K. D. et Siegfried, B. D. (2006). Comparative sensitivity of freshwater algae to atrazine. *Bulletin of Environmental Contamination and Toxicology*, *76*(1), 73-79. doi: 10.1007/s00128-005-0891-9

Makower, A. K., Schuurmans, J. M., Groth, D., Zilliges, Y., Matthijs, H. C. P. et Dittmann, E. (2015). Transcriptomics-aided dissection of the intracellular and extracellular roles of microcystin in *Microcystis aeruginosa* PCC 7806. *Applied and Environmental Microbiology*, *81*(2), 544-554. doi: 10.1128/AEM.02601-14

Meissner, S., Fastner, J. et Dittmann, E. (2013). Microcystin production revisited: conjugate formation makes a major contribution. *Environmental Microbiology*, *15*(6), 1810-1820. doi: 10.1111/1462-2920.12072

Meissner, S., Steinhauser, D. et Dittmann, E. (2015). Metabolomic analysis indicates a pivotal role of the hepatotoxin microcystin in high light adaptation of *Microcystis*. *Environmental Microbiology*, *17*(5), 1497-1509. doi: 10.1111/1462-2920.12565

Miller, N. T., Vaughn, M. D. et Burnap, R. L. (2021). Electron flow through NDH-1 complexes is the major driver of cyclic electron flow-dependent proton pumping in cyanobacteria. *Biochimica et Biophysica Acta - Bioenergetics*, *1862*(3), 148354. doi: 10.1016/j.bbabio.2020.148354

Müller, P., Li, X.-P. et Niyogi, K. K. (2001). Non-Photochemical Quenching. A Response to Excess Light Energy. *Plant Physiology*, *125*(4), 1558-1566. doi: 10.1104/pp.125.4.1558

Munoz, G., Vo Duy, S., Roy-Lachapelle, A., Husk, B. et Sauvé, S. (2017). Analysis of individual and total microcystins in surface water by on-line preconcentration and desalting coupled to liquid chromatography tandem mass spectrometry. *Journal of Chromatography A*, *1516*, 9-20. doi: 10.1016/j.chroma.2017.07.096

Murata, N., Takahashi, S., Nishiyama, Y. et Allakhverdiev, S. I. (2007). Photoinhibition of photosystem II under environmental stress. *Biochimica et Biophysica Acta - Bioenergetics*, *1767*(6), 414-421. doi: 10.1016/j.bbabio.2006.11.019

Muzzopappa, F. et Kirilovsky, D. (2020). Changing Color for Photoprotection: The Orange Carotenoid Protein. *Trends in Plant Science*, *25*(1), 92-104. doi: 10.1016/j.tplants.2019.09.013

Nikkanen, L., Solymosi, D., Jokel, M. et Allahverdiyeva, Y. (2021). Regulatory electron transport pathways of photosynthesis in cyanobacteria and microalgae: Recent advances and biotechnological prospects. *Physiologia Plantarum*, *173*(2), 514-525. doi: 10.1111/ppl.13404

Nishiyama, Y., Yamamoto, H., Allakhverdiev, S. I., Inaba, M., Yokota, A. et Murata, N. (2001). Oxidative stress inhibits the repair of photodamage to the photosynthetic machinery. *EMBO Journal*, *20*(20), 5587-5594. doi: 10.1093/emboj/20.20.5587

Niyogi, K. K. (1999) Photoprotection revisited: Genetic and molecular approaches. *: Vol. 50. Annual Review of Plant Biology* (pp. 333-359).

Niyogi, K. K. (2000). Safety valves for photosynthesis. *Current Opinion in Plant Biology*, *3*(6), 455-460. doi: 10.1016/S1369-5266(00)00113-8

Omidi, A., Esterhuizen-Londt, M. et Pflugmacher, S. (2018). Still challenging: the ecological function of the cyanobacterial toxin microcystin - What we know so far. *Toxin Reviews*, *37*(2), 87-105.

Orr, P. T. et Jones, G. J. (1998). Relationship between microcystin production and cell division rates in nitrogen-limited *Microcystis aeruginosa* cultures. *Limnology and Oceanography*, *43*(7), 1604-1614. doi: 10.4319/lo.1998.43.7.1604

Packer, J. E., Mahood, J. S., Mora-Arellano, V. O., Slater, T. F., Willson, R. L. et Wolfenden, B. S. (1981). Free radicals and singlet oxygen scavengers: Reaction of a peroxy-radical with β-carotene, diphenyl furan and 1,4-diazobicyclo(2,2,2)-octane. *Biochemical and Biophysical Research Communications*, *98*(4), 901-906. doi: 10.1016/0006-291X(81)91196-7

Perron, M. C. et Juneau, P. (2011). Effect of endocrine disrupters on photosystem II energy fluxes of green algae and cyanobacteria. *Environmental Research*, *111*(4), 520-529. doi: 10.1016/j.envres.2011.02.013

Phelan, R. R. et Downing, T. G. (2011). A growth advantage for microcystin production by microcystin PCC7806 under high light. *Journal of Phycology*, *47*(6), 1241-1246. doi: doi:10.1111/j.1529-8817.2011.01056.x

Potter, T. L., Truman, C. C., Webster, T. M., Bosch, D. D. et Strickland, T. C. (2011). Tillage, cover-crop residue management, and irrigation incorporation impact on fomesafen runoff. *Journal of agricultural and food chemistry*, *59*(14), 7910-7915.

Qian, H., Pan, X., Chen, J., Zhou, D., Chen, Z., Zhang, L. et Fu, Z. (2012). Analyses of gene expression and physiological changes in *Microcystis aeruginosa* reveal the phytotoxicities of three environmental pollutants. *Ecotoxicology*, *21*(3), 847-859. doi: 10.1007/s10646-011-0845-4

Qian, H., Tsuji, T., Endo, T. et Sato, F. (2014a). PGR5 and NDH pathways in photosynthetic cyclic electron transfer respond differently to sublethal treatment with photosystem-interfering herbicides. *Journal of Agricultural and Food Chemistry*, *62*(18), 4083-4089. doi: 10.1021/jf500143f

Qian, H., Wei, Y., Bao, G., Huang, B. et Fu, Z. (2014b). Atrazine affects the circadian rhythm of *Microcystis aeruginosa*. *Chronobiology International*, *31*(1), 17-26. doi: 10.3109/07420528.2013.817414

Qian, H., Yu, S., Sun, Z., Xie, X., Liu, W. et Fu, Z. (2010). Effects of copper sulfate, hydrogen peroxide and N-phenyl-2-naphthylamine on oxidative stress and the expression of genes involved photosynthesis and microcystin disposition in *Microcystis aeruginosa*. *Aquatic Toxicology*, *99*(3), 405-412.

R Core Team. (2020). R: A language and environment for statistical computing. R Foundation for Statistical Computing.

Rachedi, R., Foglino, M. et Latifi, A. (2020). Stress signaling in cyanobacteria: A mechanistic overview. *Life*, *10*(12), 1-24. doi: 10.3390/life10120312

Rakhimberdieva, M. G., Vavilin, D. V., Vermaas, W. F. J., Elanskaya, I. V. et Karapetyan, N. V. (2007). Phycobilin/chlorophyll excitation equilibration upon carotenoid-induced non-photochemical fluorescence quenching in phycobilisomes of the cyanobacterium *Synechocystis sp.* PCC 6803. *Biochimica et Biophysica Acta - Bioenergetics*, *1767*(6), 757-765. doi: 10.1016/j.bbabio.2006.12.007

Rantala, A., Fewer, D. P., Hisbergues, M., Rouhiainen, L., Vaitomaa, J., Börner, T. et Sivonen, K. (2004). Phylogenetic evidence for the early evolution of microcystin synthesis. *Proceedings of the National Academy of Sciences of the United States of America*, *101*(2), 568-573. doi: 10.1073/pnas.0304489101

Raps, S., Kycia, J. H., Ledbetter, M. C. et Siegelman, H. W. (1985). Light Intensity Adaptation and Phycobilisome Composition of *Microcystis aeruginosa*. *Plant Physiology*, *79*(4), 983-987. doi: 10.1104/pp.79.4.983

Rippka, R., Deruelles, J. et Waterbury, J. B. (1979). Generic assignments, strain histories and properties of pure cultures of cyanobacteria. *Journal of General Microbiology*, *111*(1), 1-61.

Schmetterer, G. (ed.), (2016). The Respiratory Terminal Oxidases (RTOs) of Cyanobacteria. In W. Cramer et T. Kallas (dir.), *Cytochrome Complexes: Evolution, Structures, Energy Transduction, and Signaling. Advances in Photosynthesis and Respiration* (vol. 41, p. 331-355). Dordrecht, NL : Springer.

Schuurmans, J. M., Brinkmann, B. W., Makower, A. K., Dittmann, E., Huisman, J. et Matthijs, H. C. P. (2018). Microcystin interferes with defense against high oxidative stress in harmful cyanobacteria. *Harmful Algae*, *78*, 47-55. doi: 10.1016/j.hal.2018.07.008

Shinopoulos, K. E., Yu, J., Nixon, P. J. et Brudvig, G. W. (2014). Using site-directed mutagenesis to probe the role of the D2 carotenoid in the secondary electron-transfer pathway of photosystem II. *Photosynthesis Research*, *120*(1-2), 141-152. doi: 10.1007/s11120-013-9793-6

Skafi, M., Vo Duy, S., Munoz, G., Dinh, Q. T., Simon, D. F., Juneau, P. et Sauvé, S. (2021). Occurrence of microcystins, anabaenopeptins and other cyanotoxins in fish from a freshwater wildlife reserve impacted by harmful cyanobacterial blooms. *Toxicon*, *194*, 44-52. doi: 10.1016/j.toxicon.2021.02.004

Spoof, L. et Arnaud, C. (ed.), (2017). Appendix 3: Tables of Microcystins and Nodularins. In J. Meriluoto, L. Spoof et G. A. Codd (dir.), *Handbook of Cyanobacterial Monitoring and Cyanotoxin Analysis* (p. 526-537). Chichester, UK : John Wiley & Sons.

Stachowski-Haberkorn, S., JérÔme, M., Rouxel, J., Khelifi, C., Rincé, M. et Burgeot, T. (2013). Multigenerational exposure of the microalga *Tetraselmis suecica* to diuron leads to spontaneous long-term strain adaptation. *Aquatic Toxicology*, *140-141*, 380-388. doi: 10.1016/j.aquatox.2013.06.016

Suominen, S., Brauer, V. S., Rantala-Ylinen, A., Sivonen, K. et Hiltunen, T. (2017). Competition between a toxic and a non-toxic *Microcystis* strain under constant and pulsed nitrogen and phosphorus supply. *Aquatic Ecology*, *51*(1), 117-130. doi: 10.1007/s10452-016-9603-2

Tamary, E., Kiss, V., Nevo, R., Adam, Z., Bernát, G., Rexroth, S., Rögner, M. et Reich, Z. (2012). Structural and functional alterations of cyanobacterial phycobilisomes induced by high-light stress. *Biochimica et Biophysica Acta - Bioenergetics*, *1817*(2), 319-327. doi: 10.1016/j.bbabio.2011.11.008

Tonk, L., Visser, P. M., Christiansen, G., Dittmann, E., Snelder, E. O. F. M., Wiedner, C., Mur, L. R. et Huisman, J. (2005). The Microcystin Composition of the Cyanobacterium *Planktothrix agardhii* Changes toward a More Toxic Variant with Increasing Light Intensity. *Applied and Environmental Microbiology*, *71*(9), 5177-5181. doi: 10.1128/aem.71.9.5177-5181.2005

Tóth, T. N., Chukhutsina, V., Domonkos, I., Knoppová, J., Komenda, J., Kis, M., Lénárt, Z., Garab, G., Kovács, L., Gombos, Z. et Van Amerongen, H. (2015). Carotenoids are essential for the assembly of cyanobacterial photosynthetic complexes. *Biochimica et Biophysica Acta - Bioenergetics*, *1847*(10), 1153-1165. doi: 10.1016/j.bbabio.2015.05.020

Wang, X., Wang, P., Wang, C., Qian, J., Feng, T. et Yang, Y. (2018). Relationship between photosynthetic capacity and microcystin production in toxic microcystis aeruginosa under different Iron regimes. *International Journal of Environmental Research and Public Health*, *15*(9), 1954. doi: 10.3390/ijerph15091954

Weiner, J. A., DeLorenzo, M. E. et Fulton, M. H. (2004). Relationship between uptake capacity and differential toxicity of the herbicide atrazine in selected microalgal species. *Aquatic Toxicology*, *68*(2), 121-128. doi: 10.1016/j.aquatox.2004.03.004

Wiedner, C., Visser, P. M., Fastner, J., Metcalf, J. S., Codd, G. A. et Mur, L. R. (2003). Effects of light on the microcystin content of *Microcystis* strain PCC 7806. *Applied and Environmental Microbiology*, *69*(3), 1475-1481. doi: 10.1128/AEM.69.3.1475-1481.2003

Yang, Z., Kong, F., Shi, X., Yu, Y. et Zhang, M. (2015). Effects of UV-B radiation on microcystin production of a toxic strain of *Microcystis aeruginosa* and its competitiveness against a non-toxic strain. *Journal of Hazardous Materials*, *283*, 447-453. doi: 10.1016/j.jhazmat.2014.09.053

Young, F. M., Morrison, L. F., James, J. et Codd, G. A. (2008). Quantification and localization of microcystins in colonies of a laboratory strain of *Microcystis* (Cyanobacteria) using immunological methods. *European Journal of Phycology*, *43*(2), 217-225. doi: 10.1080/09670260701880460

Young, F. M., Thomson, C., Metcalf, J. S., Lucocq, J. M. et Codd, G. A. (2005). Immunogold localisation of microcystins in cryosectioned cells of *Microcystis*. *Journal of Structural Biology*, *151*(2), 208-214. doi: 10.1016/j.jsb.2005.05.007

Yu, X., Huang, C., Wu, L., Hua, S., Ye, J., Meng, L. et Xu, C. (2021). Effects of the herbicides quizalofop-p-ethyl and quizalofop-ethyl on the physiology, oxidative damage, synthesis, and release of microcystin-LR in *Microcystis aeruginosa*. *Science of the Total Environment*, *776*, 146036. doi: 10.1016/j.scitotenv.2021.146036

Zhang, M., Wang, X., Tao, J., Li, S., Hao, S., Zhu, X. et Hong, Y. (2018). PAHs would alter cyanobacterial blooms by affecting the microcystin production and physiological characteristics of *Microcystis aeruginosa*. *Ecotoxicology and Environmental Safety*, *157*, 134-142. doi: 10.1016/j.ecoenv.2018.03.052

Zhang, Q., Song, Q., Wang, C., Zhou, C., Lu, C. et Zhao, M. (2017). Effects of glufosinate on the growth of and microcystin production by *Microcystis aeruginosa* at environmentally relevant concentrations. *Science of The Total Environment*, *575*, 513-518. doi: 10.1016/j.scitotenv.2016.09.011

Zhang, Y., Whalen, J. K., Vo Duy, S., Munoz, G., Husk, B. R. et Sauvé, S. (2020). Improved extraction of multiclass cyanotoxins from soil and sensitive quantification with on-line purification liquid chromatography tandem mass spectrometry. *Talanta*, *216*, 120923. doi: 10.1016/j.talanta.2020.120923

Zhu, Y., Graham, J. E., Ludwig, M., Xiong, W., Alvey, R. M., Shen, G. et Bryant, D. A. (2010). Roles of xanthophyll carotenoids in protection against photoinhibition and oxidative stress in the cyanobacterium *Synechococcus* sp. strain PCC 7002. *Archives of Biochemistry and Biophysics*, *504*(1), 86-99. doi: 10.1016/j.abb.2010.07.007

Zilliges, Y., Kehr, J. C., Meissner, S., Ishida, K., Mikkat, S., Hagemann, M., Kaplan, A., Börner, T. et Dittmann, E. (2011). The cyanobacterial hepatotoxin microcystin binds to proteins and increases the fitness of Microcystis under oxidative stress conditions. *PLoS ONE*, *6*(3), e17615. doi: 10.1371/journal.pone.0017615

[Cette page a été laissée intentionnellement blanche]

CHAPITRE 3

PHOTOSYNTHETIC INTERSYSTEM ELECTRON FLOW BETWEEN A MICROCYSTIN-PRODUCING STRAIN OF *MICROCYSTIS AERUGINOSA* PCC 7806 AND A MICROCYSTIN-LACKING MUTANT HOMOLOGUE PCC 7806 *mcy*B$^-$ REVEALS POTENTIAL SITES OF INTERACTION BETWEEN INTRACELLULAR MICROCYSTIN AND THE ELECTRON TRANSPORT CHAIN

Jonathan Naoum[1] and Philippe Juneau[1]

[1]Département des Sciences Biologiques, GRIL-TOXEN-EcotoQ, Ecotoxicology of Aquatic Microorganisms Laboratory, University du Québec à Montréal, Succursale Centre-ville, C.P. 8888 Montréal, Québec H3C 3P8, Canada

Will be submitted to mBio

[Cette page a été laissée intentionnellement blanche]

3.1 Résumé

Les microcystines (MCs) intracellulaires ont étés reliées aux processus en lien à la dissipation de l'énergie ainsi que les mécanismes qui font pression sur le P700 (Chapitre 2). Or, l'origine de ces différences reste largement incomprise. De ce contexte, ce papier vise à identifier les conséquences de la perte de production de MCs sur des processus en lien aux voies alternatives de transport d'électrons et l'état redox de la chaîne intermédiaire de transport d'électrons. Pour ce faire, il a été question de comparer PCC 7806 et son homologue mutant dépourvu de la capacité de produire les MCs PCC 7806 *mcy*B$^-$ au niveau de la proportion d'énergie absorbée par le PSII, la production et la consommation d'oxygène, les cinétiques d'oxydoréduction du P700, Cyt *f* et de la PlastoC de même que l'abondance maximale de la forme photo-oxydable de ces composantes et le pourcentage de transport cyclique d'électron autour du PSI. De cette comparaison, il a été possible de déterminer que la perte de production de MCs a entraîné une diminution dans la vitesse des cinétiques en aval du PSII soit au niveau du PSI et de PlastoC ainsi qu'une augmentation dans l'abondance en PlastoC photo-oxydable. Aussi, la perte de production de MCs a mené à une diminution dans la production et la consommation d'O_2, une diminution dans la proportion de lumière absorbée par le PSII et une augmentation dans la proportion en transport cyclique autour du PSI. Ainsi, il a été possible de relier la capacité à produire les MCs à la régulation des processus responsables du maintien de l'homéostasie de l'état d'oxydoréduction de la chaîne de transport d'électron comme les transports alternatifs d'électrons. Par extension, il est possible de spéculer sur un rôle physiologique des MCs intracellulaires au niveau des processus régulés par l'état d'oxydoréduction de la chaîne de transport d'électrons comme l'expression génique régulée par l'état redox de la réserve de PQ, les états de transition et la distribution de l'énergie lumineuse ainsi que le taux d'assemblage et de dégradation des phycobilisomes.

Mots clés: Microcystines, homéostasie, transporteurs d'électrons intersystème, P700, cytochrome *f*, plastocyanine, proportion de lumière absorbée par le PSII, production d'oxygène, consommation d'oxygène, transport cyclique d'électrons

[Cette page a été laissée intentionnellement blanche]

3.2 Abstract

Intracellular microcystins (MCs) have been linked to processes related to energy dissipation as well as mechanisms that put pressure on the P700 (Chapter 2). However, the origin of these differences remains largely unknown. In this context, this paper aimed to identify the consequences of the loss of MC production on processes related to alternative electron transport pathways and the redox state of the intersystem electron transport chain. To this end, PCC 7806 and its mutant homologue unable to produce MCs PCC 7806 *mcy*B$^-$ were compared with respect to the proportion of energy absorbed by PSII, oxygen production/consumption, redox kinetics of P700, Cyt *f* and PlastoC as well as the maximum abundance of the photo-oxidizable form of these components and the proportion of cyclic electron transport around PSI. From this comparison, it was possible to determine that the loss of MC production resulted in a decrease in the rate of kinetics downstream of the PSII (within PSI and PlastoC) as well as an increase in the abundance of photo-oxidizable PlastoC. Also, the loss of MC production led to a decrease in O_2 production and consumption, a decrease in the proportion of light absorbed by the PSII and an increase in the proportion of cyclic electron flow around PSI. Thus, it was possible to link the ability to produce MCs to the regulation of processes responsible for maintaining the homeostasis of the redox state of the electron transport chain such as alternative electron transport. By extension, it is possible to speculate on a physiological role of intracellular MCs in relation with processes regulated by the redox state of the electron transport chain such as the PQ pool redox-controlled gene expression, state transition and light energy distribution as well as the rate of assembly and disassembly of phycobilisomes.

Keywords: Microcystins, homeostasis, intersystem electron flow, P700, cytochrome *f*, plastocyanin, proportion of light absorbed by PSII, oxygen production, oxygen consumption, cyclic electron flow

[Cette page a été laissée intentionnellement blanche]

3.3 Introduction

Cyanobacteria are one of the earliest groups of oxygenic photosynthetic microorganisms which originated nearly 2.4 billion years ago (Sánchez-Baracaldo and Cardona, 2020). For photosynthesis to occur in cyanobacteria, light energy is first captured by phycobilisomes then redirected to reaction centers of photosystem II (PSII) and photosystem I (PSI) (Ueno *et al.*, 2017). In proximity of the PSII, light energy enables the oxygen evolving complex to breaks down water molecules in order to supply electrons to the electron transport chain (ETC) (Krewald *et al.*, 2015). The linear electron flow refers to the supply of electrons originating from the breakdown of water which crosses the PSII then the PSI to ultimately reduce NADP+ into NADPH (Stirbet *et al.*, 2020). In parallel, H+ are being released from water as well as pumped across the thylakoid membrane in order to establish a proton gradient that will enable the proton-translocating ATP synthase to form ATP through the binding of ADP and inorganic phosphate (Mullineaux, 2014). Otherwise, electrons can be reintroduced in or redirected from the ETC through multiple alternative electron pathways (AEPs) which are crucial to the proper function of the photosynthetic ETC. AEPs serve to prevent overreduction of the ETC in the event that the Calvin-Benson-Bassham cycle becomes saturated, thus limiting the generation of reactive oxygen species (ROS) (Nikkanen *et al.*, 2021). When ROS production becomes excessive, the photosystems are subject to degradation. Although overproduction of ROS can inhibit de novo synthesis of the D1 protein in PSII, reparation of a damaged PSI is a much slower process (Tikkanen *et al.*, 2014). Consequently, the PSI is at the center of most AEPs to ensure proper suppression of excessive excitation pressure. Multiple AEPs have been identified in cyanobacteria which implicate flavodiiron (FLV) proteins that enables a Mehler-like reaction (Bersanini *et al.*, 2014), respiratory terminal oxidases (RTOs) such as the cytochrome *bd* quinol oxidase (Cyd) and the aa_3-type cytochrome *c* oxidase (COX) complex which participate in the regulation of electron flow to PSI (Berry *et al.*, 2002, Ermakova *et al.*, 2016) and the NADH dehydrogenase-like (NDH) complex that mostly coordinates the reuptake of electrons from ferredoxin (FR) towards the pool of plastoquinones (PQ) (Miller *et al.*, 2021). The latter AEP functions as the main pathway for cyclic electron flow around PSI which can alternatively be mediated by the proton gradient regulation 5 (PGR5) and PGR-like-1 (PGRL1) where electrons are recirculated in the ETC after crossing the PSI in order to produce ATP without generating NADPH

(Lea-Smith *et al.*, 2016, Ma *et al.*, 2021). Because of the lack of compartmentalization in cyanobacteria, the respiratory electron transport chain and the photosynthetic ETC are closely intertwined (Ogawa *et al.*, 2021). Consequently, there is a significant reuptake of electrons in the ETC coming from respiratory electron flow towards the plastoquinone (PQ) pool via the NDH-1 and the succinate dehydrogenase (SDH) complexes (Liu, 2016) or may be directly transferred to the PSI instead of respiratory terminal oxidases (Liu *et al.*, 2012).

Cyanobacteria are known to produce a family of cyanotoxins called microcystins (MCs) which were found to be present during the early evolution of these photosynthetic microorganisms (Rantala *et al.*, 2004). While MCs are classified as secondary metabolites, mounting evidences point toward strong relationship between these toxins and important physiological functions such as modulation of proteins and enzymes as well as playing a role in protection against oxidative stress by possibly interacting with the antioxidant system or by scavenging ROS (Dziallas and Grossart, 2011, Malanga *et al.*, 2019). Furthermore, MCs were found to bind to specific proteins by way of redox-sensitive cysteines and that oxidative conditions, such as high light stress or addition of H_2O_2, enhance the binding of MCs (Zilliges *et al.*, 2011). The RbcL subunit of the enzyme RuBisCO was also found to be the target of MCs indicating a possible physiological role of MCs in carbon fixation/photorespiration (Zilliges *et al.*, 2011). Photorespiration competes with carbon assimilation and consumes oxygen through RuBisCO-catalyzed oxygenation (Tcherkez, 2016) which lowers photosynthetic capacity in order to dissipate excess photosynthetic energy (Busch, 2020). Moreover, changing light conditions can affect the ratio between NADPH and $NADP^+$ which can affect the PQ redox status and ultimately promote or inhibit photorespiration rate (Nawrocki *et al.*, 2019). It has become increasingly clear that MCs may serve a significant function in relation with photosynthesis and its regulation as MCs were found to be preferentially located on the thylakoidal membrane (Djediat *et al.*, 2020, Young *et al.*, 2008, Young *et al.*, 2005) and light may modulate the biosynthesis of MCs (Deblois and Juneau, 2010, Kaebernick *et al.*, 2000, Wiedner *et al.*, 2003). Furthermore, as MCs were found to be directly involved in multiple redox-sensitive processes, these toxins may also be closely connected with AEPs as well as redox-controlled regulation of gene expression or functional plasticity of intracellular components. However, literature lacks findings about a potential relationship between MCs and such processes.

Thus, the objective of this research is to determine if there is a difference between a wild MC-producing strain of *Microcystis aeruginosa* PCC 7806 and its non-MC-producing mutant homologue strain PCC 7806 *mcy*B$^-$ in regard to processes related to the redox state on intersystem components. Consequently, this research put emphasis on a possible link between the capacity of producing MCs and the redox state of intersystem photosynthetic components and how they are affected by the inactivation of MC production and may provide valuable insights on the potential physiological role of intracellular MCs in relation with these redox-sensitive processes.

3.4 Methods

3.4.1 Cultures

The strains used in this research were obtained from the Pasteur Culture collection of Cyanobacteria (PCC, Pasteur Institute, Paris, France). The wild microcystin-producing strain of *Microcystis aeruginosa* PCC 7806 (WT) and its microcystin-deficient counterpart PCC 7806 *mcy*B$^-$ (MT) were maintained in mid-exponential growth phase prior to the experiment. MT was deprived of its capacity to produce microcystin through deletion of the *mcy*B gene in the operon responsible for MC biosynthesis (Dittmann *et al.*, 1997). Cells were inoculated at 1 000 000 cells per ml. Growth occurred at 24°C in sterile BG-11 media (pH 7.4, (Rippka *et al.*, 1979)) under 35 µmol photons $\cdot$ m^{-2} $\cdot$ s^{-1} illumination with a light:dark photoperiod of 12h:12h provided by a combination of incandescent bulbs (Philips 60W) and white fluorescent lamps (Philips, F72T8/TL841/HO, USA). Cultures were sampled after 7 days of growth (exponential phase) and samples were concentrated to 2.5 µg/ml Chl *a* prior to every analysis excepted for the determination of photosynthetic activity using Pulse-Amplitude-Modulated fluorimetry.

3.4.2 Maximal and operational PSII quantum yields

Before every measurement, cultures were dark-acclimated for 15 min to allow reoxidation of the electron transport chain components. Following dark acclimation, culture samples were loaded in a liquid culture adapter of a Pulse-Amplitude-Modulated fluorometer (WATER-PAM, Heinz Walz GmbH, Effeltrich, Germany) for the determination of the maximal and operational PSII quantum yields. Then, we recorded the initial fluorescence for a dark-acclimated sample (F_0) in

the absence of actinic illumination which was followed by a flash of saturating light (800 ms, 1685 µmol photons · m^{-2} · s^{-1}) to induce the maximal fluorescence signal for a dark-acclimated sample (F_M). Afterwards, the sample was exposed to actinic light (35 µmol photons · m^{-2} · s^{-1}) for 60 seconds followed by a pulse of saturating light (800 ms, 1685 µmol photons · m^{-2} · s^{-1}) before and during which the fluorescence signal was recorded to obtain F_s and F'_M, respectively. Subsequently, actinic illumination was closed and the fluorescence signal was allowed to stabilize. Then, DCMU was added to the sample (final concentration of 10 µM) and a flash of saturating light (800 ms, 1685 µmol photons · m^{-2} · s^{-1}) was applied in order to record the maximal fluorescence when the PSII reaction centers are fully reduced ($F_{M\ DCMU}$) (Campbell et al., 1998). From these fluorescence values, we calculated the maximal (ϕ_M) and operational (ϕ'_M) PSII quantum yields according to Kitajima and Butler (1975) and Genty *et al.* (1989), respectively.

3.4.3 Photosynthetic oxygen evolution and cell respiration

Photosynthetic oxygen production and respiratory oxygen consumption were measured on whole-cells using a Clark-type oxygen electrode (Chlorolab 2, Hansatech Instruments, Norfolk, UK) as described in González *et al.* (2001). Prior to the oxygen evolution measurements, Chl *a* normalized cultures were dark acclimated for 15 min at room temperature. Oxygen evolution was followed for 5 min under actinic light at 650 nm with a PAR of 500 µmol photons · m^{-2} · s^{-1} then respiratory oxygen consumption was immediately measured for 5 min in the dark. The rate of oxygen production and subsequent oxygen consumption was determined using the Oxytrace+ software (Hansatech Instruments, Norfolk, UK).

3.4.4 Proportion of light energy absorbed by PSII

Relative PSII and PSI content were obtained from the determination of PSII specific and whole-cell Chl *a* absorption coefficient as described in Deblois *et al.* (2013). First, *in vivo* light absorption spectra of Chl *a* normalized cultures were obtained between 350 and 750 nm using a Cary 300 UV-VIS spectrophotometer (Varian Instruments, Walnut Creek, CA) fitted with an integrating sphere attachment. The same concentrated cultures were then transferred into a Cary Eclipse spectrofluorometer (Varian Instruments, Walnut Creek, CA) for the determination of the *in vivo*

fluorescence excitation spectrum between 400 and 700 nm with monitoring at 730 nm. A long pass glass filter (RG695, Schott, AG, Mainz, Germany) was placed in front of the emission beam to negate the contribution of light scattering to the measurements. The same measurement was repeated following addition of DCMU (final concentration of 50 µM) and exposure to white light at 500 µmol photons · m^{-2} · s^{-1} for 1 min to eliminate variable fluorescence. The *in vivo* light absorption spectra was corrected at 750 nm and the absorbance value at each wavelength was converted to the Chl *a* specific absorption coefficient $a^*_{\varphi}(\lambda)$ (m^2 · mg Chl a^{-1}) using eq. 1.

$$a^*_{\varphi}(\lambda) = \frac{2.3 \cdot (\text{O.D.})}{(d \cdot \text{Chl})} \qquad (1)$$

where *d* is the cuvette path length and Chl is the chlorophyll a concentration (mg · m^{-3}). To correct for instrument specific wavelength variation of the excitation beam intensity, the fluorescence excitation spectra was quantum corrected using a solution of Basic Blue 3 dye (4.1 g L^{-1}) dissolved in ethylene glycol.

3.4.5 P700, cytochrome *f* (Cyt *f*) and plastocyanin (PlastoC) kinetics

P700 kinetics was determined according to Joliot and Joliot (2005) and Cyt *f* and PlastoC kinetics were obtained as described in Ungerer et al. (2018). Prior to every redox kinetic measurement, Chl *a* normalized cultures were dark acclimated for 15 min. Using a JTS-10 pump probe spectrophotometer (JTS-10, Spectrologix, USA), variations in change in absorbance were measured during 5 sec actinic illumination followed by 5-10 sec of darkness. For P700, actinic illumination occurred under 630 nm at 150 µmol photons · m^{-2} · s^{-1} to excite both PSII and PSI. To isolate P700 kinetics, the LED detection light array was in the Far red portion of the light spectra (705-740 nm, 1400 µmol photons · m^{-2} · s^{-1}) and P700 cutoff filters (thickness of 6 mm, Schott) were placed in front of the sample and reference photodiode. To correct for unspecified contributions from the P700 kinetic, this measurement was first obtained using an interference filter at 705 nm then repeated using an interference filter at 740 nm. The final P700 kinetic was obtained from the subtraction of the kinetic measured at 740 nm from the kinetic recorded at 705 nm. Half-time of $P700^+$ re-reduction in darkness was extracted from the resulting kinetic.

Kinetic correction and half-time determination were obtained using the JTS-10 software from BioLogic. The electron turnover rates were calculated from the half-time of relaxation decay using the formula: K (turnover in electrons) = 0.693 / half-time of $P700^+$ re-reduction in seconds (Lou *et al.*, 2018).

Cyt *f* and PlastoC redox kinetics were obtained from the deconvolution of variations in absorbance changes measured at 546, 554, 563 and 573 nm with their respective interference filters (10 nm). Sample and reference photodiode were covered with 3 mm thick BG39 filters (Schott) to prevent scattering. Actinic illumination occurred under 630 nm at 150 µmol photons · m^{-2} · s^{-1} and detection pulses were provided with white light. To reduce noise, kinetics measured at 573 nm was the result of the average of 5 technical replicates. Deconvolution of the four kinetics was performed using the JTS-10 BioLogic software. The half-time of re-reduction of photo-oxidized Cyt *f* and PlastoC were used to calculate electron turnover rate through Cyt *f* and PlastoC as previously described for $P700^+$ re-reduction kinetics.

3.4.6 Determination of the proportion of cyclic electron flow around PSI

The proportion of cyclic electron flow around PSI during photosynthesis was determined according to Du *et al.* (2019). P700 redox kinetic was first obtained as described for the determination of P700 redox kinetics with simultaneous excitation of the PSII and PSI then the same measurement was repeated following addition of DCMU (10 µM, 0.3% EtOH). The electron turnover rates were determined as described for P700 kinetics determination. To obtain the relative contribution of cyclic electron flow, the PSI electron turnover rates determined from measurements with DCMU (cyclic electron flow around PSI only) were divided by the rates calculated in the absence of DCMU (reflecting total or linear + cyclic electron flow). The result was expressed in percentage relative to total electron flow.

3.4.7 Determination of maximal photo-oxidizable P700, Cyt *f* and PlastoC content

Concentration of photo-oxidizable P700 in whole cells was estimated using a JTS-10 spectrophotometer in the presence of DCMU (10 µM) and DBMIB (20 µM) according to a method adapted from Ungerer *et al.* (2018). Recordings were performed under 5 sec far-red illumination

(1400 µmol photons · m^{-2} · s^{-1}) followed by a saturation pulse (630 nm, 2500 µmol photons · m^{-2} · s^{-1}) to completely photo-oxidize P700. Detection pulses were provided by LED at 820 nm and RG780 cutoff filters (820 nm, thickness of 6 mm) were placed in front of the sample and reference photodiode. To remove the contribution of PlastoC, the same measurement was repeated with detection pulses provided by LED at 880 nm and with RG850 cutoff filters (880 nm, thickness of 3 mm) then the resulting redox kinetic was subtracted from the kinetics obtained at 820 nm. The value of the maximum variation in absorbance change was extracted then the maximum photo-oxidizable P700 concentration per cell was estimated using the reduced minus oxidized difference absorption coefficient (Δε) of 8 $mM^{-1} \cdot cm^{-1}$ (Hiyama and Ke, 1972). For the determination of Cyt *f* and PlastoC concentration, redox kinetics and deconvolution were repeated as described in the determination of Cyt *f* and PlastoC kinetics but following addition of DCMU (10 µM), DBMIB (20 µM) and methyl viologen (20 µM) according to Ungerer *et al.* (2018). From the maximum variation in absorbance change, the concentration of Cyt *f* and PlastoC per cell were estimated using a Δε of 25 (Metzger *et al.*, 1997) and 3.75 $mM^{-1} \cdot cm^{-1}$ (Schreiber, 2017), respectively.

3.4.8 Statistical analysis

The results were expressed as the average of three replicates with error bars representing standard deviation. Prior to the statistical analysis, normality and heterogeneity of variance was evaluated on residuals using the Shapiro-Wilk and Brown-Forsythe tests, respectively. Data transformation was applied when residuals were not normally distributed and showed heterogenous variance. For every parameter, the difference between WT and MT was evaluated using a Student's t-test.

3.5 Results and discussion

Although ϕ_M and ϕ'_M did not differ between strains ($P > 0.05$; Figure 3.1A-B), the MC-producing strain showed higher oxygen production (49%, $P < 0.01$, Figure 3.1C) and consumption rate (56%, $P < 0.01$, Figure 3.1D), higher relative proportion of light energy absorbed by PSII (7%, $P < 0.05$, Figure 3.2B), faster kinetics downstream of the PSII in particular for P700 (15%, $P < 0.05$, Figure 3.3B) and PlastoC (39%, $P < 0.01$, Figure 3.3F) as well as higher proportion of cyclic electron flow around PSI (73%, $P < 0.01$, Figure 3.4B) in comparison to its non-MC-producing mutant homologue. These results indicate that inactivation of MC production in PCC 7806 *mcy*B$^-$ altered processes at the center of the regulation of electron flow between the photosynthetic and respiratory electron transport chain and as well as the distribution of light energy between PSII and PSI.

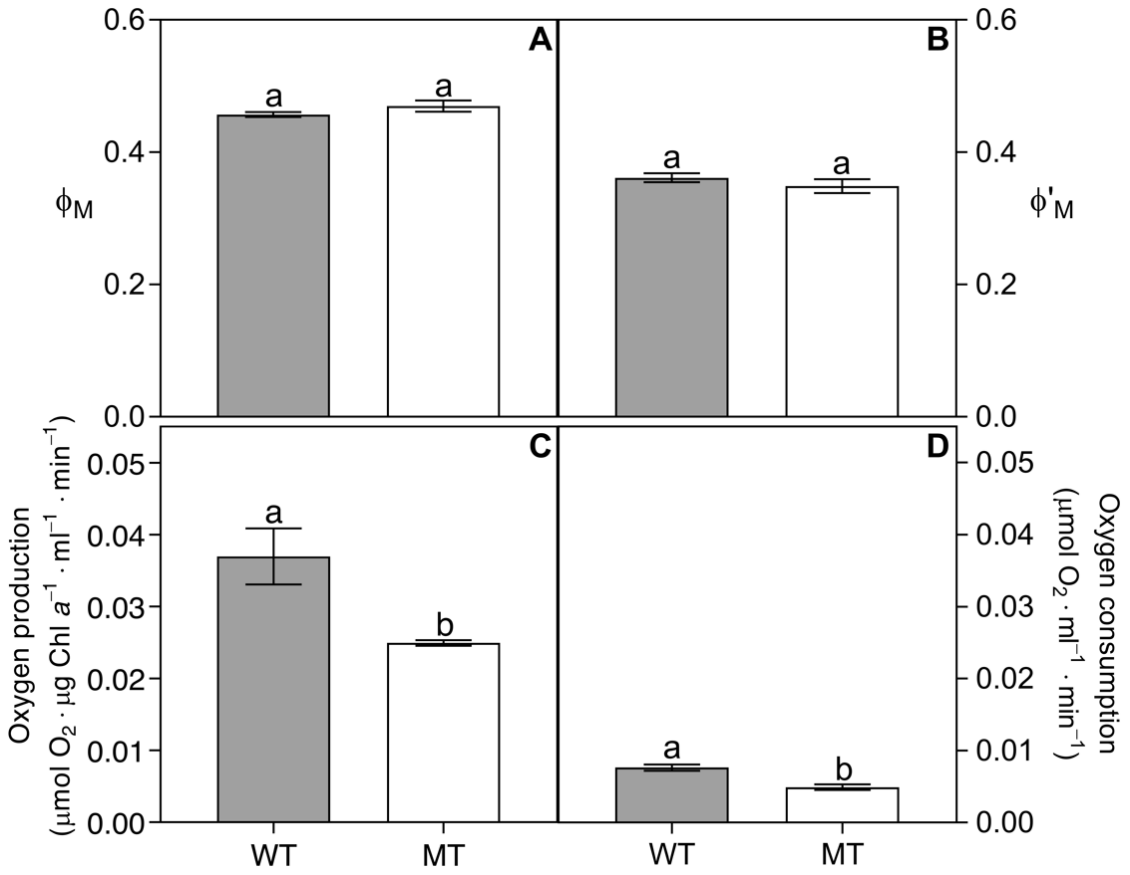

Figure 3.1 Maximal (**A**) and operational PSII quantum yield (**B**), oxygen production normalized to Chl *a* concentration (**C**) and oxygen consumption (**D**) of *M. aeruginosa* PCC 7806 (WT) and PCC 7806 *mcy*B$^-$ (MT). Means (n = 3) not connected by the same letter are significantly different according to the Student's t-test.

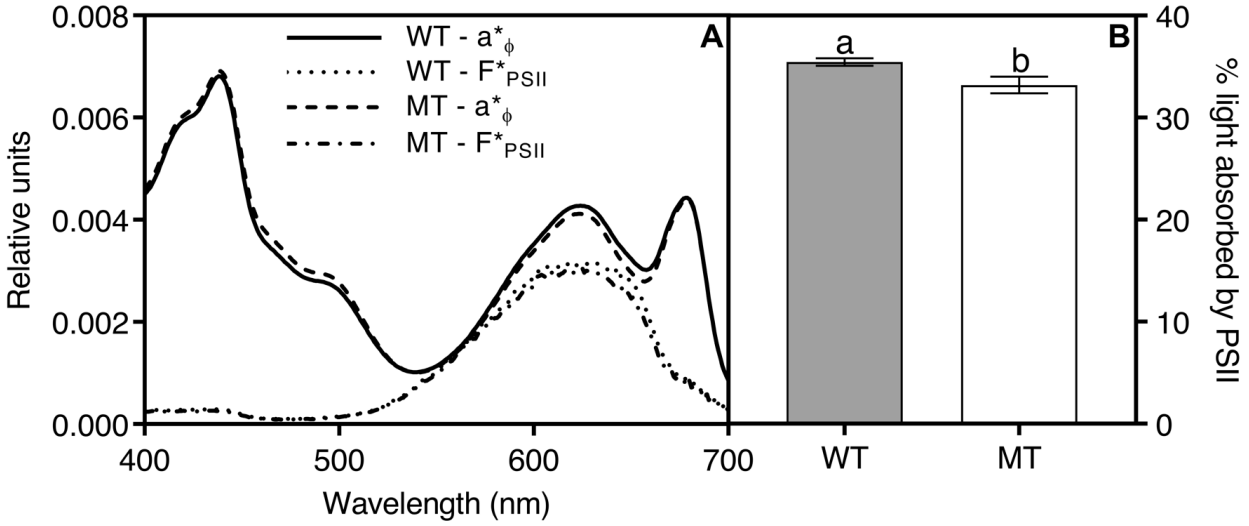

Figure 3.2 *In vivo* absorption and fluorescence spectra normalized to unity (**A**) and proportion of light energy absorbed by PSII (**B**) of *M. aeruginosa* PCC 7806 (WT) and PCC 7806 *mcy*B$^-$ (MT). Means (n = 3) not connected by the same letter are significantly different according to the Student's t-test.

Upon illumination, the P700 of a dark-adapted cyanobacterial sample is quickly oxidized and its absorptivity decreases (Nguyen *et al.*, 2017, Shubin *et al.*, 2008). During our investigation of P700 redox kinetics for WT and MT (Figure 3.3A), we observed a similar amplitude in the initial decrease in absorbance upon illumination. Afterwards, significant reduction occurs around 0.5 sec actinic illumination as shown by the sharp rise in absorbance between 0.5 sec and 1 sec illumination most likely from the initial electron influx coming from PSII. This reduction phase brought the pool of oxidized P700 to near resting state and was also similar between both strains which can be explained by their similar maximal concentration in photo-oxidizable P700 (Figure 3.5B). After 1 sec illumination, the rate at which electrons are pulled downstream of the PSI begins to overtake the rate at which electrons arrive from the acceptor side of PSI and absorbance begins to decrease as there is more oxidation than reduction of the P700 pool. At this step, both strains showed a reversal in P700 absorption at a similar time. Following this, sustained actinic illumination continuously decreases P700 absorbance until the rate of P700 oxidation/reduction reach a balance. In PCC 7806 and PCC 7806 *mcy*B$^-$, this step occurred between 1 sec and 3 sec illumination and was significantly altered by loss of MC production.

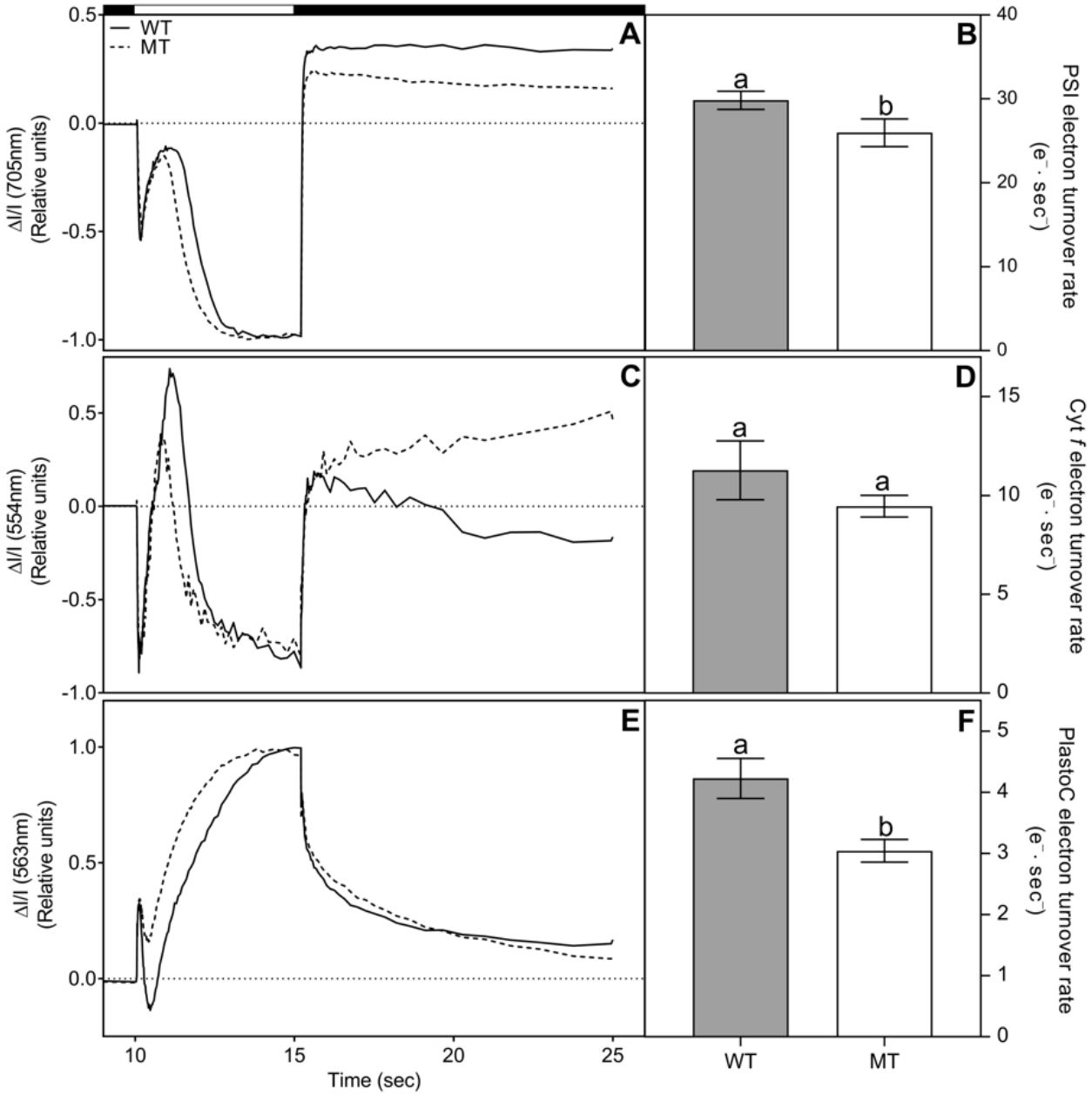

Figure 3.3 P700 redox kinetics (**A**), PSI electron turnover rate (**B**), Cyt *f* redox kinetics (**C**), Cyt *f* electron turnover rate (**D**), PlastoC redox kinetics (**E**) and PlastoC electron turnover rate (**F**) of *M. aeruginosa* PCC 7806 (WT) and PCC 7806 *mcy*B$^-$ (MT). Means (n = 3) not connected by the same letter are significantly different according to the Student's t-test.

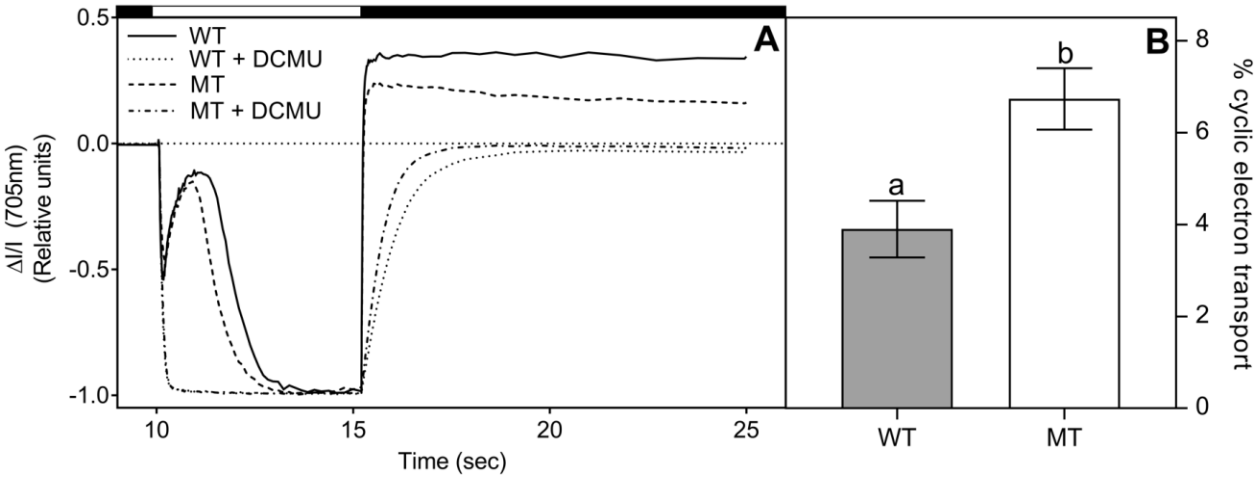

Figure 3.4 P700 redox kinetics before and after addition of DCMU (**A**) and the proportion of cyclic electron flow during photosynthesis (**B**) of *M. aeruginosa* PCC 7806 (WT) and PCC 7806 *mcy*B$^-$ (MT). Means (n = 3) not connected by the same letter are significantly different according to the Student's t-test.

Indeed, P700 of WT showed a slower reversal in P700 absorbance change followed by a faster decrease which allowed both strains to reach an equilibrium between rate of P700 oxidation/reduction at a similar time. This could be explained by the higher oxygen consumption rate of WT (Figure 3.1D) which may consequently result in more electrons being fed from the respiratory electron transport chain into the PQ pool for WT compared to MT during illumination (Ogawa *et al.*, 2021). Also, the lower proportion of cyclic electron flow rate around PSI of WT (Figure 3.4B) while showing similar photosynthetic yield than MT (Figure 3.1A-B) could explain this slower reversal in absorbance change as cyclic electron flow can generate a significant proportion of electron flow through PSI (Theune *et al.*, 2021). The higher PSI electron turnover rate of WT in comparison with MT (Figure 3.3B) can explain the faster decrease in absorbance before reaching redox equilibrium between 1 sec and 3 sec of actinic illumination for WT. Following closure of the actinic light, the pool of oxidized P700 returned to a fully reduced state faster for WT than MT which can be explained by the higher dark respiration rates of WT than MT (Figure 3.1D) as respiratory electron flow to PQ or directly to PSI (Liu *et al.*, 2012) can significantly contribute to the re-reduction of $P700^+$ in the dark.

When actinic illumination is applied on a dark-adapted sample, absorption of Cyt *f* rapidly drops in response to electrons being pulled by oxidized P700 (Metzger et al., 1997). Then, electrons coming from PSII reduce Cyt *f* which sharply increases absorption. In turn, this increase in absorption slows down and reverses as electrons are being pulled faster by PSI than are being replaced from PSII. Gradually, the rate of electrons coming from the acceptor side of Cyt *f* and drawn at the donor side of Cyt *f* reach equilibrium shortly before actinic illumination was turned off whereupon Cyt *f* becomes fully re-reduced in the dark.

We evaluated the Cyt *f* redox kinetics of PCC 7806 and PCC 7806 *mcy*B$^-$ normalized to a similar Chl *a* concentration to determine if the loss of MC production induced changes in the balance of processes governing the redox kinetics of Cyt *f* (Figure 3.3C). Comparison between the redox kinetics of Cyt *f* between both strains allowed to uncover a bottleneck in the ETC. The similar maximal concentration of photo-oxidizable P700$^+$ (Figure 3.5B) explains why the initial decrease in absorption after initial illumination has similar amplitude between strains. On the other hand, the decrease in proportion in light energy absorbed by PSII (Figure 3.2B) and the lower oxygen production rate of MT (Figure 3.1C) may explain why the subsequent rise in absorption around 150 ms illumination has a lower amplitude for MT than for WT. This observation indicates that loss of MC production affected the rate at which the pool of oxidized Cyt *f* accepts electrons to reach a more reduced state following the initial sharp oxidation phase. Since samples were equalized to a similar Chl *a* concentration and that the maximal and operational photosynthetic yields of PSII were not different between strains (Figure 3.1A-B), but more electrons were accepted by the oxidized pool of Cyt *f* in WT, higher electron flux within Cyt *f* of WT must be allowed between the first 0.5 sec to 2.5 sec of illumination. Afterwards, steady illumination allowed the influx and efflux of electrons in Cyt *f* to reach equilibrium at a similar time between strains. Following closure of the actinic light, the re-reduction rate of Cyt *f* was also similar between strains (Figure 3.3D).

Contrary to P700 and Cyt *f*, oxidation of PlastoC leads to an increase in absorbance while the opposite occurs with reduction (Schreiber, 2017). Next, we observed the PlastoC redox kinetics

of PCC 7806 and PCC 7806 *mcy*B$^-$ to evaluate if the inactivation of MC production affected the homeostasis between processes which directly influence the redox kinetics of PlastoC (Figure 3.3E). Upon actinic illumination of a dark-adapted sample, oxidation of P700 draws electron from PlastoC which oxidizes the pool of PlastoC as shown by the sharp rise in absorbance until 150 ms illumination. There was a similar amplitude in absorbance change during this step for both WT and MT. Then, the oxidized pool of PlastoC is rapidly reduced by the first electrons arriving from PSII across the Cyt *f* which causes a quick decrease in absorbance. For PCC 7806 and PCC 7806 *mcy*B$^-$, this step occurred between 150 ms and 0.5 sec illumination and the amplitude of decrease in absorbance was significantly larger in WT than MT which allowed the pool of oxidized PlastoC in the former to reach a fully reduced state while the latter did not. We may advance that the larger pool of photo-oxidizable PlastoC for MT than WT (4%, $P < 0.05$, Figure 3.6D) is partly responsible for what we observed. At this point, the efflux of electrons leaving the donor side of the PlastoC pool into the pool of oxidized P700 begins to overtake the influx from the acceptor side of the PlastoC pool until a PlastoC redox equilibrium is reached. This step was represented by a large rise in absorbance which gradually stabilized between 0.5 sec and 4.5 sec. During this phase, comparison between the redox kinetics of PlastoC between both strains provided further evidence of a bottleneck in the ETC as a significantly larger increase in the absorbance of the PlastoC pool occurred for WT than MT within the same time frame which suggests a faster electron transport rate through the PlastoC pool. In support of this result, closure of the actinic light allowed near complete reduction of the oxidized pool of PlastoC after 10 sec in darkness that occurred faster for WT than MT which translates to a higher PlastoC electron turnover rate for WT in comparison with MT (Figure 3.3F). Despite the increase in maximal photo-oxidizable PlastoC observed when the capacity to produce MCs was absent (Figure 3.6D), this change was not sufficient to induce a significant difference in the stoichiometry between photo-oxidizable PlastoC and P700 or Cyt *f* (Table 3.1). As such, the change in maximal photo-oxidizable PlastoC is unlikely to be a significant contributor in most of the difference observed in the redox kinetics which further point toward alterations in AEPs.

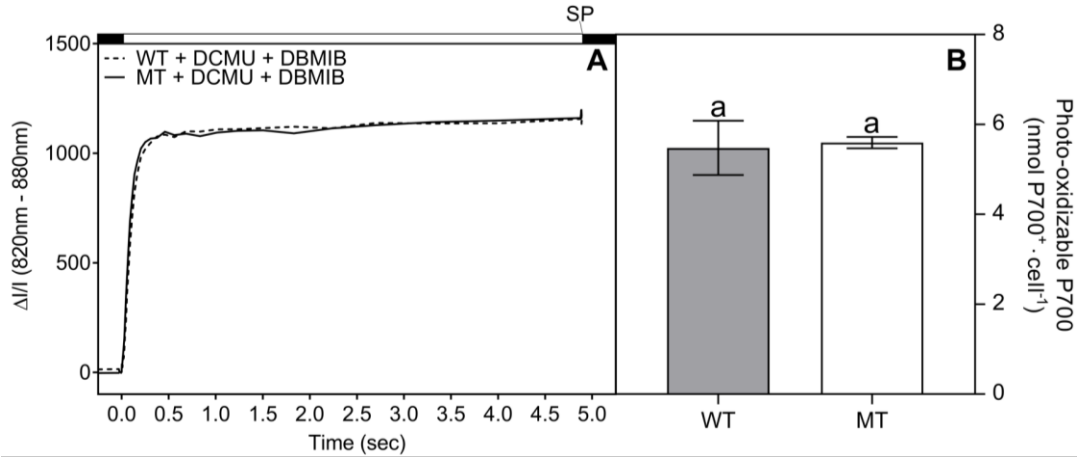

Figure 3.5 P700 redox kinetics after addition of DCMU and DBMIB (**A**) and maximum concentration of photo-oxidizable P700 (**B**) for *M. aeruginosa* PCC 7806 (WT) and PCC 7806 *mcy*B$^-$ (MT). Means (n = 3) not connected by the same letter are significantly different according to the Student's t-test. SP refers to saturation pulse.

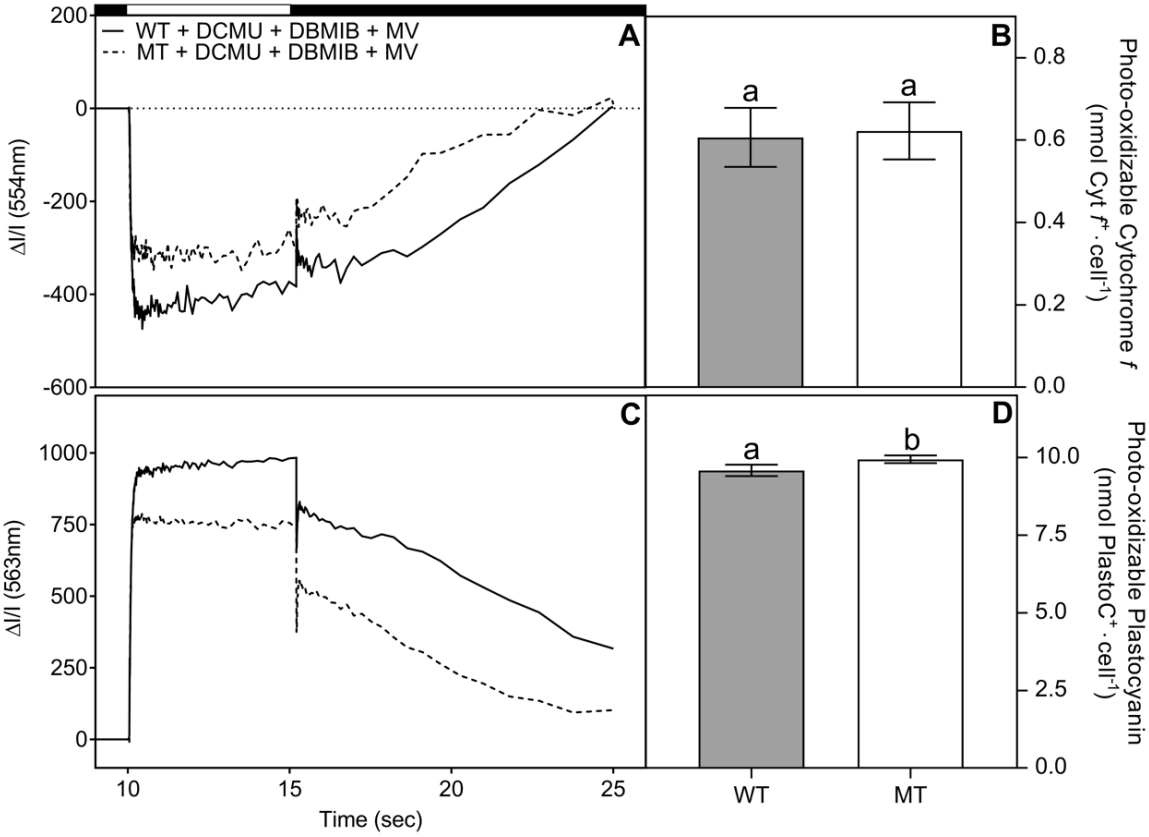

Figure 3.6 Cytochrome *f* (Cyt *f*) redox kinetics after addition of DCMU, DBMIB and MV (**A**), maximum concentration of photo-oxidizable Cyt *f* (**B**), plastocyanin (PlastoC) redox kinetics after addition of DCMU, DBMIB and MV (**C**) and maximum concentration of photo-oxidizable PlastoC (**D**) for *M. aeruginosa* PCC 7806 (WT) and PCC 7806 *mcy*B$^-$ (MT). Means (n = 3) not connected by the same letter are significantly different according to the Student's t-test.

Table 3.1 Ratios between maximum photo-oxidizable P700, cytochrome *f* (Cyt *f*) and plastocyanin (PlastoC) content for *M. aeruginosa* PCC 7806 and 7806 *mcy*B$^-$.

Parameter	WT	MT
PlastoC/P700	1.76 (0.2)[a]	1.78 (0.04)[a]
PlastoC/Cyt *f*	15.92 (1.69)[a]	16.11 (1.69)[a]
P700/Cyt *f*	9.13 (1.64)[a]	9.06 (1.0)[a]

Means (*n* = 3) are indicated with standard deviation in parentheses. Means not connected by the same letter are significantly different according to the Student's t-test.

As both pathways share the PQ pool and PSI acceptors (Lea-Smith *et al.*, 2016, Ogawa *et al.*, 2021, Peschek *et al.*, 2004), the observed differences in the redox kinetics between WT and MT may point toward a significant *mcy*-deletion-mediated change in the balance between photosynthetic and respiratory electron flow. For example, Cyd can redirect electrons coming from PQ (Berry *et al.*, 2002) while COX deprives PSI of electrons coming from PlastoC (Ermakova *et al.*, 2016) and both processes reduce oxygen into water (Howitt and Vermaas, 1998). Moreover, since RTOs and cyclic electron flow can interact with each other, electrons can alternatively circulate toward PSI or RTOs (Kusama *et al.*, 2022). Additionally, FLVs also work as electron sink by redirecting electrons toward O_2 under illumination downstream of PSI which can compete with cyclic electron flow or uptake of electrons for CO_2 fixation (Helman *et al.*, 2003, Lea-Smith *et al.*, 2016, Santana-Sanchez *et al.*, 2019).

Precise control of the rate of production and consumption of O_2 is very important to prevent overexcitation of PSI (Shimakawa and Miyake, 2018). Our work demonstrated that *mcy*-deletion induced a significant decrease in the rates of oxygen production and consumption. These results may point at a significant change in the abundance of AEPs constituents or the rate of AEPs-related electron flow following loss of microcystin production. During rapidly alternating dark to light conditions, Lea-Smith *et al.* (2013) observed that deletion of the respiratory terminal oxidases Cyd and COX in *Synechocystis sp.* PCC 6803 significantly decreased net photosynthetic oxygen production but this was not the case under continuous illumination. Furthermore, cyanobacterial ΔCOX + ΔCyd mutants grown under 12h/12h high light/dark cycles showed increased ROS production and cell death suggesting a critical role of these RTOs in limiting photoinhibition in various changing light conditions (Ermakova *et al.*, 2016, Lea-Smith *et al.*, 2013).

Ermakova *et al.* (2016) also demonstrated that mutants deprived of Cyd or COX exhibited lower dark respiration and this process was nearly imperceptible when both Cyd and COX were removed. Light-enhanced respiration (LER) is also affected by a change in O_2-consumption-related AEPs constituents as shown by Shimakawa *et al.* (2021) where a Δc*yd*/*cox*/*arto* mutant of *Synechocystis sp.* PCC 6803 showed significantly lower LER than the wild-type strain. Furthermore, there is direct evidence that MCs are involved in the response to ROS generation as shown by the binding of MCs to specific proteins in oxidative conditions (Zilliges *et al.*, 2011) and may also serve as a possible antioxidant through ROS scavenging (Malanga *et al.*, 2019). A decrease in ROS production in the presence of MCs could allow for lower inhibition of the D1 protein repair cycle by ROS (Nishiyama *et al.*, 2001) and could also mitigate the potential of PSI photodamage by the scavenging of ROS produced from the reduction of O_2 by photo-oxidized P700 (Shimakawa and Miyake, 2018) which would allow these components to tolerate higher levels of ROS generation. These properties could explain some of the differences we observed when the capacity to produce MCs was absent such as higher proportion of light energy absorbed by the PSII for WT.

In parallel, MCs are known protein phosphatase inhibitors in animals and higher plants (MacKintosh *et al.*, 1990) and were found to affect the regulation of a wide array of redox-sensitive genes (Makower *et al.*, 2015). This suggests that MCs might also influence the functional and structural plasticity of intracellular constituents. While a substantial amount of knowledge exists about gene expression in cyanobacteria, it is unlikely that all the factors which influence the regulation of these genes have been fully identified. These genes typically involve redox-controlled transcription and translation factors modulated by reversible phosphorylation (Wilde and Hihara, 2016, Yang *et al.*, 2013) upon which intracellular MCs could directly exert influence. In this context, intracellular MCs might be involved in the cell signaling network responsible for the regulation of gene expression related to light harvesting (Li and Sherman, 2000, Muramatsu and Hihara, 2012), AEPs (El Bissati and Kirilovsky, 2001), D1 protein repair cycle (Mulo *et al.*, 2012), carbon and nitrogen metabolism (Spät *et al.*, 2021) and the oxidative stress response (Los *et al.*, 2010). Thus, the results we observed when the capacity to produce MCs was absent may have been brought by changes in the PQ pool redox status-related phosphorylation regulation of gene

transcription and translation (Harrison *et al.*, 1991). Some authors did indeed observe the direct influence of MC-LR on phosphorylation-regulated gene transcription in green microalgae (Escoubas *et al.*, 1995) or plants (Freytag *et al.*, 2021). Also, phosphorylation is known to be involved in the cyanobacterial circadian clock which in itself can affect the expression of several genes related to the central metabolism (Tseng *et al.*, 2017). Reversible phosphorylation can also dictate functional and structural plasticity of certain intracellular constituents such as PBS assembly and degradation (Piven *et al.*, 2005) as well as PBS conformational changes related to state transition which can affect energy distribution between PSII and PSI (Chen *et al.*, 2015) upon which intracellular MCs may also be involved.

In Figure 3.7, we present the consequences of inactivation of MCs production we observed on the intersystem components electron flow and abundance, light absorption by the PSII and oxygen production/consumption. Additionally, Figure 3.7 depicts other processes which we suspect were affected by the inactivation of MC production such as the PQ pool redox-controlled gene expression, state transition and energy distribution between photosystems, protection against ROS and ROS scavenging and the rate of assembly/disassembly of phycobilisomes.

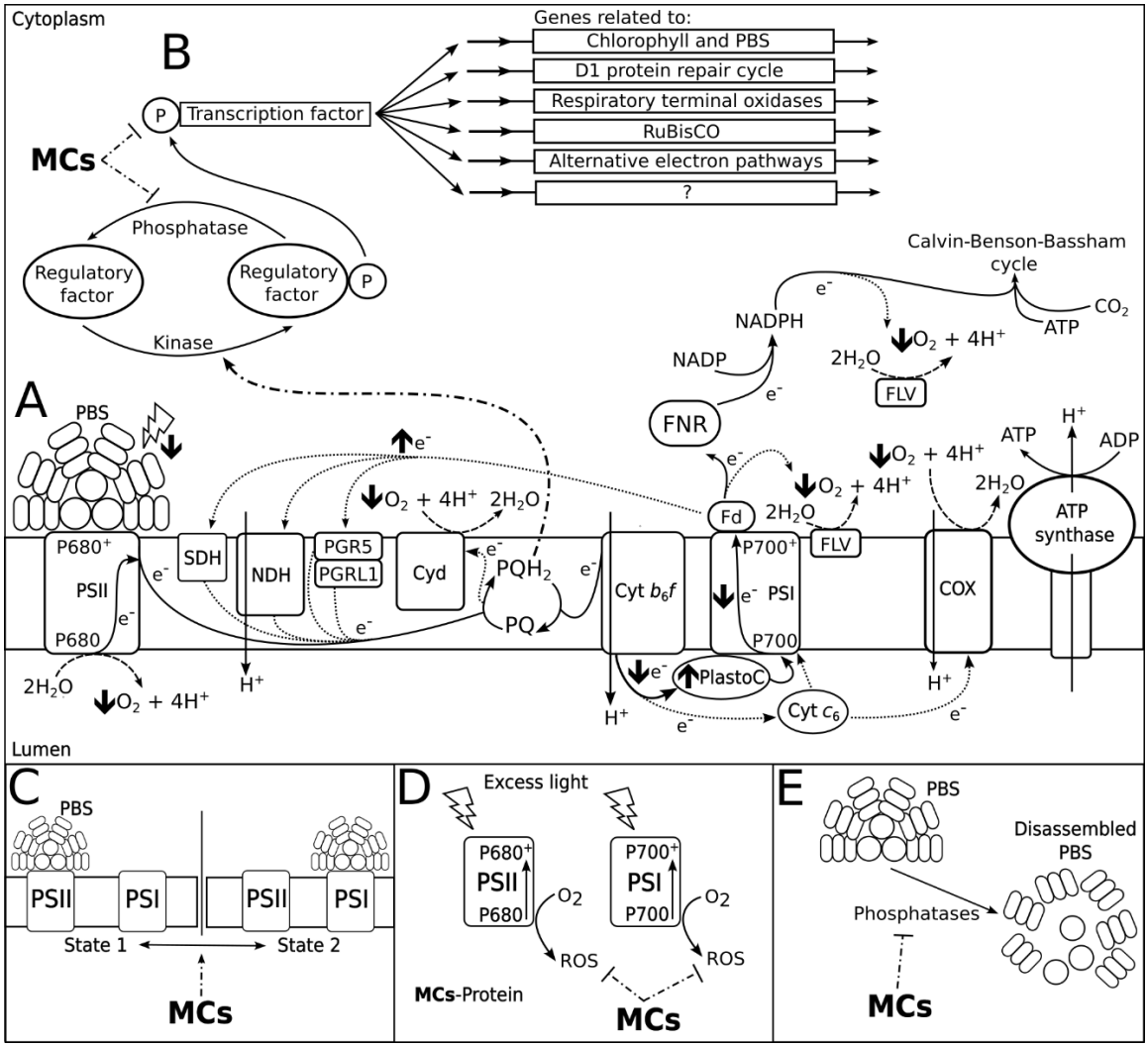

Figure 3.7 (**A**) Consequences of removal of microcystins (MCs) by insertional mutagenesis in PCC 7806 *mcy*B$^-$ we observed on the intersystem components electron flow and abundance, light absorption by the PSII and oxygen production/consumption as well as the potential involvement between intracellular MCs and processes related to (**B**) PQ pool redox-controlled gene expression, (**C**) state transition and energy distribution between photosystems, (**D**) protection against ROS and ROS scavenging and (**E**) the rate of assembly/disassembly of phycobilisomes. As depicted by the bolder black arrows, absence of MCs in the cytosol was associated with slower electron turnover rate in the PSI and PlastoC as well as higher abundance in PlastoC, lower light absorption by the PSII, lower rate of oxygen production/consumption and higher proportion of cyclic electron flow around the PSI. The physiological consequences we observed in the absence of MCs in the cytosol may be related to the known inhibitory influence of MCs on phosphatase activity and the potential roles of MCs in the response to oxidative conditions. Electrons (e^-) associated to solid arrows represent linear electron flow while dotted arrows represent alternative electron flows. Solid arrows without e^- represent known reactions. Dashed arrows represent pathways of oxygen evolution and respiration. Arrows and lines which combine dots and dashes represent unobserved but speculated processes.

3.6 Conclusion

This is the first time that the consequences of mutagenic inactivation of MC production are revealed through the evaluation of redox kinetics and abundance of photo-oxidizable Cyt *f*, PlastoC and P700 using Joliot-Type spectrophotometry from which we exposed a clear bottleneck downstream of the PSII. To our knowledge, for the very first time, we evidenced that MCs are involved in the regulation of electron transfers between the photosynthetic and respiratory electron chain necessary for the homeostatic control of the redox state of the PQ pool, in addition of photoprotection of PSI in *M. aeruginosa*. In summary, the inactivation of MC production was associated with lower PSI and PlastoC electron turnover rate and higher photo-oxidizable PlastoC content, lower proportion of light energy absorbed by the PSII, a decrease in oxygen production/consumption rates and higher proportion of cyclic electron flow around PSI. Taken together, these *mcy*-deletion-mediated changes pointed toward alterations in the balance between photosynthetic and respiratory electron flow most likely related to perturbations in AEPs. It is, however, necessary to conduct a larger investigation of AEPs and the phosphorylation of processes linked to gene expression and structural as well as functional plasticity of intracellular components to better understand and pinpoint the source of the bottleneck consequent to loss of MC production uncovered by this paper.

Author Contributions: Conceptualization, J.N., and P.J.; methodology, J.N. and P.J.; validation, J.N., and P.J.; formal analysis, J.N.; investigation, J.N.; writing—original draft preparation, J.N.; writing—review and editing, J.N. and P.J.; visualization, J.N. All authors have read and agreed to the published version of the manuscript.

3.7 References

Berry, S., Schneider, D., Vermaas, W. F. J. et Rögner, M. (2002). Electron transport routes in whole cells of *Synechocystis sp.* Strain PCC 6803: The role of the cytochrome bd-type oxidase. *Biochemistry*, *41*(10), 3422-3429. doi: 10.1021/bi011683d

Bersanini, L., Battchikova, N., Jokel, M., Rehman, A., Vass, I., Allahverdiyeva, Y. et Aro, E. M. (2014). Flavodiiron protein Flv2/Flv4-related photoprotective mechanism dissipates excitation pressure of PSII in cooperation with phycobilisomes in cyanobacteria. *Plant Physiology*, *164*(2), 805-818. doi: 10.1104/pp.113.231969

Busch, F. A. (2020). Photorespiration in the context of Rubisco biochemistry, CO_2 diffusion and metabolism. *Plant Journal*, *101*(4), 919-939. doi: 10.1111/tpj.14674

Chen, Z., Zhan, J., Chen, Y., Yang, M., He, C., Ge, F. et Wang, Q. (2015). Effects of phosphorylation of β subunits of phycocyanins on state transition in the model cyanobacterium *Synechocystis sp.* PCC 6803. *Plant and Cell Physiology*, *56*(10), 1997-2013. doi: 10.1093/pcp/pcv118

Deblois, C. P. et Juneau, P. (2010). Relationship between photosynthetic processes and microcystin in *Microcystis aeruginosa* grown under different photon irradiances. *Harmful Algae*, *9*(1), 18-24. doi: 10.1016/j.hal.2009.07.001

Deblois, C. P., Marchand, A. et Juneau, P. (2013). Comparison of photoacclimation in twelve freshwater photoautotrophs (chlorophyte, bacillaryophyte, cryptophyte and cyanophyte) isolated from a natural community. *PLoS One*, *8*(3), e57139.

Dittmann, E., Neilan, B. A., Erhard, M., Von Döhren, H. et Börner, T. (1997). Insertional mutagenesis of a peptide synthetase gene that is responsible for hepatotoxin production in the cyanobacterium *Microcystis aeruginosa* PCC 7806. *Molecular Microbiology*, *26*(4), 779-787.

Djediat, C., Feilke, K., Brochard, A., Caramelle, L., Kim Tiam, S., Sétif, P., Gauvrit, T., Yéprémian, C., Wilson, A., Talbot, L., Marie, B., Kirilovsky, D. et Bernard, C. (2020). Light stress in green and red *Planktothrix* strains: The orange carotenoid protein and its related photoprotective mechanism. *Biochimica et Biophysica Acta (BBA) - Bioenergetics*, *1861*(4), 148037. doi: 10.1016/j.bbabio.2019.06.009

Du, J., Qiu, B., Pedrosa Gomes, M., Juneau, P. et Dai, G. (2019). Influence of light intensity on cadmium uptake and toxicity in the cyanobacteria *Synechocystis sp.* PCC6803. *Aquatic Toxicology*, *211*, 163-172. doi: 10.1016/j.aquatox.2019.03.016

Dziallas, C. et Grossart, H. P. (2011). Increasing oxygen radicals and water temperature select for toxic *Microcystis* sp. *PLoS ONE*, *6*(9), e25569. doi: 10.1371/journal.pone.0025569

El Bissati, K. et Kirilovsky, D. (2001). Regulation of psbA and psaE expression by light quality in *Synechocystis* species PCC 6803. A redox control mechanism. *Plant Physiology*, *125*(4), 1988-2000. doi: 10.1104/pp.125.4.1988

Ermakova, M., Huokko, T., Richaud, P., Bersanini, L., Howe, C. J., Lea-Smith, D. J., Peltier, G. et Allahverdiyeva, Y. (2016). Distinguishing the roles of thylakoid respiratory terminal oxidases in the cyanobacterium *Synechocystis sp.* PCC 6803. *Plant Physiology*, *171*(2), 1307-1319. doi: 10.1104/pp.16.00479

Escoubas, J. M., Lomas, M., LaRoche, J. et Falkowski, P. G. (1995). Light intensity regulation of cab gene transcription is signaled by the redox state of the plastoquinone pool. *Proceedings of the National Academy of Sciences of the United States of America*, *92*(22), 10237-10241. doi: 10.1073/pnas.92.22.10237

Freytag, C., Máthé, C., Rigó, G., Nodzyński, T., Kónya, Z., Erdődi, F., Cséplő, Á., Pózer, E., Szabados, L., Kelemen, A., Vasas, G. et Garda, T. (2021). Microcystin-LR, a cyanobacterial toxin affects root development by changing levels of PIN proteins and auxin response in *Arabidopsis* roots. *Chemosphere*, *276*, 130183. doi: 10.1016/j.chemosphere.2021.130183

Genty, B., Briantais, J. M. et Baker, N. R. (1989). The relationship between the quantum yield of photosynthetic electron transport and quenching of chlorophyll fluorescence. *Biochimica et Biophysica Acta - General Subjects*, *990*(1), 87-92. doi: 10.1016/S0304-4165(89)80016-9

González, L., Bolaño, C. et Pellissier, F. (ed.), (2001). Use of oxygen electrode in measurements of photosynthesis and respiration. In M. J. Reigosa Roger (dir.), *Handbook of plant ecophysiology techniques* (1st éd., p. 141-153). Dordrecht, NL : Springer.

Harrison, M. A., Tsinoremas, N. F. et Allen, J. F. (1991). Cyanobacterial thylakoid membrane proteins are reversibly phosphorylated under plastoquinone-reducing conditions in vitro. *FEBS Letters*, *282*(2), 295-299. doi: 10.1016/0014-5793(91)80499-S

Helman, Y., Tchernov, D., Reinhold, L., Shibata, M., Ogawa, T., Schwarz, R., Ohad, I. et Kaplan, A. (2003). Genes encoding A-type flavoproteins are essential for photoreduction of O_2 in cyanobacteria. *Current Biology*, *13*(3), 230-235. doi: 10.1016/S0960-9822(03)00046-0

Hiyama, T. et Ke, B. (1972). Difference spectra and extinction coefficients of P700. *BBA - Bioenergetics*, *267*(1), 160-171. doi: 10.1016/0005-2728(72)90147-8

Howitt, C. A. et Vermaas, W. F. J. (1998). Quinol and cytochrome oxidases in the cyanobacterium *Synechocystis sp.* PCC 6803. *Biochemistry*, *37*(51), 17944-17951. doi: 10.1021/bi981486n

Joliot, P. et Joliot, A. (2005). Quantification of cyclic and linear flows in plants. *Proceedings of the National Academy of Sciences of the United States of America*, *102*(13), 4913-4918. doi: 10.1073/pnas.0501268102

Kaebernick, M., Neilan, B. A., Borner, T. et Dittmann, E. (2000). Light and the transcriptional response of the microcystin biosynthesis gene cluster. *Applied and Environmental Microbiology*, *66*(8), 3387-3392. doi: 10.1128/AEM.66.8.3387-3392.2000

Kitajima, M. et Butler, W. L. (1975). Quenching of chlorophyll fluorescence and primary photochemistry in chloroplasts by dibromothymoquinone. *BBA - Bioenergetics*, *376*(1), 105-115. doi: 10.1016/0005-2728(75)90209-1

Krewald, V., Retegan, M. et Pantazis, D. A. (2015) Principles of natural photosynthesis. *: Vol. 371. Topics in Current Chemistry* (pp. 23-48).

Kusama, S., Miyake, C., Nakanishi, S. et Shimakawa, G. (2022). Dissection of respiratory and cyclic electron transport in *Synechocystis sp.* PCC 6803. *Journal of Plant Research*, *135*(4), 555-564. doi: 10.1007/s10265-022-01401-z

Lea-Smith, D. J., Bombelli, P., Vasudevan, R. et Howe, C. J. (2016). Photosynthetic, respiratory and extracellular electron transport pathways in cyanobacteria. *Biochimica et Biophysica Acta - Bioenergetics*, *1857*(3), 247-255. doi: 10.1016/j.bbabio.2015.10.007

Lea-Smith, D. J., Ross, N., Zori, M., Bendall, D. S., Dennis, J. S., Scott, S. A., Smith, A. G. et Howe, C. J. (2013). Thylakoid terminal oxidases are essential for the cyanobacterium *Synechocystis sp.* PCC 6803 to survive rapidly changing light intensities. *Plant Physiology*, *162*(1), 484-495. doi: 10.1104/pp.112.210260

Li, H. et Sherman, L. A. (2000). A redox-responsive regulator of photosynthesis gene expression in the cyanobacterium *Synechocystis sp.* Strain PCC 6803. *Journal of Bacteriology*, *182*(15), 4268-4277. doi: 10.1128/JB.182.15.4268-4277.2000

Liu, L. N. (2016). Distribution and dynamics of electron transport complexes in cyanobacterial thylakoid membranes. *Biochimica et Biophysica Acta - Bioenergetics*, *1857*(3), 256-265. doi: 10.1016/j.bbabio.2015.11.010

Liu, L. N., Bryan, S. J., Huang, F., Yu, J., Nixon, P. J., Rich, P. R. et Mullineaux, C. W. (2012). Control of electron transport routes through redox-regulated redistribution of respiratory complexes. *Proceedings of the National Academy of Sciences of the United States of America*, *109*(28), 11431-11436. doi: 10.1073/pnas.1120960109

Los, D. A., Zorina, A., Sinetova, M., Kryazhov, S., Mironov, K. et Zinchenko, V. V. (2010). Stress sensors and signal transducers in cyanobacteria. *Sensors*, *10*(3), 2386-2415. doi: 10.3390/s100302386

Lou, W., Tan, X., Song, K., Zhang, S., Luan, G., Li, C. et Lu, X. (2018). A specific single nucleotide polymorphism in the ATP synthase gene significantly improves environmental stress tolerance of *Synechococcus elongatus* PCC 7942. *Applied and Environmental Microbiology*, *84*(18), e01222-01218. doi: 10.1128/AEM.01222-18

Ma, M., Liu, Y., Bai, C., Yang, Y., Sun, Z., Liu, X., Zhang, S., Han, X. et Yong, J. W. H. (2021). The Physiological Functionality of PGR5/PGRL1-Dependent Cyclic Electron Transport in Sustaining Photosynthesis. *Frontiers in Plant Science*, *12*, 702196. doi: 10.3389/fpls.2021.702196

MacKintosh, C., Beattie, K. A., Klumpp, S., Cohen, P. et Codd, G. A. (1990). Cyanobacterial microcystin-LR is a potent and specific inhibitor of protein phosphatases 1 and 2A from both mammals and higher plants. *FEBS Letters*, *264*(2), 187-192. doi: 10.1016/0014-5793(90)80245-E

Makower, A. K., Schuurmans, J. M., Groth, D., Zilliges, Y., Matthijs, H. C. P. et Dittmann, E. (2015). Transcriptomics-aided dissection of the intracellular and extracellular roles of microcystin in *Microcystis aeruginosa* PCC 7806. *Applied and Environmental Microbiology*, *81*(2), 544-554. doi: 10.1128/AEM.02601-14

Malanga, G., Giannuzzi, L. et Hernando, M. (2019). The possible role of microcystin (D-Leu1 MC-LR) as an antioxidant on *Microcystis aeruginosa* (Cyanophyceae). In vitro and in vivo evidence. *Comparative Biochemistry and Physiology Part - C: Toxicology and Pharmacology*, *225*, 108575. doi: 10.1016/j.cbpc.2019.108575

Metzger, S. U., Cramer, W. A. et Whitmarsh, J. (1997). Critical analysis of the extinction coefficient of chloroplasty cytochrome f. *Biochimica et Biophysica Acta - Bioenergetics*, *1319*(2-3), 233-241. doi: 10.1016/S0005-2728(96)00164-8

Miller, N. T., Vaughn, M. D. et Burnap, R. L. (2021). Electron flow through NDH-1 complexes is the major driver of cyclic electron flow-dependent proton pumping in cyanobacteria. *Biochimica et Biophysica Acta - Bioenergetics*, *1862*(3), 148354. doi: 10.1016/j.bbabio.2020.148354

Mullineaux, C. W. (2014). Electron transport and light-harvesting switches in cyanobacteria. *Frontiers in Plant Science*, *5*(JAN), 7. doi: 10.3389/fpls.2014.00007

Mulo, P., Sakurai, I. et Aro, E. M. (2012). Strategies for psbA gene expression in cyanobacteria, green algae and higher plants: From transcription to PSII repair. *Biochimica et Biophysica Acta - Bioenergetics*, *1817*(1), 247-257. doi: 10.1016/j.bbabio.2011.04.011

Muramatsu, M. et Hihara, Y. (2012). Acclimation to high-light conditions in cyanobacteria: From gene expression to physiological responses. *Journal of Plant Research*, *125*(1), 11-39. doi: 10.1007/s10265-011-0454-6

Nawrocki, W. J., Buchert, F., Joliot, P., Rappaport, F., Bailleul, B. et Wollman, F. A. (2019). Chlororespiration controls growth under intermittent light. *Plant Physiology*, *179*(2), 630-639. doi: 10.1104/pp.18.01213

Nguyen, K., Vaughn, M., Frymier, P. et Bruce, B. D. (2017). In vitro kinetics of P700+ reduction of *Thermosynechococcus elongatus* trimeric Photosystem I complexes by recombinant cytochrome c 6 using a Joliot-type LED spectrophotometer. *Photosynthesis Research*, *131*(1), 79-91. doi: 10.1007/s11120-016-0300-8

Nikkanen, L., Solymosi, D., Jokel, M. et Allahverdiyeva, Y. (2021). Regulatory electron transport pathways of photosynthesis in cyanobacteria and microalgae: Recent advances and biotechnological prospects. *Physiologia Plantarum*, *173*(2), 514-525. doi: 10.1111/ppl.13404

Nishiyama, Y., Yamamoto, H., Allakhverdiev, S. I., Inaba, M., Yokota, A. et Murata, N. (2001). Oxidative stress inhibits the repair of photodamage to the photosynthetic machinery. *The EMBO Journal*, *20*(20), 5587-5594. doi: 10.1093/emboj/20.20.5587

Ogawa, T., Suzuki, K. et Sonoike, K. (2021). Respiration Interacts With Photosynthesis Through the Acceptor Side of Photosystem I, Reflected in the Dark-to-Light Induction Kinetics of Chlorophyll Fluorescence in the Cyanobacterium *Synechocystis sp.* PCC 6803. *Frontiers in Plant Science*, *12*, 717968. doi: 10.3389/fpls.2021.717968

Peschek, G. A., Obinger, C. et Paumann, M. (2004). The respiratory chain of blue-green algae (cyanobacteria). *Physiologia Plantarum*, *120*(3), 358-369. doi: 10.1111/j.1399-3054.2004.00274.x

Piven, I., Ajlani, G. et Sokolenko, A. (2005). Phycobilisome linker proteins are phosphorylated in *Synechocystis sp.* PCC 6803. *Journal of Biological Chemistry*, *280*(22), 21667-21672. doi: 10.1074/jbc.M412967200

Rantala, A., Fewer, D. P., Hisbergues, M., Rouhiainen, L., Vaitomaa, J., Börner, T. et Sivonen, K. (2004). Phylogenetic evidence for the early evolution of microcystin synthesis. *Proceedings of the National Academy of Sciences of the United States of America*, *101*(2), 568-573. doi: 10.1073/pnas.0304489101

Rippka, R., Deruelles, J. et Waterbury, J. B. (1979). Generic assignments, strain histories and properties of pure cultures of cyanobacteria. *Journal of General Microbiology*, *111*(1), 1-61.

Sánchez-Baracaldo, P. et Cardona, T. (2020). On the origin of oxygenic photosynthesis and Cyanobacteria. *New Phytologist*, *225*(4), 1440-1446. doi: 10.1111/nph.16249

Santana-Sanchez, A., Solymosi, D., Mustila, H., Bersanini, L., Aro, E. M. et Allahverdiyeva, Y. (2019). Flavodiiron proteins 1–to-4 function in versatile combinations in O_2 photoreduction in cyanobacteria. *eLife*, *8*, e45766. doi: 10.7554/eLife.45766

Schreiber, U. (2017). Redox changes of ferredoxin, P700, and plastocyanin measured simultaneously in intact leaves. *Photosynthesis Research*, *134*(3), 343-360. doi: 10.1007/s11120-017-0394-7

Shimakawa, G., Kohara, A. et Miyake, C. (2021). Characterization of light-enhanced respiration in cyanobacteria. *International Journal of Molecular Sciences*, *22*(1), 1-13. doi: 10.3390/ijms22010342

Shimakawa, G. et Miyake, C. (2018). Oxidation of P700 ensures robust photosynthesis. *Frontiers in Plant Science*, *871*, 1617. doi: 10.3389/fpls.2018.01617

Shubin, V. V., Terekhova, I. N., Kirillov, B. A. et Karapetyan, N. V. (2008). Quantum yield of P700+ photodestruction in isolated photosystem I complexes of the cyanobacterium *Arthrospira platensis*. *Photochemical and Photobiological Sciences*, *7*(8), 956-962. doi: 10.1039/b719122g

Spät, P., Barske, T., Maček, B. et Hagemann, M. (2021). Alterations in the CO_2 availability induce alterations in the phosphoproteome of the cyanobacterium *Synechocystis sp.* PCC 6803. *New Phytologist*, *231*(3), 1123-1137. doi: 10.1111/nph.17423

Stirbet, A., Lazár, D., Guo, Y. et Govindjee, G. (2020). Photosynthesis: Basics, history and modelling. *Annals of Botany*, *126*(4), 511-537. doi: 10.1093/aob/mcz171

Tcherkez, G. (2016). The mechanism of Rubisco-catalysed oxygenation. *Plant Cell and Environment*, *39*(5), 983-997. doi: 10.1111/pce.12629

Theune, M. L., Hildebrandt, S., Steffen-Heins, A., Bilger, W., Gutekunst, K. et Appel, J. (2021). In-vivo quantification of electron flow through photosystem I – Cyclic electron transport makes up about 35% in a cyanobacterium. *Biochimica et Biophysica Acta - Bioenergetics*, *1862*(3), 148353. doi: 10.1016/j.bbabio.2020.148353

Tikkanen, M., Mekala, N. R. et Aro, E. M. (2014). Photosystem II photoinhibition-repair cycle protects Photosystem i from irreversible damage. *Biochimica et Biophysica Acta - Bioenergetics*, *1837*(1), 210-215. doi: 10.1016/j.bbabio.2013.10.001

Tseng, R., Goularte, N. F., Chavan, A., Luu, J., Cohen, S. E., Chang, Y. G., Heisler, J., Li, S., Michael, A. K., Tripathi, S., Golden, S. S., LiWang, A. et Partch, C. L. (2017). Structural basis of the day-night transition in a bacterial circadian clock. *Science*, *355*(6330), 1174-1180. doi: 10.1126/science.aag2516

Ueno, Y., Aikawa, S., Niwa, K., Abe, T., Murakami, A., Kondo, A. et Akimoto, S. (2017). Variety in excitation energy transfer processes from phycobilisomes to photosystems I and II. *Photosynthesis Research*, *133*(1-3), 235-243. doi: 10.1007/s11120-017-0345-3

Ungerer, J., Lin, P. C., Chen, H. Y. et Pakrasi, H. B. (2018). Adjustments to Photosystem Stoichiometry and Electron Transfer Proteins Are Key to the Remarkably Fast Growth of the Cyanobacterium *Synechococcus elongatus* UTEX 2973. *mBio*, *9*(1), e02327-02317. doi: 10.1128/mBio.02327-17

Wiedner, C., Visser, P. M., Fastner, J., Metcalf, J. S., Codd, G. A. et Mur, L. R. (2003). Effects of light on the microcystin content of *Microcystis* strain PCC 7806. *Applied and Environmental Microbiology*, *69*(3), 1475-1481. doi: 10.1128/AEM.69.3.1475-1481.2003

Wilde, A. et Hihara, Y. (2016). Transcriptional and posttranscriptional regulation of cyanobacterial photosynthesis. *Biochimica et Biophysica Acta - Bioenergetics*, *1857*(3), 296-308. doi: 10.1016/j.bbabio.2015.11.002

Yang, M. K., Qiao, Z. X., Zhang, W. Y., Xiong, Q., Zhang, J., Li, T., Ge, F. et Zhao, J. D. (2013). Global phosphoproteomic analysis reveals diverse functions of serine/threonine/tyrosine phosphorylation in the model cyanobacterium *Synechococcus sp.* strain PCC 7002. *Journal of Proteome Research*, *12*(4), 1909-1923. doi: 10.1021/pr4000043

Young, F. M., Morrison, L. F., James, J. et Codd, G. A. (2008). Quantification and localization of microcystins in colonies of a laboratory strain of *Microcystis* (Cyanobacteria) using immunological methods. *European Journal of Phycology*, *43*(2), 217-225. doi: 10.1080/09670260701880460

Young, F. M., Thomson, C., Metcalf, J. S., Lucocq, J. M. et Codd, G. A. (2005). Immunogold localisation of microcystins in cryosectioned cells of *Microcystis*. *Journal of Structural Biology*, *151*(2), 208-214. doi: 10.1016/j.jsb.2005.05.007

Zilliges, Y., Kehr, J. C., Meissner, S., Ishida, K., Mikkat, S., Hagemann, M., Kaplan, A., Börner, T. et Dittmann, E. (2011). The cyanobacterial hepatotoxin microcystin binds to proteins and increases the fitness of *Microcystis* under oxidative stress conditions. *PLoS ONE*, *6*(3), e17615. doi: 10.1371/journal.pone.0017615

[Cette page a été laissée intentionnellement blanche]

CONCLUSION GÉNÉRALE

Cette thèse débute par une démonstration de l'importance de la sélection des souches de *M*. *aeruginosa* pour comprendre le possible rôle physiologique des MCs intracellulaires et que, dans l'ensemble, il existe un lien entre le contenu total en MCs et les processus impliqués dans les mécanismes de photoprotection. Les deux chapitres suivants de cette thèse ont permis de démontrer que les MCs intracellulaires sont impliquées dans différents processus photosynthétiques, la réponse aux conditions oxydatives et, possiblement, les processus respiratoires chez *M*. *aeruginosa*. Une comparaison de ces processus sous plusieurs angles entre une souche possédant la capacité de produire les MCs (PCC 7806) et son homologue mutant dépourvu de celle-ci (PCC 7806 *mcy*B$^-$) nous a permis d'isoler l'influence des MCs intracellulaires sur la réponse contre la photoinhibition et le transport d'électrons au niveau de l'intersection entre la chaîne de transport d'électron photosynthétique et respiratoire.

Résultats principaux

Pour le chapitre 1, nos données provenant de l'analyse comparative des différences retrouvées entre les souches sauvages possédant ou non la capacité de produire les MCs et la souche sauvage MC+ et son homologue mutant dépourvu de sa capacité faire la synthèse de MCs ont pu démontrer que les conclusions possibles sur le rôle physiologique de la MCs provenant d'une telle analyse peut différer selon la sélection des souches de cyanobactéries. La comparaison entre PCC 7806 et PCC 7806 *mcy*B$^-$ a permis d'obtenir un portrait plus large des conséquences physiologiques de l'absence de production de MCs que la comparaison entre les souches sauvages avec ou sans la capacité de produire les MCs. De plus, nos résultats démontrent un lien clair entre la production de MCs et les processus de photoprotection et mettent l'emphase sur un rôle physiologique potentiel des MCs au niveau des processus non-photochimiques de dissipation de l'énergie via une modification des propriétés bio-optiques et la dissipation de l'énergie en trop sous forme de chaleur par l'entremise d'un lien probable entre les MCs et l'interaction entre l'OCP et le PBS. Puisqu'il existe plusieurs contradictions dans les publications qui tente de déterminer le rôle physiologique des MCs en lien à la photosynthèse et la réponse

contre le stress oxydatif, nous suggérons que les recherches futures qui tentent d'approcher cette problématique devraient inclure un nombre important de souches sauvages de cyanobactéries pouvant ou non produire les MCs ainsi que plusieurs souches homologues mutantes dépourvues cette capacité afin d'élargir les conclusions possibles à partir des résultats.

Pour élaborer davantage sur les différences physiologiques conséquentes à la présence ou non de la capacité à produire les MCs en lien aux processus de photoprotection, le chapitre 2 a permis d'isoler les processus physiologiques les plus affectés par la perte de production de MCs chez PCC 7806 *mcy*B$^-$ suite à une exposition seule ou combinée à l'effet de l'atrazine et le stress lumineux. Cette méthodologie a permis de démontrer que les MCs possèdent nécessairement un rôle physiologique au niveau des processus de photorégulation. Du point de vue de la croissance, l'impact délétère de l'atrazine était plus important pour la souche dont la production de MCs a été inactivée par rapport à son homologue sauvage. À l'inverse, l'atrazine a causé une diminution plus importante de l'activité photosynthétique chez la souche possédant la capacité de produire les MCs par rapport à MT. Aussi, la souche mutante était plus sensible à l'impact du stress lumineux que WT. Ces résultats sont d'apparence contradictoire et nécessitent plus de recherches pour en comprendre les causes à l'origine de ceux-ci. En somme, la perte de production de MCs a induit des changements physiologiques chez PCC 7806 *mcy*B$^-$ qui ont permis à cette souche de différemment tolérer l'influence de l'atrazine et le stress lumineux par rapport à PCC 7806. Principalement, ces altérations physiologiques impliquent une différence dans la composition pigmentaire et l'activité des enzymes antioxydantes qui ont permis à PCC 7806 *mcy*B$^-$ de différemment gérer la croissance en conditions qui entraînent la photoinhibition. Ces résultats pointent vers un lien entre la capacité à produire les MCs et une réorganisation de l'utilisation des réserves d'énergie, une transition dans l'efficacité des processus de dissipation de l'énergie de manière non-photochimique et un changement dans l'équilibre des processus qui régulent l'état redox du PSI.

Pour approfondir sur les processus qui gouvernent les mécanismes cités dans les conclusions du chapitre 2, le chapitre 3 a permis d'isoler les processus physiologiques impliqués dans la

régulation des transports d'électrons entre la chaîne de transport d'électrons photosynthétiques et respiratoires. Pour la toute première fois, il a été possible de directement relier la capacité à produire les MCs et la régulation des transferts d'électrons entre la chaîne de transport photosynthétique et respiratoire nécessaire au contrôle homéostatique de l'état redox du contenu en PQ en plus de la photoprotection du PSI chez *M*. *aeruginosa*. De plus, ce chapitre offre une première vision des conséquences de l'inactivation mutagénique de la production de MCs au niveau des cinétiques redox et de l'abondance de Cyt *f*, PlastoC et du P700 à l'aide de la spectrophotométrie de type Joliot. Cette étude a permis de déterminer la présence d'un goulot d'étranglement clair en aval du PSII. En somme, la perte de production de MCs a entraîné une baisse du taux de renouvellement des électrons au niveau du PSI et de PlastoC ainsi qu'une augmentation du contenu en PlastoC photo-oxydable, une baisse de la proportion d'énergie lumineuse absorbée par le PSII, une diminution des taux de production et de consommation d'oxygène ainsi qu'une augmentation de la proportion du flux cyclique d'électrons autour du PSI. Pour conclure le chapitre 3, l'intégration des différences physiologiques retrouvées en conséquence à la délétion du gène *mcy*B dans l'opéron responsable pour la production de MCs nous mène à supposer qu'il existe un lien très probable entre la production de MCs et les transports alternatifs d'électrons et/ou la phosphorylation des processus liés à l'expression des gènes et la plasticité structurelle et fonctionnelle des composantes intracellulaires.

Certains résultats du chapitre 3 viennent donc complémenter les observations du chapitre 2. La diminution dans le taux de production et de consommation d'oxygène chez la souche mutante sans MCs couplée à une plus grande proportion en transport cyclique d'électron et les différences au niveau des cinétiques d'oxydoréduction pour le P700, le Cyt *f* et la PlastoC peuvent impliquer une restructuration de l'équilibre entre les différents mécanismes de transport alternatifs d'électron. Une telle restructuration pourrait en partie expliquer le contraste au niveau de l'impact physiologique de l'atrazine et du stress lumineux entre la souche sauvage et sa souche homologue mutante dépourvue de MCs. Par exemple, la contribution plus importante du transport cyclique d'électron chez la souche mutante sans MCs pourrait avoir limité les conséquences physiologiques de l'obstruction du transport linéaire d'électron par l'atrazine. À

l'inverse, puisque les mécanismes de transport alternatifs d'électron servent principalement à réduire les pressions d'excitation au niveau des photosystèmes et limiter la génération d'espèces réactives de l'oxygène, un changement dans l'équilibre des échanges d'électron entre la chaîne de transport photosynthétique et respiratoire pourrait avoir influencé la capacité de la souche mutante sans MCs à tolérer le stress lumineux. De plus, les conséquences de la perte de MCs au niveau des échanges d'électron pourraient avoir affecté la régulation de l'expression des gènes et l'adaptabilité des composantes intracellulaires en termes de modifications structurelles et fonctionnelles associées à la réponse contre la photoinhibition. Pour isoler davantage le rôle physiologique des MCs, il aurait été idéal de pouvoir inclure des expériences sur des souches possédant la capacité de produire les MCs et dont la concentration intracellulaire en MC a été rapidement modulée sans pour autant affecter la physiologie de la cellule pour ensuite en mesurer les conséquences physiologiques. Puisqu'il n'existe pas de méthode permettant une telle manipulation, il a donc été mis en pratique de se rapprocher le plus possible d'un tel contexte en incluant une sélection de souches de type sauvage possédant ou non la capacité de synthétiser les MCs ainsi qu'une souche qui produit les MCs et sont homologue mutant dont la production de MCs a été inactivée. Ainsi, bien qu'il a été possible d'observer les différences physiologiques relevées par la présence ou l'absence des MCs sous différents contextes, il a été nécessaire de prendre en compte que les souches sauvages comportant ou non les MCs sont des souches à part entière qui ont divergé évolutivement. Dans le cas de la souche mutante dépourvue des MCs, un temps significatif s'est écoulé depuis la perte de production des MCs et, en conséquence, il n'a pas été possible d'observer les conséquences physiologiques immédiates et à très court terme de la perte de production de MCs.

Perspectives

Les résultats contenus dans cette thèse permettent d'ouvrir la porte à plusieurs avenues de recherches pour approfondir notre compréhension du rôle physiologique des MCs chez *M. aeruginosa*. Puisqu'il a été possible de directement relier la capacité à produire les MCs aux processus qui régulent l'état redox des composantes intermédiaires de la chaîne de transport photosynthétique, il est nécessaire d'explorer davantage les divers mécanismes entourant

l'équilibre homéostatique entre la chaîne de transport d'électron photosynthétique et respiratoire. Par exemple, puisque la perte de production de MCs a amené un changement dans la production/consommation d'oxygène, une autre conséquence possible de la perte de production de MCs pourrait être un changement dans l'abondance ou les flux d'électrons dans diverses composantes des transports alternatifs d'électrons comme les FLVs cyanobactériennes, car celles-ci ont pu être reliées à proportion significative de la réduction d'O_2 sous illumination (Allahverdiyeva *et al.*, 2011, Allahverdiyeva *et al.*, 2013, Ermakova *et al.*, 2014). Donc, il est impératif d'explorer davantage les conséquences de la perte de production de MCs sur les processus qui gouvernent la régulation de l'état redox des composantes intermédiaires entre la chaîne de transport d'électron photosynthétique et respiratoire, notamment FLVs, NDH-1, SDH, PGR5/PGRL1, COX, Cyd et ARTO en plus de la régulation du cycle de Calvin-Benson-Basshan et l'équilibre du taux de photorespiration. Additionnellement, il serait également important de relier les conséquences de l'inactivation de la production de MCs aux processus sensibles à l'état redox de la CTE comme la phosphorylation qui régule l'expression génique (Bairagi *et al.*, 2022, Harrison *et al.*, 1991, Hihara *et al.*, 2003, Horiuchi *et al.*, 2010, Ibrahim *et al.*, 2020, Miguel *et al.*, 2000, 2001, Sonya et George, 2000) et qui peut potentiellement moduler la plasticité fonctionnelle et structurelle des composantes intracellulaires.

Finalement, la compréhension du lien entre les MCs et les mécanismes de photoprotection, de transfert d'électrons et au niveau de la production/consommation d'oxygène chez *M. aeruginosa* ouvre la porte au développement de meilleures stratégies qui visent à prédire ou limiter la prolifération ou la toxicité des efflorescences de cyanobactéries nocives. Par exemple, une perturbation sélective des mécanismes de photoprotection chez les souches pouvant produire les MCs pourrait mener à un avantage compétitif pour les souches ne possédant pas les MCs. Aussi, une caractérisation approfondie du lien entre les MCs et la production/consommation d'oxygène pourrait mener à l'isolation des composantes intracellulaires clés impliquées dans ces processus qui pourraient être ciblés afin de perturber le métabolisme et possiblement limiter la croissance des cyanobactéries possédant les MCs.

RÉFÉRENCES (INTRODUCTION ET CONCLUSION)

Allahverdiyeva, Y., Ermakova, M., Eisenhut, M., Zhang, P., Richaud, P., Hagemann, M., Cournac, L. et Aro, E. M. (2011). Interplay between flavodiiron proteins and photorespiration in *Synechocystis sp.* PCC 6803. *Journal of Biological Chemistry*, *286*(27), 24007-24014. doi: 10.1074/jbc.M111.223289

Allahverdiyeva, Y., Mustila, H., Ermakova, M., Bersanini, L., Richaud, P., Ajlani, G., Battchikova, N., Cournac, L. et Aro, E. M. (2013). Flavodiiron proteins Flv1 and Flv3 enable cyanobacterial growth and photosynthesis under fluctuating light. *Proceedings of the National Academy of Sciences of the United States of America*, *110*(10), 4111-4116. doi: 10.1073/pnas.1221194110

Bairagi, N., Watanabe, S., Nimura-Matsune, K., Tanaka, K., Tsurumaki, T., Nakanishi, S. et Tanaka, K. (2022). Conserved Two-component Hik2-Rre1 Signaling Is Activated under Temperature Upshift and Plastoquinone-reducing Conditions in the Cyanobacterium *Synechococcus elongatus* PCC 7942. *Plant and Cell Physiology*, *63*(2), 176-188. doi: 10.1093/pcp/pcab158

Berry, S., Schneider, D., Vermaas, W. F. J. et Rögner, M. (2002). Electron transport routes in whole cells of *Synechocystis sp.* Strain PCC 6803: The role of the cytochrome *bd*-type oxidase. *Biochemistry*, *41*(10), 3422-3429. doi: 10.1021/bi011683d

Bersanini, L., Battchikova, N., Jokel, M., Rehman, A., Vass, I., Allahverdiyeva, Y. et Aro, E. M. (2014). Flavodiiron protein Flv2/Flv4-related photoprotective mechanism dissipates excitation pressure of PSII in cooperation with phycobilisomes in cyanobacteria. *Plant Physiology*, *164*(2), 805-818. doi: 10.1104/pp.113.231969

Börner, T. et Dittmann, E. (ed.), (2005). Molecular Biology of Cyanobacterial Toxins. In J. Huisman, H. C. P. Matthijs et P. M. Visser (dir.), *Harmful Cyanobacteria* (vol. 3, p. 25-40). Dordrecht, NL : Springer.

Boyer, G. L. et Dyble, J. (2009). Harmful Algal Blooms, A newly emerging pathogen in water. *Water Sci Technol*, *59*(8), 1531.

Briand, E., Bormans, M., Quiblier, C., Salençon, M. J. et Humbert, J. F. (2012). Evidence of the cost of the production of microcystins by *Microcystis aeruginosa* under differing light and nitrate environmental conditions. *PLoS ONE*, *7*(1), e29981. doi: 10.1371/journal.pone.0029981

Campbell, D., Hurry, V., Clarke, A. K., Gustafsson, P. et Öquist, G. (1998). Chlorophyll fluorescence analysis of cyanobacterial photosynthesis and acclimation. *Microbiology and Molecular Biology Reviews*, *62*(3), 667-683.

Carmichael, W. W. (1992). Cyanobacteria secondary metabolites—the cyanotoxins. *Journal of Applied Bacteriology*, *72*(6), 445-459. doi: 10.1111/j.1365-2672.1992.tb01858.x

Carmichael, W. W. (2001). Health Effects of Toxin-Producing Cyanobacteria: "The CyanoHABs". *Human and Ecological Risk Assessment*, *7*(5), 1393-1407. doi: 10.1080/20018091095087

Chaffin, J. D., Davis, T. W., Smith, D. J., Baer, M. M. et Dick, G. J. (2018). Interactions between nitrogen form, loading rate, and light intensity on *Microcystis* and *Planktothrix* growth and microcystin production. *Harmful algae*, *73*, 84-97.

Chalifour, A. et Juneau, P. (2011). Temperature-dependent sensitivity of growth and photosynthesis of *Scenedesmus obliquus*, *Navicula pelliculosa* and two strains of *Microcystis aeruginosa* to the herbicide atrazine. *Aquatic Toxicology*, *103*(1–2), 9-17. doi: http://dx.doi.org/10.1016/j.aquatox.2011.01.016

Chorus, I., Fastner, J. et Welker, M. (2021). Cyanobacteria and cyanotoxins in a changing environment: Concepts, controversies, challenges. *Water (Switzerland)*, *13*(18), 2463. doi: 10.3390/w13182463

Crowe, S. A., Døssing, L. N., Beukes, N. J., Bau, M., Kruger, S. J., Frei, R. et Canfield, D. E. (2013). Atmospheric oxygenation three billion years ago. *Nature*, *501*(7468), 535-538. doi: 10.1038/nature12426

Deblois, C. P. et Juneau, P. (2010). Relationship between photosynthetic processes and microcystin in *Microcystis aeruginosa* grown under different photon irradiances. *Harmful Algae*, *9*(1), 18-24. doi: 10.1016/j.hal.2009.07.001

Dittmann, E., Erhard, M., Kaebernick, M., Scheler, C., Neilan, B. A., Von Döhren, H. et Börner, T. (2001). Altered expression of two light-dependent genes in a microcystin-lacking mutant of *Microcystis aeruginosa* PCC 7806. *Microbiology*, *147*(11), 3113-3119. doi: 10.1099/00221287-147-11-3113

Dittmann, E., Neilan, B. A., Erhard, M., Von Döhren, H. et Börner, T. (1997). Insertional mutagenesis of a peptide synthetase gene that is responsible for hepatotoxin production in the cyanobacterium *Microcystis aeruginosa* PCC 7806. *Molecular Microbiology*, *26*(4), 779-787.

Ermakova, M., Battchikova, N., Richaud, P., Leino, H., Kosourov, S., Isojaïvi, J., Peltier, G., Flores, E., Cournac, L., Allahverdiyeva, Y. et Aro, E. M. (2014). Heterocyst-specific flavodiiron protein Flv3B enables oxic diazotrophic growth of the filamentous cyanobacterium *Anabaena sp.* PCC 7120. *Proceedings of the National Academy of Sciences of the United States of America*, *111*(30), 11205-11210. doi: 10.1073/pnas.1407327111

Ermakova, M., Huokko, T., Richaud, P., Bersanini, L., Howe, C. J., Lea-Smith, D. J., Peltier, G. et Allahverdiyeva, Y. (2016). Distinguishing the roles of thylakoid respiratory terminal oxidases in the cyanobacterium *Synechocystis sp.* PCC 6803. *Plant Physiology*, *171*(2), 1307-1319. doi: 10.1104/pp.16.00479

Fastner, J. et Humpage, A. (ed.), (2021). Hepatotoxic cyclic peptides – microcystins and nodularins In Ingrid Chorus et M. Welker (dir.), *Toxic cyanobacteria in water. A guide to their public health consequences, monitoring and management* (2nd éd., chap. 2.1, p. 21-52). Boca Raton, FL, USA : CRC press.

Flombaum, P., Gallegos, J. L., Gordillo, R. A., Rincón, J., Zabala, L. L., Jiao, N., Karl, D. M., Li, W. K. W., Lomas, M. W., Veneziano, D., Vera, C. S., Vrugt, J. A. et Martiny, A. C. (2013). Present and future global distributions of the marine Cyanobacteria *Prochlorococcus* and *Synechococcus*. *Proceedings of the National Academy of Sciences*, *110*(24), 9824-9829. doi: 10.1073/pnas.1307701110

Giannuzzi, L. et Hernando, M. (2022). The Eco-physiological role of *Microcystis aeruginosa* in a changing world. *Microorganisms*, *10*(4), 685. doi: 10.3390/microorganisms10040685

Harke, M. J. et Gobler, C. J. (2013). Global Transcriptional Responses of the Toxic Cyanobacterium, *Microcystis aeruginosa*, to Nitrogen Stress, Phosphorus Stress, and Growth on Organic Matter. *PLOS ONE*, *8*(7), e69834. doi: 10.1371/journal.pone.0069834

Harrison, M. A., Tsinoremas, N. F. et Allen, J. F. (1991). Cyanobacterial thylakoid membrane proteins are reversibly phosphorylated under plastoquinone-reducing conditions in vitro. *FEBS Letters*, *282*(2), 295-299. doi: 10.1016/0014-5793(91)80499-S

Hellweger, F. L., Martin, R. M., Eigemann, F., Smith, D. J., Dick, G. J. et Wilhelm, S. W. (2022). Models predict planned phosphorus load reduction will make Lake Erie more toxic. *Science*, *376*(6596), 1001-1005. doi: 10.1126/science.abm6791

Hesse, K., Dittmann, E. et Börner, T. (2001). Consequences of impaired microcystin production for light-dependent growth and pigmentation of *Microcystis aeruginosa* PCC 7806. *FEMS Microbiology Ecology*, *37*(1), 39-43. doi: 10.1016/S0168-6496(01)00142-8

Hihara, Y., Sonoike, K., Kanehisa, M. et Ikeuchi, M. (2003). DNA Microarray Analysis of Redox-Responsive Genes in the Genome of the Cyanobacterium *Synechocystis sp.* Strain PCC 6803. *Journal of Bacteriology*, *185*(5), 1719-1725. doi: 10.1128/JB.185.5.1719-1725.2003

Hoiczyk, E. et Hansel, A. (2000). Cyanobacterial Cell Walls: News from an Unusual Prokaryotic Envelope. *Journal of Bacteriology*, *182*(5), 1191-1199. doi: 10.1128/jb.182.5.1191-1199.2000

Horiuchi, M., Nakamura, K., Kojima, K., Nishiyama, Y., Hatakeyama, W., Hisabori, T. et Hihara, Y. (2010). The PedR transcriptional regulator interacts with thioredoxin to connect photosynthesis with gene expression in cyanobacteria. *Biochemical Journal*, *431*(1), 135-140. doi: 10.1042/BJ20100789

Huisman, J., Kardinaal, W. E. A., Jolanda, M. H. V., Sharples, J., Stroom, J. M., Visser, P. M. et Sommeijer, B. (2004). Changes in Turbulent Mixing Shift Competition for Light between Phytoplankton Species. *Ecology*, *85*(11), 2960-2970.

Huner, N. P. A., Öquist, G. et Sarhan, F. (1998). Energy balance and acclimation to light and cold. *Trends in Plant Science*, *3*(6), 224-230. doi: https://doi.org/10.1016/S1360-1385(98)01248-5

IARC. (2010). Ingested nitrate and nitrite, and cyanobacterial peptide toxins. *IARC monographs on the evaluation of carcinogenic risks to humans*, *94*, v-vii, 1-412.

Ibrahim, I. M., Wu, H., Ezhov, R., Kayanja, G. E., Zakharov, S. D., Du, Y., Tao, W. A., Pushkar, Y., Cramer, W. A. et Puthiyaveetil, S. (2020). An evolutionarily conserved iron-sulfur cluster underlies redox sensory function of the Chloroplast Sensor Kinase. *Communications Biology*, *3*(1). doi: 10.1038/s42003-019-0728-4

Jähnichen, S., Ihle, T., Petzoldt, T. et Benndorf, J. (2007). Impact of inorganic carbon availability on microcystin production by *Microcystis aeruginosa* PCC 7806. *Applied and environmental microbiology*, *73*(21), 6994-7002.

Jähnichen, S., Long, B. M. et Petzoldt, T. (2011). Microcystin production by *Microcystis aeruginosa*: Direct regulation by multiple environmental factors. *Harmful Algae*, *12*, 95-104. doi: https://doi.org/10.1016/j.hal.2011.09.002

Jankowiak, J., Hattenrath-Lehmann, T., Kramer, B. J., Ladds, M. et Gobler, C. J. (2019). Deciphering the effects of nitrogen, phosphorus, and temperature on cyanobacterial bloom intensification, diversity, and toxicity in western Lake Erie. *Limnology and Oceanography*, *64*(3), 1347-1370. doi: 10.1002/lno.11120

Johnk, K. D., Huisman, J., Visser, P. M., Sharples, J., Sommeijer, B. et Stroom, J. M. (2008). Summer heatwaves promote blooms of harmful cyanobacteria. *Global Change Biology*, *14*(3), 495-512. doi: 10.1111/j.1365-2486.2007.01510.x

Joliot, P., Beal, D. et Frilley, B. (1980). Une nouvelle méthode spectrophotométrique destinée à l'étude des réactions photosynthétiques. *Journal de Chimie Physique*, *77*, 209-216. doi: 10.1051/jcp/1980770209

Jungblut, A. D., Lovejoy, C. et Vincent, W. F. (2010). Global distribution of cyanobacterial ecotypes in the cold biosphere. *The ISME Journal*, *4*(2), 191.

Jüttner, F. et Lüthi, H. (2008). Topology and enhanced toxicity of bound microcystins in *Microcystis* PCC 7806. *Toxicon*, *51*(3), 388-397. doi:10.1016/j.toxicon.2007.10.013

Kaebernick, M., Neilan, B. A., Börner, T. et Dittmann, E. (2000). Light and the transcriptional response of the microcystin biosynthesis gene cluster. *Applied and environmental microbiology*, *66*(8), 3387-3392.

Kirilovsky, D. (2007). Photoprotection in cyanobacteria: the orange carotenoid protein (OCP)-related non-photochemical-quenching mechanism. *Photosynthesis Research*, *93*(1-3), 7-16. doi: 10.1007/s11120-007-9168-y

Kirilovsky, D. et Kerfeld, C. A. (2012). The orange carotenoid protein in photoprotection of photosystem II in cyanobacteria. *BBA - Bioenergetics*, *1817*(1), 158-166. doi: 10.1016/j.bbabio.2011.04.013

Kun, S., Yunlin, Z., Yongqiang, Z., Xiaohan, L., Guangwei, Z., Boqiang, Q. et Guang, G. (2017). Long-term MODIS observations of cyanobacterial dynamics in Lake Taihu: Responses to nutrient enrichment and meteorological factors. *Scientific Reports*, *7*, 40326. doi: 10.1038/srep40326

Latour, D., Perrière, F. et Purdie, D. (2022). Higher sensitivity to hydrogen peroxide and light stress conditions of the microcystin producer *Microcystis aeruginosa sp* PCC7806 compared to non-producer strains. *Harmful Algae*, *114*, 102219. doi: 10.1016/j.hal.2022.102219

Le Manach, S. v., Sotton, B., Huet, H. l. n., Duval, C., Paris, A., Marie, A., Yépremian, C., Catherine, A., Mathéron, L. c., Vinh, J., Edery, M. et Marie, B. (2018). Physiological effects caused by microcystin-producing and non-microcystin producing *Microcystis aeruginosa* on medaka fish: A proteomic and metabolomic study on liver. *Environmental Pollution*, *234*, 523-537. doi: 10.1016/j.envpol.2017.11.011

Lea-Smith, D. J., Bombelli, P., Vasudevan, R. et Howe, C. J. (2016). Photosynthetic, respiratory and extracellular electron transport pathways in cyanobacteria. *Biochimica et Biophysica Acta (BBA) - Bioenergetics*, *1857*(3), 247-255. doi: 10.1016/j.bbabio.2015.10.007

Liu, L. N. (2016). Distribution and dynamics of electron transport complexes in cyanobacterial thylakoid membranes. *Biochimica et Biophysica Acta - Bioenergetics*, *1857*(3), 256-265. doi: 10.1016/j.bbabio.2015.11.010

Liu, L. N., Bryan, S. J., Huang, F., Yu, J., Nixon, P. J., Rich, P. R. et Mullineaux, C. W. (2012). Control of electron transport routes through redox-regulated redistribution of respiratory complexes. *Proceedings of the National Academy of Sciences of the United States of America*, *109*(28), 11431-11436. doi: 10.1073/pnas.1120960109

Lone, Y., Bhide, M. et Koiri, R. K. (2016). Microcystin-LR induced immunotoxicity in mammals. *Journal of toxicology*, *2016*, 8048125.

Lone, Y., Koiri, R. K. et Bhide, M. (2015). An overview of the toxic effect of potential human carcinogen Microcystin-LR on testis. *Toxicology Reports*, *2*, 289-296. doi: https://doi.org/10.1016/j.toxrep.2015.01.008

Lyons, T. W., Reinhard, C. T. et Planavsky, N. J. (2014). The rise of oxygen in Earth's early ocean and atmosphere. *Nature*, *506*(7488), 307-315. doi: 10.1038/nature13068

Ma, M., Liu, Y., Bai, C., Yang, Y., Sun, Z., Liu, X., Zhang, S., Han, X. et Yong, J. W. H. (2021). The Physiological Functionality of PGR5/PGRL1-Dependent Cyclic Electron Transport in Sustaining Photosynthesis. *Frontiers in Plant Science*, *12*, 702196. doi: 10.3389/fpls.2021.702196

MacKintosh, C., Beattie, K. A., Klumpp, S., Cohen, P. et Codd, G. A. (1990). Cyanobacterial microcystin-LR is a potent and specific inhibitor of protein phosphatases 1 and 2A from both mammals and higher plants. *FEBS letters*, *264*(2), 187-192.

Makower, A. K., Schuurmans, J. M., Groth, D., Zilliges, Y., Matthijs, H. C. P. et Dittmann, E. (2015). Transcriptomics-aided dissection of the intracellular and extracellular roles of microcystin in *Microcystis aeruginosa* PCC 7806. *Applied and Environmental Microbiology*, *81*(2), 544-554. doi: 10.1128/AEM.02601-14

Massey, I. Y., Al osman, M. et Yang, F. (2022). An overview on cyanobacterial blooms and toxins production: their occurrence and influencing factors. *Toxin Reviews*, *41*(1), 326-346. doi: 10.1080/15569543.2020.1843060

McConnell, M. D., Koop, R., Vasil'ev, S. et Bruce, D. (2002). Regulation of the Distribution of Chlorophyll and Phycobilin-Absorbed Excitation Energy in Cyanobacteria. A Structure-Based Model for the Light State Transition. *Plant Physiology*, *130*(3), 1201-1212. doi: 10.1104/pp.009845

Merel, S., Walker, D., Chicana, R., Snyder, S., Baurès, E. et Thomas, O. (2013). State of knowledge and concerns on cyanobacterial blooms and cyanotoxins. *Environment International*, *59*, 303-327. doi: 10.1016/j.envint.2013.06.013

Miguel, A., Irène, P. et Diana, K. (2000). Redox Control of psbA Gene Expression in the Cyanobacterium *Synechocystis* PCC 6803. Involvement of the Cytochrome *b6*/*f* Complex. *Plant Physiology*, *122*(2), 505-515.

Miguel, A., Irène, P. et Diana, K. (2001). Redox Control of ntcA Gene Expression in *Synechocystis sp.* PCC 6803. Nitrogen Availability and Electron Transport Regulate the Levels of the NtcA Protein. *Plant Physiology*, *125*(2), 969-981.

Miller, N. T., Vaughn, M. D. et Burnap, R. L. (2021). Electron flow through NDH-1 complexes is the major driver of cyclic electron flow-dependent proton pumping in cyanobacteria. *Biochimica et Biophysica Acta - Bioenergetics*, *1862*(3), 148354. doi: 10.1016/j.bbabio.2020.148354

Mitrovic, S. M., Lorrainehardwick et Forughdorani. (2011). Use of flow management to mitigate cyanobacterial blooms in the Lower Darling River, Australia. *Journal of Plankton Research*, *33*(2), 229-241. doi: 10.1093/plankt/fbq094

Mucci, M., Guedes, I. A., Faassen, E. J. et Lürling, M. (2020). Chitosan as a Coagulant to Remove Cyanobacteria Can Cause Microcystin Release. *Toxins*, *12*(11). 711. doi: 10.3390/toxins12110711

Mullineaux, C. W. (2001). How do cyanobacteria sense and respond to light? *Molecular microbiology*, *41*(5), 965-971.

Mullineaux, C. W. (2014). Co-existence of photosynthetic and respiratory activities in cyanobacterial thylakoid membranes. *Biochimica et Biophysica Acta - Bioenergetics*, *1837*(4), 503-511. doi: 10.1016/j.bbabio.2013.11.017

Muzzopappa, F. et Kirilovsky, D. (2020). Changing Color for Photoprotection: The Orange Carotenoid Protein. *Trends in Plant Science*, *25*(1), 92-104. doi: 10.1016/j.tplants.2019.09.013

Nagarajan, A. et Pakrasi, H. B. (ed.), (2016). Membrane-Bound Protein Complexes for Photosynthesis and Respiration in Cyanobacteria. In L. John Wiley & Sons (dir.), *eLS*. Chichester, EN : John Wiley & Sons, Ltd.

Nath, K., Jajoo, A., Poudyal, R. S., Timilsina, R., Park, Y. S., Aro, E.-M., Nam, H. G. et Lee, C. H. (2013). Towards a critical understanding of the photosystem II repair mechanism and its regulation during stress conditions. *FEBS Letters*, *587*(21), 3372-3381. doi: 10.1016/j.febslet.2013.09.015

Nikkanen, L., Solymosi, D., Jokel, M. et Allahverdiyeva, Y. (2021). Regulatory electron transport pathways of photosynthesis in cyanobacteria and microalgae: Recent advances and biotechnological prospects. *Physiologia Plantarum*, *173*(2), 514-525. doi: 10.1111/ppl.13404

Nishizawa, T., Asayama, M., Fujii, K., Harada, K.-i. et Shirai, M. (1999). Genetic analysis of the peptide synthetase genes for a cyclic heptapeptide microcystin in *Microcystis spp. The Journal of Biochemistry*, *126*(3), 520-529.

Niyogi, K. K. (1999) Photoprotection revisited: Genetic and molecular approaches. *: Vol. 50. Annual Review of Plant Biology* (pp. 333-359).

Niyogi, K. K. (2000). Safety valves for photosynthesis. *Current Opinion in Plant Biology*, *3*(6), 455-460. doi: 10.1016/S1369-5266(00)00113-8

O'Neil, J. M., Davis, T. W., Burford, M. A. et Gobler, C. J. (2012). The rise of harmful cyanobacteria blooms: The potential roles of eutrophication and climate change. *Harmful Algae*, *14*, 313-334. doi: https://doi.org/10.1016/j.hal.2011.10.027

Ogawa, T., Suzuki, K. et Sonoike, K. (2021). Respiration Interacts With Photosynthesis Through the Acceptor Side of Photosystem I, Reflected in the Dark-to-Light Induction Kinetics of Chlorophyll Fluorescence in the Cyanobacterium *Synechocystis sp.* PCC 6803. *Frontiers in Plant Science*, *12*, 717968. doi: 10.3389/fpls.2021.717968

Omidi, A., Esterhuizen-Londt, M. et Pflugmacher, S. (2018). Still challenging: the ecological function of the cyanobacterial toxin microcystin - What we know so far. *Toxin Reviews*, *37*(2), 87-105.

Orr, P. T. et Jones, G. J. (1998). Relationship between microcystin production and cell division rates in nitrogen-limited *Microcystis aeruginosa* cultures. *Limnology and Oceanography*, *43*(7), 1604-1614. doi: 10.4319/lo.1998.43.7.1604

Paerl, H. (2018). Mitigating Toxic Planktonic Cyanobacterial Blooms in Aquatic Ecosystems Facing Increasing Anthropogenic and Climatic Pressures. *Toxins*, *10*(2), 76.

Paerl, H. W. et Huisman, J. (2008). Blooms like It Hot. *Science*, *320*(5872), 57-58.

Paerl, H. W. et Paul, V. J. (2012). Climate change: Links to global expansion of harmful cyanobacteria. *Water Research*, *46*(5), 1349-1363.

Passarge, J., Hol, S., Escher, M. et Huisman, J. (2006). Competition for Nutrients and Light: Stable Coexistence, Alternative Stable States, or Competitive Exclusion? *Ecological Monographs*, *76*(1), 57-72.

Pathak, J., Ahmed, H., Singh, P. R., Singh, S. P., Häder, D. P. et Sinha, R. P. (ed.), (2018). Mechanisms of Photoprotection in Cyanobacteria. In *Cyanobacteria: From Basic Science to Applications* (p. 145-171).

Pearson, L., Mihali, T., Moffitt, M., Kellmann, R. et Neilan, B. (2010). On the chemistry, toxicology and genetics of the cyanobacterial toxins, microcystin, nodularin, saxitoxin and cylindrospermopsin. *Marine drugs*, *8*(5), 1650-1680. doi: 10.3390/md8051650

Pfister, K. et Arntzen, C. J. (1979). The mode of Action of Photosystem II-Specific Inhibitors in Herbicide-Resistant Weed Biotypes. *Zeitschrift fur Naturforschung - Section C Journal of Biosciences*, *34*(11), 996-1009. doi: 10.1515/znc-1979-1123

Pimentel, J. S. M. et Giani, A. (2014). Microcystin production and regulation under nutrient stress conditions in toxic microcystis strains. *Applied and environmental microbiology*, *80*(18), 5836-5843. doi: 10.1128/AEM.01009-14

Rabalais, N. N., Díaz, R. J., Levin, L. A., Turner, R. E., Gilbert, D. et Zhang, J. (2010). Dynamics and distribution of natural and human-caused hypoxia. *Biogeosciences*, *7*(2), 585-619.

Roach, T. et Krieger-Liszkay, A. K. (2014). Regulation of photosynthetic electron transport and photoinhibition. *Current Protein & Peptide Science*, *15*(4), 351-362. doi: 10.2174/1389203715666140327105143

Sandrini, G., Huisman, J. et Matthijs, H. C. P. (2015). Potassium sensitivity differs among strains of the harmful cyanobacterium *Microcystis* and correlates with the presence of salt tolerance genes. *FEMS Microbiology Letters*, *362*(16). fnv121. doi: 10.1093/femsle/fnv121

Scherer, P. I., Raeder, U., Geist, J. et Zwirglmaier, K. (2016). Influence of temperature, mixing, and addition of microcystin-LR on microcystin gene expression in *Microcystis aeruginosa*. *MicrobiologyOpen*, *6*(1), e00393. doi: doi:10.1002/mbo3.393

Sevilla, E., Martin-Luna, B., Bes, M. T., Fillat, M. F. et Peleato, M. L. (2012). An active photosynthetic electron transfer chain required for mcyD transcription and microcystin synthesis in *Microcystis aeruginosa* PCC7806. *Ecotoxicology*, *21*(3), 811-819. doi: 10.1007/s10646-011-0842-7

Shi, L., Carmichael, W. W. et Kennelly, P. J. (1999). Cyanobacterial PPP family protein phosphatases possess multifunctional capabilities and are resistant to microcystin-LR. *Journal of Biological Chemistry*, *274*(15), 10039-10046. doi: 10.1074/jbc.274.15.10039

Sinang, S. C., Reichwaldt, E. S. et Ghadouani, A. (2015). Local nutrient regimes determine site-specific environmental triggers of cyanobacterial and microcystin variability in urban lakes. *Hydrol. Earth Syst. Sci.*, *19*(5), 2179-2195. doi: 10.5194/hess-19-2179-2015

Smith, V. H. (1983). Low nitrogen to phosphorus ratios favor dominance by blue-green algae in lake phytoplankton. *Science*, *221*(4611), 669-671. doi: 10.1126/science.221.4611.669

Sonya, L. K. et George, W. O. (2000). Redox-Regulated RNA Helicase Expression. *Plant Physiology*, *124*(2), 703-713.

Spoof, L. et Arnaud, C. (ed.), (2017). Appendix 3: Tables of Microcystins and Nodularins. In J. Meriluoto, L. Spoof et G. A. Codd (dir.), *Handbook of Cyanobacterial Monitoring and Cyanotoxin Analysis* (p. 526-537). Chichester, UK : John Wiley & Sons.

Stanier, G. (ed.), (1988). Fine structure of cyanobacteria. In *Methods in Enzymology* (vol. 167, p. 157-172). Academic Press.

Straub, C., Quillardet, P., Vergalli, J., de Marsac, N. T. et Humbert, J.-F. (2011). A Day in the Life of *Microcystis aeruginosa* Strain PCC 7806 as Revealed by a Transcriptomic Analysis. *PLOS ONE*, *6*(1), e16208. doi: 10.1371/journal.pone.0016208

Taiz, L. et Zeiger, E. (ed.), (2006). Plant Cells. In *Plant Physiology* (4th ed., chap. 1, p. 15). Sunderland, EN : Sinauer Associates, Inc.

Tikkanen, M., Mekala, N. R. et Aro, E. M. (2014). Photosystem II photoinhibition-repair cycle protects Photosystem i from irreversible damage. *Biochimica et Biophysica Acta - Bioenergetics*, *1837*(1), 210-215. doi: 10.1016/j.bbabio.2013.10.001

Tilzer, M. M. (1987). Light-dependence of photosynthesis and growth in cyanobacteria: implications for their dominance in eutrophic lakes. *New Zealand Journal of Marine and Freshwater Research*, *21*(3), 401-412.

Tonk, L., Visser, P. M., Christiansen, G., Dittmann, E., Snelder, E. O. F. M., Wiedner, C., Mur, L. R. et Huisman, J. (2005). The Microcystin Composition of the Cyanobacterium *Planktothrix agardhii* Changes toward a More Toxic Variant with Increasing Light Intensity. *Applied and Environmental Microbiology*, *71*(9), 5177-5181. doi: 10.1128/aem.71.9.5177-5181.2005

Trebst, A. (1972) Measurement of Hill Reactions and Photoreduction. *: Vol. 24. Methods in Enzymology* (pp. 146-165).

Trebst, A. (2007). Inhibitors in the functional dissection of the photosynthetic electron transport system. *Photosynthesis Research*, *92*(2), 217-224. doi: 10.1007/s11120-007-9213-x

Utkilen, H. et Gjølme, N. (1992). Toxin production by *Microcystis aeruginosa* as a function of light in continuous cultures and its ecological significance. *Applied and Environmental microbiology*, *58*(4), 1321-1325.

Utkilen, H. et Gjølme, N. (1995). Iron-stimulated toxin production in *Microcystis aeruginosa*. *Applied and Environmental Microbiology*, *61*(2), 797-800.

Van de Waal, D. B., Verspagen, J. M. H., Finke, J. F., Vournazou, V., Immers, A. K., Kardinaal, W. E. A., Tonk, L., Becker, S., Van Donk, E., Visser, P. M. et Huisman, J. (2011). Reversal in competitive dominance of a toxic versus non-toxic cyanobacterium in response to rising CO_2. *The ISME journal*, *5*(9), 1438-1450. doi: 10.1038/ismej.2011.28

Vézie, C., Rapala, J., Vaitomaa, J., Seitsonen, J. et Sivonen, K. (2002). Effect of Nitrogen and Phosphorus on Growth of Toxic and Nontoxic *Microcystis* Strains and on Intracellular Microcystin Concentrations. *Microbial Ecology*, *43*(4), 443-454. doi: 10.1007/s00248-001-0041-9

Walsby, A. E., Hayes, P. K., Boje, R. et Stal, L. J. (1997). The Selective Advantage of Buoyancy Provided by Gas Vesicles for Planktonic Cyanobacteria in the Baltic Sea. *The New Phytologist*, *136*(3), 407-417.

Wang, X., Wang, P., Wang, C., Qian, J., Feng, T. et Yang, Y. (2018). Relationship between Photosynthetic Capacity and Microcystin Production in Toxic *Microcystis Aeruginosa* under Different Iron Regimes. *International journal of environmental research and public health*, *15*(9), 1954. doi: 10.3390/ijerph15091954

Waterbury, J. B., Watson, S. W., Guillard, R. R. L. et Brand, L. E. (1979). Widespread occurrence of a unicellular, marine, planktonic, cyanobacterium. *Nature*, *277*, 293. doi: 10.1038/277293a0

Wiedner, C., Visser, P. M., Fastner, J., Metcalf, J. S., Codd, G. A. et Mur, L. R. (2003). Effects of light on the microcystin content of *Microcystis* strain PCC 7806. *Applied and Environmental Microbiology*, *69*(3), 1475-1481. doi: 10.1128/AEM.69.3.1475-1481.2003

Wilson, K. E., Ivanov, A. G., Öquist, G., Grodzinski, B., Sarhan, F. et Huner, N. P. (2006). Energy balance, organellar redox status, and acclimation to environmental stress. *Botany*, *84*(9), 1355-1370.

Wynne, M. et Bold, H. C. (1978). *Introduction to algae: structure and reproduction.* (p. 623). Upper Saddle River, NJ : Prentice-Hall Inc.

Yang, H., Xie, P., Xu, J., Zheng, L., Deng, D., Zhou, Q. et Wu, S. (2006). Seasonal Variation of Microcystin Concentration in Lake Chaohu, a Shallow Subtropical Lake in the People's Republic of China. *Bulletin of Environmental Contamination and Toxicology*, *77*(3), 367-374. doi: 10.1007/s00128-006-1075-y

Yang, J. R., Lv, H., Isabwe, A., Liu, L., Yu, X., Chen, H. et Yang, J. (2017). Disturbance-induced phytoplankton regime shifts and recovery of cyanobacteria dominance in two subtropical reservoirs. *Water Research*, *120*, 52-63. doi: 10.1016/j.watres.2017.04.062

Young, F. M., Morrison, L. F., James, J. et Codd, G. A. (2008). Quantification and localization of microcystins in colonies of a laboratory strain of *Microcystis* (Cyanobacteria) using immunological methods. *European Journal of Phycology*, *43*(2), 217-225. doi: 10.1080/09670260701880460

Young, F. M., Thomson, C., Metcalf, J. S., Lucocq, J. M. et Codd, G. A. (2005). Immunogold localisation of microcystins in cryosectioned cells of *Microcystis*. *Journal of Structural Biology*, *151*(2), 208-214. doi: https://doi.org/10.1016/j.jsb.2005.05.007

Yu, Y., Zeng, Y., Li, J., Yang, C., Zhang, X., Luo, F. et Dai, X. (2019). An algicidal *Streptomyces amritsarensis* strain against *Microcystis aeruginosa* strongly inhibits microcystin synthesis simultaneously. *Science of The Total Environment*, *650*, 34-43. doi: https://doi.org/10.1016/j.scitotenv.2018.08.433

Zegura, B. (2016). An overview of the mechanisms of microcystin-LR genotoxicity and potential carcinogenicity. *Mini reviews in medicinal chemistry*, *16*(13), 1042-1062.

Zilliges, Y., Kehr, J. C., Meissner, S., Ishida, K., Mikkat, S., Hagemann, M., Kaplan, A., Börner, T. et Dittmann, E. (2011). The cyanobacterial hepatotoxin microcystin binds to proteins and increases the fitness of *Microcystis* under oxidative stress conditions. *PLoS ONE*, *6*(3), e17615. doi: 10.1371/journal.pone.0017615

Zurawell, R. W., Chen, H., Burke, J. M. et Prepas, E. E. (2005). Hepatotoxic Cyanobacteria: A Review of the Biological Importance of Microcystins in Freshwater Environments. *Journal of Toxicology and Environmental Health, Part B*, *8*(1), 1-37. doi: 10.1080/10937400590889412